AD-A191 698 STUDY OF THE STRUCTURE OF TURBULENCE IN ACCELERATING TRANSITIONAL BOUNDAR..(U) UNITED TECHNOLOGIES RESEARCH CENTER EAST HARTFORD CT M F BLAIR ET AL. 23 DEC 87 1/3

UNCLASSIFIED UTRC/R87-956900-1 AFOSR-TR-88-0017 F/G 20/4 NL

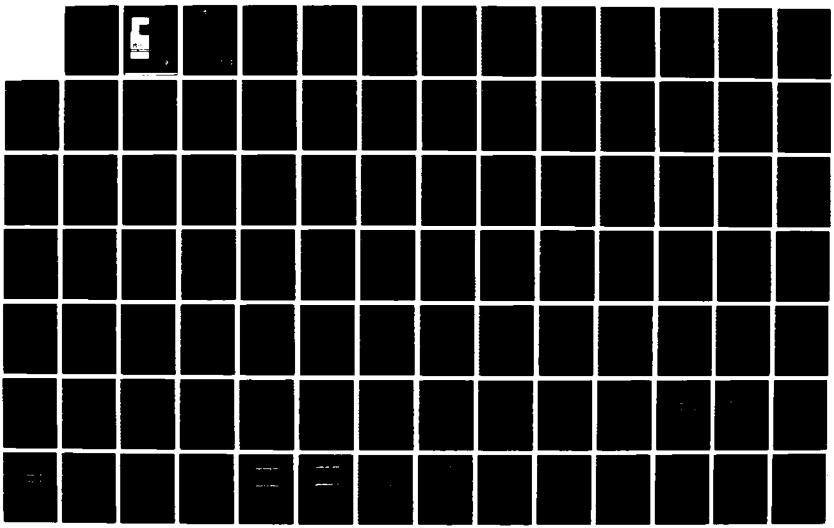

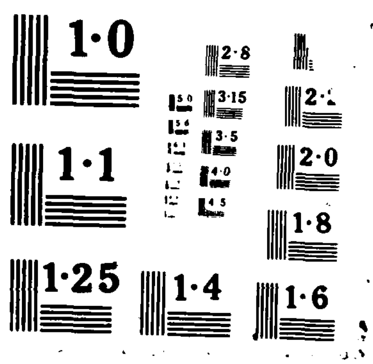
1·0
2·8
3·15
3·5
4·0
4·5
1·1
2·0
1·8
1·25
1·4
1·6

DTIC FILE COPY

(2)

AFOSR-TR- 88-0017

AD-A191 698

R87-956900-1

Study of the Structure of Turbulence in Accelerating Transitional Boundary Layers

Contract No. F49620-84-C-0050

UNITED TECHNOLOGIES RESEARCH CENTER

UNITED TECHNOLOGIES RESEARCH CENTER

East Hartford, Connecticut 06108

DTIC
ELECTE
FEB 2 5 1988
D
H

DISTRIBUTION STATEMENT A

Approved for public release;
Distribution Unlimited

2

UNITED
TECHNOLOGIES
RESEARCH
CENTER
East Hartford, Connecticut 06108

R87-956900-1

Study of the Structure of
Turbulence in Accelerating
Transitional Boundary Layers

Contract No. F49620-84-C-0050

REPORTED BY M. F. Blair
M. F. Blair

Olaf L Anderson
O. L. Anderson

APPROVED BY Robert P Dring
R. P. Dring

DATE December 1987

DISTRIBUTION STATEMENT A

Approved for public release;
Distribution Unlimited

88 2 24 143

UNCLASSIFIED

SECURITY CLASSIFICATION OF THIS PAGE

REPORT DOCUMENTATION PAGE

1a. REPORT SECURITY CLASSIFICATION UNCLASSIFIED	1b. RESTRICTIVE MARKINGS
2a. SECURITY CLASSIFICATION AUTHORITY	3. DISTRIBUTION/AVAILABILITY OF REPORT Approved for public release; distribution unlimited.
2b. DECLASSIFICATION / DOWNGRADING SCHEDULE	
4. PERFORMING ORGANIZATION REPORT NUMBER(S) R-87-956900-1	5. MONITORING ORGANIZATION REPORT NUMBER(S) AFOSR-TR- [illegible]
6a. NAME OF PERFORMING ORGANIZATION United Technologies Research Center; 6b. OFFICE SYMBOL (If applicable)	7a. NAME OF MONITORING ORGANIZATION Air Force Office of Scientific Research
6c. ADDRESS (City, State, and ZIP Code) Silver Lane East Hartford, CT 06108	7b. ADDRESS (City, State, and ZIP Code) Bldg. 410 Bolling Air Force Base D.C. 20332
8a. NAME OF FUNDING/SPONSORING ORGANIZATION AFOSR/NA Bolling AFB, DC 20332; 8b. OFFICE SYMBOL (If applicable) NA	9. PROCUREMENT INSTRUMENT IDENTIFICATION NUMBER F49620-84-C-0050
8c. ADDRESS (City, State, and ZIP Code) AFOSR/NA Bolling AFB, DC 20332	10. SOURCE OF FUNDING NUMBERS: PROGRAM ELEMENT NO. 61102F; PROJECT NO. 2307; TASK NO. A2; WORK UNIT ACCESSION NO.

11. TITLE (Include Security Classification)
Study of the Structure of Turbulence in Accelerating Transitional Boundary Layers

12. PERSONAL AUTHOR(S)
Blair, Michael F. & Anderson, Olof L.

13a. TYPE OF REPORT	13b. TIME COVERED	14. DATE OF REPORT (Year, Month, Day)	15. PAGE COUNT
Final Technical	FROM 84/5/10 TO 87/9/22	1987 Dec. 23	218

16. SUPPLEMENTARY NOTATION

17. COSATI CODES			18. SUBJECT TERMS (Continue on reverse if necessary and identify by block number)
FIELD	GROUP	SUB-GROUP	Boundary Layers, Transition, Turbulence, Intermittency, Acceleration
20	04		

19. ABSTRACT (Continue on reverse if necessary and identify by block number)

A combined experimental and analytical program has been conducted to examine transitional, accelerating boundary layer flows with high levels of freestream turbulence. This program was designed to complement a parallel study conducted previously under AFOSR funding (Contract No. F49620-78-C-0064). ~~The~~ A earlier program focused on measurement of transitional heat transfer distributions for four combinations of streamwise acceleration and freestream turbulence. The present program was designed to document the boundary layer turbulence structure and spectral distributions for the same four test conditions. The results from the present program have shown that transition in accelerating flows consists of an acceleration dominated stage of slowly developing intermittency followed by a second stage with the same general characteristics as zero-pressure-gradient transition. Conditionally sampled fluctuating velocity profile measurements indicated that the boundary layer turbulence was highly anisotropic in the early stages of transition. Conditionally sampled mean velocity

20. DISTRIBUTION/AVAILABILITY OF ABSTRACT ☐ UNCLASSIFIED/UNLIMITED ☒ SAME AS RPT ☐ DTIC USERS	21. ABSTRACT SECURITY CLASSIFICATION UNCLASSIFIED
22a. NAME OF RESPONSIBLE INDIVIDUAL James M McMichael	22b. TELEPHONE (Include Area Code) [illegible] ; 22c. OFFICE SYMBOL [illegible]

DD FORM 1473, 84 MAR — 83 APR edition may be used until exhausted. All other editions are obsolete.

SECURITY CLASSIFICATION OF THIS PAGE

UNCLASSIFIED

measurements showed that within the intermittent turbulent patches the mean velocity profiles were very similar to those of an equilibrium turbulent boundary layer. Spectral distribution data indicated that preferred amplification of the most unstable (as predicted by linear stability theory) frequencies occurred upstream of the onset of transitional bursting.

In addition to the experimental portion of this investigation, numerical experiments were undertaken to assess the ability of currently existing methods to predict heat transfer during transition in accelerating flows. Comparisons of these numerical results with the present experimental data indicate that excellent predictions of both heat transfer and boundary layer development can be achieved with case-specific knowledge of the streamwise intermittency distribution. General predictions, which required intermittency correlations as input, were much less satisfactory.

ABSTRACT

A combined experimental and analytical program has been conducted to examine transitional, accelerating boundary layer flows with high levels of freestream turbulence. This program was designed to complement a parallel study conducted previously under AFOSR funding (Contract No. F49620-78-C-0064). The earlier program focused on measurement of transitional heat transfer distributions for four combinations of streamwise acceleration and freestream turbulence. The present program was designed to document the boundary layer turbulence structure and spectral distributions for the same four test conditions. The results from the present program have shown that transition in accelerating flows consists of an acceleration dominated stage of slowly developing intermittency followed by a second stage with the same general characteristics as zero-pressure-gradient transition. Conditionally sampled fluctuating velocity profile measurements indicated that the boundary layer turbulence was highly anisotropic in the early stages of transition. Conditionally sampled mean velocity measurements showed that within the intermittent turbulent patches the mean velocity profiles were very similar to those of an equilibrium turbulent boundary layer. Spectral distribution data indicated that preferred amplification of the most unstable (as predicted by linear stability theory) frequencies occurred upstream of the onset of transitional bursting.

In addition to the experimental portion of this investigation, numerical experiments were undertaken to assess the ability of currently existing methods to predict heat transfer during transition in accelerating flows. Comparisons of these numerical results with the present experimental data indicate that excellent predictions of both heat transfer and boundary layer development can be achieved with case-specific knowledge of the streamwise intermittency distribution. General predictions, which required intermittency correlations as input, were much less satisfactory.

CONTENTS

I. INTRODUCTION

Accurate calculation of airfoil boundary layer development is a prerequisite for the prediction of turbine heat transfer distributions and aerodynamic performance (efficiency). Such calculations, however, are exceptionally difficult in that the nature of boundary layers on turbine airfoils and the numerous mechanisms that affect them are extremely complicated. Turbine airfoil boundary layers have regions where they are laminar, transitional (forward and reverse) and fully turbulent. They are also subject to the interacting effects of streamwise curvature, freestream turbulence, pressure gradients and three-dimensionality.

Precise prediction of airfoil profile heat loads is of critical importance because the maximum turbine inlet temperatures nearly always exist in the midspan region of the airfoil away from the endwalls. Fortunately, for the vast majority of turbine configurations, the airfoil profile boundary layers are two-dimensional for most of the span. Only near the root and tip is this situation complicated by the presence of three-dimensional secondary endwall flows. There is, then, an important need to be able to accurately compute two-dimensional boundary layer development and heat transfer for the turbine environment.

The boundary layers which develop along the suction and pressure surfaces of modern high camber turbine airfoils have vastly different streamwise pressure histories. Along the suction (convex) surface there is typically a half chord of moderately high acceleration upstream of the airfoil minimum pressure region followed by a moderate deceleration to the airfoil trailing edge. Depending upon the fore-chord acceleration level and the freestream turbulence the suction surface boundary layer may become transitional anywhere from upstream of the maximum velocity region to as far downstream as the adverse pressure gradient zone.

Along the pressure (concave) surface the developing boundary layer experiences approximately half a chord of low, near-constant velocity followed by a length of extremely high acceleration to the airfoil trailing edge. The state of turbulence in the pressure surface boundary layer is determined by an extremely complex interaction of phenomena. In addition to the destabilizing effects of the high freestream turbulence, the concave wall curvature produces destabilizing streamwise vortex systems within the boundary layer. Countering these turbulence promoting effects, the extreme aft-chord accelerations can be sufficient to relaminarize even fully turbulent boundary layers. Since local heat transfer rates are very sensitive to the state of the boundary layer (laminar, transitional or turbulent) the ability to predict transition onset and length is very important. As an illustration of the importance, it is not uncommon for the boundary layer to be transitional for over half the chord for a typical turbine airfoil.

There is a widely recognized need to improve existing analytical models for prediction of boundary layer development (profile loss) and heat transfer distributions for transitional turbine airfoils. One family of cases for which particularly large discrepancies between prediction and experiment have been observed are transitional flows with streamwise acceleration and high freestream turbulence. Brown and Martin (Ref. 1) made special note of the current lack of adequate understanding of this problem in their comprehensive heat transfer review paper. Additional examples of important discrepancies between state-of-the-art airfoil boundary layer predictive schemes and the best available experimental data are given by Han, Chait, Boyee and Rapp (Ref. 2), Hylton, Mihelc, Turner, Nealy and York (Ref. 3) and Rae, Taulbee, Civenskas and Dunn (Ref. 4).

Currently the most highly mature portion of the analytical prediction of transition is the computation of unstable normal modes in boundary layers with small (linear) single frequency (Tollmien-Schlichting) disturbances. Much effort has also been expended to develop methods for predicting the amplification process through which the single frequency disturbances grow to nonlinear levels and culminate in turbulent spot formation (see Ref. 5 for a description of the e^9 and "modified e^9" amplitude ratio methods). In addition, Mack (Ref. 6) has developed techniques for applying stability theory to boundary layers exposed to a wideband disturbance spectrum (e.g., freestream isotropic or near-isotropic turbulence). Using numerical computational techniques for a family of Falkner-Skan family acceleration profiles, Mack has successfully predicted the trends, known long from experimental testing, of streamwise acceleration to retard and of freestream turbulence to promote the transition process.

The analytical techniques discussed above apply exclusively to low-intensity disturbances in laminar boundary layers. For large levels of exterior disturbances both Morkovin (Ref. 5) and Reshotko (Ref. 7) subscribe to the concept of the "high intensity bypass" (complete jump of the linear amplification stage of transition). The bypass mode of transition is thought to occur when disturbances to the boundary layer are so large that they are already at non-linear levels without Tollmien-Schlichting amplification. The available experimental evidence supports this concept in that the highest freestream turbulence levels for which Tollmien-Schlichting waves have ever been detected are 0.45% for flat wall transition (Ref. 8) and 0.5% for turbine airfoil transition (Ref. 9 and 10). One portion of this present program was designed to provide new information on the "bypass" mode. For relatively high freestream turbulence levels the spectral distribution of the boundary layer disturbances upstream of the onset of transition were examined to detect preferential amplification of the bandwidth of predicted unstable frequencies.

Downstream of the "onset" of transition, i.e., downstream of the first appearance of turbulent bursts in the test boundary layers, the present study examined the development of the intermittent boundary layer turbulence structure. A common method of dealing with transition in current finite-difference boundary layer computations is to presume that it occurs over zero length. The flow is assumed to be fully laminar at one computation station and to have an equilibrium turbulence structure at the next. Other analytical models have attempted to incorporate the experimentally observed facts that (1) real transition extends over a distance of many boundary layer thicknesses (sometimes hundreds) and (2) the flow in the transitional region is intermittent in character--sometimes laminar and sometimes turbulent. Some of the more widely used transitional flow turbulence models of this type include those of McDonald and Fish (Ref. 10), Price and Harris (Ref. 11 and 12) and Forest (13). All of these models rely upon the assumption that at any location along the length of transition certain turbulence quantities (e.g., the Reynolds stress structural coefficient $u'v'/q^2$ for Ref. 10 or the eddy viscosity for Ref. 13) are equal to the equilibrium turbulent boundary layer value times the local intermittency. Since all these models rely upon unverified assumed distributions of turbulence quantities they can be accurately described as speculative in nature. The program was designed to provide the data required to incorporate more realistic physics into such transition models.

This present program was designed to complement a parallel study conducted previously under AFOSR funding (Contract No. F49620-78-C-0064). The earlier program focused on measurement of transitional heat transfer distributions for four combinations of streamwise acceleration and freestream turbulence. The present program was designed to document the boundary layer turbulence structure for the same four test conditions. The measurements from the earlier program combined with the present results provide a comprehensive examination of accelerating transitional boundary layer flow. Analytical results include comparisons between these various measurements and a variety of numerical transitional boundary layer computation procedures.

II. DESCRIPTION OF TEST EQUIPMENT

1. UTRC BOUNDARY LAYER WIND TUNNEL

All experimental data for the present investigation were obtained in the United Technologies Research Center (UTRC) Boundary Layer Wind Tunnel. A complete description of this facility is given in Reference 14. This tunnel was designed for conducting fundamental studies of two-dimensional, incompressible flat wall boundary layer flow. Incorporated in the tunnel is a versatile, adjustable test section constructed so that laminar, transitional, or turbulent boundary layers can be subjected to favorable, zero, or adverse pressure gradients. In addition, test boundary layers can be subjected to a wide range of freestream turbulence levels. Low freestream turbulence flows can be investigated in this facility since it is designed to have a very low residual test section turbulence level. Higher turbulence levels can be generated within the test section through the use of various rectangular grids.

An overall sketch of the Low Speed Boundary Layer Tunnel is shown in Figure 1. The tunnel is of recirculating design and consists of a blower, a settling chamber/plenum, a contraction nozzle, the boundary layer test section, a downstream diffuser, and a return duct. The settling chamber/plenum consists of a series of perforated part span baffles which even out gross irregularities in the flow from the blower and a honeycomb which removes large-scale flow swirl. Downstream of the honeycomb are a series of fine mesh damping screens which progressivly reduce both the flow nonuniformity and the residual tunnel turbulence level. A nozzle with a 2.8:1 contraction ratio mounted downstream of the damping screens accelerates the flow to produce the required test section Reynolds number. Following the contraction nozzle the flow passes through the 34-in. wide flat wall boundary layer test section. At the entrance to the test section an upstream facing scoop bleed assembly forms the leading edge of the boundary layer test surface. The purpose of this leading edge bleed scoop is to remove all the flow near the tunnel upper wall. With this arrangement the test section flow consists of the uniform "core" flow from the main contraction nozzle. The scoop assembly consists of a two-stage leading edge adjustable bleed attached to the flat wall boundary layer test surface. The upstream and by far the larger of the two scoops removes the flow nearest the upper wall of the contraction exit duct. This large scoop is intended to trap both the two-dimensional boundary layer which develops along the contraction nozzle wall and the vortices which develop in the contraction corners. The local scoop flow rate can be adjusted to produce uniform pressure (in the transverse direction) at the static taps along the entire scoop. The downstream and much smaller of the two scoops is mounted directly on the front edge of the boundary layer test surface. The test section boundary layer begins growing at the leading edge of this smaller scoop. The leading edge of the small downstream scoop is a 4 x 1 elliptical shape in order to prevent a local separation bubble and a premature transition of the test surface boundary layer.

The test section of the Boundary Layer Wind Tunnel consists of a flat, smooth, aluminum upper wall test surface, a lower flexible, adjustable stainless steel wall and transparent vertical sidewalls. The vertical sidewalls were constructed of plexiglass to facilitate positioning of boundary layer probes and for purposes of conducting flow visualization studies. Downstream of the test section a diffuser/corner combination reduces the flow velocity and delivers the flow to the return duct. Mounted in this return duct are an air filter and a liquid chilled heat exchanger which controls and stabilizes the tunnel air temperature at approximately 70°F.

2. TURBULENCE GENERATING GRIDS

As described in Reference 14, this wind tunnel has a relatively low residual test section turbulence level (< 1/4%). Higher turbulence levels required for this study were generated by inserting various square array biplane grids constructed from rectangular bars at the entrance to the main tunnel contraction (see Fig. 1). Three turbulence generating grids were designed using the correlations of Reference 15. The grids will be referred to as Grids 1, 2, and 3 corresponding to mesh widths, M, of 7/8, 2 9/16, and 7 in. (see Fig. 2). Details of the grid configuration are given in Reference 14. This present arrangement differs from that used for nearly all the earlier investigations of this subject in which the turbulence grids were located in the test section just upstream of the boundary layer test surface. The benefits derived from locating the grids at the contraction entrance were that the generated turbulence was more homogeneous and had a lower decay rate along the test section. Since grid generated turbulence decays approximately as $u'/U \propto (x/b)^{-5/7}$ (Ref. 15), the change in turbulence level with distance along the test section was reduced by increasing the distance from the grid to the test section entrance. In addition, the results of Reference 15 indicate that approximately 10 grid mesh lengths are required to establish a uniform turbulent flow. Locating the grid a distance upstream of the test section requires, of course, a more coarse grid to achieve a given test section turbulence intensity.

Another effect considered was the expected influence of the contraction on the components of the grid generated turbulence. It was recognized that rearrangement of the relative magnitudes of the turbulence components would occur due to the contraction. However, since the contraction ratio was small (2.8), it was concluded that any effects of induced anisotropy would be small in comparison to the advantages gained in homogeneity and reduced decay rate. As part of an earlier study of transitional heat transfer in this same facility (Refs. 16 and 17) all three components of the test section tubulence were documented for these same test grids. Repeat measurement (at a reduced number of locations) of these three-component freestream turbulence data were also obtained as part of this present program.

3. TEST SECTION INSERTS

Two test section inserts, to be installed opposite the flat aluminum test wall, were designed to produce flows with a nearly-constant acceleration parameter ($K = \nu/U^2 \; \partial U/\partial X = 0.2$ and 0.75×10^{-6}, wedges 1 and 2 respectively). These two test section inserts, sketches of which are shown in Figure 3, consist of simple wedge-shaped bodies with a 2 in. long steeper wedge attached to the leading edge. These "modified shape" wedges were designed, using the inviscid potential flow analysis of Reference 18 to provide a near constant acceleration of the test section flow along the entire test wall. Important dimensions of the two wedge inserts are given in Figure 3. Probe traverse slots, aligned with slots in the test section bottom wall, have been incorporated into the wedge inserts.

4. INSTRUMENTATION AND DATA ACQUISITION

a. Hot Wire probes--Measurements of fluctuating velocities in the test boundary layers were obtained using multi-element hot wire anemometry techniques. Both vertical and horizontal x-type two wire probes as well as single horizontal wire probes were employed. In order to minimize potential errors for these measurements (errors largely arising from the inherent mean velocity gradients in the flows and the finite probe size) the hot wire probes were custom designed and fabricated specifically for boundary layer measurements. A comprehensive description of the design of these probes is given in Reference 19. Included in Reference 19 are detailed examples of velocity statistics measured in zero pressure gradient boundary layers.

Following a preliminary "burn in" and a resistance-temperature calibration each sensor was calibrated for velocity and angular sensitivity in a low-turbulence 1 1/2-in. dia. jet flow for approximately twenty jet flow speeds ranging from 7 to 130 ft/s. The mean response equation of each sensor was assumed to be of the form

$$N_u = A_1 + B_1 R_e{}^{0.45} \tag{1}$$

which can be algebraically manipulated to

$$E_w{}^2 = \frac{A_2(R_s + R_w)^2}{R_w} T^{0.76} (T_w - T) + \frac{B_2(R_s + R_w)^2}{R_w} (T_w - T) U_E{}^{0.45} \tag{2}$$

where E_w = wire voltage
R_s = probe body, cable and internal anemometer resistance

R_w = sensor resistance
T = air temperature
T_w = sensor temperature
U_E = effective velocity
A_2, B_2 = empirical constants

The constants A_2 and B_2 were determined for each sensor from a least-squares fit of the data to Equation (2). Next, for the x-wire probes, pitch angle versus voltage data were obtained with the probes rotated from +20° to -20° in steps of 5°. The center of pitch coincided with the intersection of the wires of the x. The angular sensitivity of the wires was assumed to conform to Champagne's k^2 law (Ref. 20),

$$U_E^{\,2}(\phi) = U^2(\phi = 0)\ (\cos^2 \phi + k^2 \sin^2 \phi) \tag{3}$$

where ϕ = angle between wire and direction normal to the flow ($\phi \approx 45°$ with probe stem normal to the flow)
U_E = effective velocity

Using a least-squares routine to find a best fit of the pitch-voltage data to Champagne's equation, optimum values of k were determined for each sensor.

In summary, the temperature-resistance, mean velocity and pitch calibrations were used to determine the following calibration constants.

(1) R_{32} - sensor resistance at 32°F
(2) α - temperature-resistance coefficient
(3) A_2 and B_2 - empirical constants (Eq. 2)
(4) k - empirical constant (Eq. 3).

b. <u>Anemometry and signal processing equipment</u>--Thermo Systems Inc. (TSI) model 1050 constant temperature anemometers were employed to drive the hot wire sensors. Standard square-wave techniques were used to assure that the sensor/anemometer frequency response exceeded 50 KHz. Signals from the anemometers were first passed through 5 KHz low-pass anti-aliasing filters, reduced with a precise D. C. offset, passed through a wide band amplifier (Preston Model 8300 XWB) and then digitized using a TSI Model 1075 Multichannel Digitizer. A feature of this particular analog-to-digitial converter which is important to this application is that the various channels are sampled and held simultaneously. This simultaneous sample-hold feature permits cross-products of the various fluctuating quantities to be computed. The buck and gain system permits the maximum 12 bit resolution of the digitizer to be utilized.

Signals were sampled for 5 seconds at 7813 samples/sec for a total of 39060 continuous numbers per channel. The bandwidth of frequency resolution, then, was 1/5 to 3900 Hz. A Perkin Elmer 3205 minicomputer with 800 K Bytes available RAM was used to control the digitizer and temporarily store a stream of data. Longer term storage of the raw voltage-time records was achieved using 25 M Byte hard disks and digital tape. Reduction of the voltage-time records to velocity-time and mean velocity statistics was also accomplished using the PE 3205. Computed quantities included the mean values of first through fourth moments of the velocity fluctuations and the double (Reynolds stress) and triple velocity products.

III. TEST CONDITIONS

1. TEST SECTION VELOCITY DISTRIBUTIONS

The acceleration configurations (1 and 2) were designed to produce "sink" or constant acceleration parameter flows. Idealized "sink" flow is represented in the following sketch.

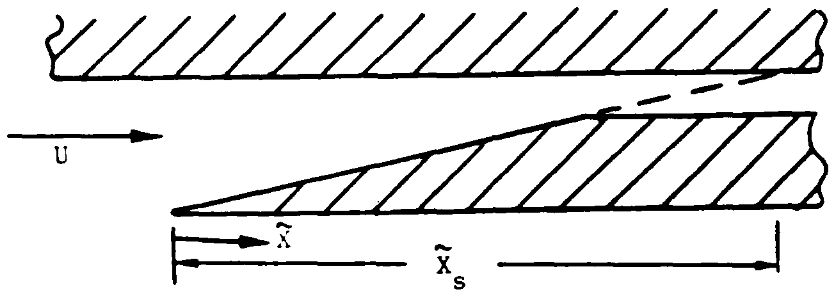

where $\tilde{X}$ is the distance from the beginning of acceleration and $\tilde{X}_s$ is the distance to the potential "origin". The velocity distribution for idealized sink flow is

$$U = C(\tilde{X}_s - \tilde{X})^{-1} \tag{4}$$

The velocity distribution produces a constant acceleration parameter

$$K = \nu/U^2 \; \partial U/\partial\tilde{X} = \nu/C = \text{constant} \tag{5}$$

For the present test program the wedges were carefully adjusted to reproduce the exact velocity distributions employed in References 16 and 17. In this way the present intermittent turbulence structure data and the wall Stanton numbers obtained in the previous study can be combined to form a single comprehensive set of transitional boundary layer information. The velocity distributions reported in References 16 and 17 are reproduced in Figure 4 and 5. The present data agreed within ± 1% of these previously measured distributions. An examination of Figures 4 and 5 reveals that the flows generated in the two acceleration configurations closely approximate ideal sink flow. Test boundary layers developing along the flat test wall were subjected to nearly constant acceleration. The velocity ratio curve plotted for Figure 4 is the analytical relationship determined from the velocity distribution data:

$$U = 14{,}800\ (200 - X)^{-1.066} \tag{6}$$

where U is in ft/s and X is in inches. The acceleration parameter K was calculated using this same analytical relationship. As shown in Figure 4 the acceleration parameter is nearly constant along the entire test wall with a value very near the design target of $K = \nu/U^2\ \partial U/\partial X = 0.2 \times 10^{-6}$.

For Figure 5 the velocity ratio and acceleration plots were calculated from the relationship

$$U = 3780\ (83.3 - X)^{-1.075} \tag{7}$$

where again U is in ft/s and X is in inches. The streamwise acceleration parameter was nearly constant along the entire test wall with $K = 0.75 \times 10^{-6}$.

2. FREESTREAM TURBULENCE DISTRIBUTIONS

Boundary layer turbulence statistics were measured at various streamwise stations along the test wall for the following four acceleration/turbulence combinations:

Flow Condition	K $\times 10^6$	Grid No.	Denoted
1	0.20	1	K.20G1
2	0.20	2	K.20G2
3	0.75	2	K.75G2
4	0.75	3	K.75G3

These combinations reproduced the same test conditions for which mean velocity and temperature profiles and wall Stanton number were recorded for References 16 and 17.

As part of References 16 and 17 the axial distributions of the freestream turbulence intensity and streamwise integral length scale were documented for the four test cases. All three components of the freestream turbulence were recorded at numerous streamwise stations. These previous freestream turbulence measurements were obtained using x-type cylindrical hot film probes and linearized constant temperature anemometers. The individual velocity components were separated using sum-and-difference circuits. Figure 6 presents the turbulence intensity and streamwise length scale data obtained at the test section entrance for Reference 16. These data, obtained for all three turbulence generating grids, indicate that both the intensity and scale were independent of flow speed over the range of testing. Multi-component freestream turbulence intensity data obtained for the present program outside the boundary layers are presented in Figures 7 through 12. These new data, obtained with the previously described hot wire and A/D data acquisition system, are plotted along with the earlier data of Reference 16. The three components of turbulence measured for $K = 0.2 \times 10^{-6}$ and Grids 1 and 2 are presented in Figures 7 and 8 respectively. The present results are in very good agreement with the earlier measurements. Agreement between the present and previous results is also excellent for Figure 9 in which the total turbulence distributions for the two cases are compared. The individual component distributions for Grids 2 and 3 with $K = 0.75 \times 10^{-6}$ (Figs. 10 and 11) compared less favorably to the similar previous data. In contrast, however, the total turbulence measured for these two cases (Fig. 12) agreed very well with the earlier results. The apparent disagreement shown in Figure 10 and 11 resulted from the fact that the two sets of intensity measurements were obtained at different distances from the wall. The data of Reference 16 represent results measured in the mid-channel region while the present results were obtained at $Y > \delta$ but less than an integral scale from the wall. As a result the normal (v) component was suppressed relative to the true freestream value. Note that Figure 12 indicates that the total freestream turbulence kinetic energy measured for the present program was in excellent agreement with the values recorded far from the wall for Reference 16.

Freestream streamwise integral length scale measurements obtained for both the present program and for Reference 16 are presented in Figure 13. The results from the two studies are in very good agreement. The data are consistent with other similar studies (Ref. 21) indicating that acceleration can produce very large growth rates of streamwise length scale.

IV. CONDITIONAL SAMPLING TECHNIQUES

The detection of intermittent turbulent bursts in the test boundary layer flows was accomplished using conditional sampling techniques. These procedures are well established as an accurate means for discrimination of instantaneous flow conditions and are thoroughly described in References 22 through 24. In brief, a fluctuating velocity record was numerically examined to determine which portions should be designated as turbulent. Specifically, the conditional sampling criteria were selected such that periods of high frequency, larger magnitude fluctuations of velocities and/or Reynolds stresses were identified as turbulent. The turbulent criterion were met when a detector function (averaged over a very short smoothing period) exceeded a predetermined threshold level. The particular choices for the detector function, smoothing period and threshold level, then, each influenced the turbulent/nonturbulent discrimination process.

Three independent detector functions were examined as part of this study. For the single horizontal hot wire records the square of the streamwise velocity fluctuations $\left(\frac{\partial u}{\partial t}\right)^2$ was selected. Squares of the Reynolds fluctuation $\left(\frac{\partial uv}{\partial t}\right)^2$ and $\left(\frac{\partial uw}{\partial t}\right)^2$ were used for the vertical and horizontal wires respectively. As demonstrated in References 22 through 24, use of the square of the fluctuations provides a clearer discrimination than the temporal derivative alone.

Using the instantaneous values of these three detector functions velocity-time and Reynolds stress-time records were examined, as follows, to empirically select smoothing times and threshold levels. As described under Data Acquisition, the P-E minicomputer was employed to reduce the x-type or single-wire signals to velocity-time records. A comprehensive signal processing software package (SPAG - Cranfield Data Systems) then permitted convenient displays of the velocity-time records on a computer monitor. As an example the u, v and uv product over a period of time could be displayed on the screen. The conditional sampling discrimination procedure was programmed to produce a display showing times when the turbulent criterion was satisfied. Hundereds of sample velocity records covering the entire test ranges of free-stream turbulence and intermittency were then tested against candidate smoothing times and threshold levels. The values eventually selected proved to be capable of reliably identifying turbulent periods over a very broad range of conditions. A smoothing period of 0.0005 sec. was selected for use with all test records. This smoothing window corresponds to approximately 60 - 100 Kolmogorov length scales for most of the data. Very similar smoothing periods were employed for both References 22 and 23. The threshold level selected consisted of a multiple of an upstream reference (pre-bursting, near-wall) value of that quantity for that particular test boundary layer. For the uv and uw records the criteria for the beginning of bursts was that $\left(\frac{\partial uv}{\partial t}\right)^2 > 10 \left(\frac{\partial uv}{\partial t}\right)^2_{upstream}$ or $\left(\frac{\partial uw}{\partial t}\right)^2 > 10 \left(\frac{\partial uw}{\partial t}\right)^2_{upstream}$ respectively. For the single wire a burst beginning was satisfied if $\left(\frac{\partial u}{\partial t}\right)^2 > 6 \left(\frac{\partial u}{\partial t}\right)^2_{upstream}$.

Identification of the end of turbulent periods proved to be considerably more difficult. The leading edges of bursts were consistently sharp (hence the large multiplication factor on the threshhold criterion). There were, however, usually periods within a burst where the fluctuations were relatively reduced but still very large compared to the upstream "reference" value. Examination of hundreds of velocity-time displays revealed that the end of bursts consisted of a "tailing off" of the high-frequency fluctuations by a return to "upstream reference" conditions. These observations were accommodated into the conditional sampling routine by requiring that 8 smoothing periods in a row fall below a "turbulent-end" criterion before a "stop" was identified. The possible error introduced by this logic was that 2 or more short bursts could be lumped together into a single artificially long burst. Ensemble averaged velocity profile data to be presented later in this report indicate that any such errors were not important. The "transition-end" criterion used for the various records were $\left(\frac{\partial uv}{\partial t}\right)^2 < 2 \left(\frac{\partial uv}{\partial t}\right)^2_{upstream}$ $\left(\frac{\partial uw}{\partial t}\right)^2 < 2 \left(\frac{\partial uw}{\partial t}\right)^2_{upstream}$ and $\left(\frac{\partial u}{\partial t}\right)^2 < 1.5 \left(\frac{\partial u}{\partial t}\right)^2_{upstream}$.

Sample displays of velocities, Reynolds stresses and the turbulence detector function are presented in Figures 14 through 24. These particular samples were selected to display the performance of the turbulence detector for a wide range of intermittency levels and freestream turbulence intensities. In order to present the time resolution of events, time blocks of only 200 ms are displayed. These, then, represent only 4% of the 5 seconds of continuous sample obtained for each total record. The location, acceleration level, freestream turbulence intensity and intermittency level (over the entire 5 second record) are given for each figure.

Sample verical-x-wire and single-wire records taken at $Y/\delta = 0.275$ for a low freestream turbulence intensity, moderate intermittency flow are presented in Figure 14. Note that the x-wire (14a) and the single-wire (14b) data were not obtained simultaneously so the u-time records should not correlate. Figure 14a gives the u,v and Reynolds stress records and the detector function based on the uv product. Starts of turbulent periods correspond to the + spikes of the detector, stops to the - spikes. Figure 14b gives the single-wire u-time record and the detector function based on u. For both 14a and 14b the starts and stops of turbulence as selected by the conditional sampling routine coincide with distinctly active portions of the records. The horizontal-x-wire data taken at the same location and conditions as for Figure 14 are presented in Figure 15 (Fig. 15b repeats Fig. 14b for convenience). As can be seen from an examination of Figure 15a, the uw discriminator also accurately identifies the starts and stops of turbulent periods of the flow.

Figures 16 and 17 are similar to Figures 14 and 15 in that they present uv, uw, and u records for a single location in a test boundary layer. In this case, however, the samples show the performance of the detectors for a high intermittency flow ($\gamma = 0.68$). Again, all the detectors (uv, uw, and u) accurately identify periods of turbulence.

Figures 18 through 23 are an abbreviated version of the turbulence-detector displays in that only the uv, uw, and u records are presented. Figures 18 through 23 present sample records for a wide range of flow conditions; Figure 18 — low T_E and low γ, Figure 19 — moderate T_E and low γ, Figure 20 — high T_E and moderate γ, Figure 21 — low T_E and high γ, Figure 22 — moderate T_E and high γ and Figure 23 — high T_E and high γ. Finally Figure

24 presents sample single-wire records for a single boundary layer at three distinctly different distances (Y/δ = 0.056, 0.193 and 0.926) from the wall. Profiles of the turbulence intensity and intermittency for this particular boundary layer are given in Figure 25. An examination of Figure 24 and 25 reveals that the u detector function was effectively able to identify turbulent periods dispite the fact that the average turbulence level varied enormously across the boundary layer. It should be pointed out, however, that the Reynolds stress detector functions performed unsatisfactorally in the outer part of the boundary layers. For $Y/\delta < 0.5$ the uv, uw, and u criteria would consistently agree within about ± 2% on the level of intermittency. Beyond this point, however, for most of the time the levels of uv and uw in the boundary layers exceeded the upstream, near-wall, pre-bursting "reference" value and the "end-of-turbulence" criterion failed. A detector using a threshold level based on local values might offer some promise for future investigation.

In summary, for all three detector functions (for $Y/\delta < 0.5$) the conditional sampling program was demonstrated to be a highly versatile and accurate procedure for detecting turbulent periods in transitional boundary layer flow.

V. EXPERIMENTAL RESULTS

1. STREAMWISE DISTRIBUTION OF INTERMITTENCY

The "universal" distribution of Dhawan and Narasimha (Ref. 25) is widely accepted as an accurate description of the development of near-wall intermittency in zero pressure gradient transitional boundary layers.

$$\gamma = 1 - \exp\left[- 0.412\ \xi^2\right] \tag{8}$$

$$\xi = \left(X - X_t\right) \lambda \tag{9}$$

$$\lambda = X\ (\gamma = 0.75) - X\ (\gamma = 0.25) \tag{10}$$

For experimentally measured intermittency distributions the beginning of transition, X_t, is most accurately determined, as per Narasimha (Ref. 26), by plotting

$$F(\gamma) = [- \ln(1 - \gamma)]^{1/2} \tag{11}$$

against streamwise location and finding the X ($\gamma = 0$) intercept. As discussed in Reference 26, in this format zero pressure gradient intermittency distribution data fall on a single straight line.

The distribution of the near-wall intermittency measured for the four test cases of the present program are presented in Figure 26. These near-wall intermittency values represent a local average of the values inferred from the uv, uw, and u detectors as described in CONDITIONAL SAMPLING TECHNIQUES. Because these independent measurements consistently agreed with each other within about ± 2% for $Y/\delta < 0.5$, their average is thought to be a highly reliable measure of the near-wall value. Figure 26 reveals that for cases K.20C1, K.20G2 and K.75G2 there was a distinct "kink" in the intermittency distributions. This same two-stage behavior for transition in favorable pressure gradients was recently reported by Narasimha (Ref. 27) where the break in the intermittency distributions was referred to as a "subtransition". Note that there was no evidence of a "subtransition" for the K.75G3 case, probably a result of the extremely high disturbance level of that test.

The intermittency data of the present study are plotted in the "universal" coordinates in Figure 27. The data are plotted in two ways; (1) the origin (X_t) was taken as the x intercept of the data (open symbols) and (2) X_t was determined by extrapolating the intermittency data for X > "subtransition" to $F(\gamma) = 0$ (solid symbols). Neither method resulted in agreement with the "universal" zero pressure gradient distribution over the entire length of transition. By using the X_t determined from extrapolation (solid symbols), however, all the data beyond the subtransition fell on the universal curve (including the K.75G3 data which had no subtransition point). The extrapolation procedure failed for the K.20G2 case because the subtransition occurred beyond $\gamma = 0.25$, the lower limit in the definition of λ. The results presented in Figures 26 and 27 as well as data of Reference 27 indicate that it is possible for acceleration to substantially inhibit the development of the intermittency until some critical stage (the "subtransition") is reached. Following the "subtransition" point the intermittency distribution appears to follow the same universal scaling low observed for zero pressure gradient transitions.

2. BOUNDARY LAYER TURBULENCE PROFILES

Boundary layer mean and fluctuating velocity profile data were obtained at approximately seven streamwise locations for each of the four experimental test cases. Single-horizontal hot wire (u component only) data were obtained at all upstream stations where the test boundary layer had not grown to sufficient thickness to permit the use of x-wire probes. For the downstream 4 stations of each test both single-wire and vertical and horizontal x-wire (u, v, and w components) data were recorded. As an example, the profile data obtained for one of the test cases ($K = 0.75 \times 10^{-6}$, GRID #2, K.75G2) are presented in Figures 28A through 28K and will be discussed here. The profile data for all four test cases are provided in both plotted and tabulated form in Appendix A.

The figures presented in this section and in Appendix A were all generated using a computer based plotting system (GOLDEN GRAPHER). For consistency, all of these figure formats (sizes, scales, labels, symbols, etc.) were kept the same for the entire data set. For each of the downstream locations 10 small plots, five per figure, of various fluctuating quantities are presented. Since only a few quantities were measured for the upstream profiles, the locations on the figures assigned for the remaining plots appear as blank areas on the page.

The profile data (u component only) obtained at the most upstream station, X = 8.8 inches, are given in Figure 28A. At this station there were no turbulent bursts detected and only the mean velocity and long term ("COMPOSITE") average U/U_E are presented. Even though there were no periods when the turbulence criterion was satisfied the turbulence intensity (u'/U_E) reached nearly 7% at about $Y/\delta = 0.3$. This location for the maximum amplitude of fluctuations is in excellent agreement with the maximum-amplitude locations found from both theoretical predictions and experimental data for low-amplitude, Tollmien-Schlichting disturbances in zero pressure gradient boundary layers (Ref. 28). This in spite of the fact that this test profile was highly subcritical. For the profile of Figure 28A $Re_\Theta \cong 230$ while the critical Reynolds number for linear disturbance amplification for this acceleration level (Ref. 28) was $Re_\Theta \cong 1580$.

In addition to the composite turbulence intensity distribution, Figure 28A also presents the long-term ("composite") mean velocity distribution. For reasons related to the clarity of presentation of the downstream profiles only straight-line segments connecting measured data (no data symbols) for $U/U_E >$ 0.6 are plotted. These hot wire mean velocity profile data were in excellent agreement with similar profile data measured with a miniature Pitot probe as part of Reference 16.

The results for the next streamwise station, X = 12.8 inches, are given in Figure 28B where, again, there were no turbulent periods detected. The maximum boundary layer turbulence intensity had grown to about 8% and was, as with Figure 28A, located at about $Y/\delta = 0.3$. Note that the local freestream turbulence intensity above the station is given for each figure and that T_E fell from 2.0 to 1.9% between the first two stations.

For the next station (X = 16.8 inches, Figure 28C) the conditional sampling procedure determined that the criteria for turbulence were met for a small fraction (about 2%) of the time. Three additional plots are presented for Figure 28C (1) the intermittency (γ) vs Y/δ, (2) the inter-turbulent-zone intensity vs Y/δ and (3) the turbulent-zone intensity versus Y/δ. The turbulent and inter-turbulent-zone plots present conditional (zonal) averages of the quantities during and between turbulent periods. The term inter-turbulent was chosen instead of laminar because of the highly disturbed character of the flow between turbulent bursts. For the test cases with high freestream turbulence there were large-amplitude, relatively low-frequency fluctuations between the relatively high-frequency turbulent fluctuations. For example see the time displays of Figure 20.

For Figure 28C, the turbulence intensity during the turbulent periods is greater in magnitude and peaks much closer to the wall than the composite profile. The composite and inter-turbulent profiles, meanwhile show an increase (from 8 to 9%) in peak intensity from the previous station. The intermittency profile indicated that this quantity was practically constant across the boundary layer at about 2%. Two additional data fairing lines, the turbulent and inter-turbulent zone average velocity ratios, can also be seen in the Mean Velocity plot. All three mean velocity ratios are plotted against Y/δ where δ is the long-term mean boundary layer thickness. As will be demonstrated later in this report, the turbulent periods correspond to regions of greatly increased boundary layer thickness. Since the boundary layer thickness during the turbulent period is much greater than the long-term boundary layer thickness the turbulent-zone mean velocity decreases relative to the composite average. Since the intermittency was so low for this case the composite and inter-turbulent average were practically identical.

Figures 28D and E present the first full set of profile data including results from both single-wire and x-wire probes. The Intermittency distribution plot of Figure 28D indicate that all three conditional detectors indicated that $\gamma \approx 0.08$ across most of the boundary layer. Sample velocity data records for this profile at $Y/\delta = 0.286$ can be seen in Figure 19.

The mean velocity and streamwise component turbulence intensity results for Figure 28D were very similar to those of the previous station. The normal and transverse profiles indicate that at this early stage of transition the turbulence is highly anisotropic with a particularly small v' component. Five additional plots must be introduced for Figure 28E. The Shear Stress and Turbulence Kinetic Energy plots display the distribution of the conditional and composite averaged values of those quantities across the boundary layer. The Structural Coefficient plots display the distributions of the direct and Reynolds shear stresses divided by the local turbulence kinetic energy.

$$a = \overline{u'u'} \;/\; \overline{q^2} \tag{12}$$

$$b = \overline{v'v'} \;/\; \overline{q^2} \tag{13}$$

$$c = \overline{w'w'} \;/\; \overline{q^2} \tag{14}$$

$$d = -\,\overline{u'v'} \;/\; \overline{q^2} \tag{15}$$

$$\text{where } \overline{q^2} = \overline{u'u'} + \overline{v'v'} + \overline{w'w'} \tag{16}$$

Figures 28F/G, 28H/I and 28J/K present a similar set of 10 plots for X = 28.8, 36.8, and 48.8 inches. Examination of these figures reveals that with increasing X the boundary layer turbulence structure progressively approached that expected for equilibrium turbulent flow. The various intermittency detector were generally in very good agreement for $Y/\delta < 0.5$. As previously discussed the uv and uw detector functions performed poorly in the outer portion of the boundary layers.

Similar sets of turbulence profile data were obtained for the remaining three test combinations of acceleration level and turbulence intensity (see APPENDIX A). In an attempt to reach general conclusions about the development of the turbulence through transition the four structural coefficients measured for all of the test cases were combined in Figure 29. In this figure the structural coefficients are plotted as a function of the local intermittency at that particular station. The individual coefficients are normalized by the value measured for a fully turbulent equilibrium boundary layer at the same freestream turbulence intensity in the study of Ref. 29. Each figure includes the normalized coefficients based on both the composite and turbulent-zone conditional averages. Although considerable scatter is evident when the data are plotted in this format it is possible to draw three conclusions from the trends. (1) For all four plots the present data indicate that the structural coefficents approached the equilibrium turbulent boundary layer values (Ref. 29) as the intermittency reached 100 percent. (2) The turbulent-zone conditionally averaged structural coefficients showed much less variation with intermittency than did the composite values. In fact the turbulent-zone conditionally averaged direct stress coefficients (a, b, and c) were nearly equal to the fully turbulent values for all intermittencies. (3) The trends of coefficients a and b reveal the extreme anisotropy of the turbulence, especially in the early stages of transition. Commonly used equilibrium values for a and b are 0.5 and 0.2 respectively giving a ratio a/b = 2.5. The present data indicate that at the early stages of turbulent bursting this ratio was approximately 13.

3. CONDITIONALLY AVERAGED MEAN VELOCITY PROFILES

Momentum and displacement integral thicknesses were computed for each of the conditionally averaged mean velocity profiles. For each intermittent profile integral thicknesses were determined for the turbulent zone, the inter-turbulent zone and the composite average. It was observed that the inter-turbulent profiles were laminar-like with shape factors ($H = \delta^*/\theta$) generally equal to 2.0 or greater. Because of their laminar-like shapes skin friction coefficients were computed for these inter-turbulent zone profiles using the molecular viscosity and the near-wall normal velocity derivative. It was also observed that the turbulent zone profiles were turbulent-like with shape factors equal to about 1.5. When plotted in the universal turbulent coordinates, U + versus Y +, these turbulent zone profiles could be well represented by the turbulent law-of-the-wall. Skin friction coefficients for these turbulent zone profiles were determined by a least-squares best fit to the standard log-wall relationship

$$\frac{U}{U_\tau} = \frac{1}{0.41} \ln \frac{YU_\tau}{\nu} + 5.0 \qquad (17)$$

The conditionally averaged mean velocity profile results for the four test cases are presented in Figures 30 through 33. For each figure the shape factor δ^*/Θ, momentum thickness, Θ, Reynolds number based on Θ and skin friction coefficient distributions are plotted as a function of streamwise distance along the test plate. The turbulent-zone, inter-turbulent-zone and composite values are given for each plot. The composite skin friction coefficients were computed by weighting the turbulent and inter-turbulent contributions according to the local intermittency.

$$C_{f_{comp}} = \gamma C_{f_{turb}} + (1-\gamma)\, C_{f_{inter-turb}} \qquad (18)$$

The solid symbols downstream of the present transitional results indicate data obtained for these same test conditions using miniature Pitot tubes (Ref. 16). These transitional mean profile data will be compared with predictions from boundary layer computation procedures in a later section of this report.

4. ENSEMBLE AVERAGED TURBULENT-ZONE PROFILES

Ensemble averaging techniques were employed to examine the variation of the mean streamwise velocity profiles through the turbulent periods of the flow. An ensemble averaging data reduction program was constructed to uniquely identify each individual turbulent period and determine the time interval between its beginning and end. The "start" of a turbulent period (as determined by the $\left(\frac{\partial u}{\partial t}\right)^2$ burst detector) is defined as $t = 0$ for these ensemble computations while the time period from beginning to end is designated as $\Delta\tau$.

For each detected turbulent period the velocity versus time record was broken into intervals of $\frac{\Delta\tau}{10}$ with an average velocity computed for each interval. For each burst interval-averaged velocities were computed for five intervals prior to t = 0, ten intervals during the turbulent period and, finally, for five intervals following $t = \Delta\tau$. The velocities at each particular fraction of a turbulent period averaged over all the turbulent periods constituted the ensemble-averaged local velocity. These ensemble-averaged velocities were constructed from the individual velocity versus time record (5 seconds long) representing the instantaneous velocity at a fixed location from the wall. The ensemble routine computed the ensemble-averaged mean velocity variation through the turbulent periods for that particular distance from the wall.

A single probe at a fixed location in a transitional boundary layer detects a wide range of turbulent period lengths ($\Delta\tau$'s). These differing periods can correspond to the passage of turbulent patches of different size or to random transverse locations of the patches relative to the probe (the edge of a large patch clipping the probe appears as a short turbulent period). During the examination of these ensemble averaged distributions it was observed that the results were much more coherent if only the burst lengths within about the middle 60% of the length distribution were included in the ensembles. The very short and very long, about the extreme 20% of each end of the distribution, turbulent periods were excluded from the computations. For most of the results presented here about 50 to 100 turbulent periods were included in each ensemble distribution.

In order to reveal the presence or lack of general trends in these results, turbulent-zone mean velocity profile variations were examined for four distinctly different test conditions. These four particular cases were selected based upon two criteria: (1) each case corresponded to a different one of the four acceleration/turbulence test combinations and (2) each case corresponded to a different intermittency level. The ensemble-averaged velocity distributions for these four cases are presented in Figures 34 through 37. The following Table lists the test conditions, locations and intermittencies for these figures.

FIG NO	K $\times 10^6$	X inches	T_E %	γ (near wall)
34	0.75	4.8	4.7	0.12
35	0.20	16.8	1.7	0.78
36	0.75	28.8	1.4	0.31
37	0.20	44.8	0.74	0.68

There are a number of features common to these four figures. The ordinate for Figures 34 through 37 is the time-interval ensemble-averaged velocity (< U >) normalized by the freestream mean velocity. For each profile, velocity histories are given for 20 normal locations ranging from about $Y/\delta = 0.05$ to about $Y/\delta = .85$. The ensemble-averaged velocities are plotted as a function of turbulent period fraction ($t/\Delta\tau$). Zero corresponds to the "start" time of the detector function. It is important to point out that these ensemble-averaged plots are based on locally determined timing of the turbulent periods. The beginning and end of turbulent periods was determined at that specific distance from the wall. This technique does not consider the shape of the leading and trailing faces of the turbulent patches in that all the $t = 0$ and $t = \Delta\tau$ events were plotted as if they were simultaneous.

The most distinct feature of Figures 34 through 37 is the sharp increase in velocity near the wall at $t = 0$ followed by a fall to about the upstream value. The velocity histories for the outer portion of the boundary layers indicates a significant deceleration at the arrival of the turbulent patch followed by a gradual return to the inter-turbulent velocity. Discussion of the individual cases follows.

The velocity-history plots of Figure 34 are for a case with a very high freestream turbulence intensity ($T_E = 4.7\%$) and a very low near-wall intermittency level ($\gamma = 0.12$). The ensemble-averaged velocity histories of Figure 34, then, portray very small, young turbulent patches in a very highly disturbed environment. This case evidenced the lowest degree of "organization" of the four cases studied. Note that the upstream ($t < 0$) and downstream ($t > \Delta\tau$) velocities do not agree well for all normal locations. The apparent "disorganization" of the flow of Figure 34 probably indicates that the individual turbulent patches were still developing at this near-onset location.

Figure 35 presents a case with moderate (T_E = 1.7%) freestream turbulence and high intermittency (γ = 0.78). The individual velocity histories are much smoother and more correlated for Figure 35 than for Figure 34 indicating that there was a greater burst-to-burst consistency. The upstream ($t < 0$) and downstream ($t > \Delta\tau$) velocities are not constant for Figure 35, a consequence of the high intermittency. At this late stage of transition the inter-turbulent intervals were small compared to $\Delta\tau$ (see Figs. 17 and 21). By including samples $\pm \frac{\Delta\tau}{2}$ upstream and downstream of the edges of the turbulent periods, random samples from neighboring turbulent patches have been lumped into the inter-turbulent ensembles.

Figure 36 presents results quite similar to those of Figure 35. In this case, however, the intermittency level was much lower (γ = 0.31) and the upstream and downstream velocities are both constant and in near agreement.

Finally, a case with very low freestream turbulence (T_E = 0.74%) is given in Figure 37. Again, because of the high intermittency (γ = 0.68), "leakage" from neighboring turbulent patches has contaminated the upstream and downstream ensembles. The velocity histories of Figure 37 were cross-plotted into "instantaneous" ensemble-averaged profiles for Figure 38. The ensemble-averaged ratios are plotted against $Y/\bar{\delta}$ where $\bar{\delta}$ is the long-term average of the boundary layer thickness. The relative time (in burst-length fraction, $t/\Delta\tau$) for each profile is given near the boundary layer edge. Note the enormous increase in boundary layer thickness and change in profile shape as the turbulent patch passes by. Selected profiles from Figure 38 are presented in Figure 39 in the universal turbulent profile coordinates. The upstream and downstream profiles ($t/\Delta\tau$ = - 0.3 and 1.3) are seen to be in excellent agreement with each other and to exhibit a standard laminar shape. At $t = 0$ $U+ > Y+$ for a few of the near wall points hinting of a possible instantaneous adverse pressure gradient. By $t/\Delta\tau = 0.1$ the profile begins to appear transitional and by the midpoint ($t/\Delta\tau = 0.5$) it agrees very well with the fully turbulent law-of-the-wall. The variation of selected profile quantities for the "instantaneous" ensemble-averaged profiles are plotted in Figure 40. Figure 40 presents the overall boundary layer thickness, δ, the momentum thickness, θ, the shape factor, δ^*/θ and, finally the skin friction coefficient. As indicated in the skin friction plot these instantaneous skin friction values were computed from the laminar viscosity for the inter-turbulent profiles, from the law-of-the-wall for the turbulent profiles and by a simple numerical average of the two for the others. The results presented in Figure 40 reveal the extreme discrepancies between the inter-turbulent flow and that in the turbulent patches. A turbulent patch appears to be typically 3 times thicker than the surrounding inter-turbulent boundary layer with a momentum thickness nearly twice as large as the interturbulent value. The shape factor is seen to plunge from about 2.3 to about 1.6 and then return to the upstream value. The skin friction is nearly 5 times greater at midpoint in the turbulent patch than computed for the inter-turbulent profile. Note that these "instantaneous" ensemble-averaged profile results are in very good agreement with the average conditional results (T-turbulent, IT-inter-turbulent, C-composite) marked on the plots.

5. SPECTRAL DISTRIBUTIONS

A Fast-Fourier-Transform (FFT) routine contained in the Cranfield Data Systems package was employed to compute the spectral distribution of individual velocity-time data records. The previously described conditional sampling program was configured such that spectral distributions could be computed for the total (composite) data sample or for just the turbulent or inter-turbulent portions of the record. The individual inter-turbulent and turbulent periods were arranged end-to-end to form constructed continuous records. Although this procedure does not compromise resolution of the high-frequency portions (upper limit = sampling rate/2) of the spectrum it does restrict the lower frequency limit. Only for the continuous records (composite) can it be assured that the lowest frequency resolved is equal to the reciprocal of the total sample length. Since all sampling for this program was conducted at 7813 Hz/channel the upper limit of frequency resolution for all cases was 3906 Hz.

In order to demonstrate the performance of the spectral analysis system used here the power-spectral-density (PSD) distribution computed for a post-transitional (fully turbulent) boundary layer is given in Figure 41. This figure gives the PSD for the streamwise fluctuation recorded near the wall at a station downstream of transition ($\gamma = 1.00$) for one of the test configurations. For this figure the spectral distribution is plotted in non-dimensional, turbulent boundary layer co-ordinates as suggested by Bradshaw (Ref. 30). The agreement between the present data and the results of Reference 30 are seen to be excellent.

The primary objective of the present spectral measurements was to obtain information about the nature of the disturbance distribution in transitional boundary layers. In order to achieve this, spectral distribution measurements were obtained for boundary layers at various levels of intermittency as well as for upstream pre-transitional profiles in which no turbulent periods were detected. These present transitional boundary layer spectral distribution data provide an opportunity to compare the predictions of linear stability/amplification theory with experimental measurements. It should be pointed out, however, that the experimental test cases studied for this program all involved relatively high levels of freestream turbulence with accelerating flow. In contrast, linear small-disturbance amplification theory and experiments (Refs. 31 and 32) have focused primarily in single frequency disturbances to boundary layers with very low freestrean turbulence. These present spectral data/linear theory comparisons are particularly interesting because the present test cases fall into the important category of "bypass mode" transition (Ref. 33).

Figures 42 through 49 present spectral distributions measured at successively increasing streamwise locations through the transition process for the test configuration $K = 0.2 \times 10^{-6}$, Grid No. 1. For these figures the spectral distributions are presented in dimensional coordinates since the appropriate length scale is unclear. Figure 42 presents the spectral data for the most upstream profile (X = 12.8 in) at which no turbulent periods were detected. At this station the momentum thickness Reynolds number, Re_{θ}, was 360, far below the critical ($Re_{\theta} = 680$) thickness for this acceleration level (Ref. 34). All frequencies are stable at this Re_{θ} for sufficiently small disturbances. Spectral distributions obtained at four distances from the wall are given in Figure 42. The freestream spectrum, given here for reference, is in excellent agreement with the distribution measured previously by Sato for this turbulence generating grid Reynolds number (Ref. 35). The three spectra measured in the profile show a much faster roll-off with increasing wavenumber than expected for developed turbulence. There was a ratio of nearly 6 orders of magnitude between the low and high-frequency contributions to the spectra at both $Y/\delta = 0.14$ and 0.18. These results indicate that deep in the boundary layer the spectra are radically different from the broadband, developed free-stream distribution (the driving disturbance). There is no evidence of narrowband disturbance frequency preference at this profile. Note that at the two locations closest to the wall a spike corresponding to the tunnel blower blade-passing-frequency can be discerned (BPF). This spike is almost certainly an acoustic wave and not a velocity fluctuation.

Spectral distributions for the next station downstream (X = 16.8 in) are given in Figure 43. Again the freestream spectrum is included for reference. The near-wall spectrum has changed radically from the previous station with four bands of highly amplified disturbances. The band labled F1 corresponds to the most-unstable frequency predicted by linear theory for this acceleration level (Ref. 28). The 2nd, 3rd, and 4th harmonics of F1 also match the observed amplified bands. This agreement is rather remarkable in that the boundary layer is still highly sub-critical. The observed amplified frequencies corresponded to the predicted critical frequencies for this large-amplitude disturbance level even though the linear theory would predict that Re_θ was subcritical for all wavenumbers. Note that the BPF acoustic wave is still discernable.

At the next station (X = 20.8 in, Fig. 44) the near-wall disturbances have become both more powerful and broadband. There is still some meager evidence of preferred amplification for F1 and 2F1. Note that at this station some turbulent periods were detected with $\gamma = 0.002$. The same trend continued for Figure 45 with a steadily increasing contribution from the higher wave-numbers to the near-wall spectrum. At this station $\gamma = 0.013$.

The format for the next four figures (46 through 49) differs from that of Figures 42 through 45. For these four downstream stations the spectra from only a single normal location ($Y/\delta = 0.10$) are given for each streamwise station. For these downstream stations the intermittency level was high enough so that adequate conditionally sampled turbulent spectra could be computed. For these four profiles, then, spectra are given for the composite record and for the inter-turbulent and turbulent portions of the record. The axes coordinates are subscripted with i corresponding to either the composite, inter-turbulent, or turbulent value. The conditionally sampled spectra show the distributions of the fluctuations within that particular zone. The turbulent spectra for all four streamwise locations appear to indicate fully developed turbulence. For example, the turbulent spectral distribution is seen to agree well with a -5/3 slope for Figure 48. The inter-turbulent spectra change dramatically with increasing streamwise location. At X = 28.8 in. (Fig. 46) there is a ratio of about 5 orders of magnitude between the low and high frequency contributions. By X = 52.8 in. (Fig. 49) the relative power of the high frequency content has greatly increased so that this ratio has dropped to about 3 orders of magnitude. None of the composite, inter-turbulent or turbulent spectra show any evidence of narrow-band preferred amplification.

The final two spectral distributions presented here were obtained for the test case K = 0.75 x 10^{-6}, GRID No. 2. Figure 50 shows distributions obtained at an upstream station (X = 8.8 in.) where there were no detected turbulent periods. As with Figure 42 the near-wall spectrum contained very little contribution from the high-frequency fluctuations. Again the BPF acoustic wave stand out clearly. At X = 12.8 in. (Fig. 51) the near-wall spectrum contains much more power in the high frequency range with some evidence of selective amplification. The most-unstable frequency for the acceleration associated with the data of Figure 51 (F1) appears to roughly coincide with one of the preferred bandwidths.

VI. ASSESSMENT OF ANALYTICAL PREDICTIONS OF TRANSITION

Numerical experiments were undertaken to assess the ability of current methods for predicting heat transfer during transition in accelerating flows with various levels of freestream turbulence. The analytical predictions were made using the UTRC ABLE boundary layer code developed by Edwards et al. (Ref. 34). These predictions are compared with the experimental data base obtained by Blair (Ref. 16) for two different rates of acceleration and several different freestream turbulence levels. Analytical predictions of transition use essentially three different methods. The first and earliest (Refs. 13, 25, 35, 36, 37, and 38) use empirical correlations for the start and end of transition usually using Reynolds number Re_θ based on boundary layer momentum thickness and then some intermittency distribution to produce a smooth transition from laminar to turbulent flow. Of these methods, only the first two predict both the beginning and end of transition. The others predict only the start of transition (Ref. 36), the end of transition (Ref. 37), or the intermittency (Refs. 25 and 38).

These empirical correlations generally suffer from difficulty in application and interpretation in flows which have varying freestream conditions (i.e., flow history). Indeed the transition from laminar to turbulent flow will depend on flow history and thus these methods will always have this problem. In view of this, a second method has been developed which depends on the solution of a differential equation (usually the turbulence kinetic energy equation). The most successful of these was developed by McDonald and Fish (Ref. 10) and improvements were later made by McDonald and Kreskovsky (Ref. 39). This method attacks the problem of transition on a more fundamental level and hence presumably is applicable to a wider range of problems if the turbulence has been properly modeled. However, these methods require a deeper understanding of the structure of turbulence during and after transition and considerably more data to evaluate empirical constants. These methods, however, have an advantage over methods based on empirical correlations because there is less ambiguity in application to flows with a varying flow history (i.e., varying freestream conditions — pressure gradient and freestream turbulence and varying wall conditions — wall temperature or heat flux).

With the development of the two equation models of turbulence (Refs. 40 and 41) came the possibility of predicting transition directly (Refs. 42-47), since these models solve partial differential equations for the turbulence properties. Of these methods, References 45 and 48 appear the best documented and appear to predict many of the qualitative and quantitative features of transition in both constant and accelerating freestream flows. An attractive feature of these methods is that since the history of turbulence is modeled, transition is allowed to take place in a more natural manner. The accuracy of such predictions for general flow situations depends very much on the universality of the empirical coefficients used in the various models. Thus, although it is quite possible to make ad hoc adjustments to these empirical constants so that transition can be predicted for a limited number of cases, it is not clear that such ad hoc changes represent a phenomenological modeling of the turbulent processes, particularly when nominal constants are permitted to change. The only true procedure for verifying these constants is to obtain detailed experimental data of the turbulent parameters so that all empirical constants can be phenomenologically modeled. At a minimum, this would require measurements of dissipation, a difficult but not impossible task so that both dependent variables in the $\kappa - \varepsilon$ model are known experimentally. Thus, the third method for predicting transition requires an even deeper understanding of the structure of turbulence during and after transition and even more experimental data to evaluate empirical constants.

The following study concentrates on only the first two methods and will be limited to the empirical method of AbuGannom and Shaw (Ref. 35) (AGS) and the modified one equation method of McDonald and Kreskovsky (Ref. 39) (MFK). The (AGS) method is primarily a method for predicting the intermittency distribution. Since this report presents measurements of intermittency γ during transition, a more detailed evaluation of this method can be made than was previously possible. The (MKF) method is primarily a method for predicting a mixing length scale ℓ_∞ during transition. The primary empirical factors are the structual coefficients a, b, d (especially d) which vary during transition. Again this report presents measurements of these structural coefficients and a more detailed evaluation of this method is possible. A proper evaluation of a two equation $\kappa - \varepsilon$ model of turbulence for predicting transition requires at a minimum the measurement of dissipation ε. Unfortunately this data is not available at the present time and so this model will not be considered.

1. COMPARISON OF CALCULATIONS WITH EXPERIMENTAL DATA

The cases shown in the following figures, are all presented in the same manner. In addition to the prediction of the heat transfer during transition from laminar to turbulent flow, these figures also contain the prediction for completely laminar flow (i.e., no grid) as well as completely turbulent flow which has been tripped at the leading edge. In all cases it was found that the thermal history of the boundary layer (i.e., wall temperature history) was important. Therefore all cases were calculated using the measured wall temperature distribution. For the completely turbulent boundary layer case, measurements were not made of either heat transfer or wall temperature, therefore the wall temperature for the completely laminar flow (no grid) case was used. This latter calculation should be considered as a reference only. The test matrix of flow conditions to be examined is shown in Table 1. They consist of two different pressure gradients K = 0.20E-06 and K = 0.75E-06 where

$$K = \frac{\nu}{U^2}\frac{dU}{dX} \tag{19}$$

and four different turbulence levels (including no freestream turbulence). The nominal upstream turbulence levels are given on Table 1 for a position 12.0 in upstream of the leading edge where

$$Tu = \sqrt{\frac{\overline{u'u'}}{U_e^2}} \tag{20}$$

The matrix of test conditions calculated is shown on Table 2 showing the combinations of accelerations and freestream turbulence levels. The results are presented in terms of the variations of Stanton number (St_e) with X where

$$St_e = \frac{\dot{q}_w}{\rho U_e C_p (T_w - T_e)} \tag{21}$$

It is noted that wall is not heated for the first 2.19 in and therefore an adiabatic wall is assumed.

2. ABUGANNOM-SHAW PREDICTIONS

Figure 52 shows a comparison of the predictions using the (AGS) model with experimental data for both the weak and strong acceleration cases. For

Table 1: Matrix of Measured Flow Conditions

	Weak Acceleration K = 0.20E0 - 6	Strong Acceleration K = 0.75E - 06
No Grid	0.000	0.000
Grid 1	0.012	
Grid 2	0.026	0.027
Grid 3		0.066

Table 2: Matrix of Calculated Flow Conditions

	K = 0.20E - 06	K = 0.75E - 06
(AGS) AbuGannom-Shaw [3]	Grid 1 Grid 2 laminar turbulent	Grid 2 Grid 3 laminar turbulent
(MFK) Mcdonald-Kreskovsky [10]	Grid 1 Grid 2 laminar turbulent	Grid 2 Grid 3 laminar turbulent
(INP) Experimental Intermittency	Grid 1 Grid 2 laminar turbulent	Grid 2 Grid 3 laminar turbulent
(INA) Experimental Structural Coefs.	Grid 1 Grid 2 laminar turbulent	Grid 2 Grid 3 laminar turbulent

these cases, the Cebeci-Smith (Ref. 49) eddy viscosity turbulence model was used. Since the flow has varying freestream conditions, the following procedure was used to predict transition. Let Re_Θ be the local Reynolds number based on momentum thickness and let $Re_{\Theta s}$ be the predicted start of transition using theAbuGannom-Shaw transition model and local conditions. Transition was assumed to occur when $Re_\Theta = Re_{\Theta s}$. It can be seen from these figures, that the (AGS) transition model produces a fairly good prediction for the start of transition, but poorly predicts the end of transition. Clearly the intermittency distribution is not predicted well for these cases.

3. MCDONALD - FISH - KRESKOVSKY PREDICTIONS

Figure 53 shows a comparison of the predictions using the (MFK) model with experimental data for both the weak and strong acceleration cases. For these cases, the experimental freestream turbulence was also input. As can be seen from these comparisons, the (MFK) model does not predict the start of transition nor does the model fully capture the fully turbulent flow region. A comparison of the results for the weak acceleration Figure 53a with the results for the strong acceleration Figure 53b appear to indicate that this model overestimates the impact of acceleration. It should be noted that at the time that the model was developed, the structural coefficients a, b, d, given by equations 12, 13, and 15, and the dissipation length scale L_d given by,

$$L_d = (\overline{- u'u'})^{3/2}/\varepsilon \qquad (22)$$

were not known for transitional flow, and hence various assumptions were made to obtain them by comparison of mean flow predictions with experimental data.

4. CEBECI-SMITH PREDICTIONS WITH EXPERIMENTAL INTERMITTENCY

Since the intermittency distribution was measured for these cases, the flow field and heat transfer were recalculated using the measured intermittency distributions together with the Cebeci-Smith (Ref. 49) turbulence model. The results are shown on Figures 54 through 57 and the predictions for heat transfer, skin friction, and momentum thickness appear to be quite good. One may then conclude from these results that the use of the intermittency distribution is a valid method for providing a smooth transition from laminar to turbulent flow and that if one had good correlations for the beginning and end of transition quite good predictions could be made even though no provision is made in the Cebeci-Smith turbulence model for the effects for freestream turbulence.

5. MCDONALD-KRESKOVSKY PREDICTIONS WITH STRUCTURAL COEFFICIENTS

Empirical correlations for the structural coefficients a, b, d as a function of intermittency γ are given by;

$$a = 0.600\ [1.30 + (1.00 - 1.30)\gamma] \qquad (23)$$

$$b = 0.250\ [0.25 + (1.00 - 0.25)\gamma] \qquad (24)$$

$$d = 0.1215\gamma^{1/2} \qquad (25)$$

These correlations were programmed in the ABLE code and the cases rerun with the experimental intermittency distributions. The predictions for heat transfer are shown on Figure 57. These predictions show some improvement over the predictions using the (MFK) model alone and give encouragement to the basic concept. It should be noted that measurements of dissipation length L_d have not been made so that it is not possible to completely test the procedure. Since an improved model is desireable, it is strongly recommended that measurements of dissipation ε be made.

VII. CONCLUSIONS

A combined experimental and analytical program has been conducted to examine transitional, accelerating boundary layer flows with high levels of freestream turbulence. This program was designed to complement a parallel study conducted previously under AFOSR funding. The earlier program focused on measurement of transitional heat transfer distributions for four combinations of streamwise acceleration and freestream turbulence. The present program was designed to document the boundary layer turbulence structure for the same four test conditions. In addition spectral distribution data were obtained both within the test boundary layers and in the freestream flow. The measurements from the earlier program combined with the present results provide a comprehensive examination of accelerating transitional boundary layer flow. Analytical results include comparisions between these various measurements and a variety of numerical transitional boundary layer computation procedures. Specific conclusions reached from the experimental and analytical programs were as follows.

1. EXPERIMENTAL PROGRAM

1) Documentation of the flow conditions for each of the four test cases consisted of measurements of the streamwise freestream velocity (static pressure) distributions, all three components of the turbulence beyond the edge of the test boundary layers, distributions of the streamwise integral length scale, the spectral distribution of the freestream turbulence and, finally, the location and extent of the boundary layer transition zones.

Measurements of all these quantities were obtained for both the previous and present experiments (using different techniques and in differing detail). Agreement between the present and earlier data was excellent assuring that the present test conditions duplicated those of the earlier AFOSR contract.

2) The hot-wire conditional sampling routine developed as part of this study has been shown to be consistently capable of discriminating between turbulent and non-turbulent periods in transitional boundary layer flow. The discrimination routine proved to be reliable for a wide range of freestream turbulence intensities and intermittency levels. The conditional sampling routine made possible computation of zonal (turbulent or "inter-turbulent") mean and fluctuating boundary layer flow quantities and ensemble-averaged velocity distributions within and between the turbulent patches.

3) The streamwise distributions of near-wall intermittency measured for the various test cases indicate that there are two distinctly separate stages of the transition process for accelerating flow. These data indicate that it is possible for acceleration to substantially inhibit the development of intermittency until a critical point (the "subtransition") is reached. Following the "subtransition" point the intermittency distribution appears to follow the same universal scaling law observed for zero pressure gradient transitions. It appears that the feasibility of accurate computation of transitional boundary layer development could be significantly improved if a generalized procedure were available for the prediction of the location and extent of both stages of this two-step process.

4) Profiles of the conditionally sampled direct and Reynolds stresses across the test boundary layers were obtained at several streamwise stations

for all four flow conditions. At stations upstream of intermittent turbulent bursting the amplitude distribution of the streamwise fluctuations was very similar to that predicted by linear small-disturbance theory. The profiles obtained at locations with very low intermittency indicate that at this early stage of transition the turbulence is highly anisotropic with a particularly small v' component. The ratio between the streamwise and normal velocity fluctuations was over five times larger for these low intermittency flows than for equilibrium turbulent boundary layers. The turbulence components steadily approached the equilibirium turbulent boundary layer arrangement as the intermittency approached unity. Suggested functional relationships are given for the distributions of the turbulence structural coefficients through transition.

5) Momentum and displacement integral thicknesses and skin friction coefficients were computed for each of the conditionally sampled mean velocity profiles. It was observed that the turbulent zone profiles could be well represented by the fully-turbulent law-of-the-wall. It was also observed that the inter-turbulent zone profiles were laminar-like with shape factors equal to 2.0 or greater.

6) The passage of "typical" turbulent patches was examined by computing relative time (in burst-length fractions), ensemble-averaged "instantaneous" mean velocity profiles. In this format the inter-turbulent zone profiles were shown to exhibit the standard laminar shape while the mid-patch turbulent profiles agreed very well with the turbulent law-of-the-wall. These results revealed the extreme discrepancies between the inter-turbulent flow and that

in the turbulent patches. A turbulent patch appears to be typically three times thicker than the surrounding inter-turbulent boundary layer with a momentum thickness nearly twice as large as the inter-turbulent value. The skin friction is nearly five times greater at midpoint in the turbulent patch than computed for the inter-turbulent profile.

7) Spectral analysis of the fluctuations in a boundary layer upstream of the onset of intermittency have revealed a band of highly amplified disturbances near the most-unstable frequency predicted by linear theory. This result is rather remarkable in that the boundary layer at that location was highly subcritical. The result reveals the preferred amplification of selected strong (non-linear) disturbances and demonstrates at least one possible path of a "bypass" transition. Conditionally averaged spectral distributions indicate that the turbulent zone spectra are very similar to those of an equilibrium turbulent boundary layer for the entire length of transition. The inter-turbulent zone spectra, however, exhibit a much lower fraction of high frequency power for low intermittencies and only assume an equilibrium turbulent boundary layer distribution as the intermittency approaches unity.

2. ANALYTICAL PROGRAM

1) An assessment of the AbuGannom-Shaw (Ref. 35) empirical correlations for the prediction of transition in accelerating flows shows that this procedure predicts the onset of transition quite well but does not predict the length of transition.

2) An assessment of the McDonald-Kreskovsky (Ref. 39) one equation model for the prediction of transition in accelerating flows shows that this procedure does not predict the onset of transition nor does it fully capture the fully turbulent flow.

3) Use of the experimental intermittency distribution in place of empirical correlations produced very good predictions of transition. This result indicates that the modeling of transition using case-specific intermittency distributions is a valid concept and that better empirical correlations for the intermittency could produce accurate predictions of transition.

4) Use of experimental values in place of fully turbulent values for the structural coefficients in the McDonald-Kreskovsky (Ref. 39) one equation model produced better predictions for transition. This result indicates that better correlations for the structural coefficients and the dissipation length could perhaps produce better predictions.

VIII. LIST OF SYMBOLS

a,b,c,d	Turbulence structural coefficients (equations 12-15)
c_f	Skin friction coefficient
c_p	Specific heat at constant pressure
K	Acceleration parameter (equation 5)
H	Shape factor, δ^*/θ
L_d	Dissipation length scale (equation 22)
q^2	Turbulence kinetic energy (equation 16)
Re	Reynolds number
Re_θ	Reynolds number based on momentum thickness
t	Time from beginning of turbulent period
T	Turbulence intensity
T_w	Wall temperature
T_e	Freestream temperature
u,v,w	Instantaneous value of velocity components
u',v',w'	Fluctuating velocity components
U	Mean streamwise velocity
U^+	Dimensionless velocity, u/U_τ
U_τ	Friction velocity
$\langle U \rangle$	Ensemble averaged velocity
$u'^2(f)$	Velocity fluctuations (squared) per Hertz
X	Distance from leading edge
Y	Distance from wall

LIST OF SYMBOLS (Cont'd)

Y^{+}	Dimensionless distance, YU_{τ}/ν
γ	Intermittency
δ	Boundary layer thickness
δ^{*}	Displacement thickness
$\overline{\delta}$	Long-term average boundary layer thickness
$\Delta\tau$	Time interval from beginning to end of a turbulent period
Θ	Momentum thickness
Λ	Streamwise integral length scale
ν	Kinematic viscosity

Subscripts

E	Freestream
FT	Fully turbulent
U	Upstream

REFERENCES

1. Brown, A. and Martin, B. W.: A Review of the Basis of Predicting Heat Transfer to Gas Turbine Rotor Blades. ASME Paper 74-GT-27, 1974.

2. Han, L. S., Chait, A., Boyee, W. F. and Rapp, J. R.: Heat Transfer on Three Turbine Airfoils, AFWAL-TR-82-2124, Aero Propulsion Laboratory, Air Force Wright Aeronautical Laboratories, Air Force Systems Command, Wright-Patterson Air Force Base, Ohio 45433, January 1, 1982.

3. Hylton, L. D., Mihelc, M. B., Turner, E. R., Nealy, D. A. and York, R. E.: Analytical and Experimental Evaluation of the Heat Transfer Distribution Over the Surfaces of Turbine Vanes, NASA CR 168015, Final Report for Contract No. NAS3-22761, May, 1983.

4. Rae, W. J., Taulbee, D. B., Civinskas, K. C. and Dunn, M. G.: Turbine-Stage Heat Transfer: Comparison of Shock-Duration Measurements With State-of-the-Art Prediction, AIAA Paper No. AIAA-86-1465, submitted to the AIAA Journal of Propulsion and Power.

5. Morkovin, M. V.: Instability, Transition to Turbulence and Predictability, AGARDograph 236, July, 1978.

6. Mack, L.: Transition and Laminar Instability, JPL Publication 77-15, May 15, 1977, also appears as Chapter 3 of Application and Fundamentals of Turbulence, based on Short Course; University of Tennessee Space Institute, Tullahoma, TN, Plenum Press, 1977.

7. Reshotko, E.: Boundary Layer Stability and Transition, Annual Review of Fluid Mechanics, Vol. 8, 311-350, 1976.

8. Bennet, H. W.: An Experimental Study of Boundary Layer Transition, Kimberly-Clark Corp. Report, Neenah, WI (1953) - See Ref. I-26, pp. 37-38.

9. Dring, R. P., Joslyn, H. D., Hardin, L. W. and Wagner, J. H.: Turbine Rotor-Stator Interaction, ASME Journal of Engineering for Power, Vol. 104, pp. 729-742, October, 1972.

10. McDonald, H., Fish, R. W.: Practical Calculations of Transitional Boundary Layers. International Journal of Heat and Mass Transfer, Vol. 16, No. 9, pp. 1729-1744.

REFERENCES (Cont'd)

11. Harris, J. E.: Numerical Solution of the Equations for Compressible Laminar Transitional and Turbulent Boundary Layers and Comparisons with Experimental Data, NASA TR R-368, 1971.

12. Price, J. M. and Harris, J. E.: Computer Program for Solving Compressible Non-similar-Boundary-Layer Equations for Laminar, Transitional, or Turbulent Flows of a Perfect Gas, NASA TM X-2458, 1972.

13. Forest, A. E.: Engineering Predictions of Transitional Boundary Layers, Laminar-Turbulent Transition, AGARD-CP-224, Paper 22, 1977.

14. Blair, M. F., Bailey, D. A. and Schlinker, R. H.: Development of a Large Scale Wind Tunnel for the Simulation of Turbomachinery Airfoil Boundary Layer. ASME paper 81-GT-6 to be presented at ASME Gas Turbine Conference, March, 1981.

15. Baines, W. D. and Peterson, E. G.: An Investigation of Flow Through Screens. Trans. of ASME, Vol. 73, pp. 467-480, July, 1951.

16. Blair, M. F. and Werle, M. J.: Combined Influence of Free Stream Turbulence and Favorable Pressure Gradients on Boundary Layer Transition and Heat Transfer, UTRC Report R81-914388-17, AFOSR Contract No.F49620-78-C-0064.

17. Blair, M. F.: Influence of Free-Stream Turbulence on Boundary Layer Transition in Favorable Pressure Gradients, ASME Paper No. 82-GT-5, and Journal of Engineering for Power, October, 1982, Vol. 102, pp. 743-750.

18. Caspar, J. R., Hobbs, D. E. and Davis, R. L.: Calculation of Two-Dimensional Potential Cascade Flow Using Finite Area Methods. AIAA Journal, Vol. 18, No. 1, January, 1980.

19. Blair, M. F. and Bennett, J. C.: Hot-Wire Measurements of Velocity and Temperature Fluctuations in a Heated Turbulent Boundary Layer, J. Physics E: Sci. Instruments 20 (1987), pp. 209-216.

20. Champagne, F. H., SLeicher, C. A. and Wehrmann, O. H.: Turbulence Measurements with Inclined Hot-Wires Part I - Heat Transfer Experiments with Inclined Hot-Wires, Part II Hot-Wire Response Equations, JFM, Vol. 28, 1967, pp. 153-182.

21. Tan-atichat, J., Nagib, H. M. and Drubka, R. E.: Effects of Axisymmetric Contractions on Turbulence of Various Scales. NASA CR 165136, September, 1980.

REFERENCES (Cont'd)

22. Antonia, R. A.: Conditionally Sampled Measurements Near the Outer Edge of a Turbulent Boundary Layer. JFM, 1972, Vol. 56, pp. 1-18.

23. Hedley, T. B. and Keffer, J. F.: Turbulent/non-Turbulent Decisions in an Intermittent Flow. JFM, 1974, Vol. 64, pp. 625-644.

24. Blackwelder, R. F. and Kaplan, R. E.: On the Wall Structure of the Turbulent Boundary Layer. JFM, 1976, Vol. 76, pp. 89-112.

25. Dhawan, S. and Narasimha, R.: Some Properties of Boundary Layer Flow During Transition From Laminar to Turbulent Motion, JFM, 3, 1958, pp. 418-436.

26. Narasimha, R.: The Laminar-Turbulent Transition Zone in The Boundary Layer, Prog. Aero. Sci., Vol. 22, 1985, pp. 29-80.

27. Narasimha, R.: Subtransitions in the Transition Zone, Proc. 2nd IUTAM Symb. Laminar-Turbulent Transition. Novosibirsk, July, 1984, pp. 141-151.

28. Schlichting, H.: Boundary Layer Theory, 6th Ed., McGraw-Hill Co., Inc., New York, 1978, pp. 460-461 and 470-471.

29. Blair, M. F. and Edwards, D. E.: The Effects of Freestream Turbulence on the Turbulence Structure and Heat Transfer in Zero Pressure Gradient Boundary Layers, UTRC Report R82-915634-2, November, 1982.

30. Bradshaw, P.: The Turbulence Structure of Equilibrium Boundary Layers. JFM, Vol. 29, part 4, 1967, pp. 625-645.

31. Schubauer, G. B. and Skramstad, H. K.: Laminar Boundary-Layer Oscillations and Transition on a Flat Plate, N.A.C.A. Report No. 909 (1948).

32. Rosenhead, L.: Laminar Boundary Layers, Oxford at the Clarendon Press, 1963, p. 542.

33. Hinze, J.: Turbulence, Second Edition, McGraw-Hill, Inc., New York, 1975, p. 251.

34. Edwards, D. E., J. E. Carter and M. J. Werle: Analysis of Boundary Layer Equations Including a New Composite Coordinate Transformation, UTRC Report No. UTRC81-30, May, 1982.

REFERENCES (Cont'd)

35. AbuGannom, B. J. and Shaw, R.: Natural Transition of Boundary Layers - The Effect of Turbulence, Pressure Gradient, and Flow History, Journal of Mechanical Engineering Science, Vol. 22, No. 5, 1980.

36. Dunham, J.: Prediction of Boundary Layer Transition in Turbomachinery Blades, Tech. Paper I-3, AGARD-AG0164, December, 1972.

37. Hall, D. J. and Gibbings, J. C.: Influence of Free Stream Turbulence and Pressure Gradient upon Boundary Layer Transition, Journal of Mechanical Engineering Sciences, Vol. 14, pp. 134-146, 1972. NACA TR 1289, 1956.

38. Schubauer, G. B. and P. S. Klebanoff: Contributions on the Mechanics of Boundary Layer Transition.

39. McDonald, H. and Kreskovsky, J. P.: Effects of Free Stream Turbulence on the Turbulent Boundary Layer, International Journal of Heat and Mass Transfer, Vol. 17, pp. 705-716, 1974.

40. Launder, B. E., Pridden, C. H. and Sharma, B. I.: The Calculations of Turbulent Boundary Layers on Spinning and Curved Surfaces, Trans. ASME J. Fluids Eng., March, 1977, p. 231.

41. Jones, W. P. and Launder, B. E.: The Prediction of Laminarization With a Two Equation Model of Turbulence, Int. J. Heat and Mass Transfer, Vol. 15, 1972, p. 301.

42. Wang, J. H., Jen, H. F. and Hartel, E. O.: Airfoil Heat Transfer Calculation Using a Low Reynolds Number Version of a Two Equation Turbulence, Model, Trans. ASME Journal of Engineering for Gas Turbines and Power, Vol. 107, pp. 60-67, January, 1985.

43. Lam, C. K. G., and Bremhorst, K.: A Modified Form of the κ-ε Model for Predicting Wall Turbulence, J. Fluids Engineering, Vol. 103, Sept. 1981, pp. 456-460.

44. Schmidt, R. C., and Patankar, S. V.: Development of Low Reynolds Number Two Equation Turbulence Models for Predicting Heat Transfer on Turbine Blades, Proceedings of the 1986 Turbine Engine Hot Section Technology Conference, NASA Lewis Research Center, NASA Conference Proceedings Publication 2444, Oct. 1986, pp. 219-239.

REFERENCES (Cont'd)

45. Schmidt, R. C. and Patankar, S. V.: Prediction of Transition on a Flat Plate Under the Influence of Free Stream Turbulence Using Low Reynolds Number Two-Equation Turbulence Models, ASME Paper 87-HT-32, 1987.

46. Rodi, W. and Scheuerer, G.: Calculation of Heat Transfer to Convection-Cooled Gas Turbine Blades, J. of Engineering for Gas Turbines and Power, Vol. 107, July 1985, pp. 620-627.

47. Rodi, W. and Scheuerer, G.: Calculation of Laminar-Turbulent Boundary Layer Transition on Turbine Blades, AGARD-CPP-390.

48. Patankar, S. V. and Smith, R. C.: A Low-Reynolds-Number Two-Equation Turbulence Model for Predicting Heat Transfer on Turbine Blades, Proceedings of the 1987 Turbine Engine Hot Section Technology Conference, NASA Lewis Research Center, NASA Conference Proceedings Publication 2493, Oct. 1987, pp. 155-167.

49. Cebeci, T. and Smith, A. M. O.: Analysis of Turbulent Boundary Layers, Academic Press, New York, 1974.

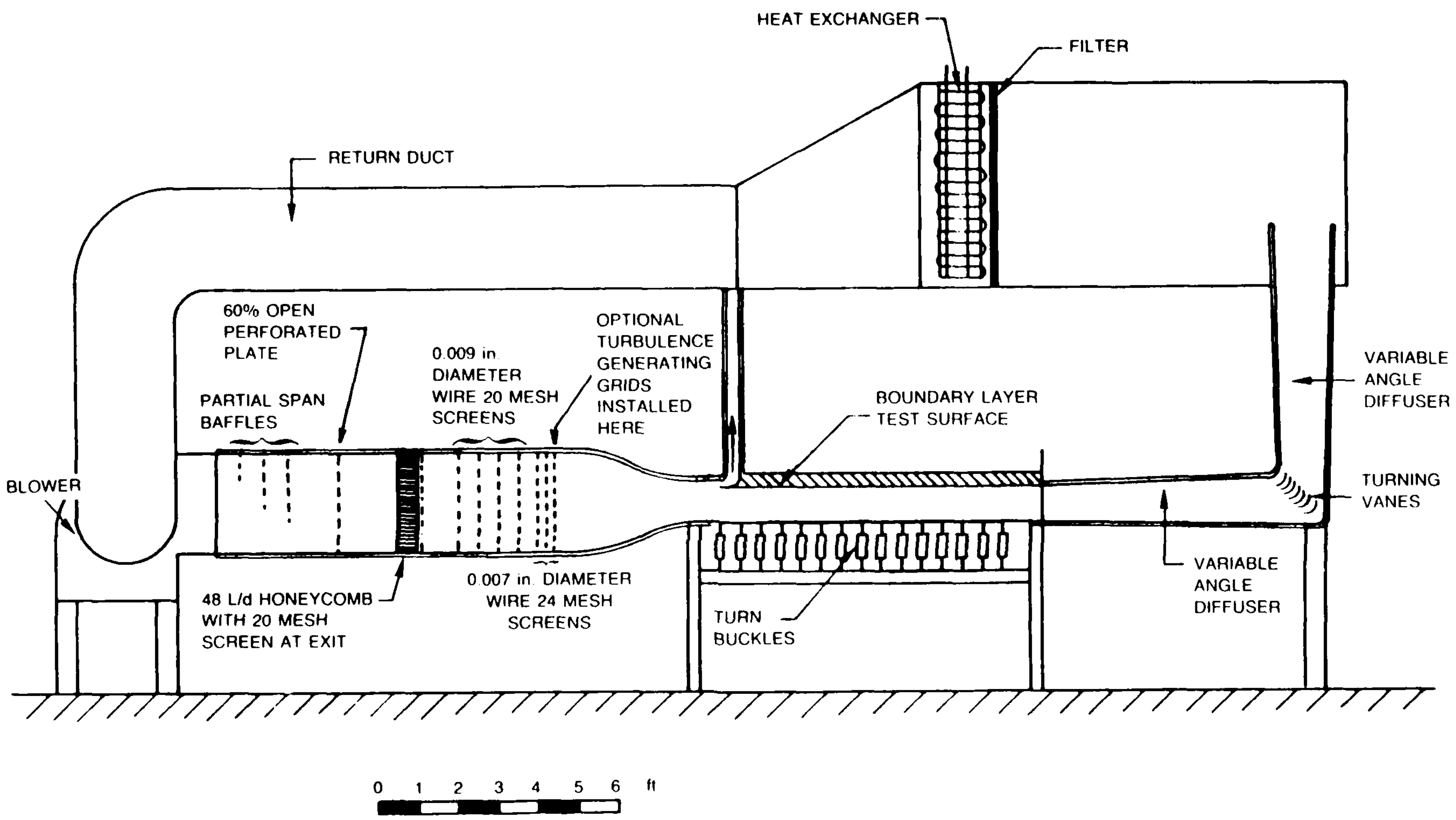

Figure 1. United Technologies Research Center Boundary Layer Wind Tunnel

8⁷-10-44-54

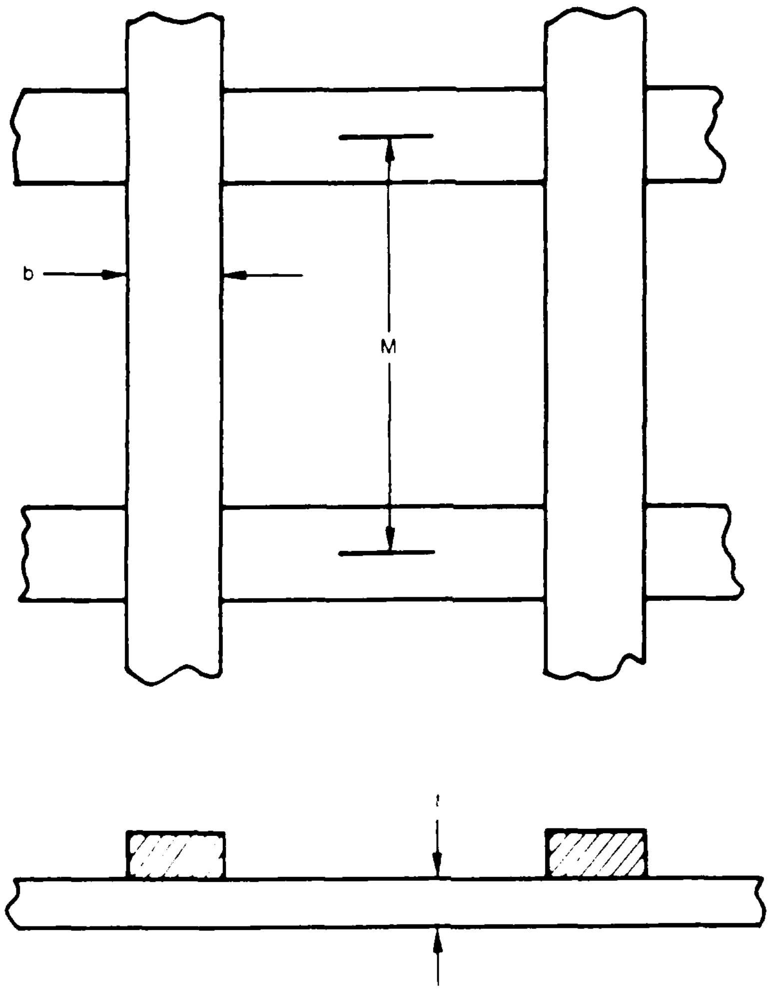

GRID NUMBER	b (inches)	M (inches)	t (inches)	M/b	% OPEN AREA
1	3/16	7/8	3/16	4 67	62
2	1/2	2 9/16	3/8	5.13	65
3	1 1/2	7	1/2	4 67	62

Figure 2. Turbulence Generating Grid Configurations for the Boundary Layer Wind Tunnel

87-10-44-56

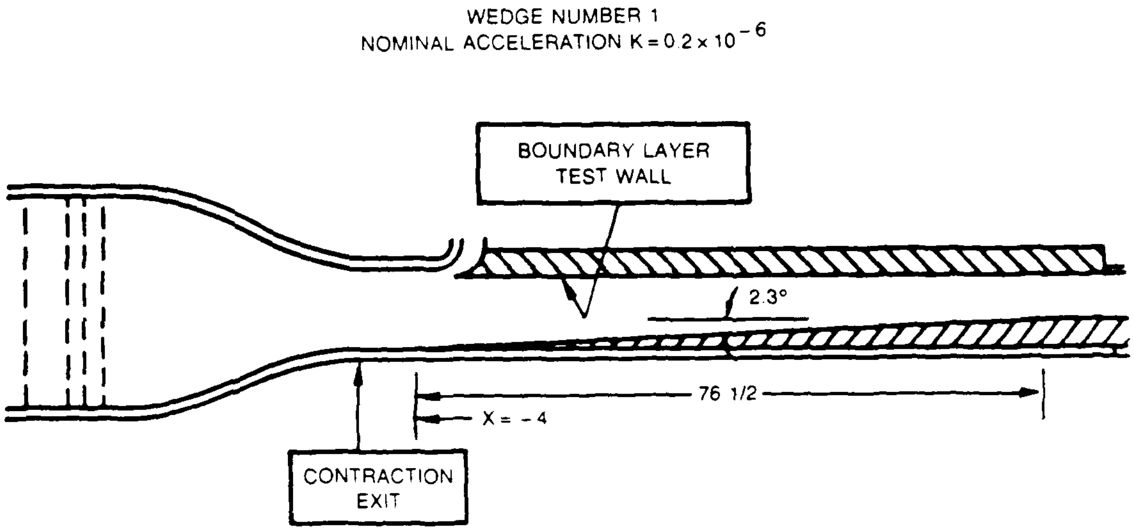

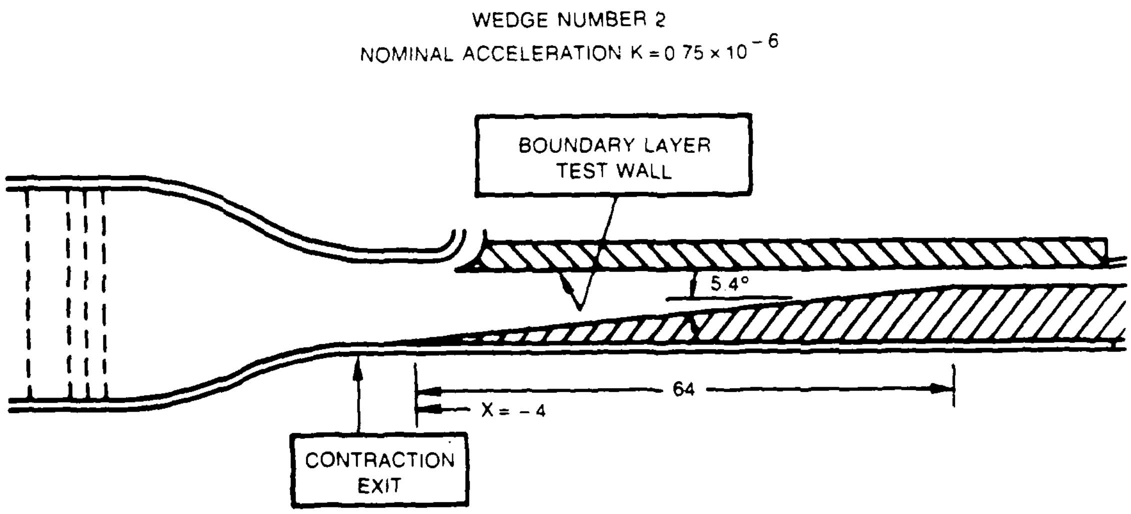

Figure 3. Diagrams of the Wedge Inserts Installed in the Wind Tunnel Test Section

87 - 10 - 44 - 55

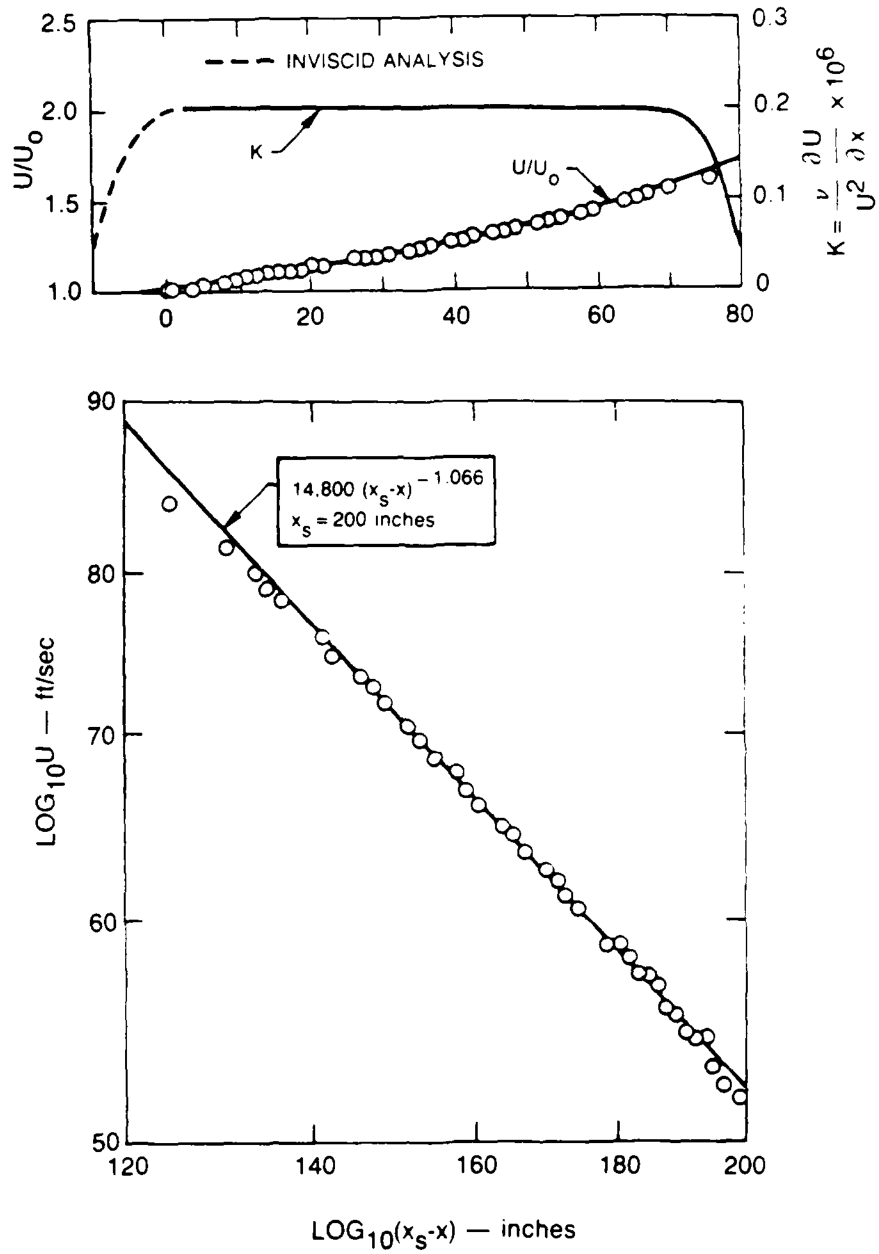

Figure 4. Velocity Distribution Along the Flat Test Wall with the 2.3° Angle Wedge (Wedge 1) and No Turbulence Grid

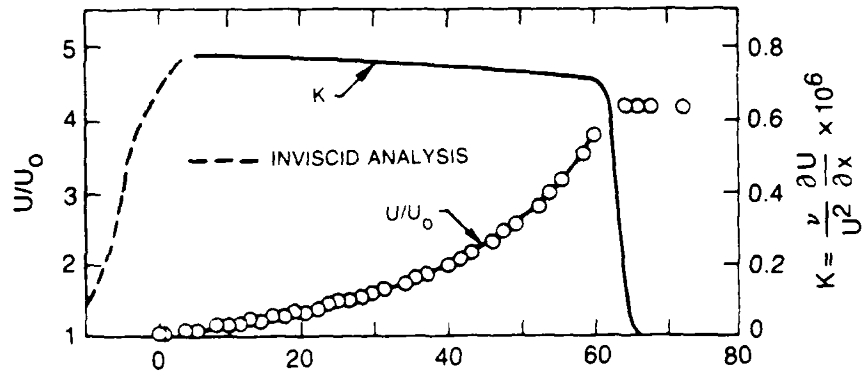

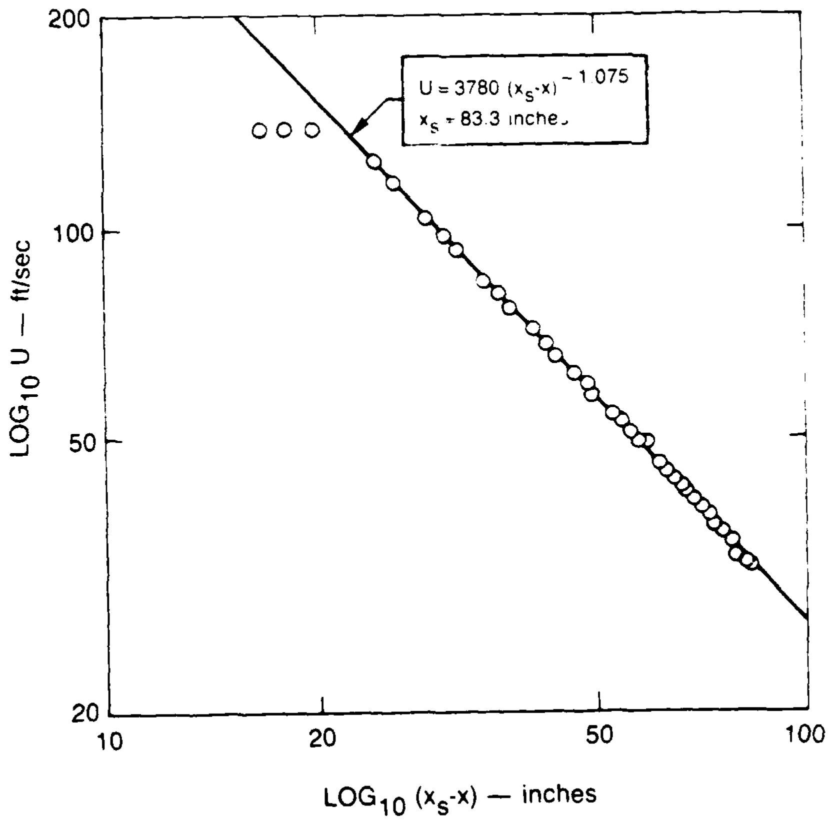

Figure 5. Velocity Distribution Along the Flat Test Wall with the 5.4° Angle Wedge (Wedge 2) and No Turbulence Grid

87-10-44-58

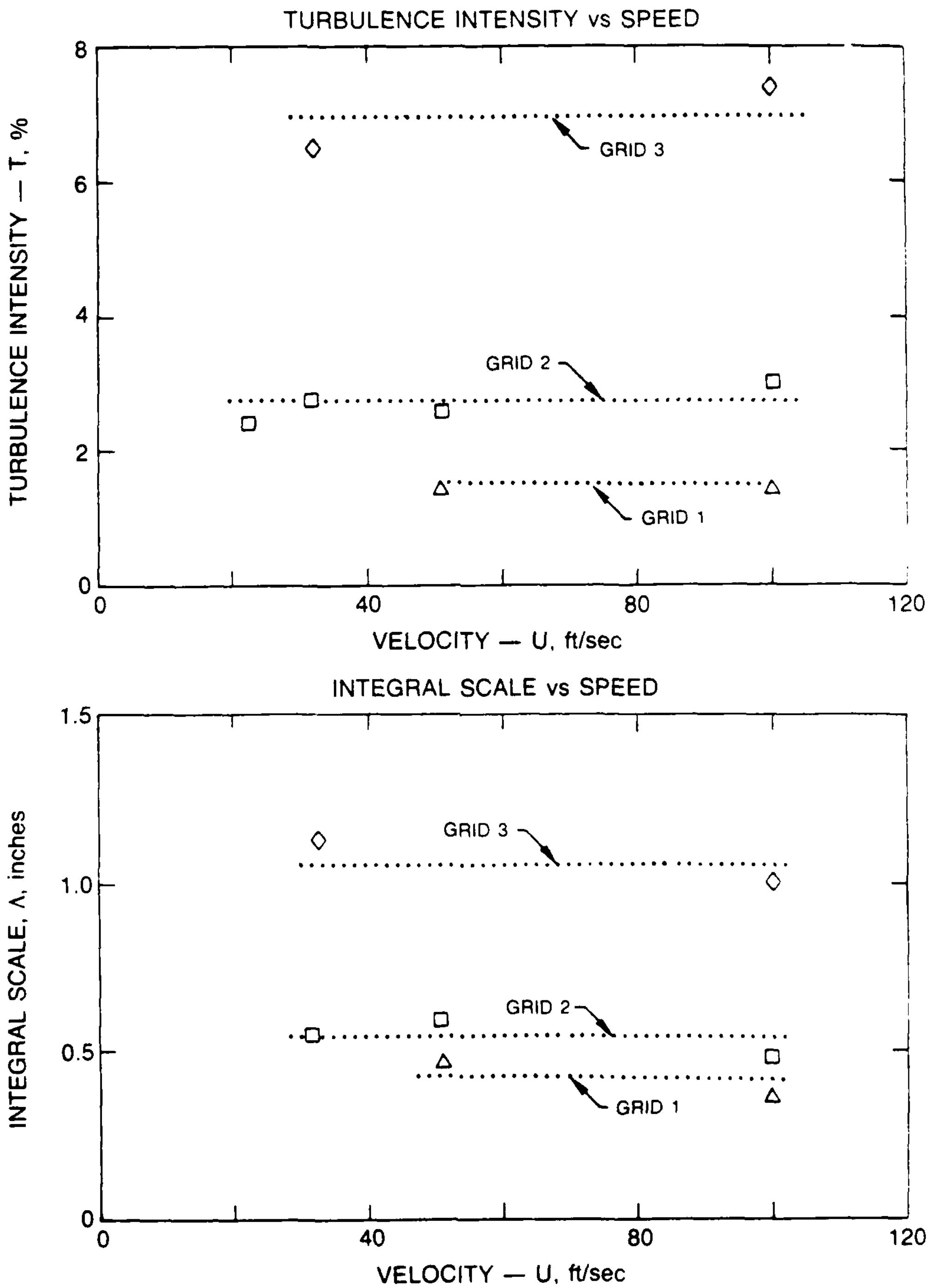

Figure 6. Turbulence Intensity and Longitudinal Integral Scale as a Function of Speed at the Entrance to the Tunnel Test Section — Turbulence *Grids 1, 2, and 3*

87 - 10 - 44 - 59

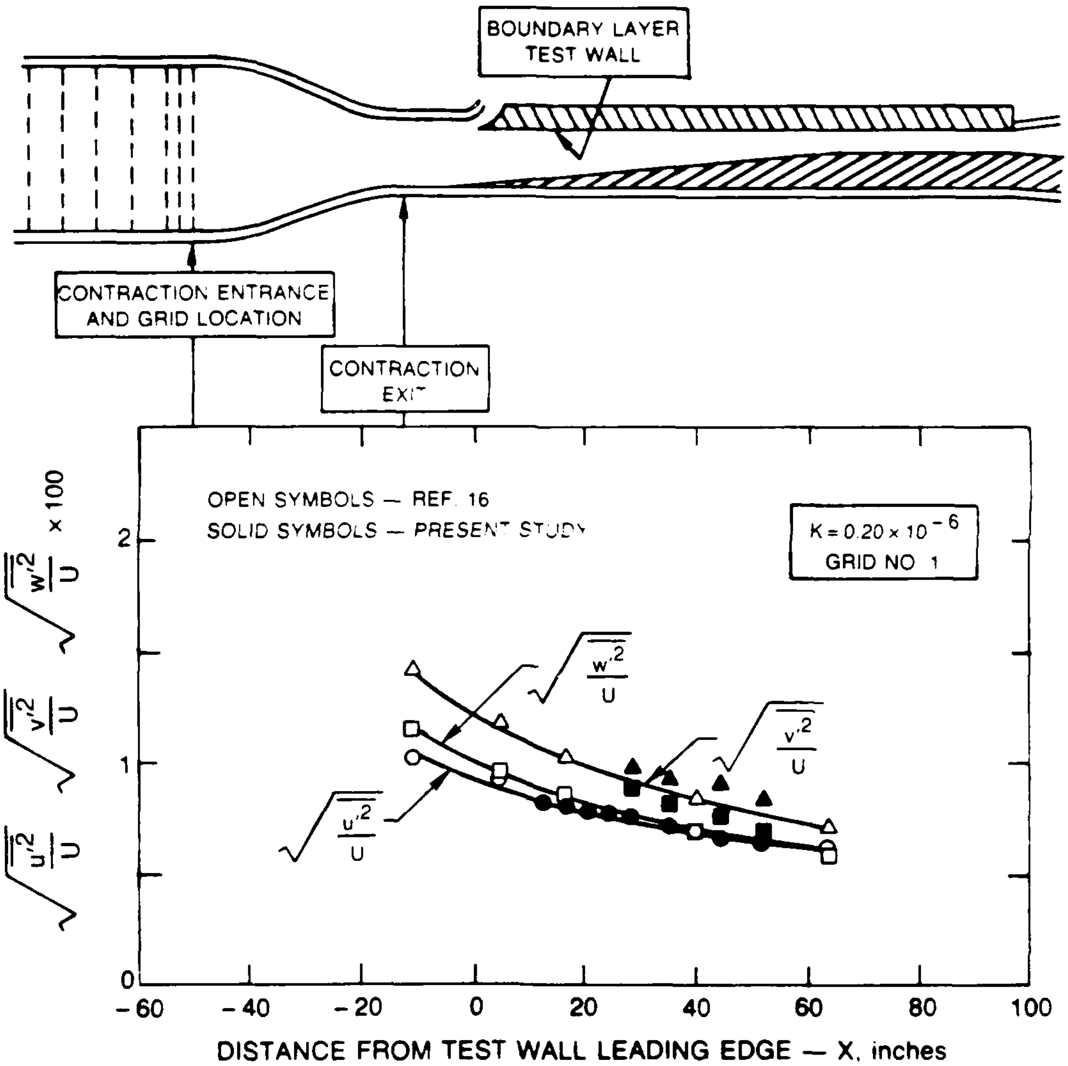

Figure 7. Distribution of the Components of the Turbulence in the Test Section for $K = 0.20 \times 10^{-6}$ and Grid 1

87-10-44-66

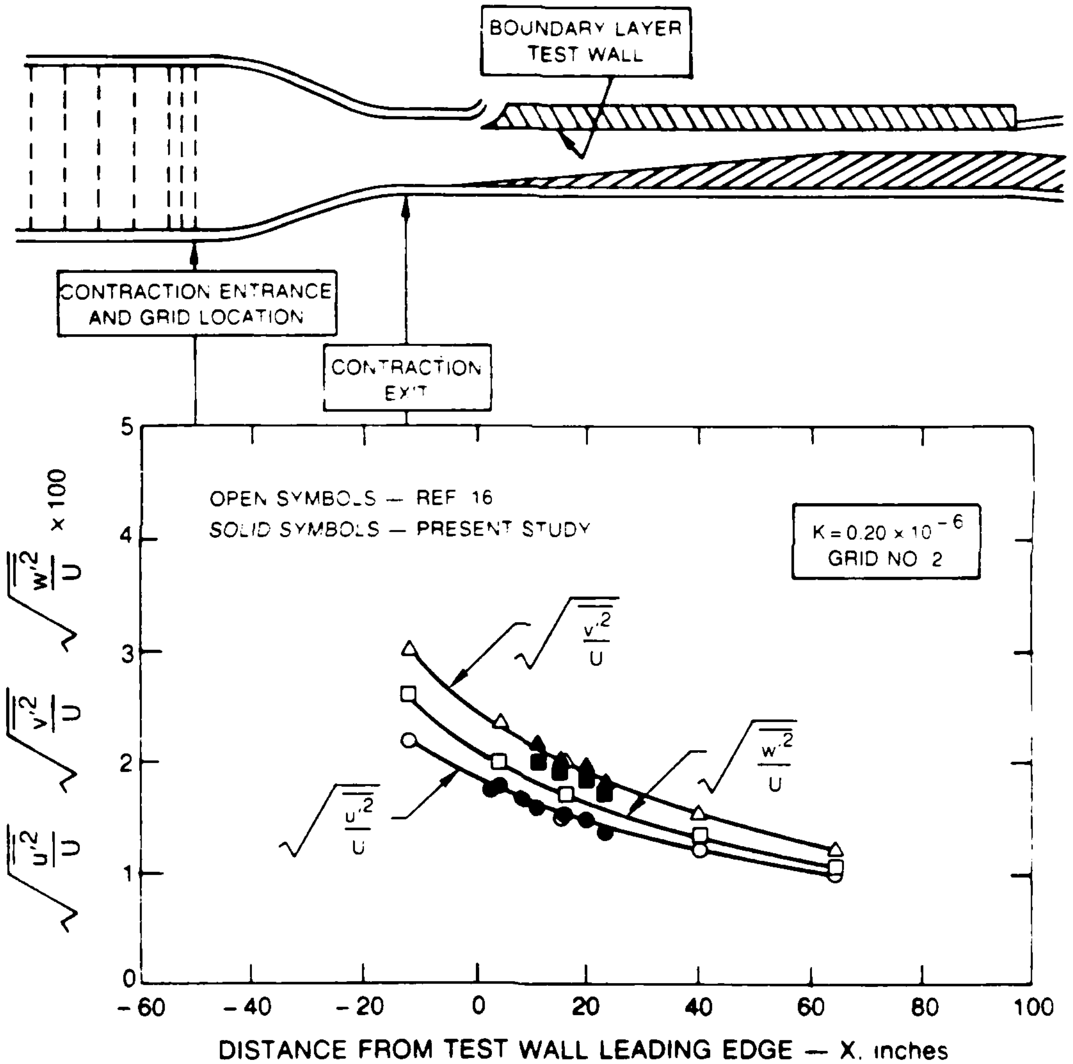

Figure 8. Distribution of the Components of the Turbulence in the Test Section for $K = 0.20 \times 10^{-6}$ and Grid 2

87-10-44-60

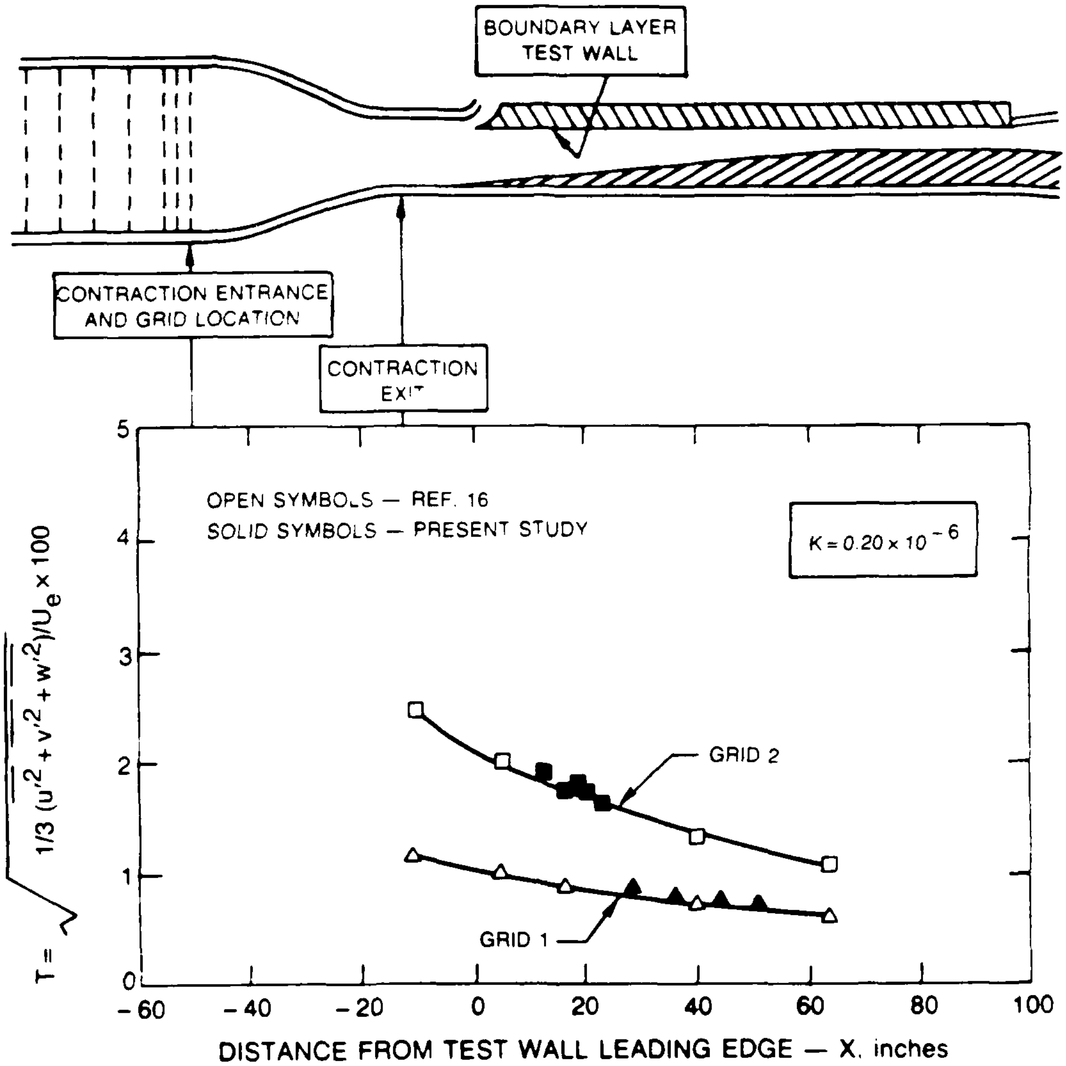

Figure 9. Distributions of Total Turbulence Intensity in the Test Section for $K = 0.20 \times 10^{-6}$

87 - 10 - 44 - 61

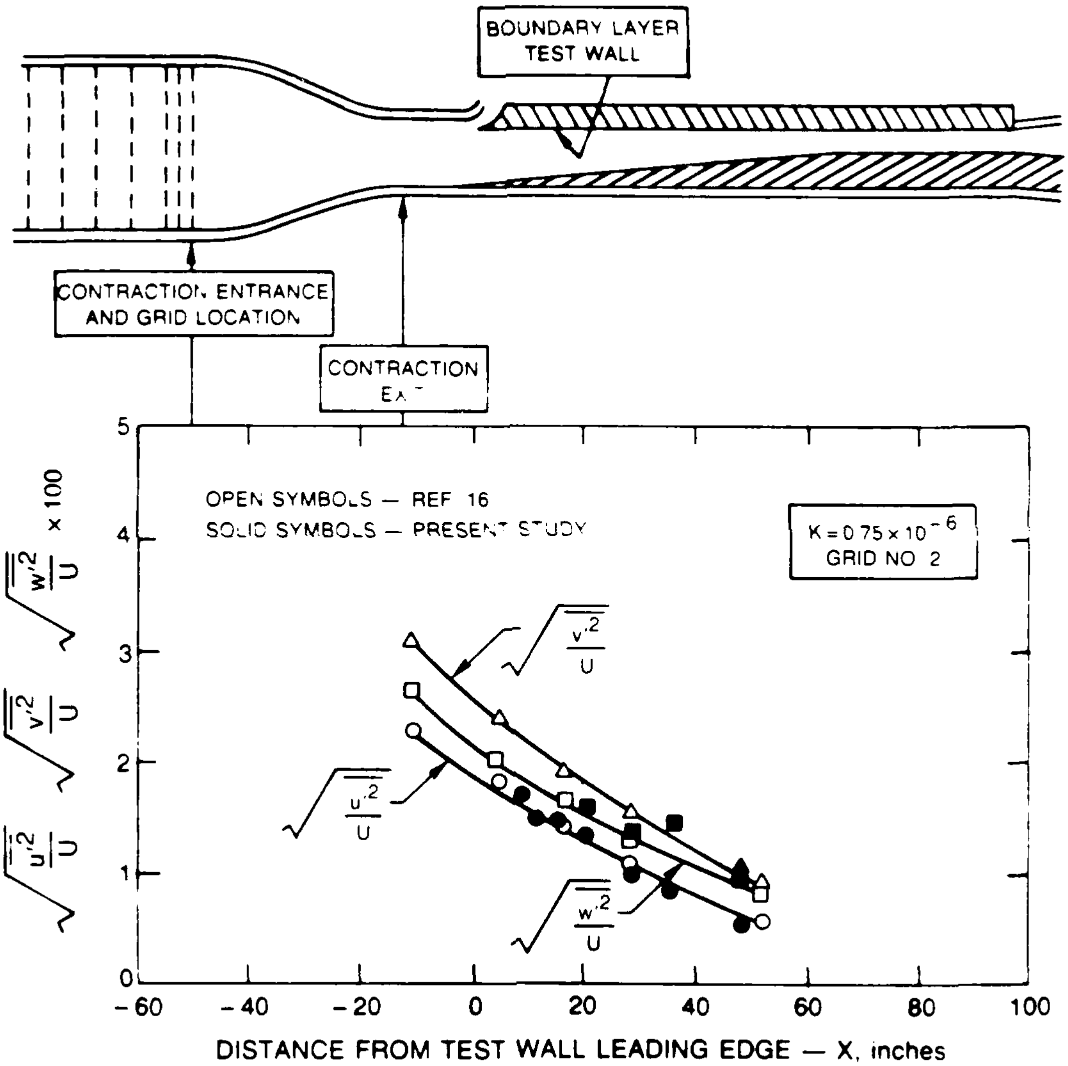

Figure 10. Distribution of the Components of the Turbulence in the Test Section for $K = 0.75 \times 10^{-6}$ and Grid 2

87-10-44-62

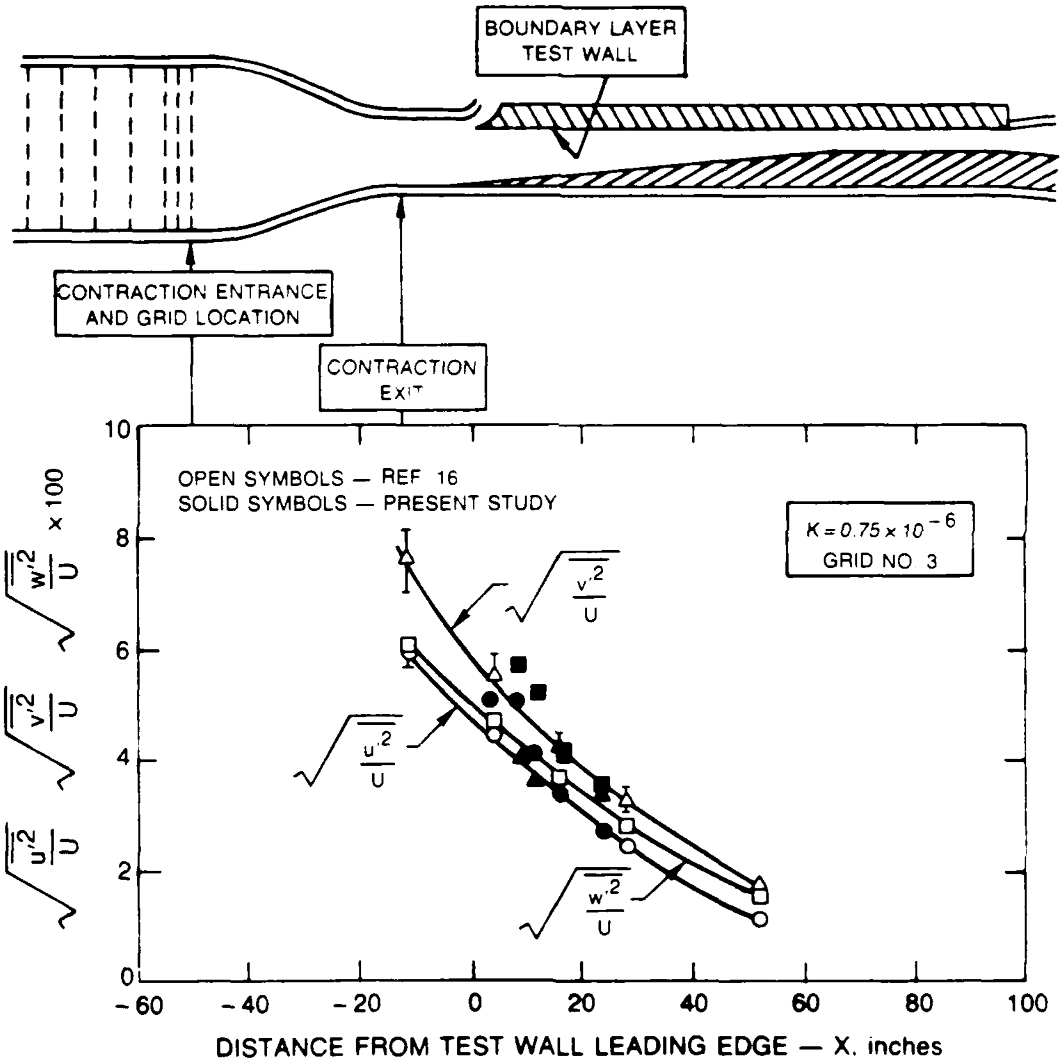

Figure 11. Distribution of the Components of the Turbulence in the Test Section for $K = 0.75 \times 10^{-6}$ and Grid 3

87-10-44-63

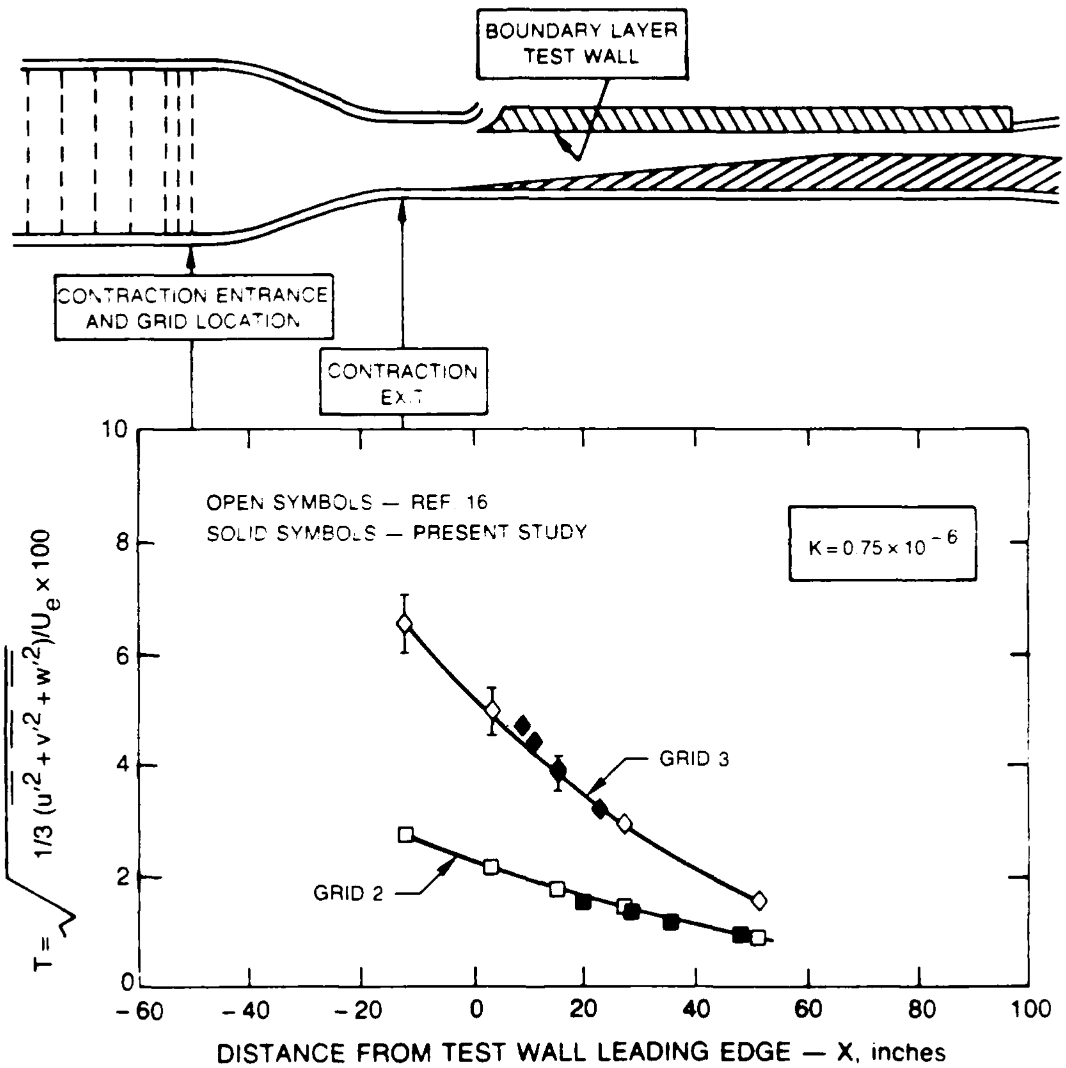

Figure 12. Distributions of Total Turbulence Intensity in the Test Section for $K = 0.75 \times 10^{-6}$

87 - 10 - 44 - 64

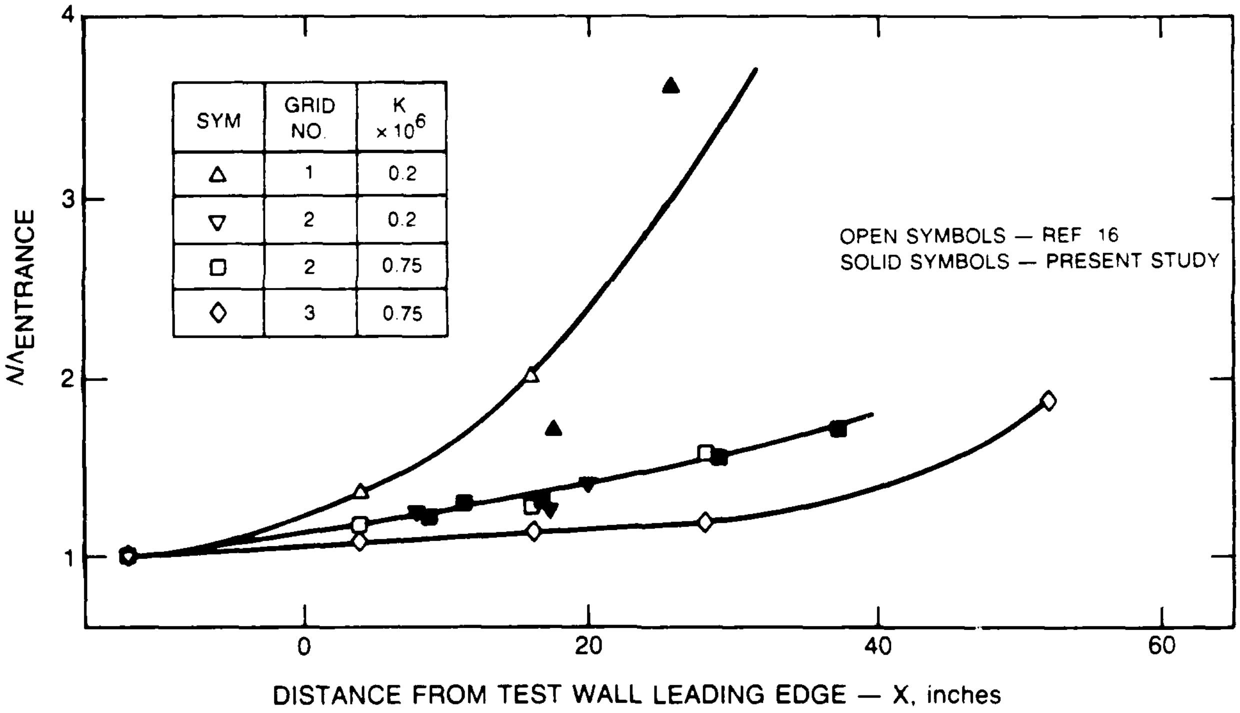

Figure 13. Distributions of the Streamwise Integral Length Scale in the Test Section for the Four Acceleration/Grid Combinations

87-10-44-65

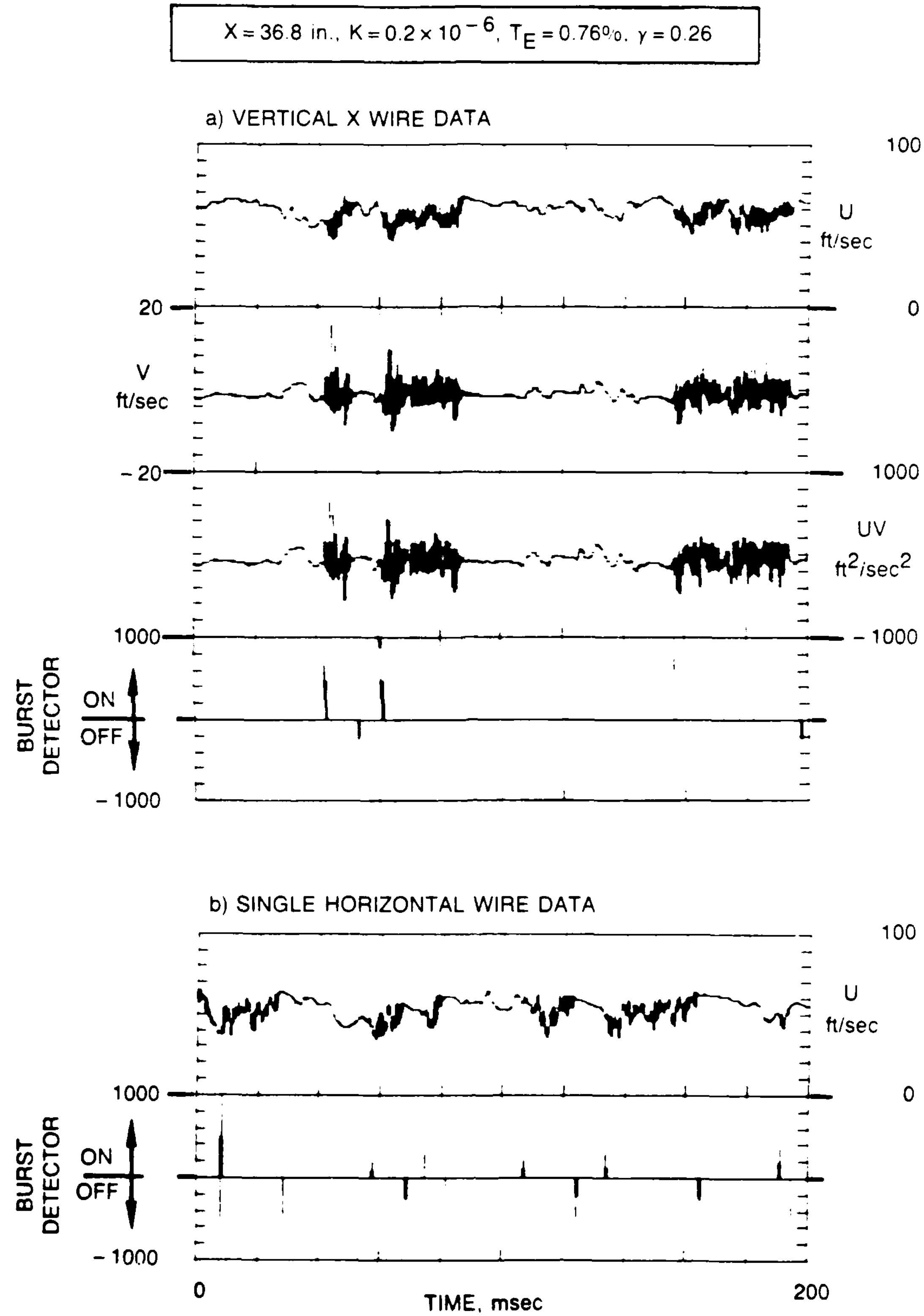

Figure 14. U & V-Time Records Showing a Low Freestream Turbulence, Moderate Intermittency Flow, $Y/\delta = 0.275$

87-10-44-11

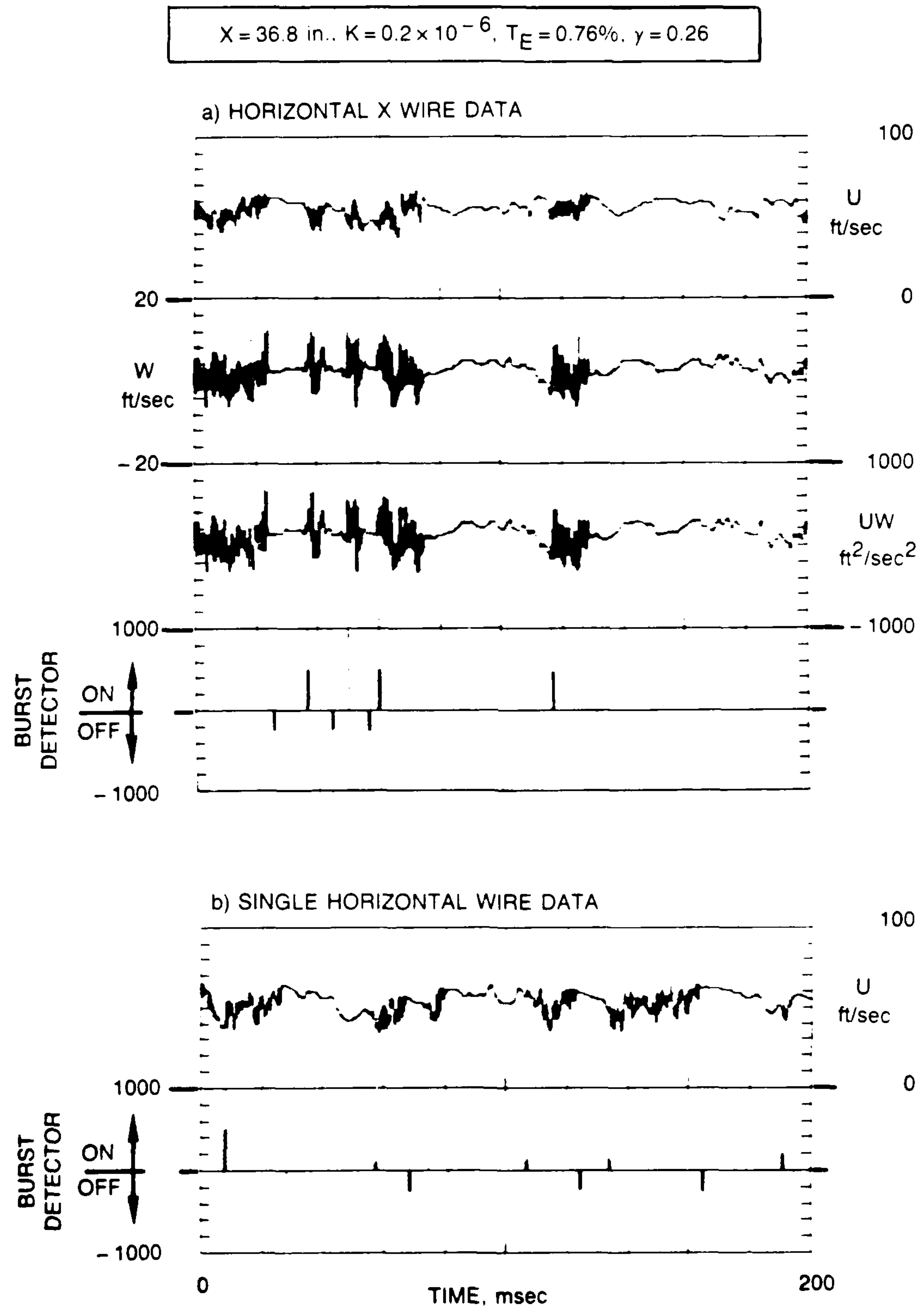

Figure 15. Sample U & W-Time Records Showing a Low Freestream Turbulence, Moderate Intermittency Flow, $Y/\delta = 0.275$

87-10-44-10

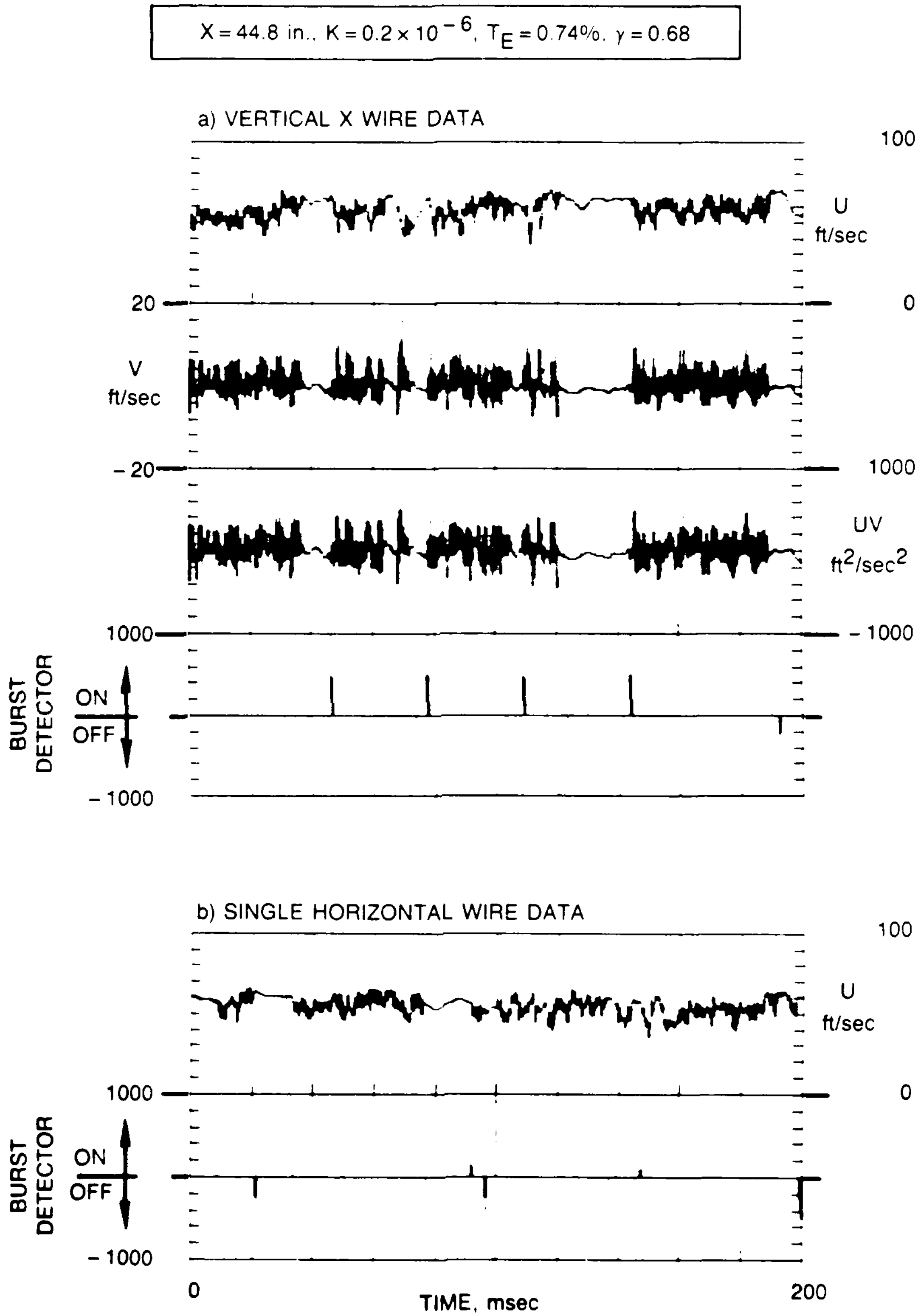

Figure 16. Sample U & V-Time Records Showing a Low Freestream Turbulence, High Intermittency Flow, $Y/\delta = 0.183$

87-10-44-9

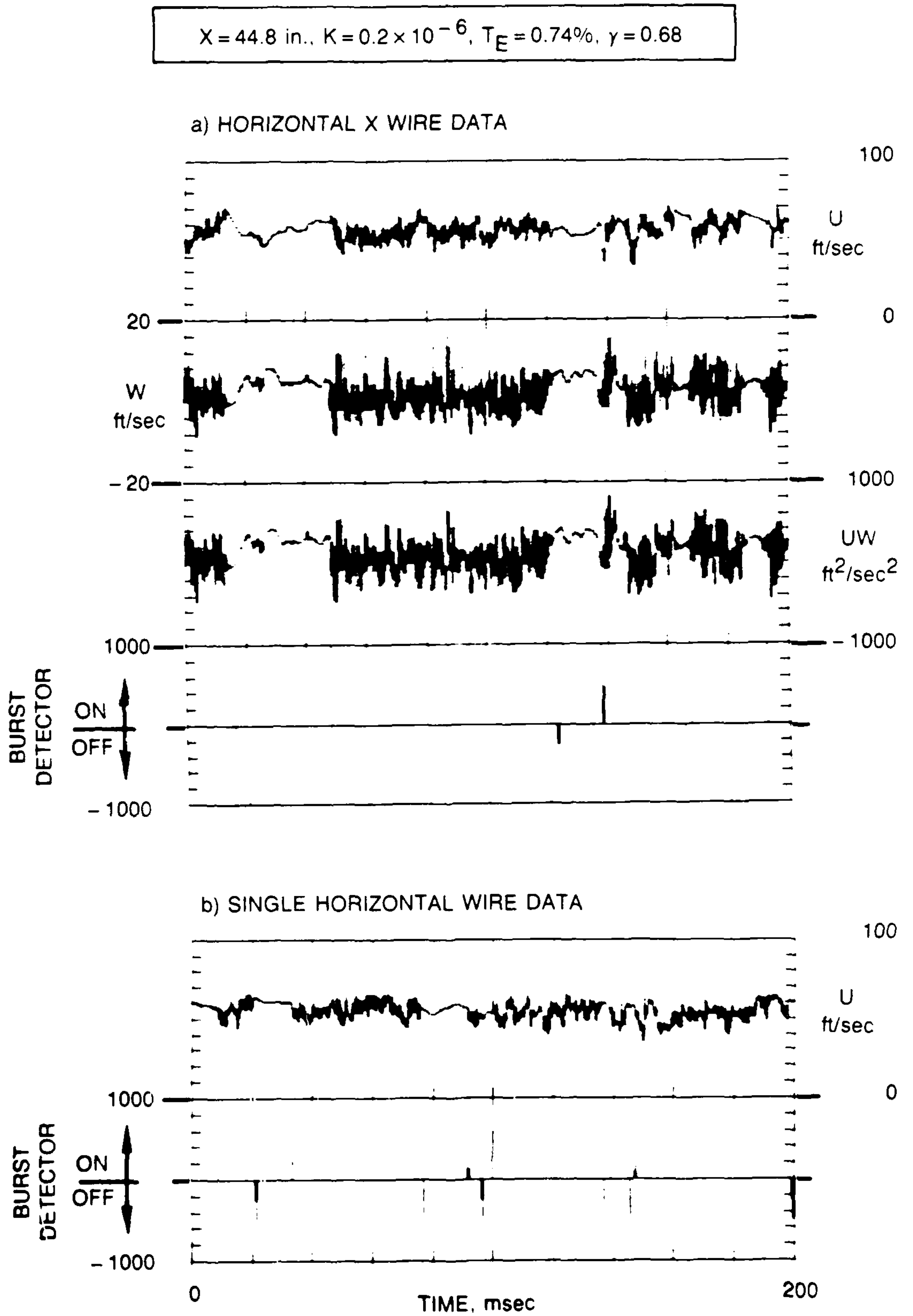

Figure 17. Sample U & W-Time Records Showing a Low Freestream Turbulence, High Intermittency Flow, $Y/\delta = 0.183$

87-10-44-6

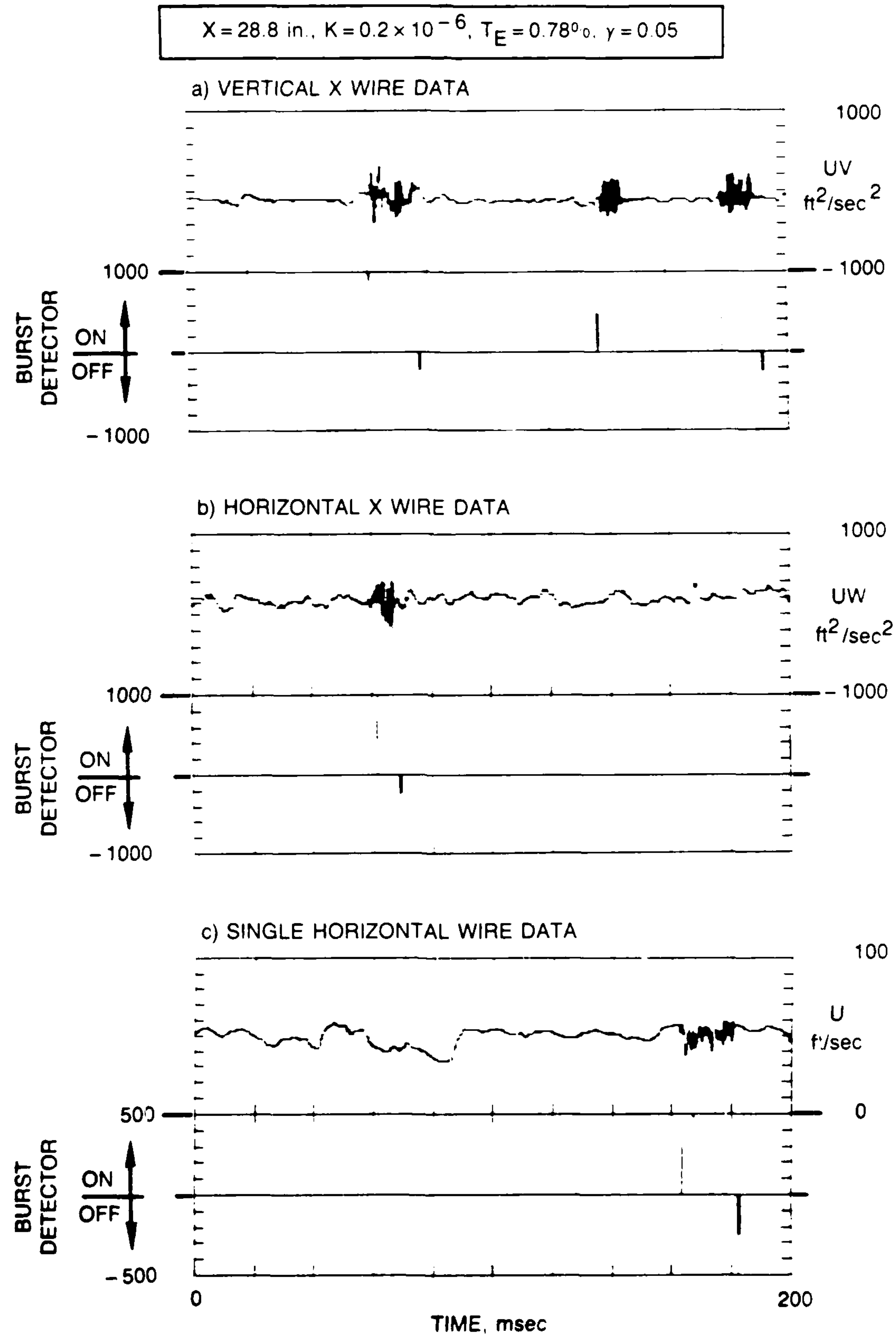

Figure 18. Sample UV, UW & U-Time Records Showing a Low Freestream Turbulence, Low Intermittency Flow, $Y/\delta = 0.355$

87 - 10 - 44 - 7

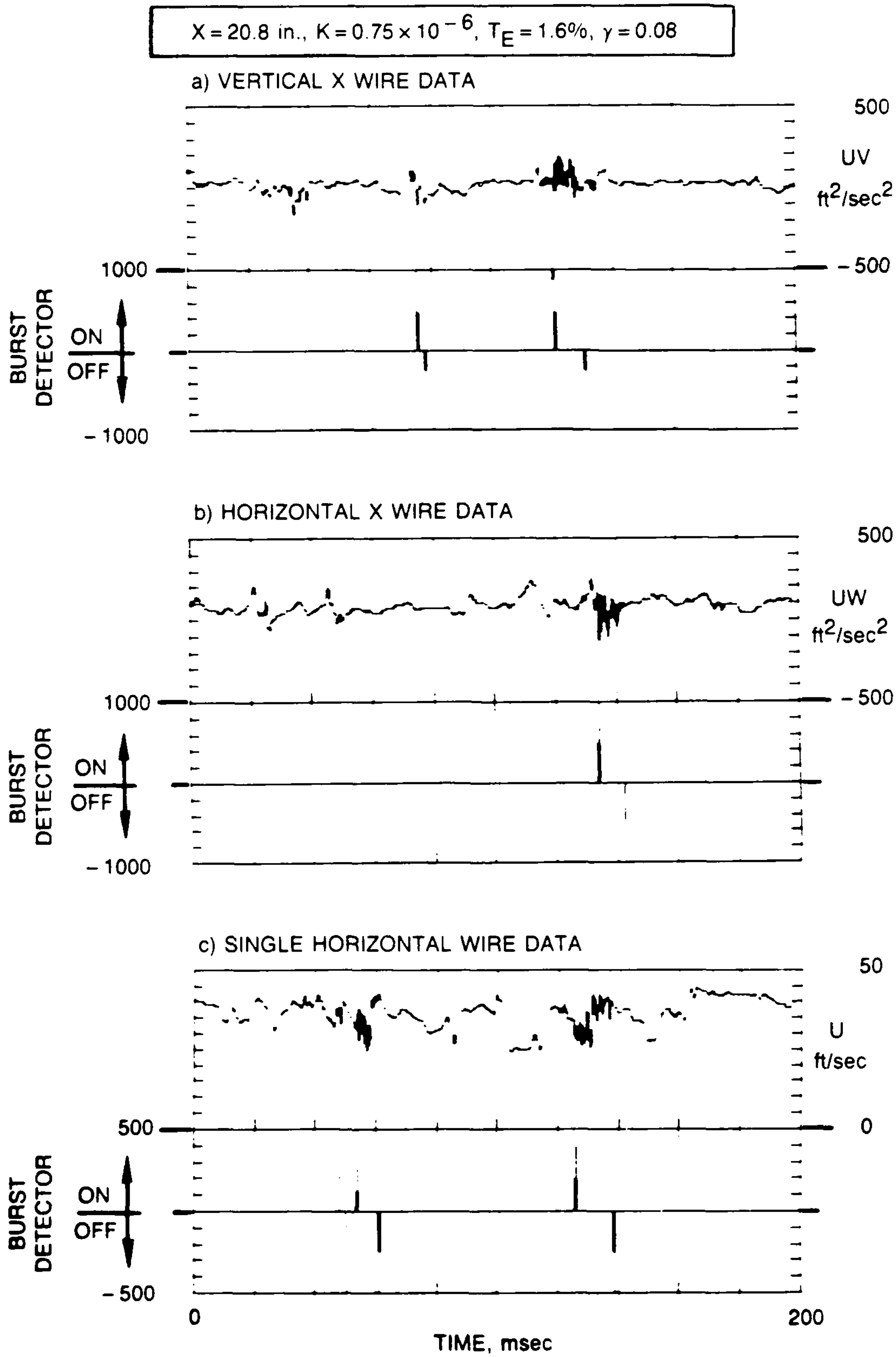

Figure 19. Sample UV, UW, & U-Time Records Showing a Moderate Freestream Turbulence, Low Intermittency Flow, Y/δ = 0.286

87 - 10 - 44 - 6

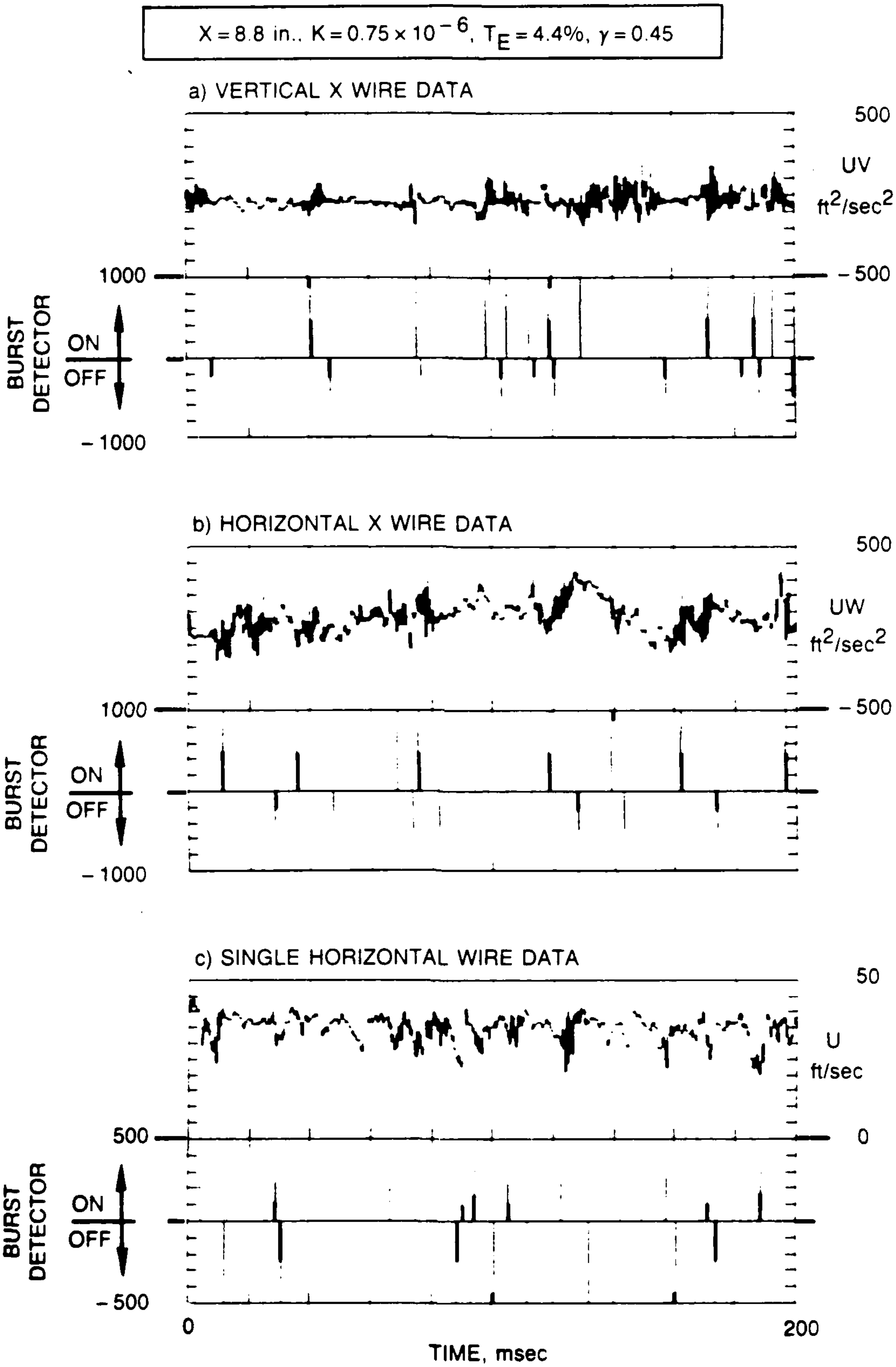

Figure 20. Sample UV, UW, & U-Time Records Showing a High Freestream Turbulence, Moderate Intermittency Flow, $Y/\delta = 0.297$

87 - 10 - 44 - 5

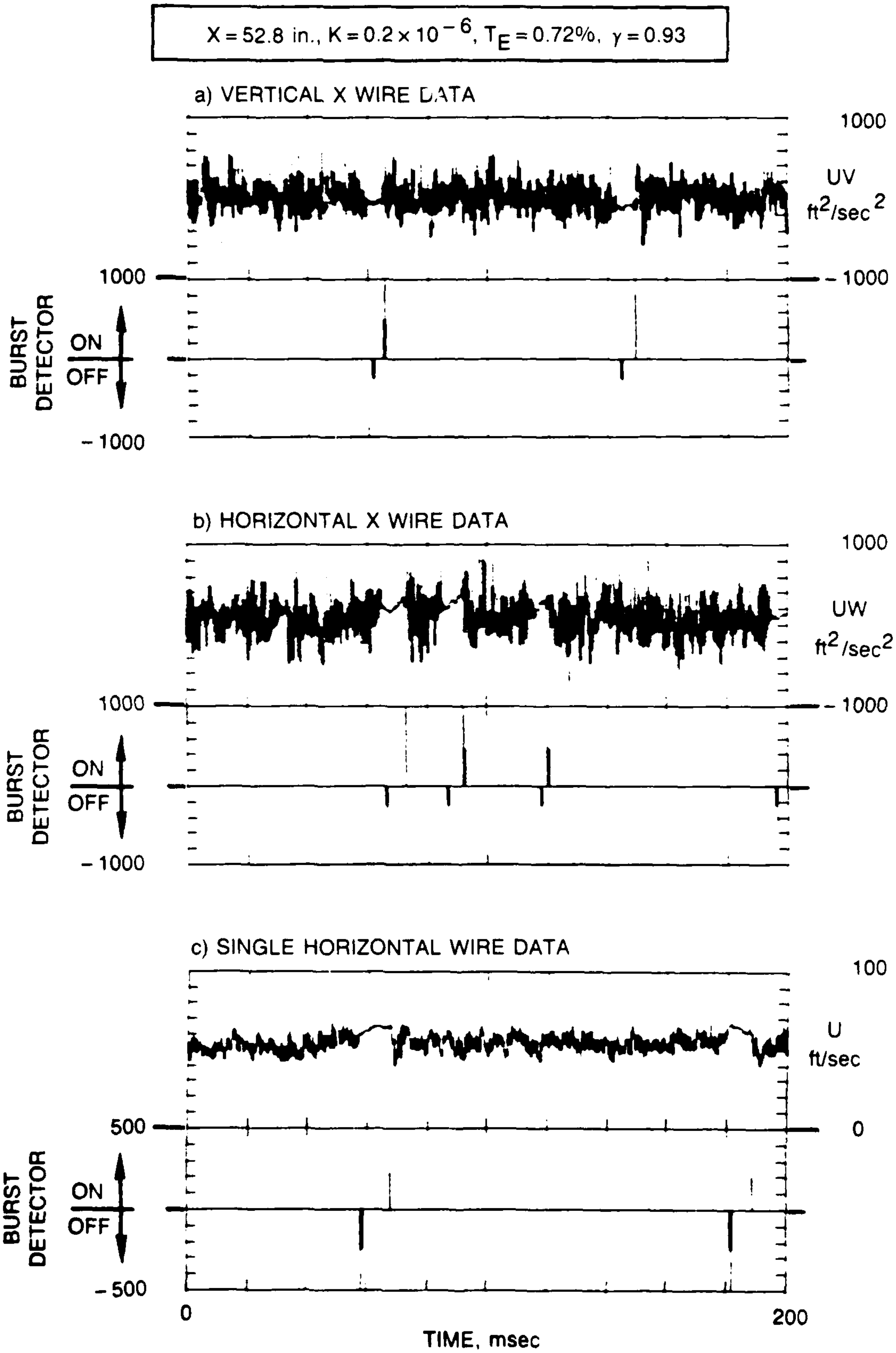

Figure 21. Sample UV, UW, & U-Time Records Showing a Low Freestream Turbulence, High Intermittency Flow, $Y/\delta = 0.145$

87 - 10 - 44 - 4

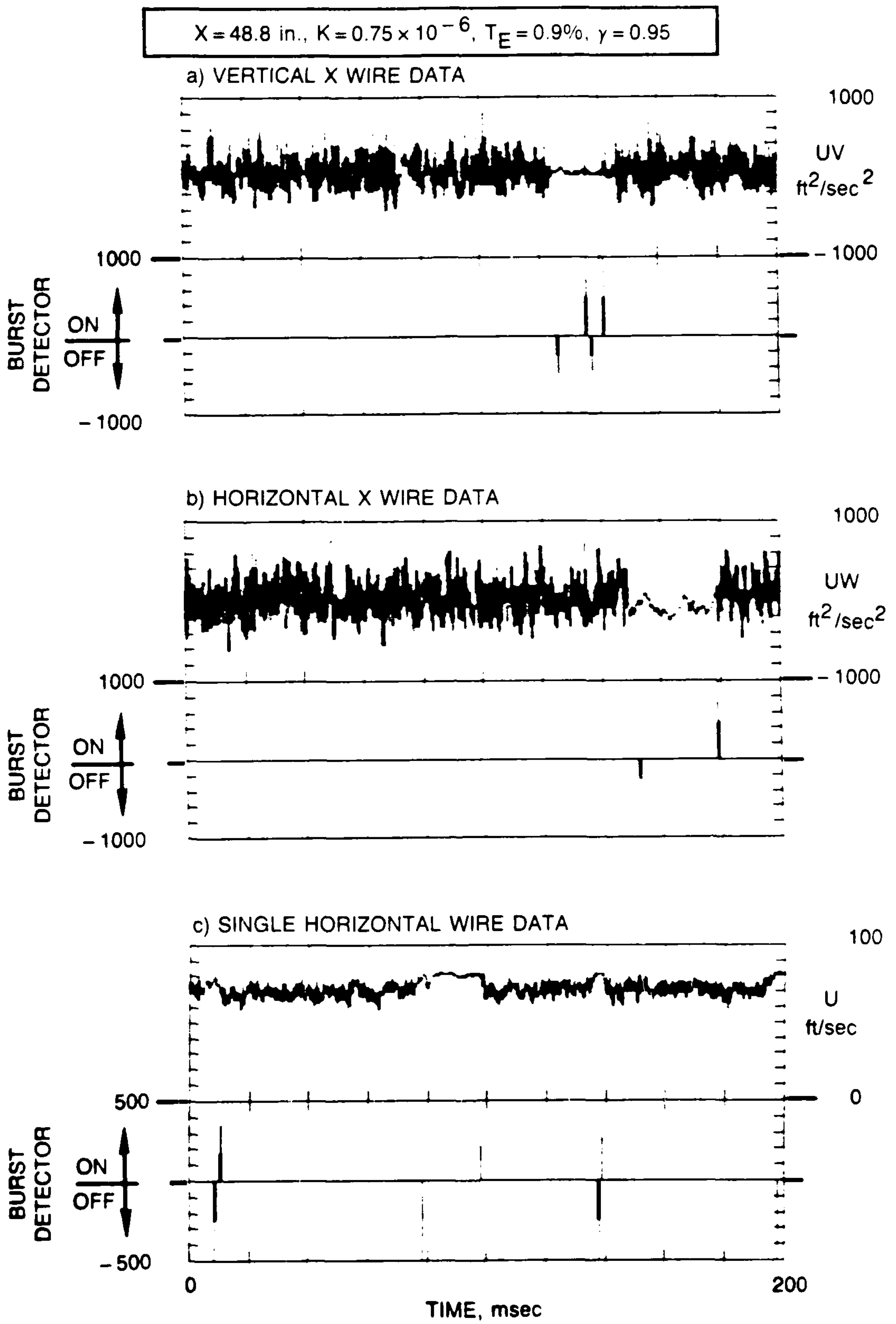

Figure 22. Sample UV, UW & U-Time Records Showing a Moderate Freestream Turbulence, High Intermittency Flow, Y/δ = 0.172

87 - 10 - 44 - 3

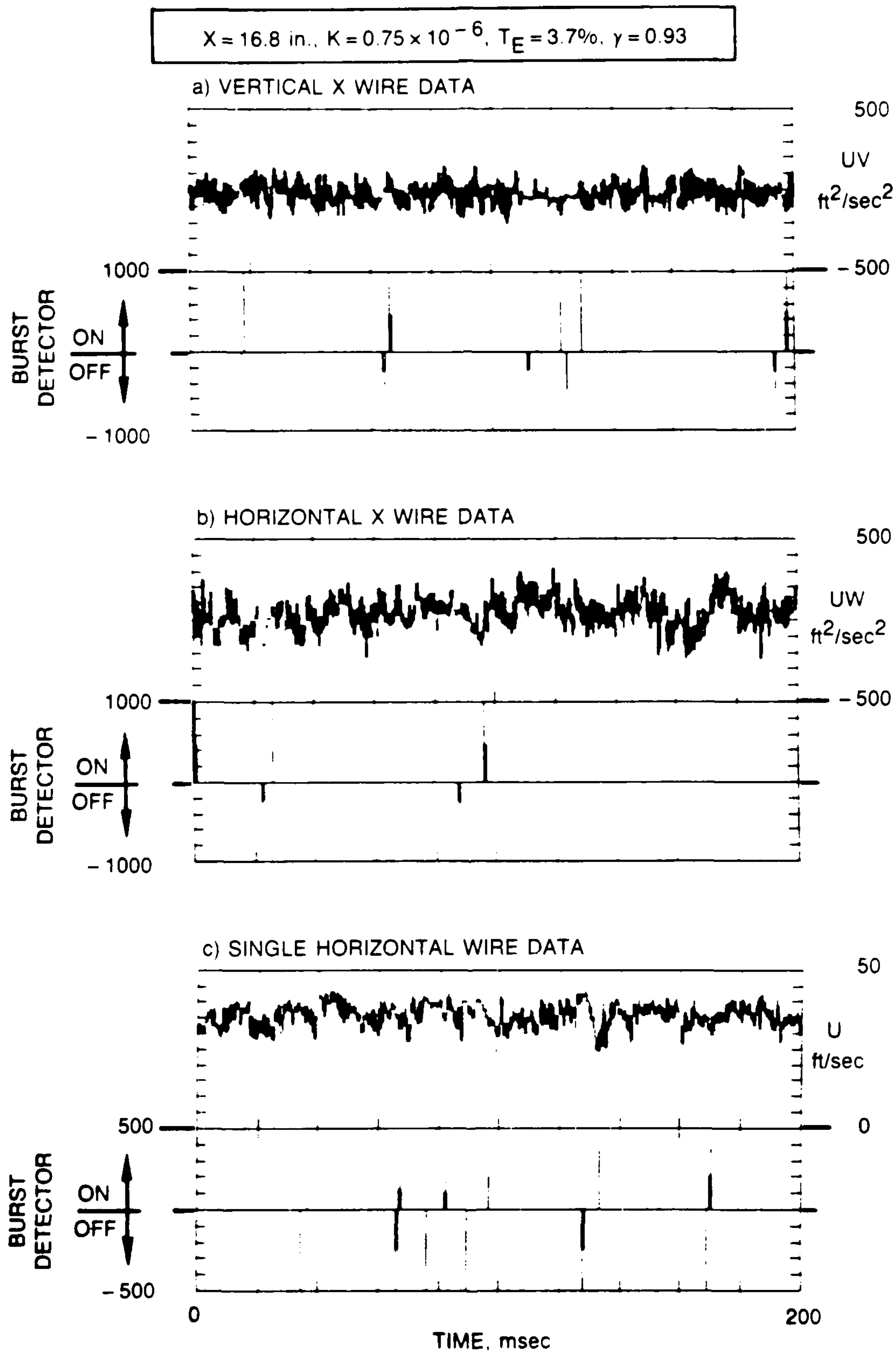

Figure 23. Sample UV, UW & U-Time Records Showing a High Freestream Turbulence, High Intermittency Flow, $Y/\delta = 0.183$

87 - 10 - 44 - 2

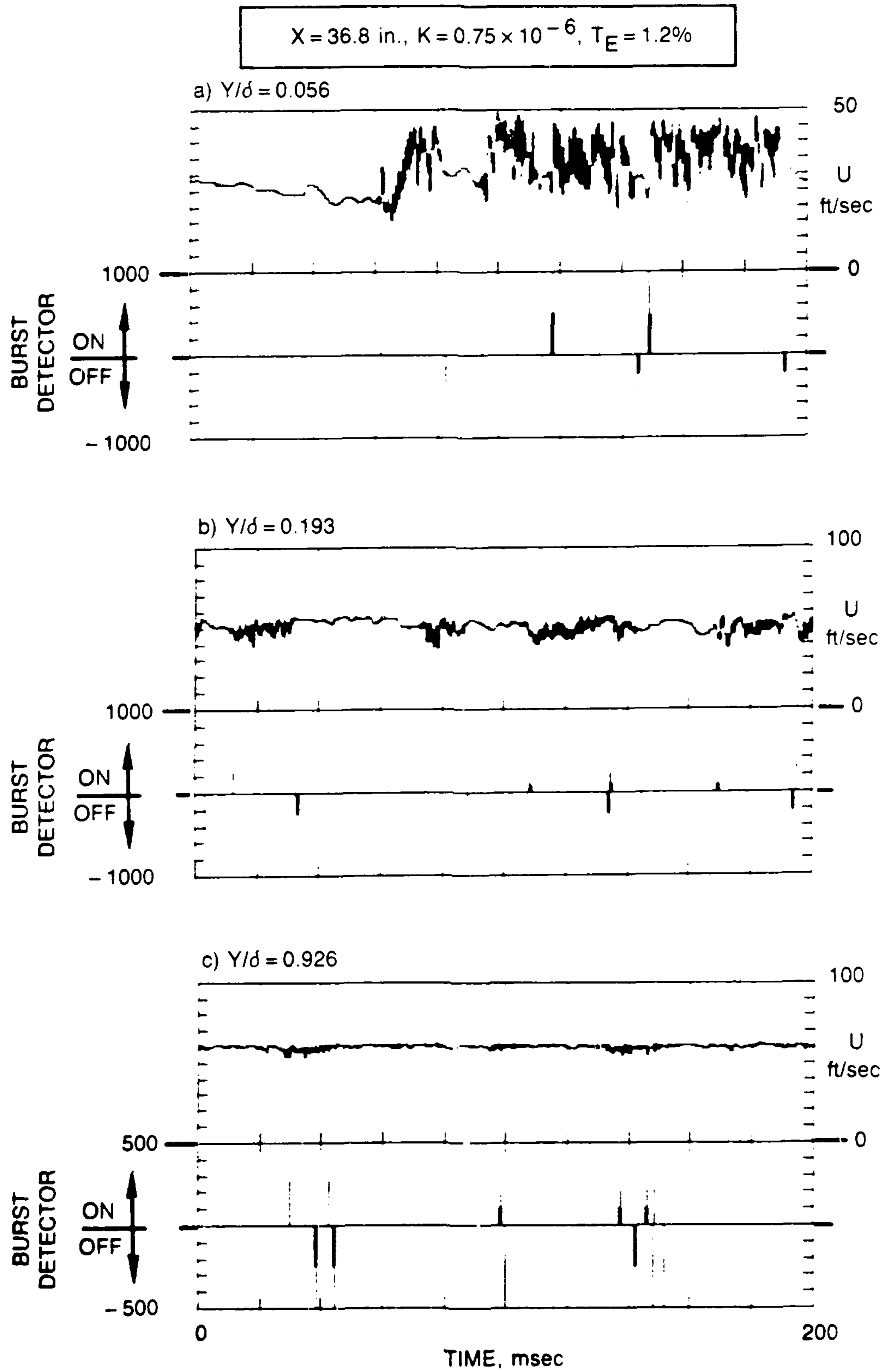

Figure 24. Sample U-Time Records at 3 Distances From the Wall for a Moderate Freestream Turbulence, Moderate Intermittency Flow

87 - 10 - 44 - 1

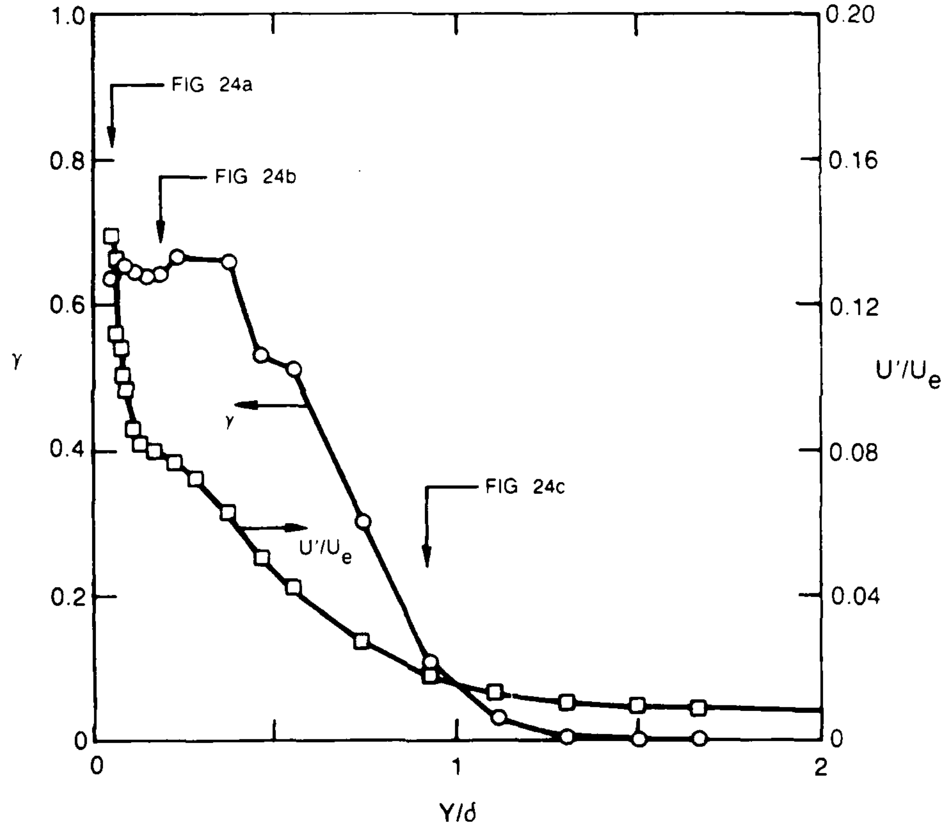

Figure 25. Turbulence Intensity and Intermittency Distributions for the Profile of Figure 24 X = 36.8 in., $K = 0.75 \times 10^{-6}$, $T_E = 1.2\%$

87-10-44-67

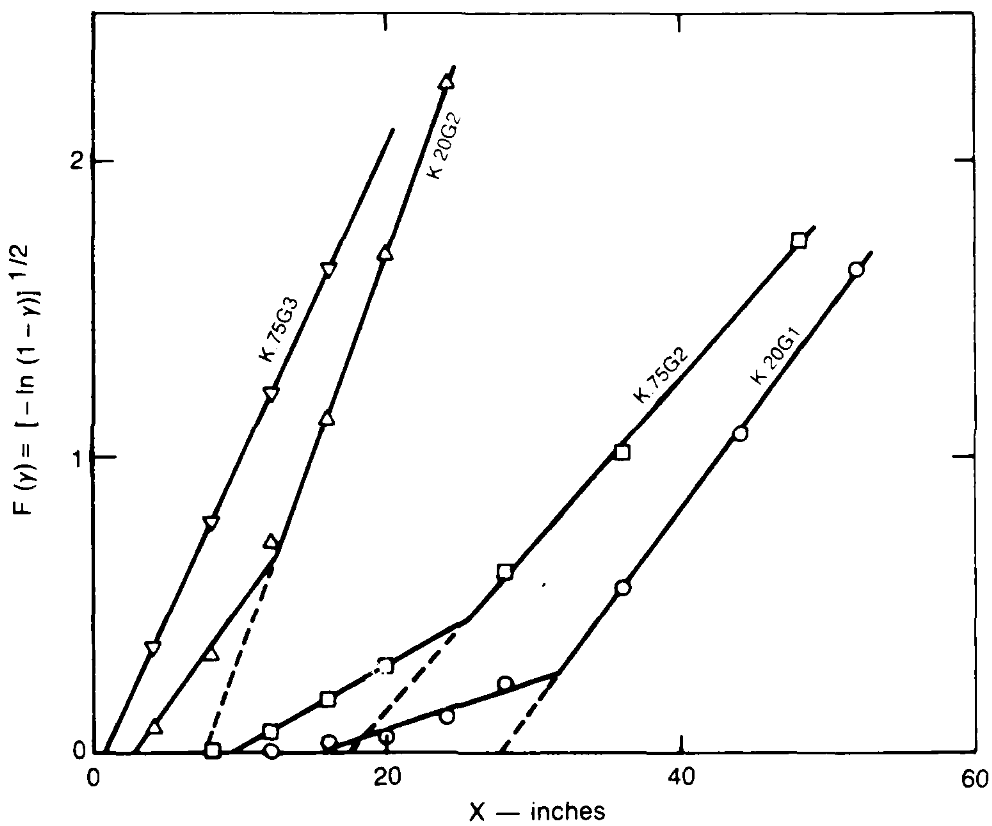

Figure 26. Near-Wall Intermittency Distributions for the Four Test Cases

87 - 10 - 44 - 40

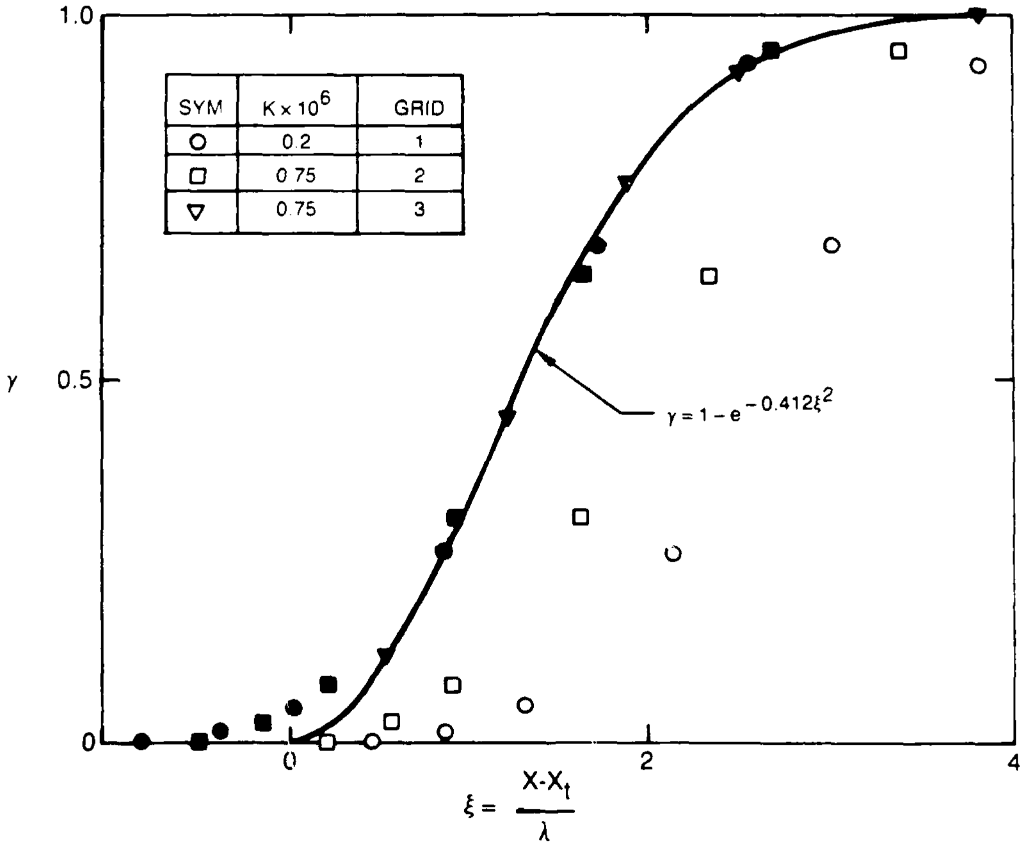

Figure 27. Intermittency Distributions in the Universal Coordinates of Narasimha

87 - 10 - 44 - 41

X = 8.8 K = 0.75 E−6 TE = 2.0 %

MEAN VELOCITY

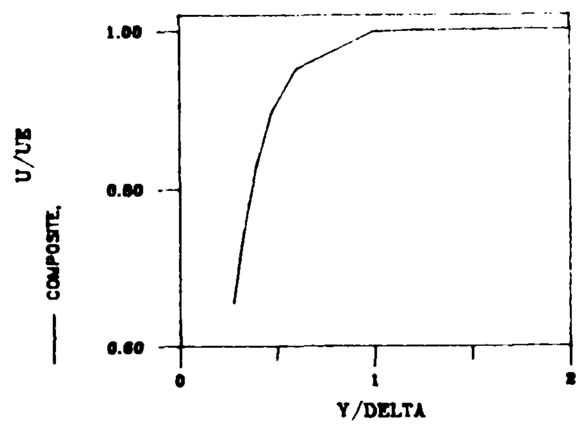

TURBULENCE COMPONENTS

COMPOSITE AVERAGE

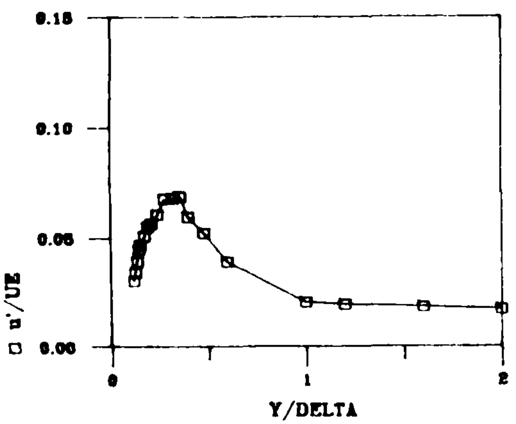

Figure 28A. Profiles of Mean and Fluctuating Quantities

8?-10-44-23

X = 12.8 K = 0.75 E-6 TE = 1.9 %

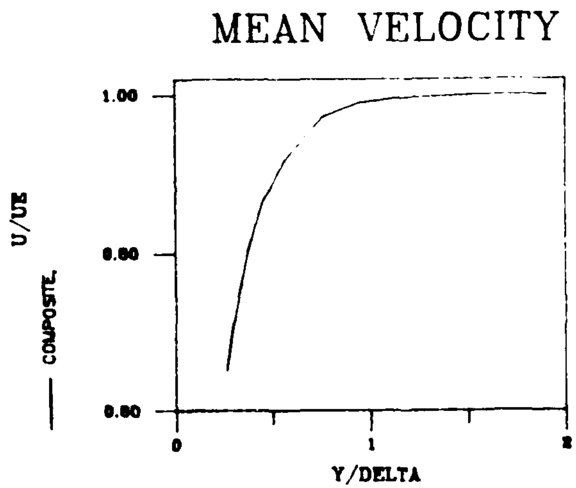

TURBULENCE COMPONENTS

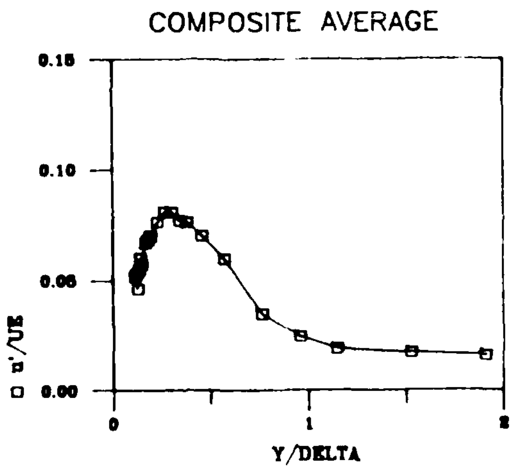

Figure 28B. Profiles of Mean and Fluctuating Quantities

87-10-44-24

X = 16.8 K = 0.75 E-6 TE = 1.7 %

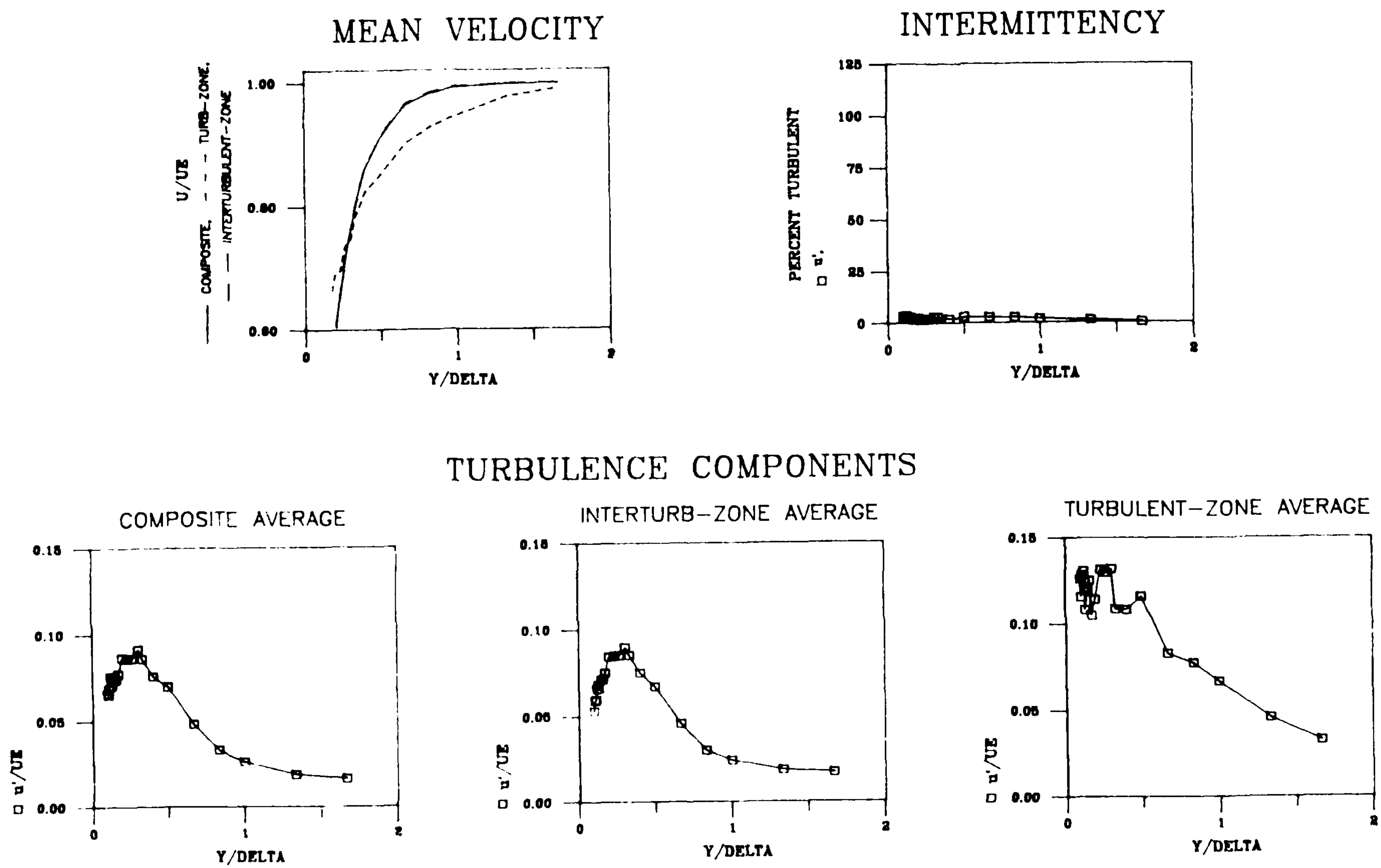

Figure 28C. Profiles of Mean and Fluctuating Quantities

87-10-44-25

AD-A191 690 STUDY OF THE STRUCTURE OF TURBULENCE IN ACCELERATING 2/3
TRANSITIONAL BOUNDAR..(U) UNITED TECHNOLOGIES RESEARCH
CENTER EAST HARTFORD CT M F BLAIR ET AL. 23 DEC 87
UNCLASSIFIED UTRC/R87-956900-1 AFOSR-TR-88-0017 F/G 20/4 NL

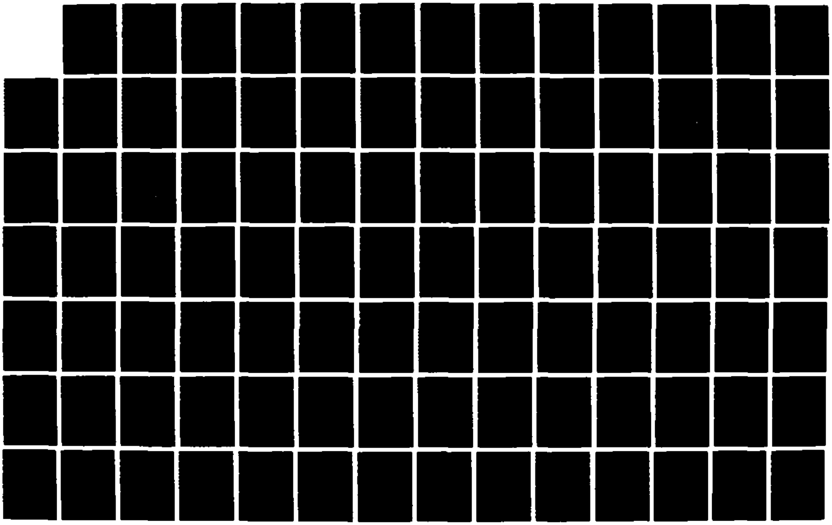

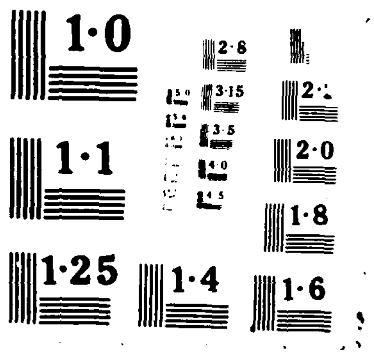
1·0
2·8
3·15
3·5
2·0
1·1
1·8
1·25
1·4
1·6

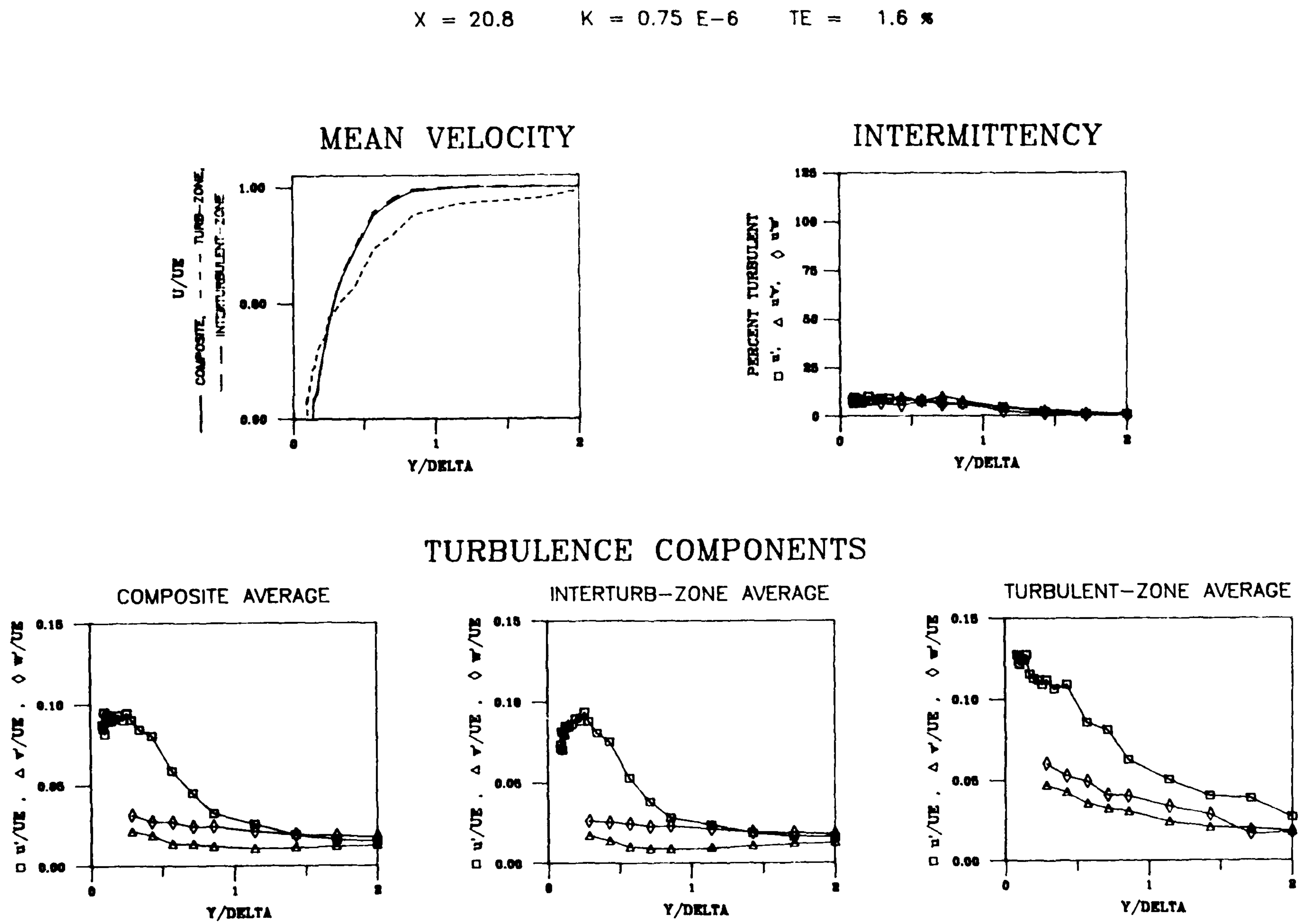

Figure 28D. Profiles of Mean and Fluctuating Quantities

87-10-44-26

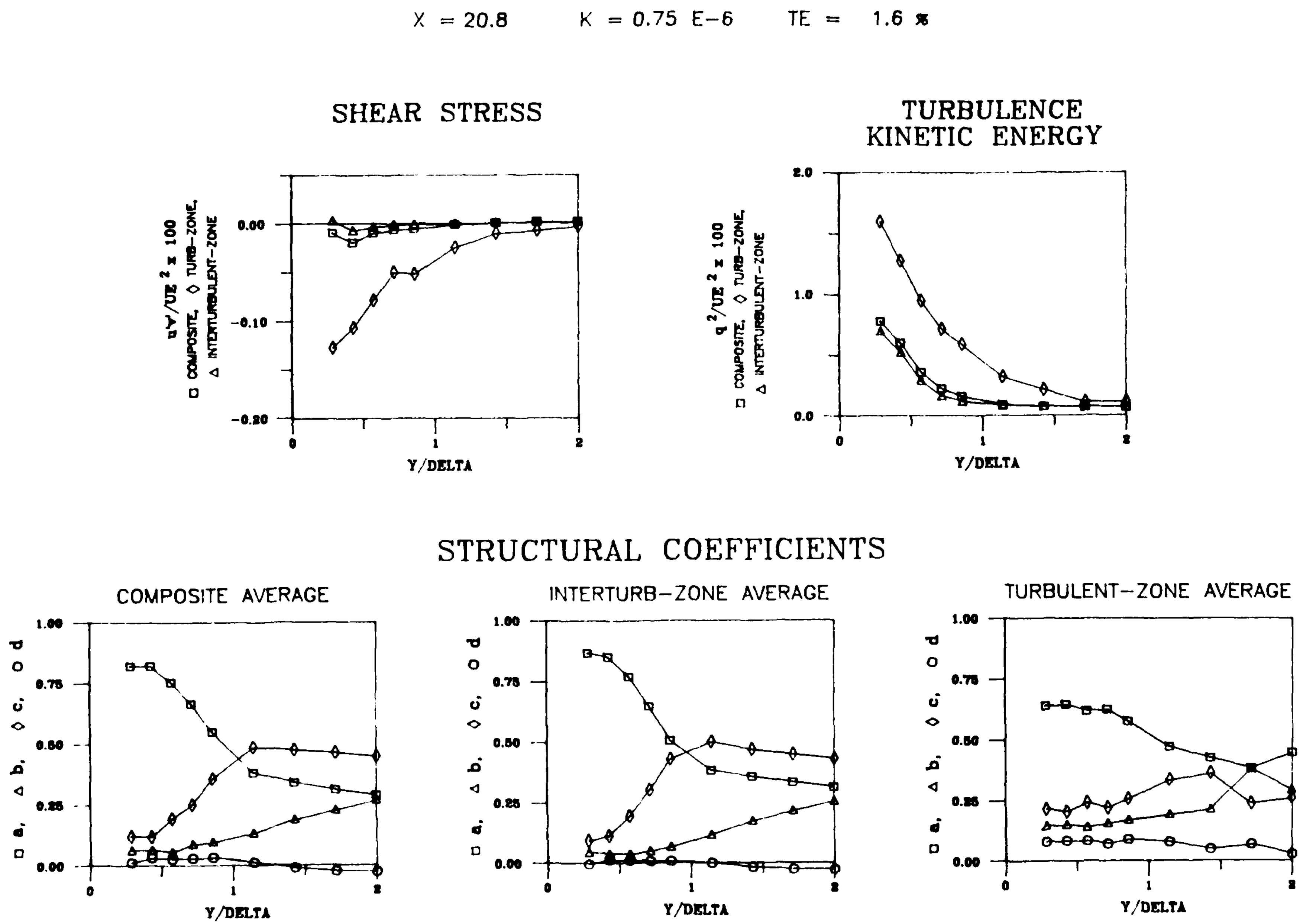

87-10-44-27

Figure 28E. Profiles of Turbulence Stresses

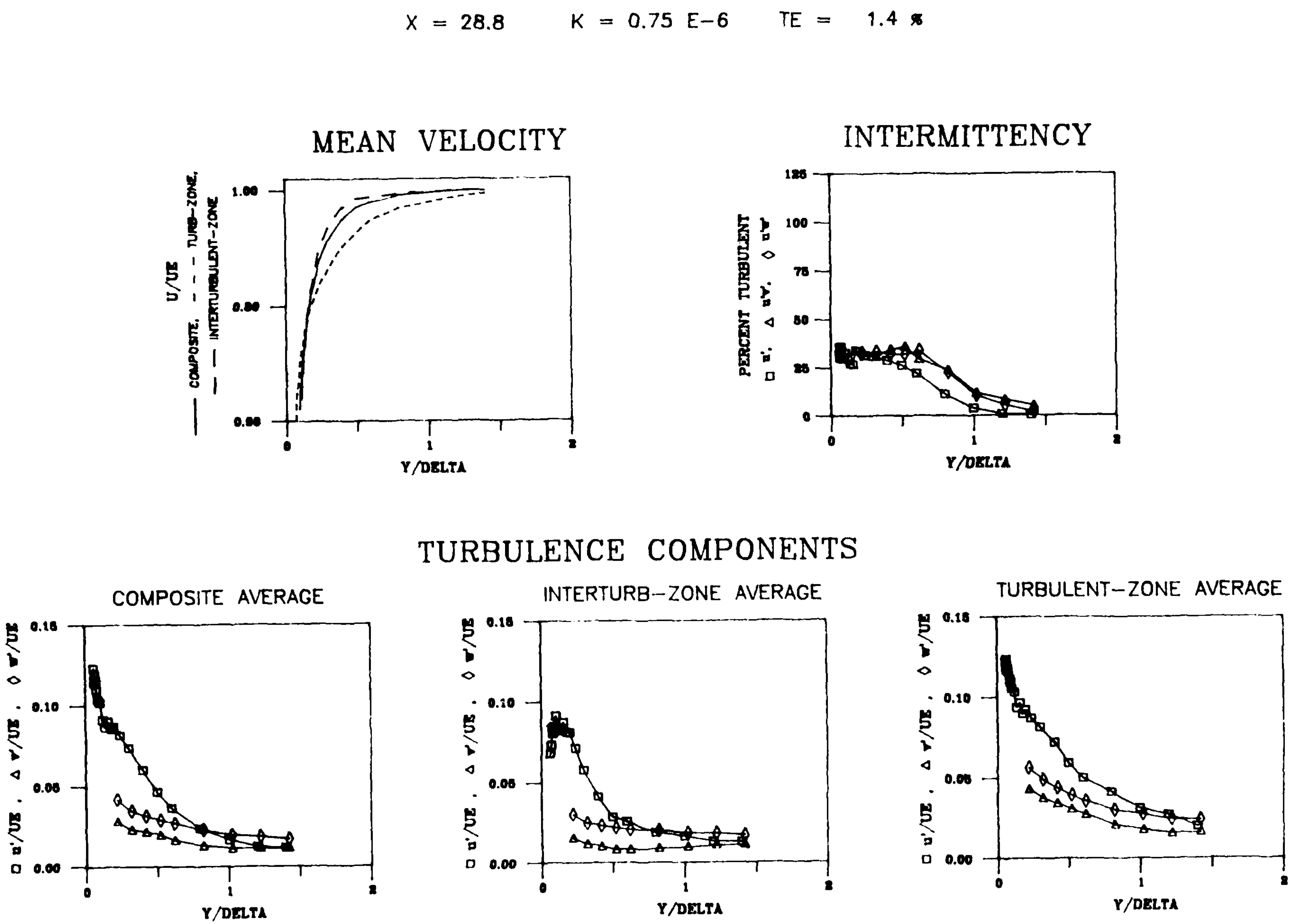

87-10-44-28

Figure 28F. Profiles of Mean and Fluctuating Quantities

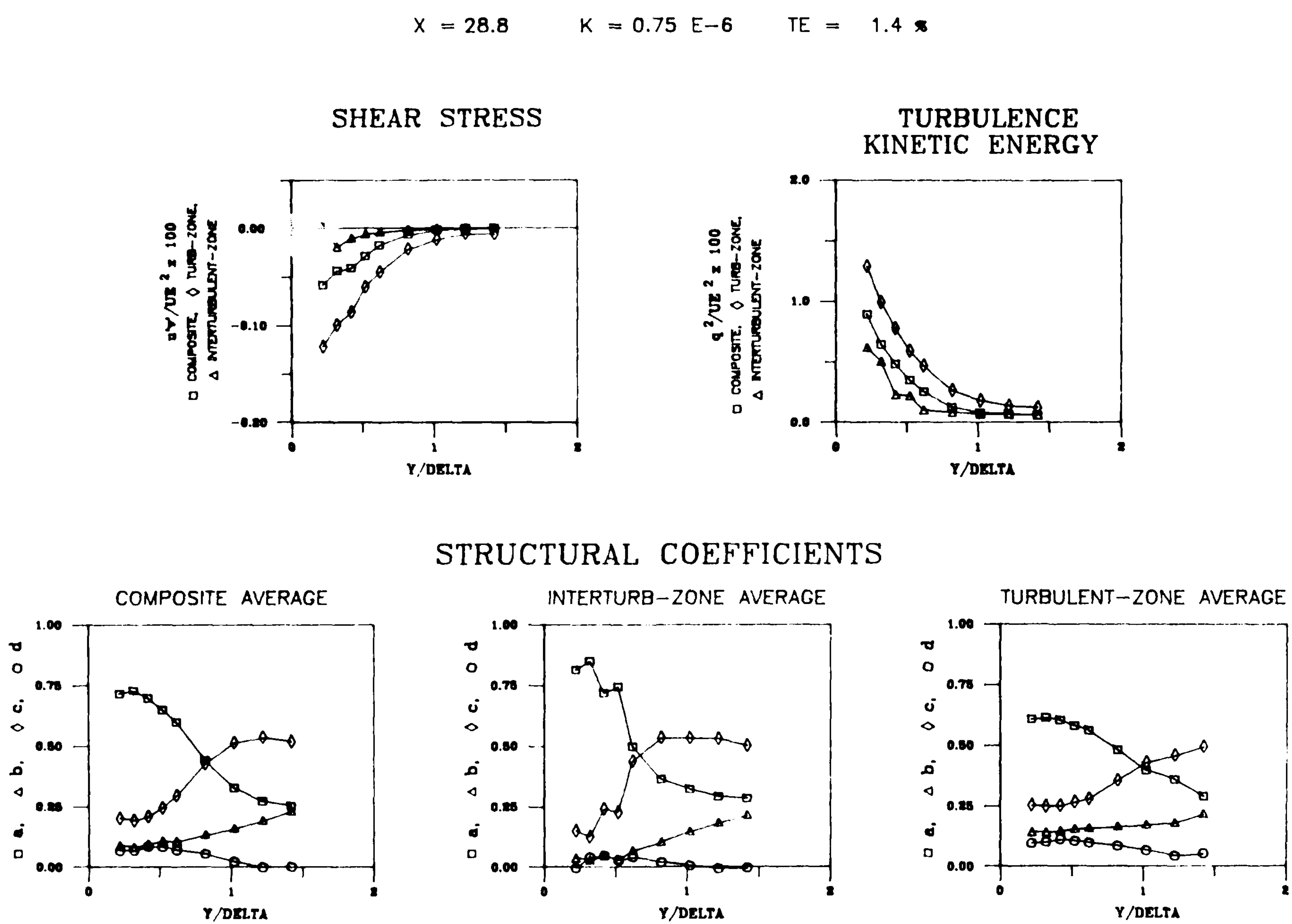

Figure 28G. Profiles of Turbulent Stresses

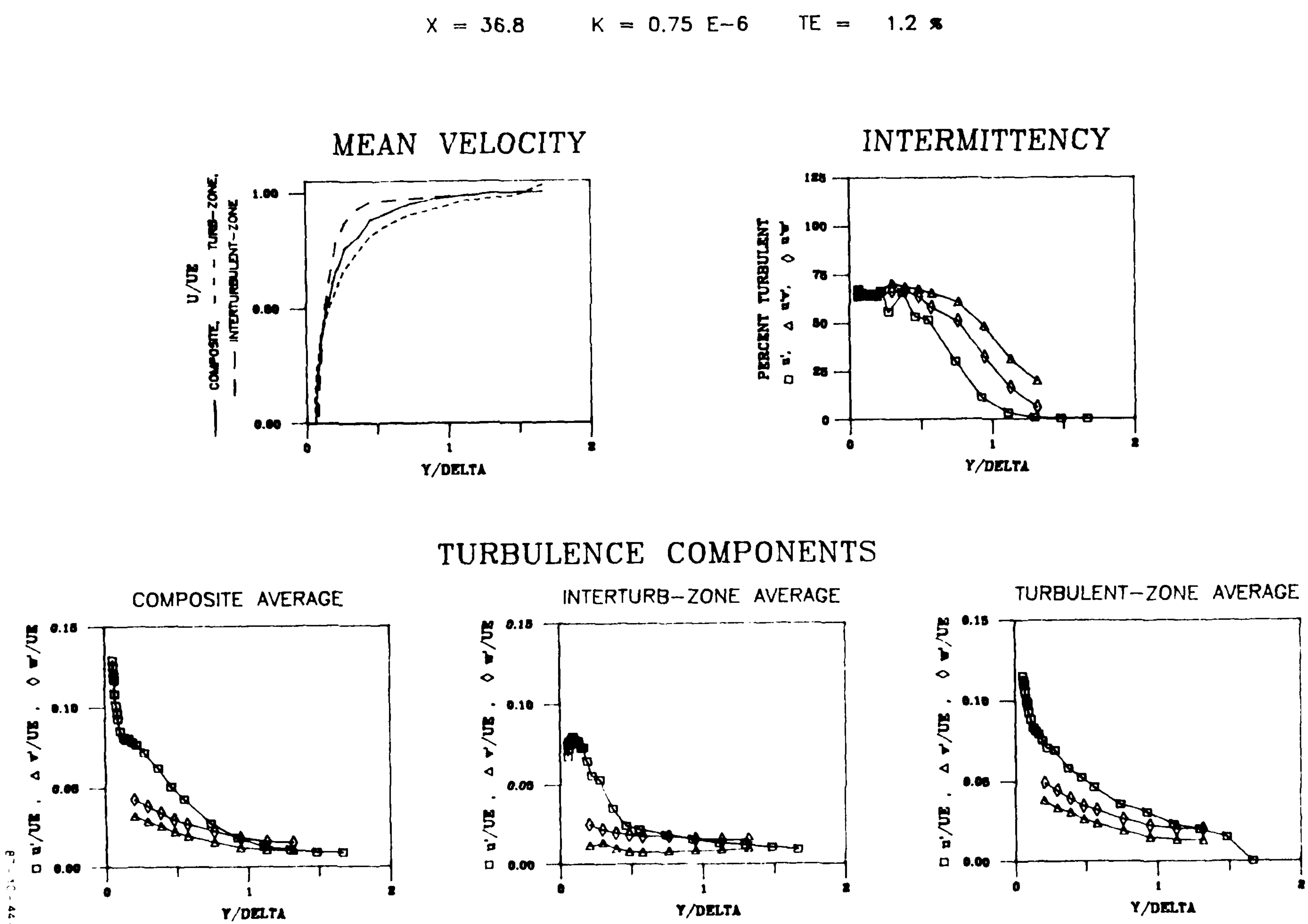

Figure 28H. Profiles of Mean and Fluctuating Quantities

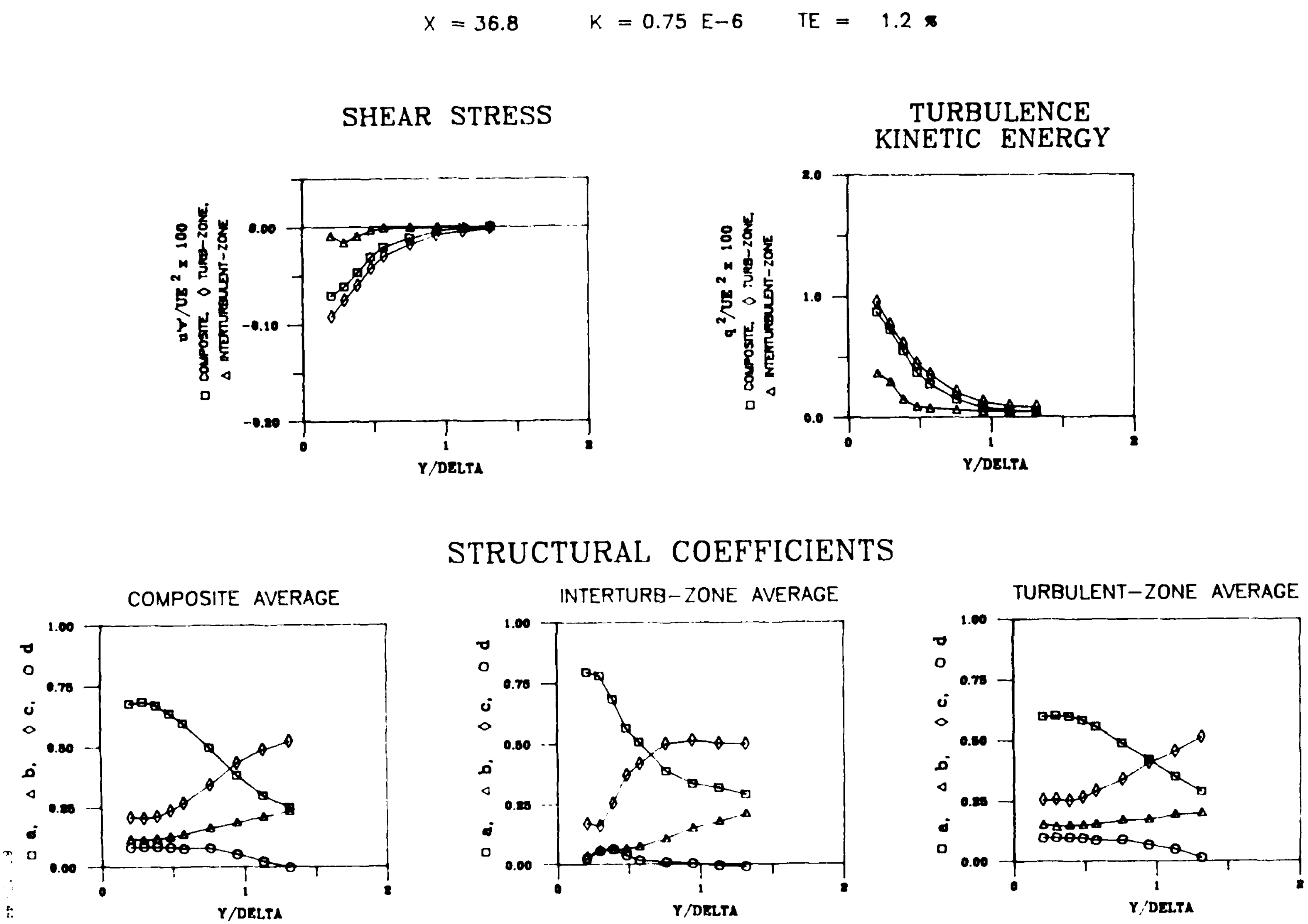

Figure 28I. Profiles of Turbulent Stresses

X = 48.8 K = 0.75 E-6 TE = 0.9 %

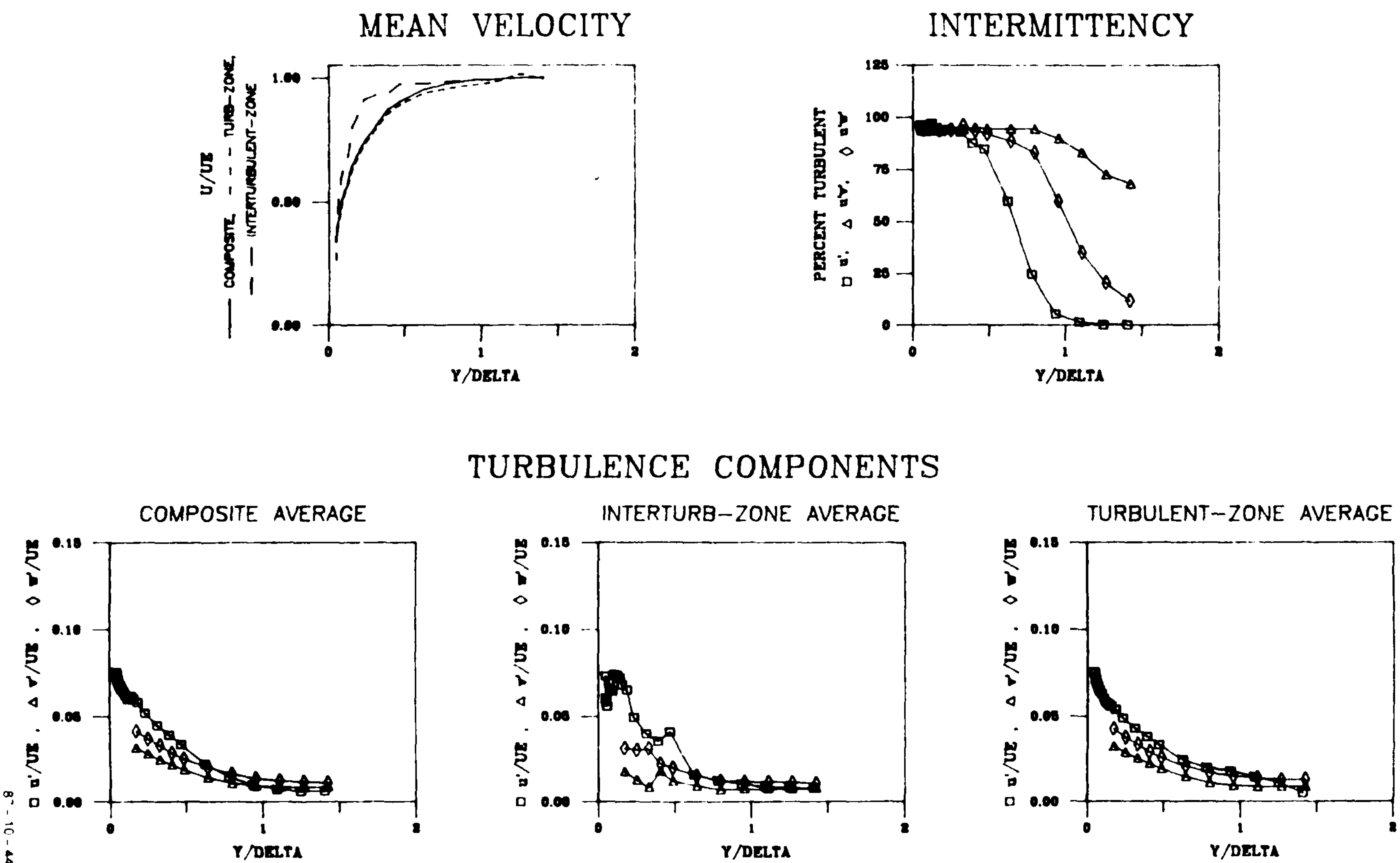

Figure 28J. Profiles of Mean and Fluctuating Quantities

87-10-44-32

X = 48.8 K = 0.75 E-6 TE = 0.9 %

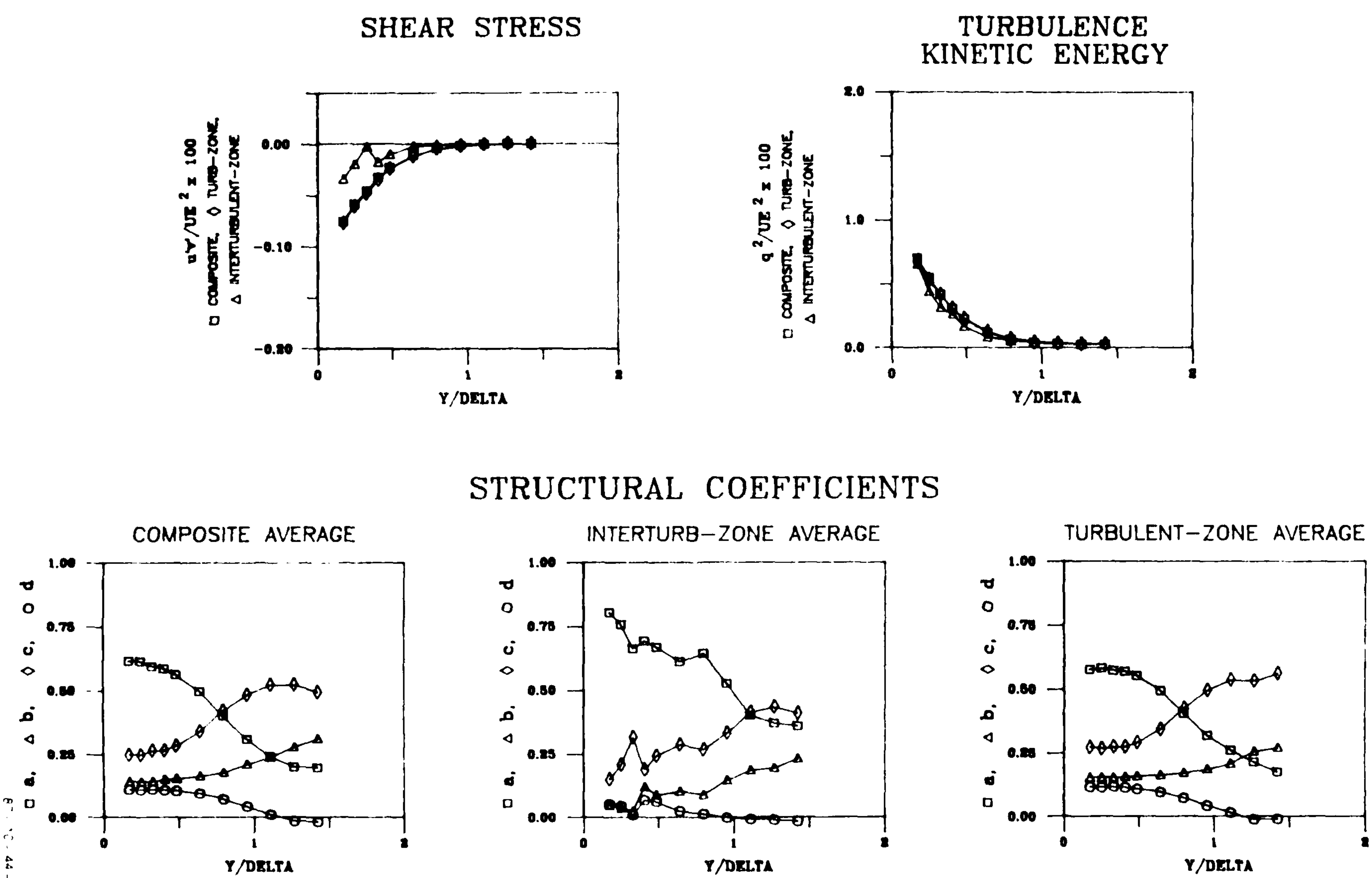

Figure 28K. Profiles of Turbulent Stresses

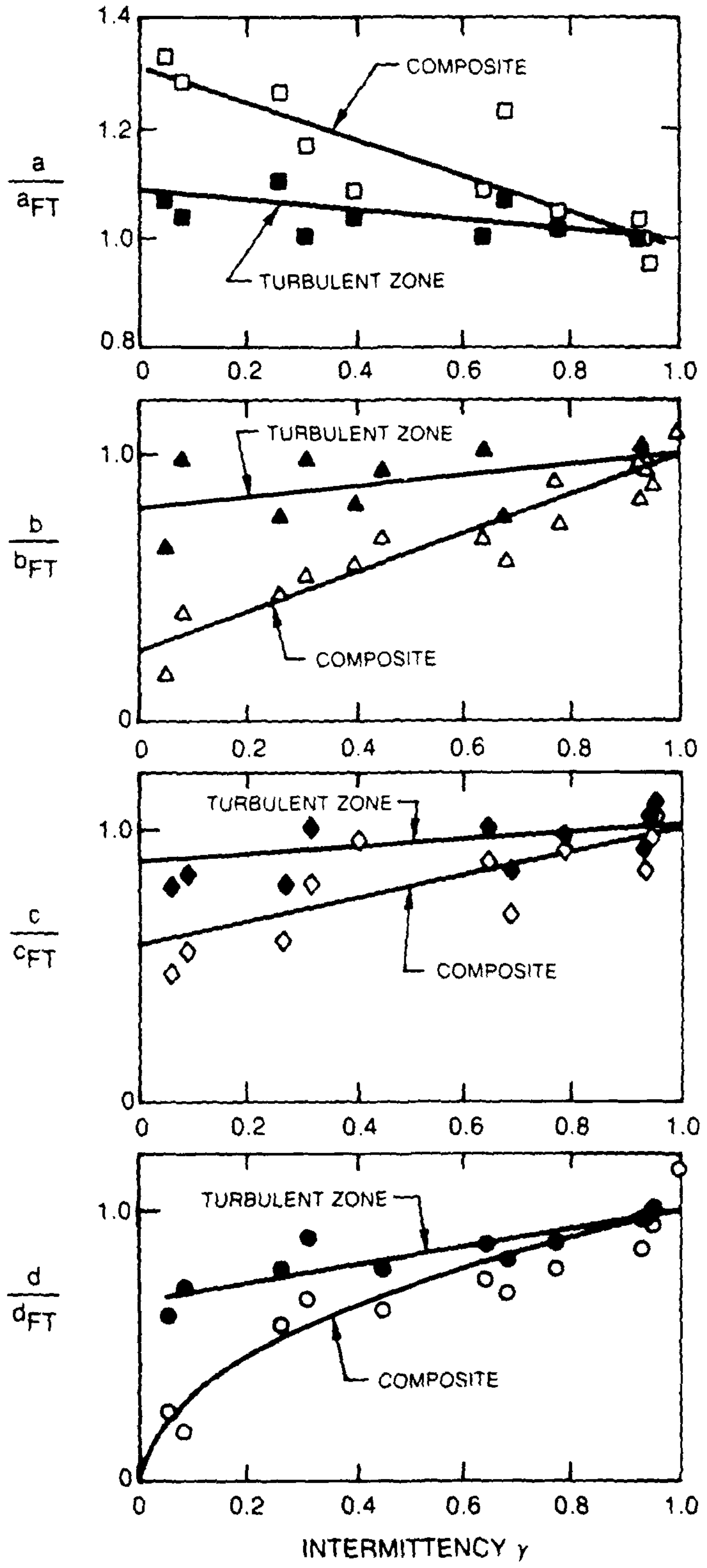

Figure 29. Distribution of the Turbulence Structural Coefficients as a Function of Intermittency

87-10-44-42

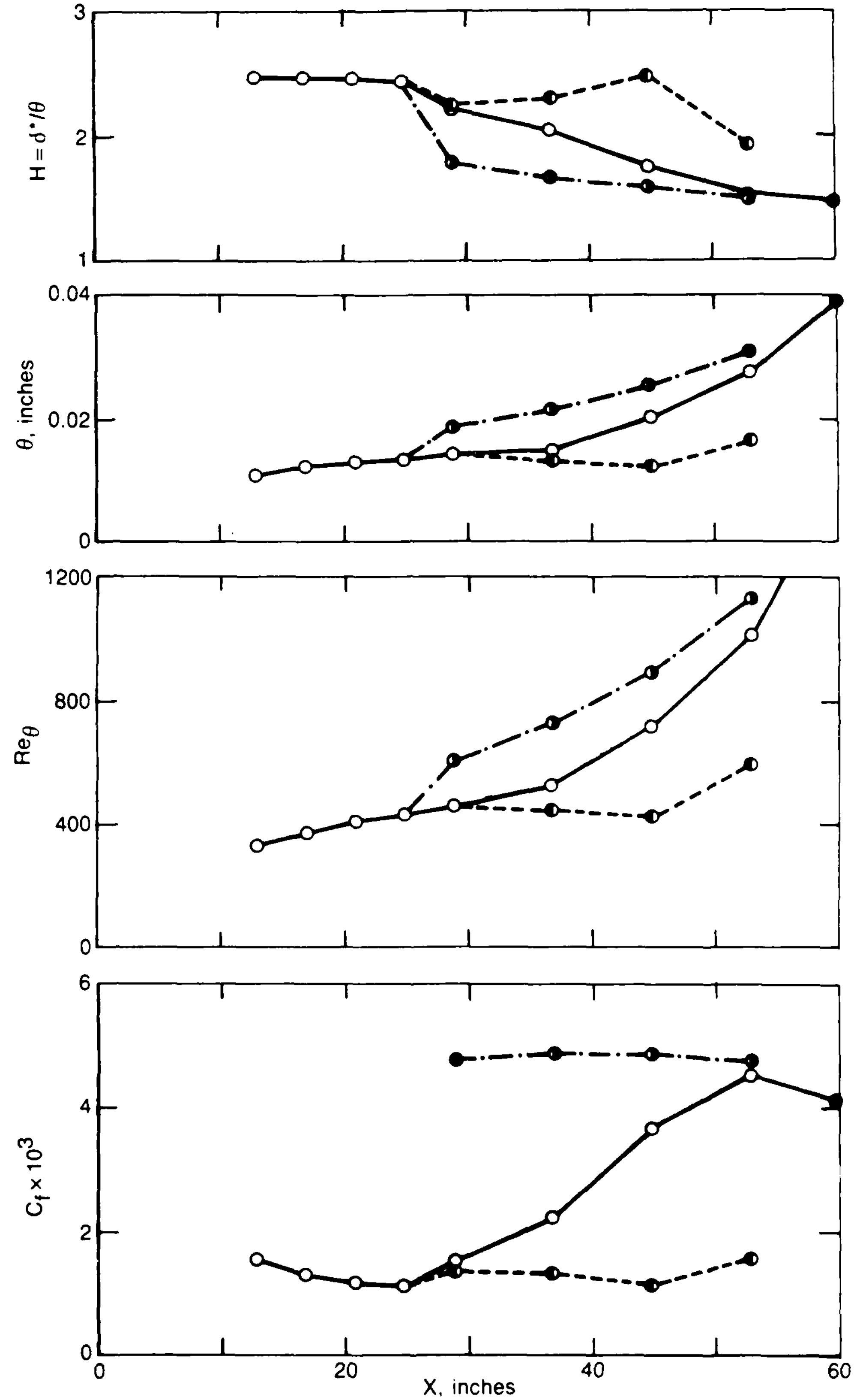

Figure 30. Development of the Mean Velocity Profile Through Transition for $K = 0.2 \times 10^{-6}$ and Grid No. 1 -○——○- Composite, -◐-·-·-◐- Turbulent, -◐----◐- Inter-Turbulent

87-10-44-43

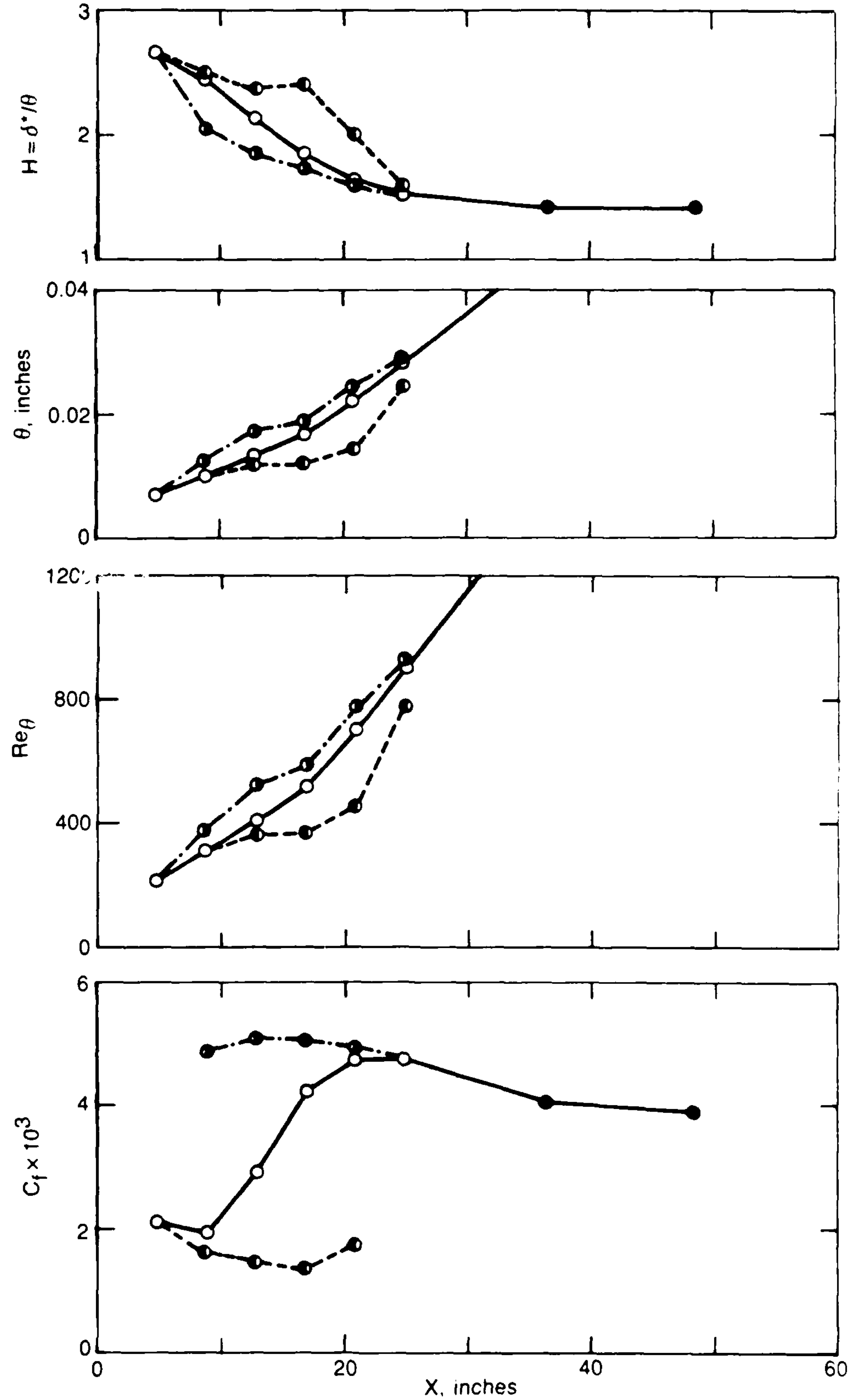

Figure 31. Development of the Mean Velocity Profile Through Transition for $K = 0.2 \times 10^{-6}$ and Grid No. 2 -○———○- Composite, -◐-·—·-◐- Turbulent, -◐----◐- Inter-Turbulent

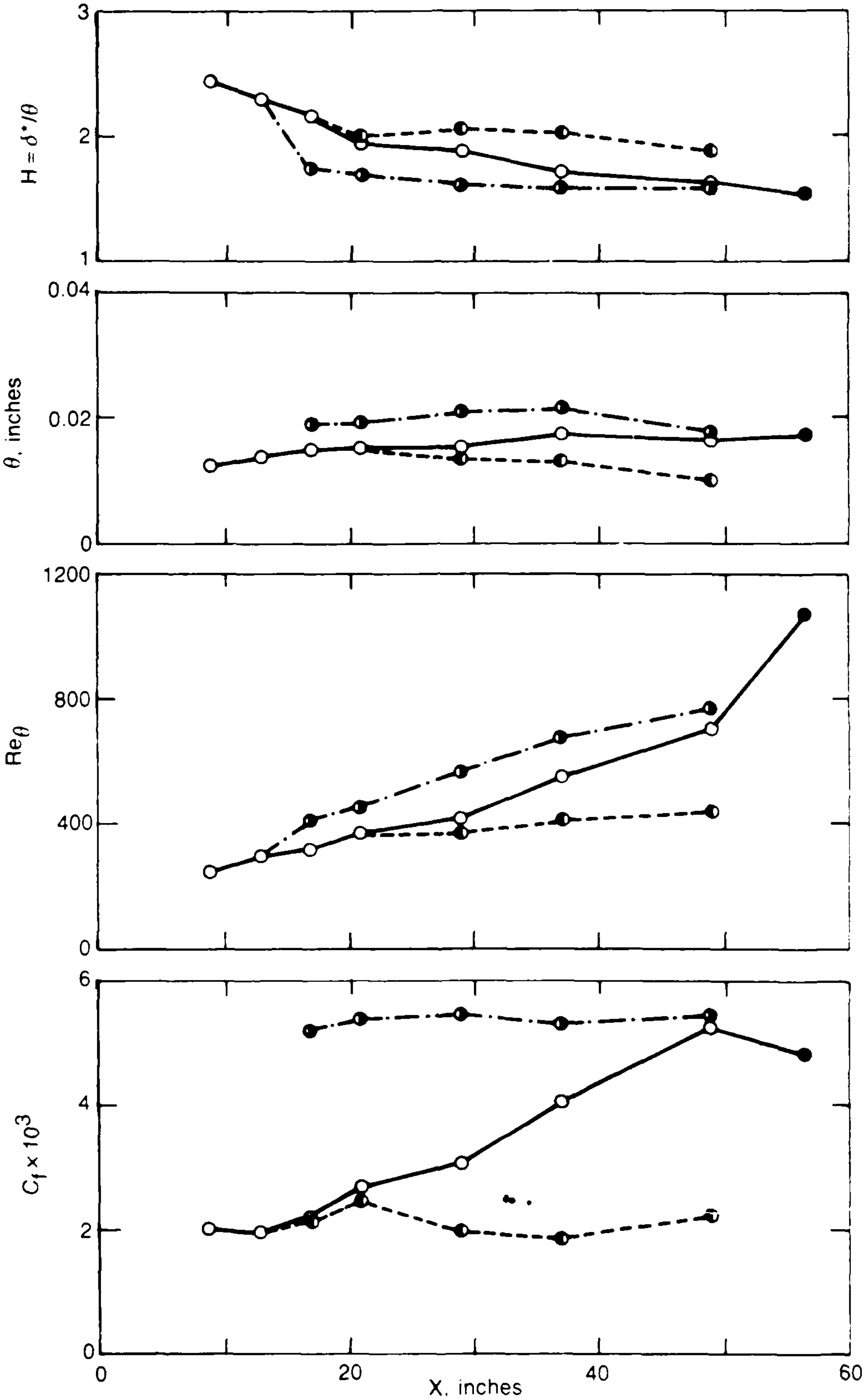

Figure 32. Development of the Mean Velocity Profile Through Transition for $K = 0.75 \times 10^{-6}$ and Grid No. 2 -○——○- Composite, -◑—·—◑- Turbulent, -◐- - - -◐- Inter-Turbulent

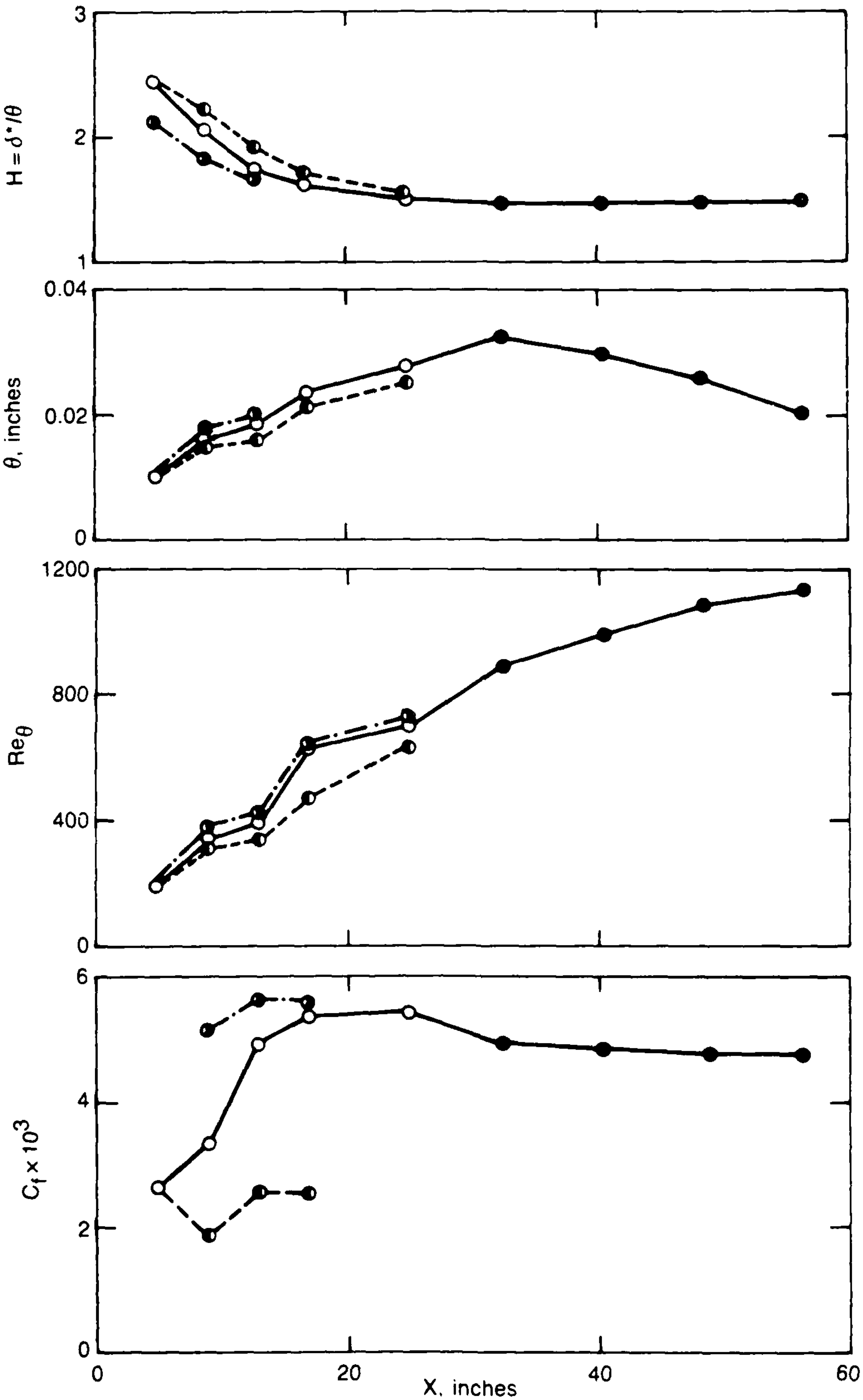

Figure 33. Development of the Mean Velocity Profile Through Transition for $K = 0.75 \times 10^{-6}$ and Grid No. 3 -o——o- Composite, -◐-·—-◐- Turbulent, -◐---◐- Inter-turbulent

87 - 10 - 44 - 46

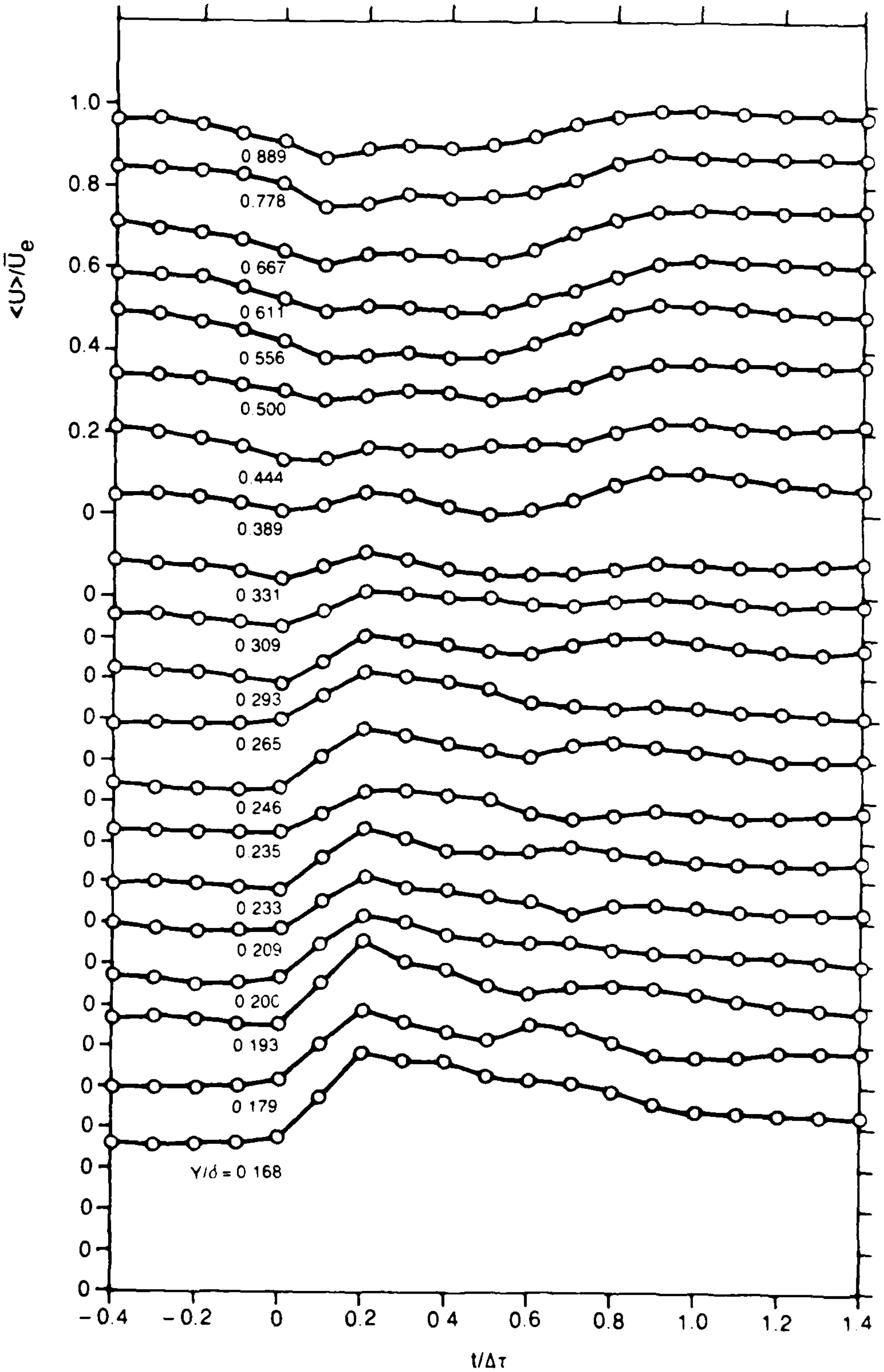

Figure 34. Ensemble Averaged Velocity Variations Through the Turbulent Zone at Various Distances From the Wall X = 4.4 in., $K = 0.75 \times 10^{-6}$, $T_e = 4.7\%$, $\gamma_{(near\text{-}wall)} = 0.12$

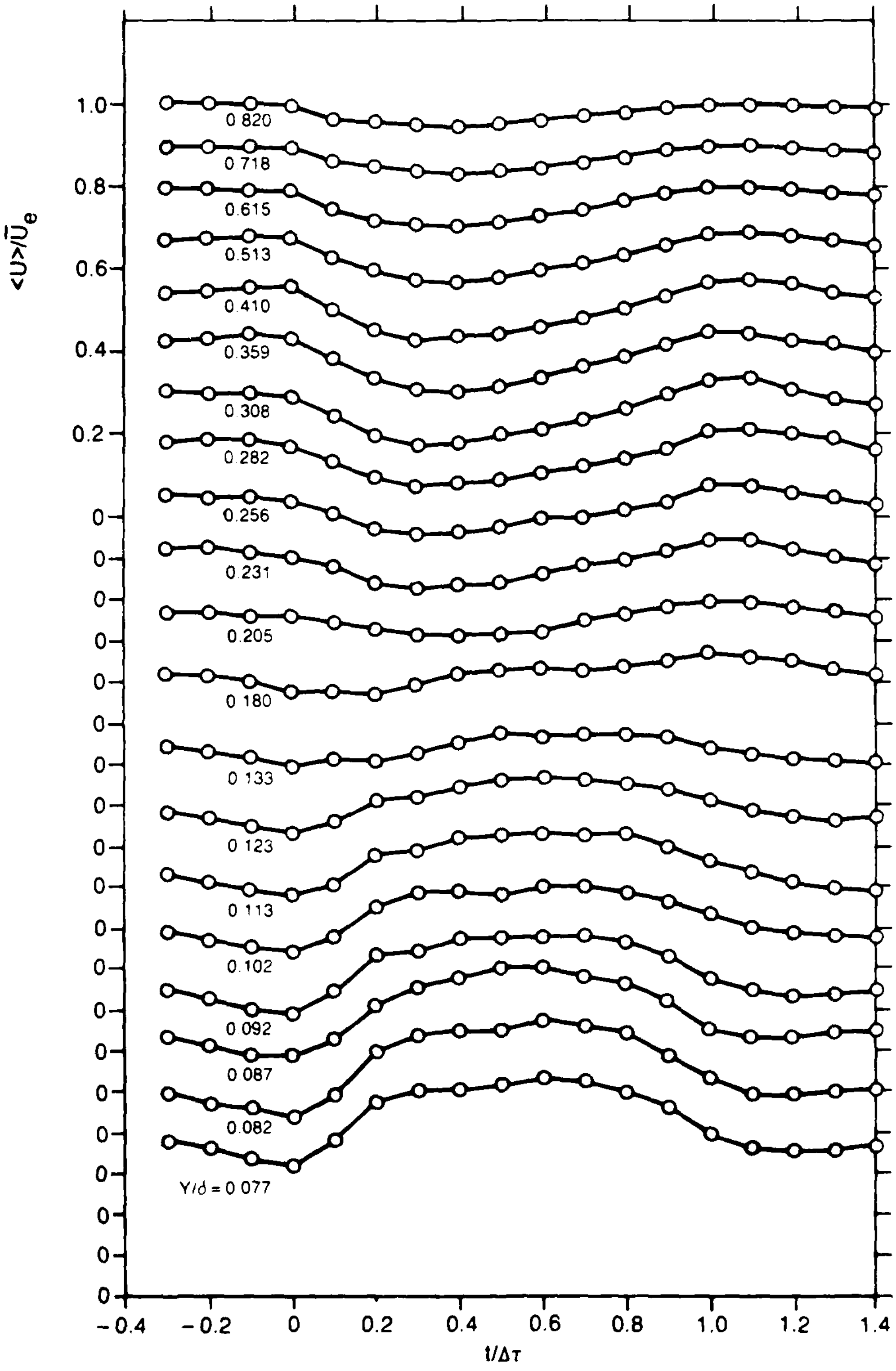

Figure 35. Ensemble Averaged Velocity Variations Through the Turbulent Zone at Various Distances From the Wall X = 16.8 in., $K = 0.2 \times 10^{-6}$, $T_e = 1.7\%$, $\gamma_{(\text{near-wall})} = 0.78$

87 - 10 - 44 - 50

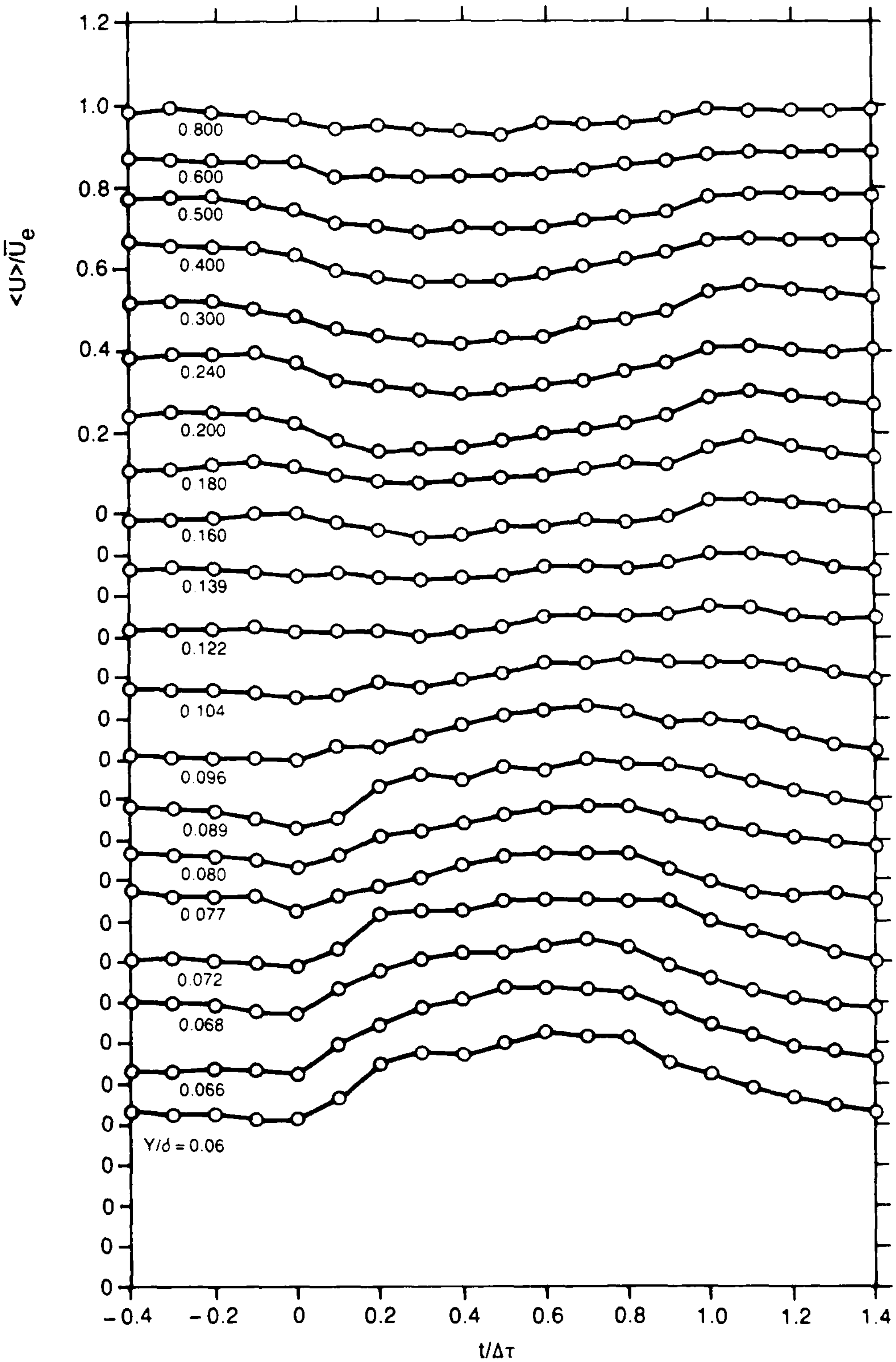

Figure 36. **Ensemble Averaged Velocity Variations Through the Turbulent Zone at Various Distances From the Wall X = 28.8 in., K = 0.75×10^{-6}, T_e = 1.4%. $\gamma_{(near\text{-}wall)} = 0.31$**

8? - 10 - 44 - 52

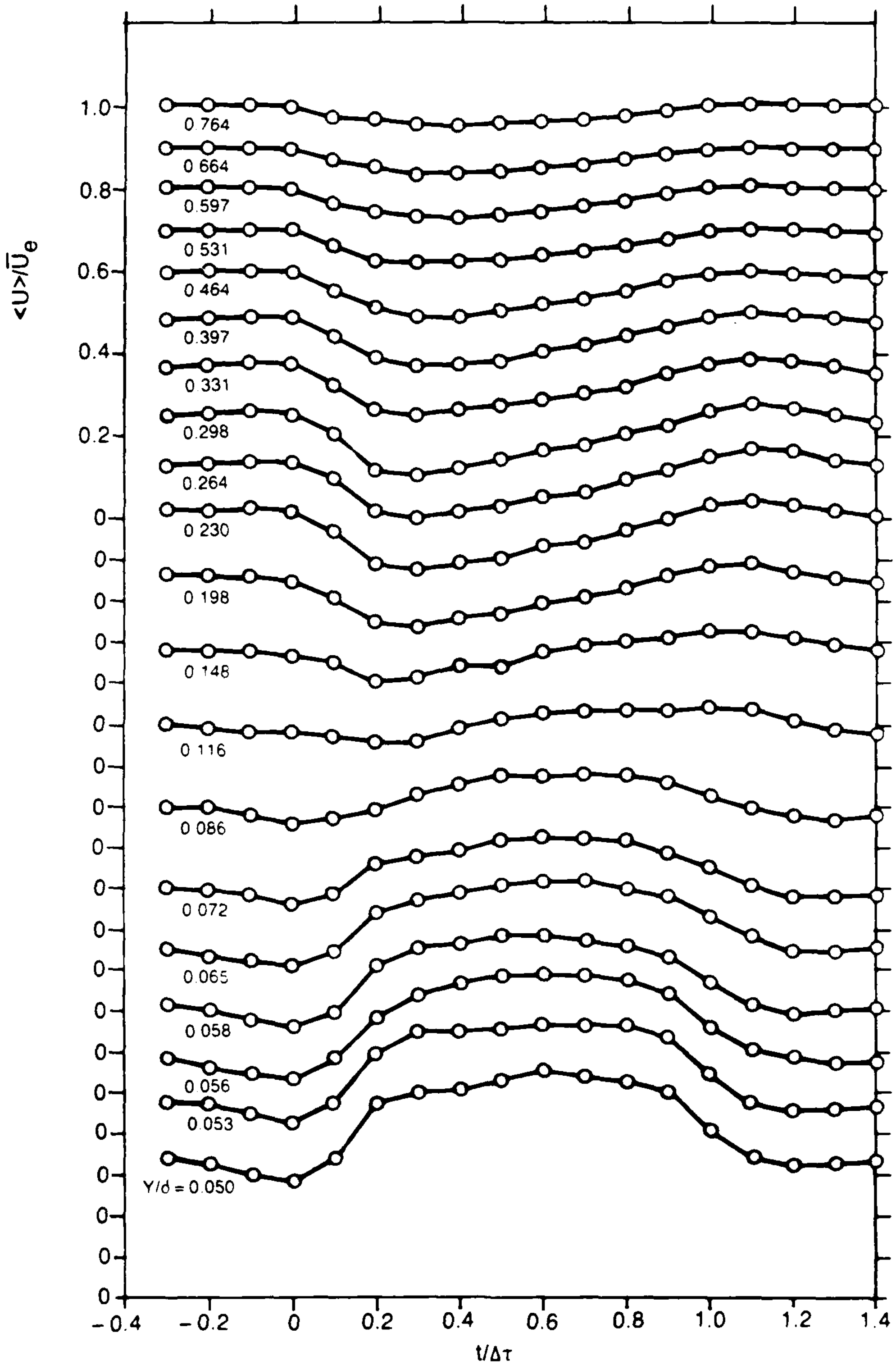

Figure 37. Ensemble Averaged Velocity Variations Through the Turbulent Zone at Various Distances From the Wall X = 44.8 in., $K = 0.2 \times 10^{-6}$, $T_E = 0.74\%$, $\gamma_{(near\text{-}wall)} = 0.68$

87 - 10 - 44 - 51

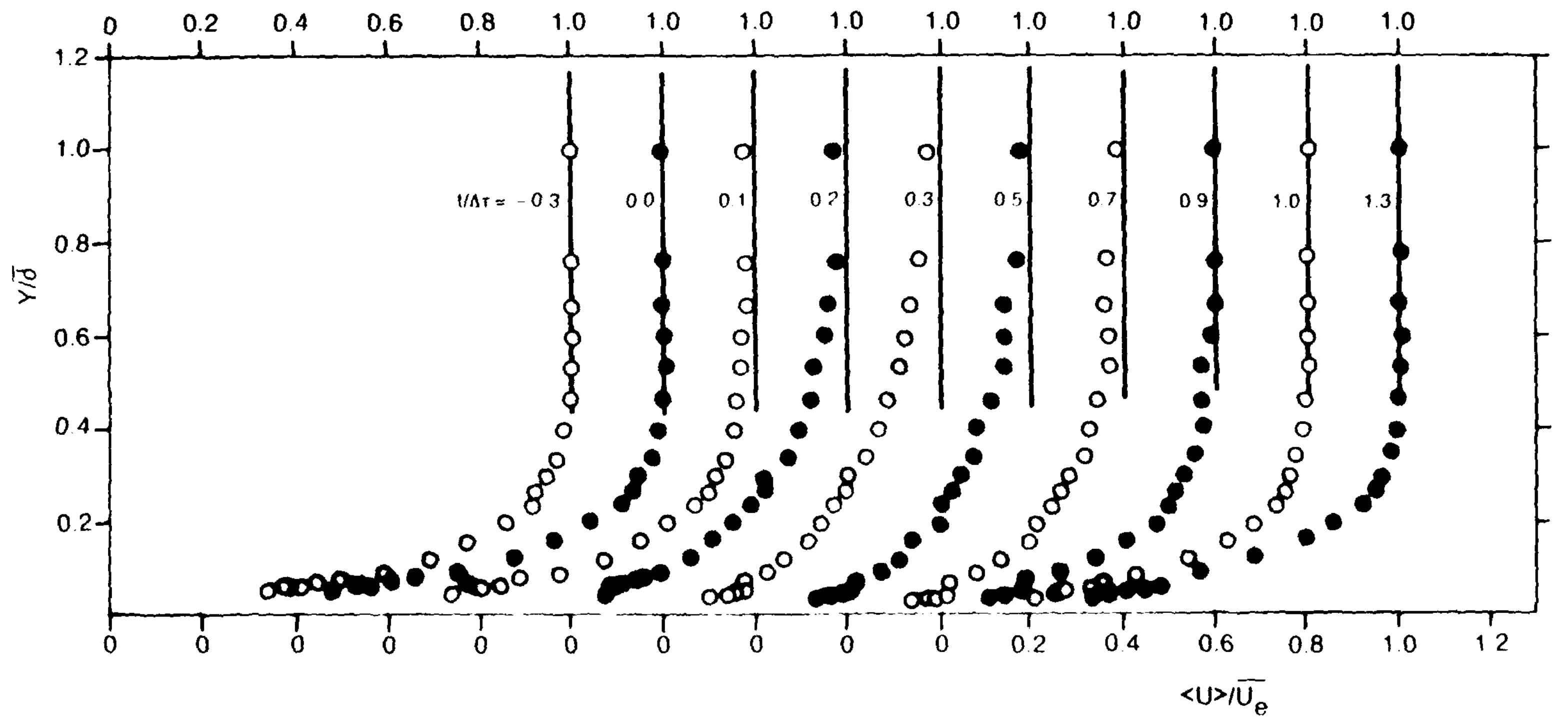

Figure 38. Ensemble Averaged Velocity Profiles Through the Turbulent Zone (From Fig. 37) $X = 44.8$ in., $K = 0.2 \times 10^{-6}$, $T_E = 0.74\%$, $\gamma_{(near\text{-}wall)} = 0.68$

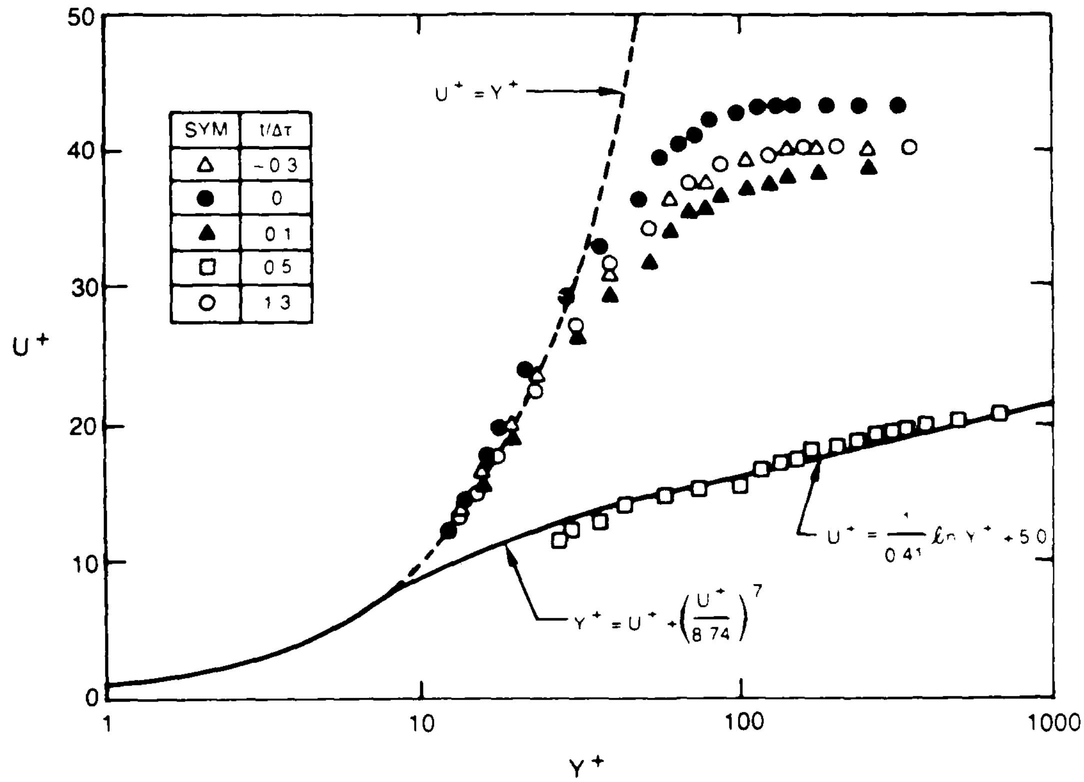

Figure 39. **Ensemble Averaged Velocity Profiles Through the Turbulent Zone in Turbulent Boundary Layer Co-Ordinates X = 44.8 in., K = 0.2 × 10^{-6}, T$_E$ = 0.74%, $\gamma_{\text{(near-wall)}}$ = 0.68**

8? - 10 - 44 - 4?

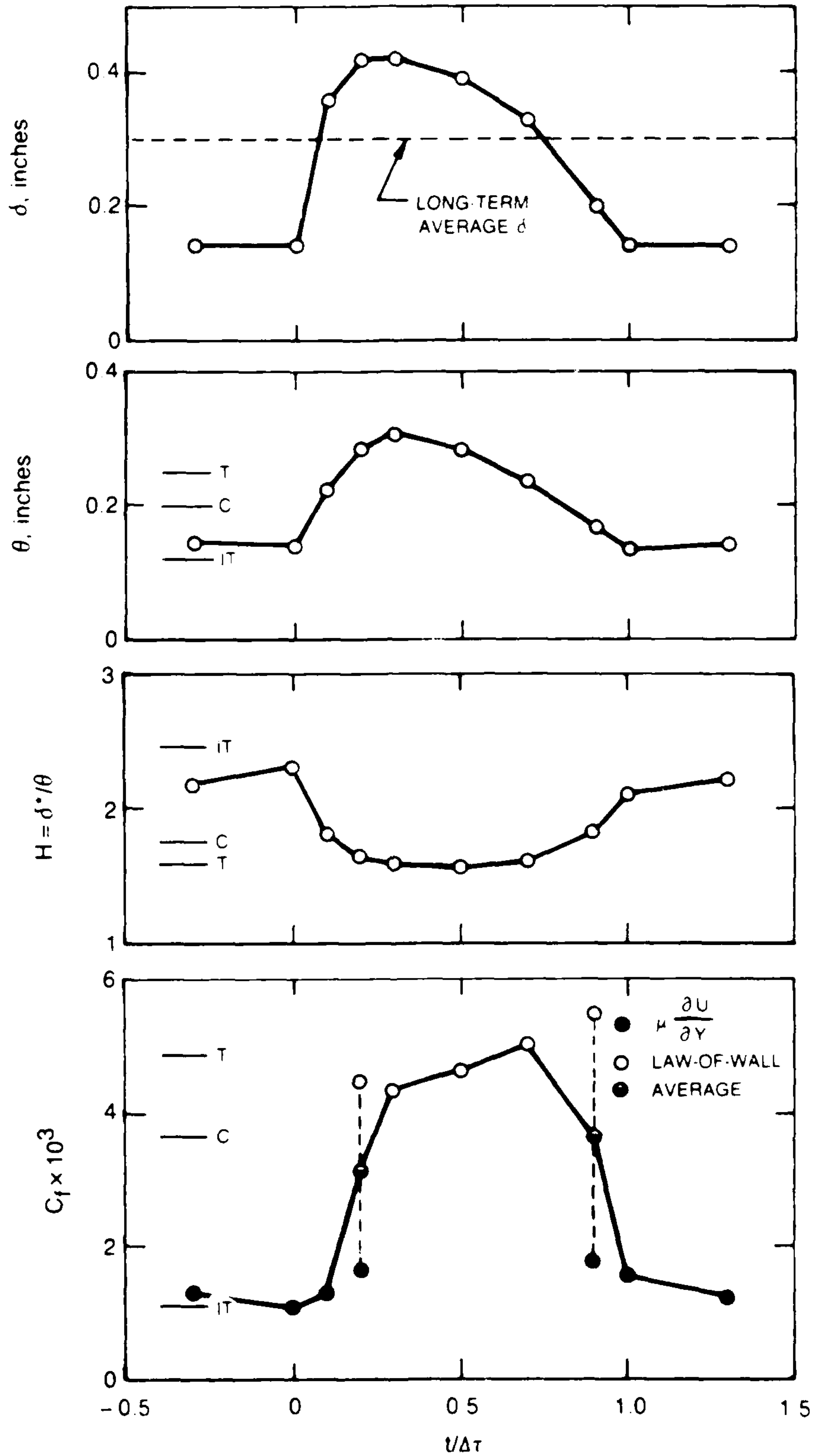

Figure 40. Profile and Skin-Friction Variations Through the Turbulent Zone Computed From the Ensemble Averaged Velocity Profiles X = 44.8 in., $K = 0.2 \times 10^{-6}$, $T_E = 0.74\%$, $\gamma_{(near\text{-}wall)} = 0.68$

8? - 10 - 44 - 46

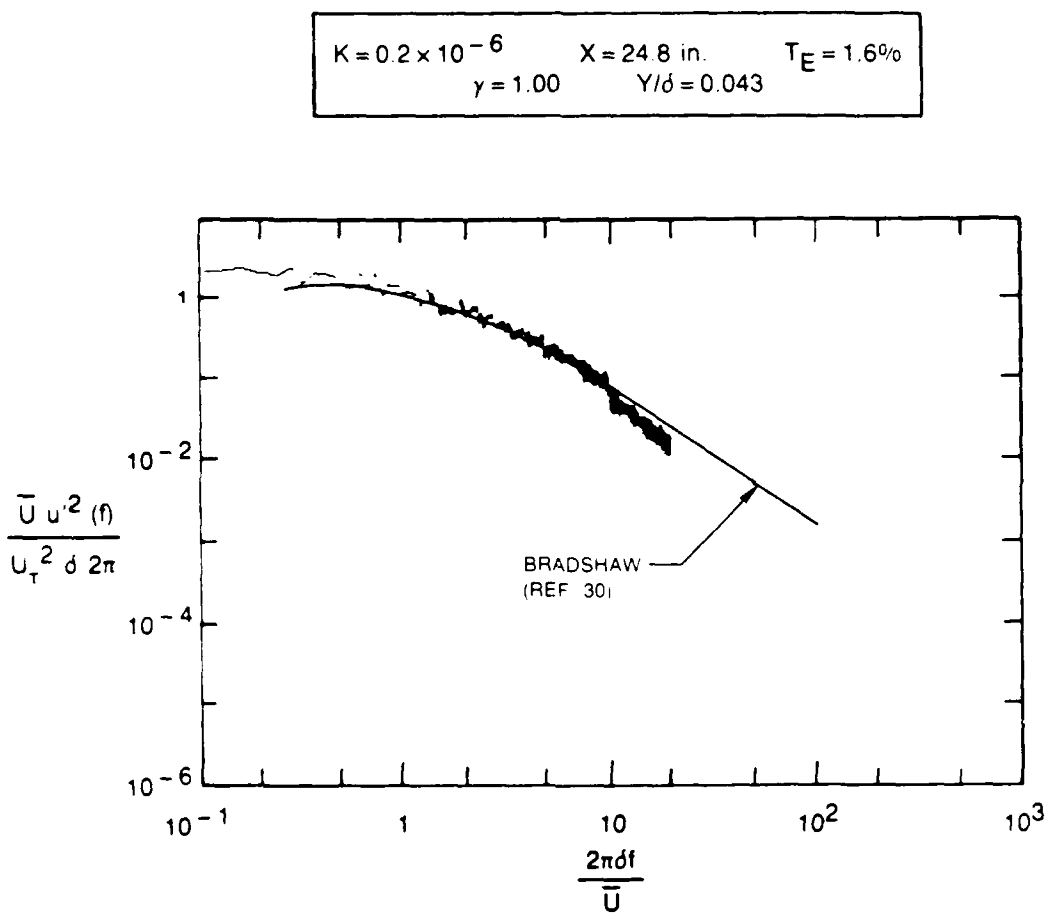

Figure 41. Power Spectral Density Distribution for a Fully Turbulent Profile.

87 - 10 - 44 - 16

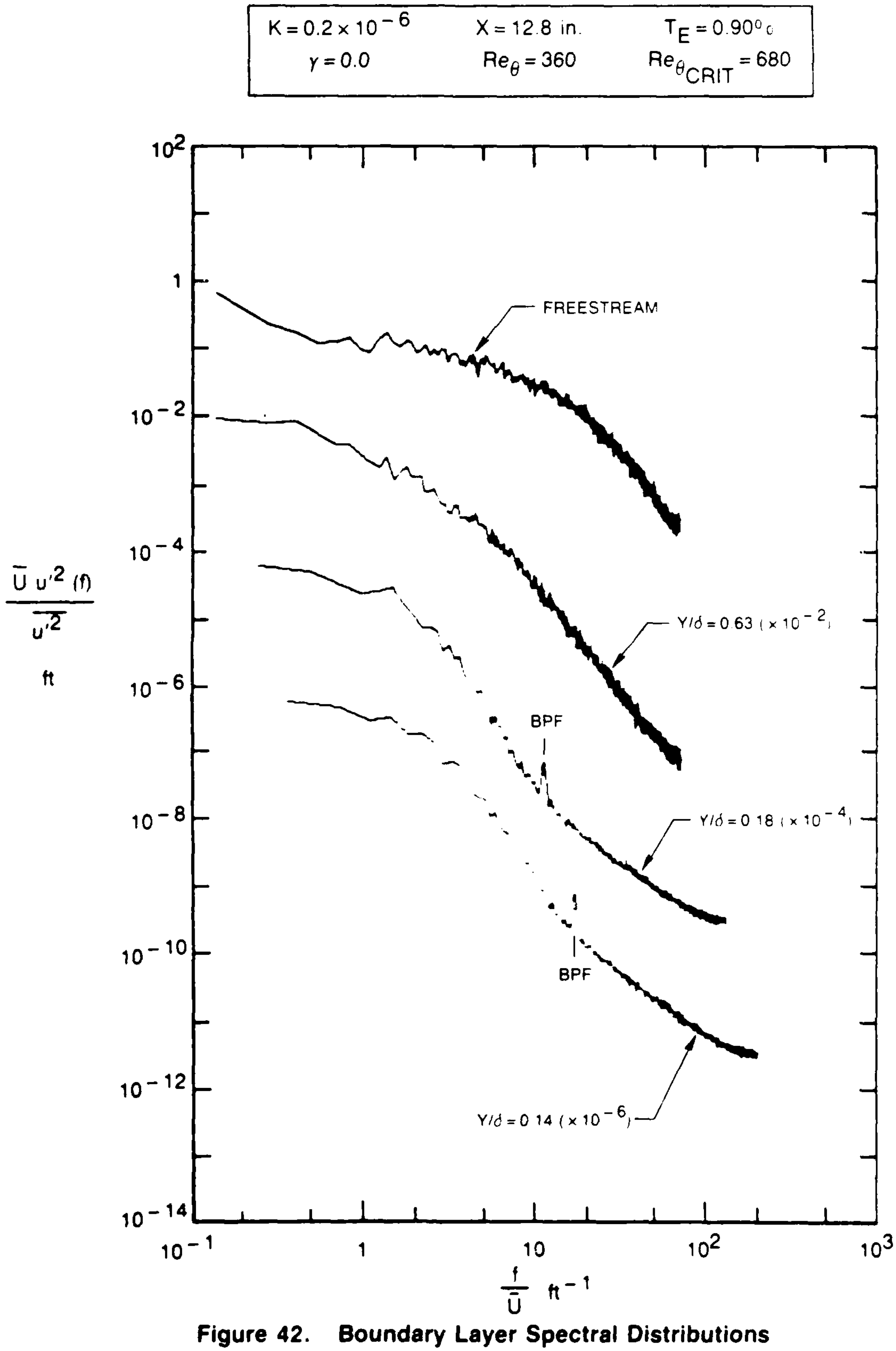

Figure 42. Boundary Layer Spectral Distributions

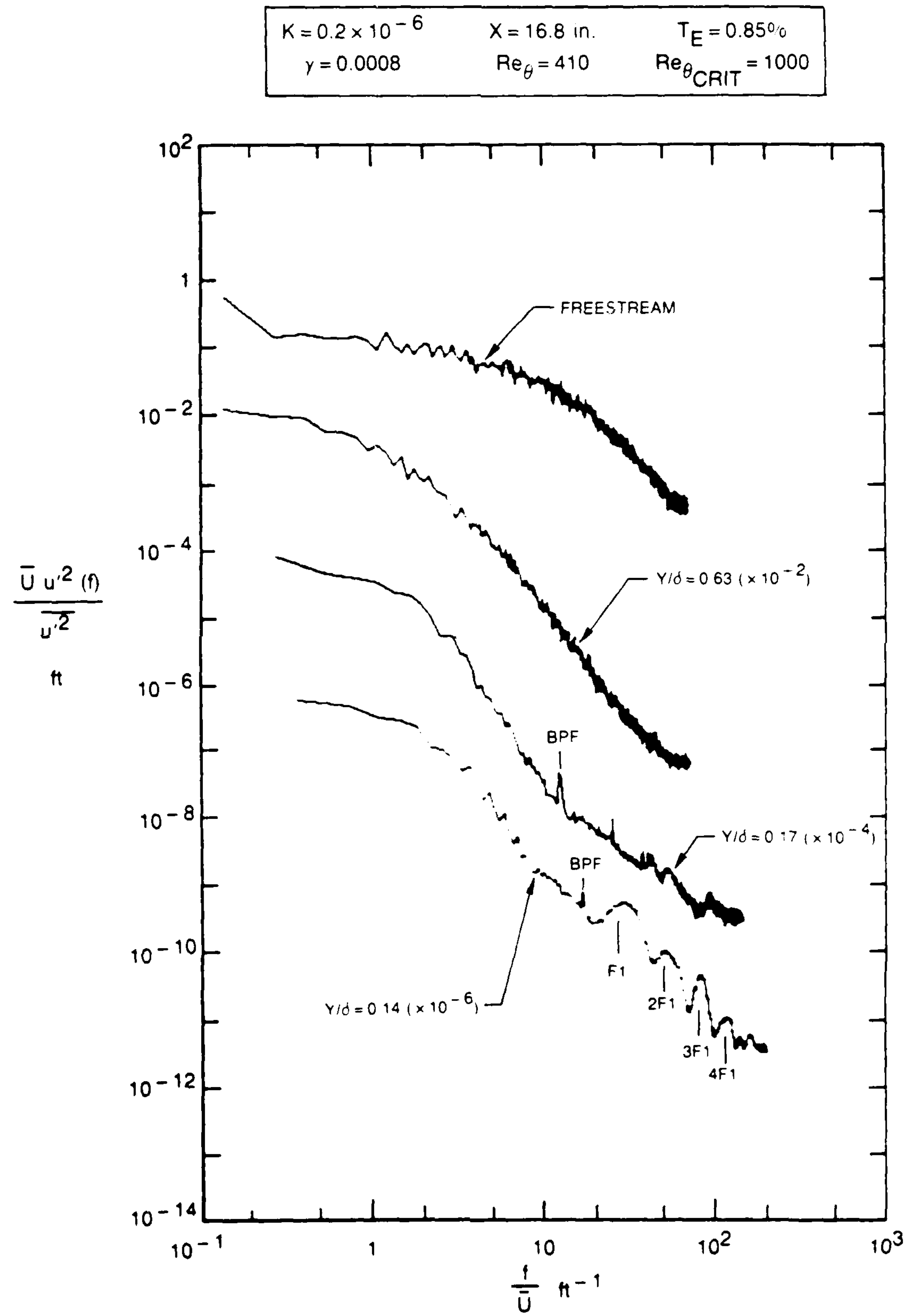

Figure 43. Boundary Layer Spectral Distributions

87 - 10 - 44 - 18

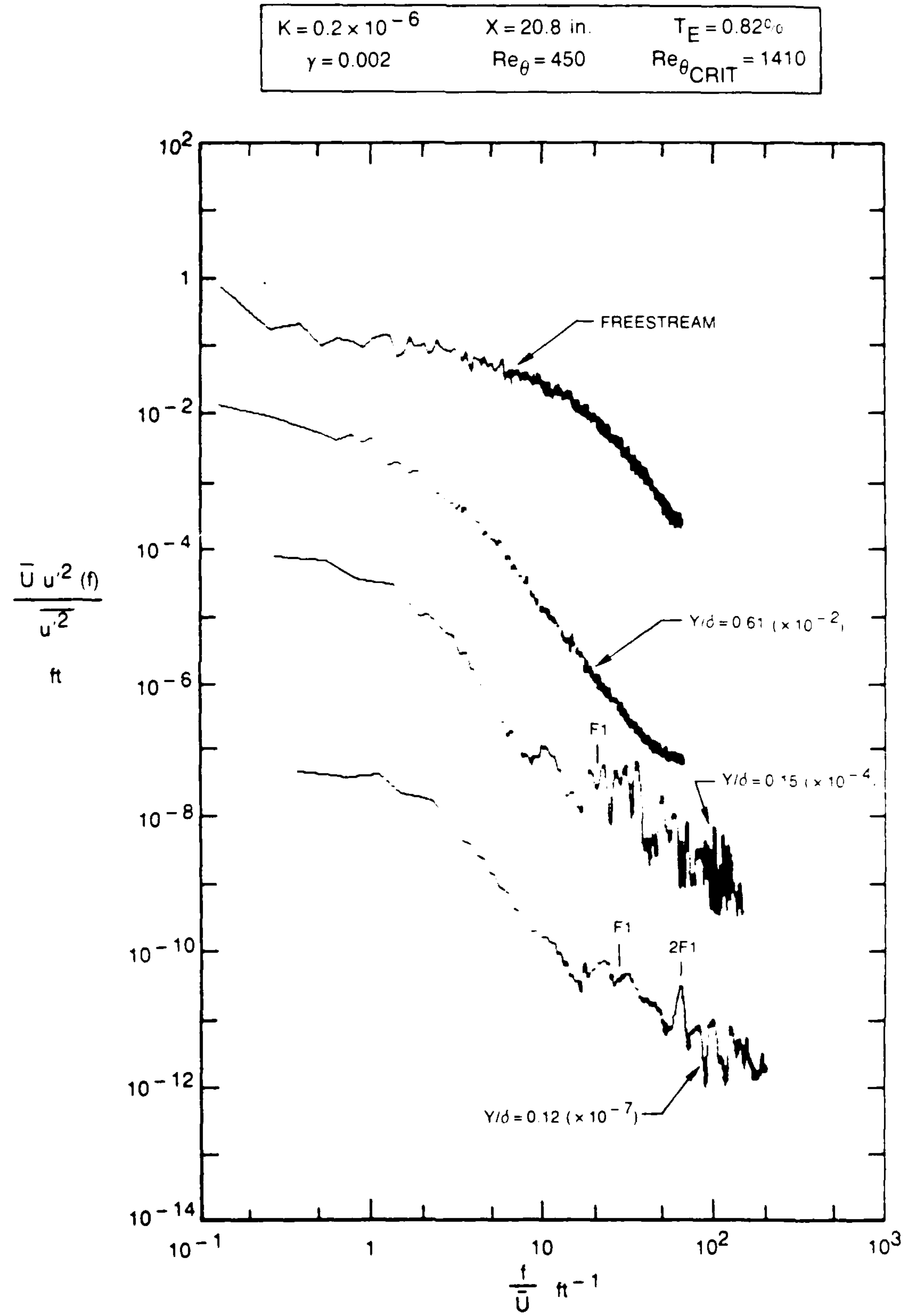

Figure 44. Boundary Layer Spectral Distributions

87-10-44-19

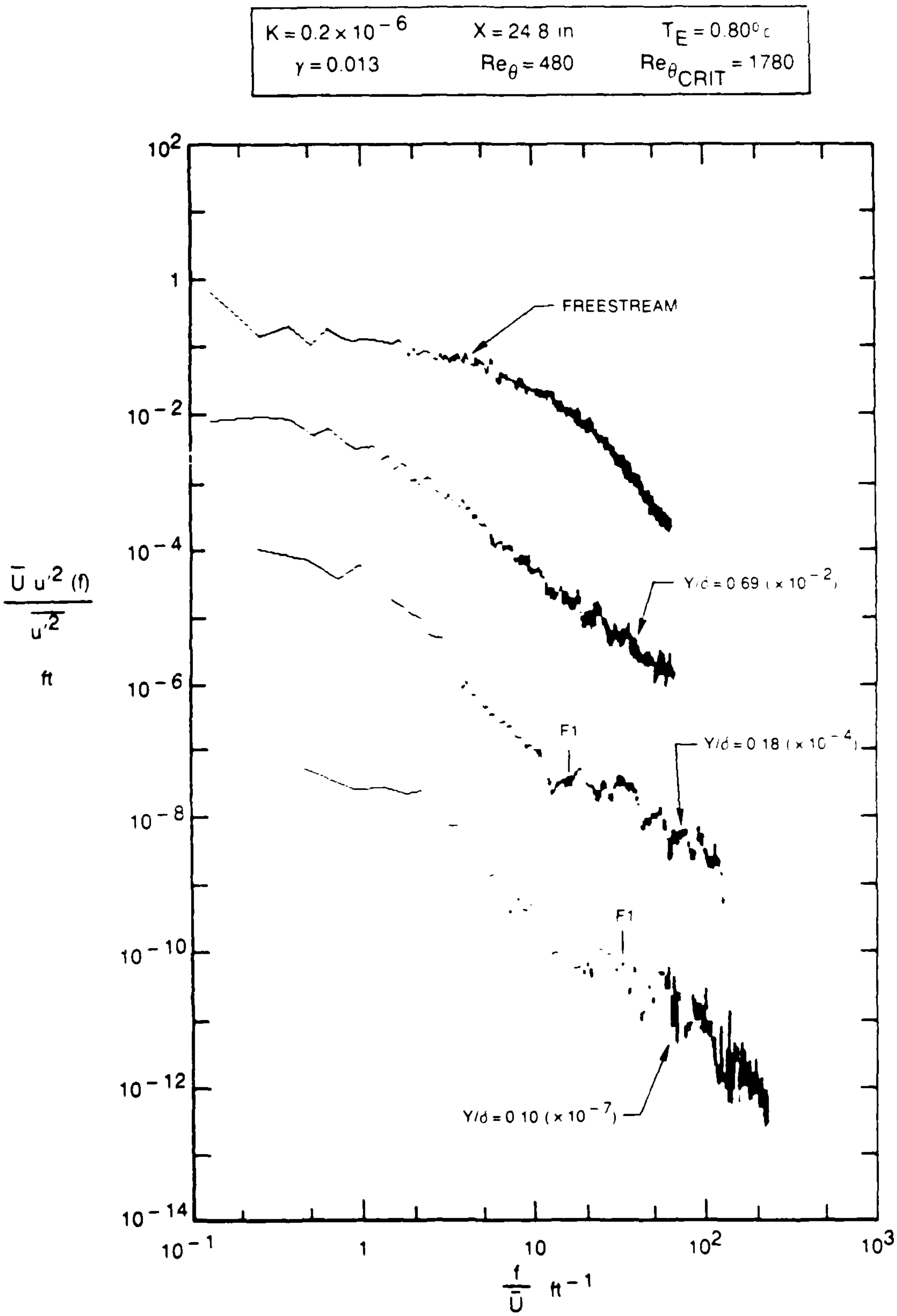

Figure 45. Boundary Layer Spectral Distributions

8? - 10 - 44 - 20

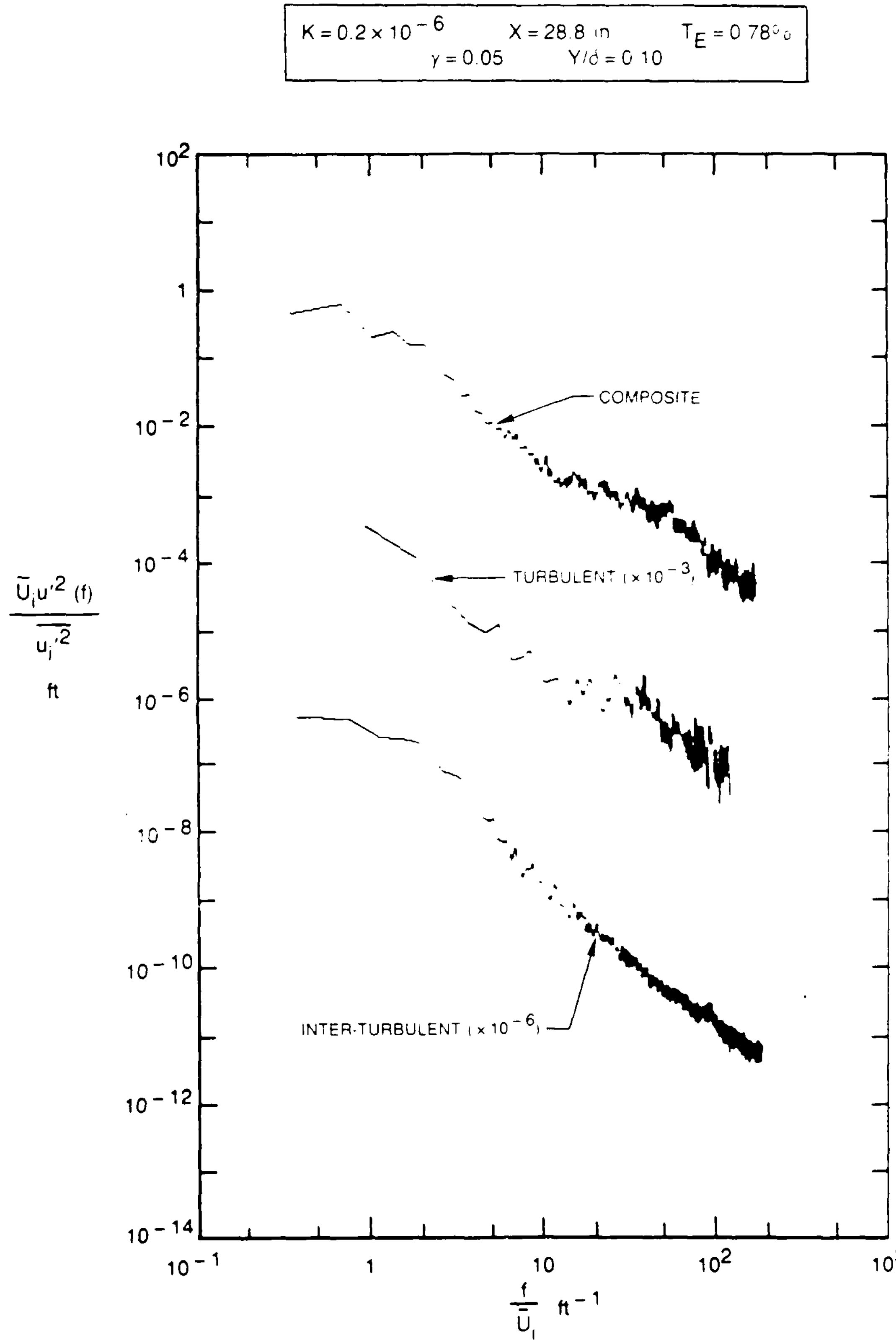

Figure 46. Conditionally Sampled Boundary Layer Spectral Distributions

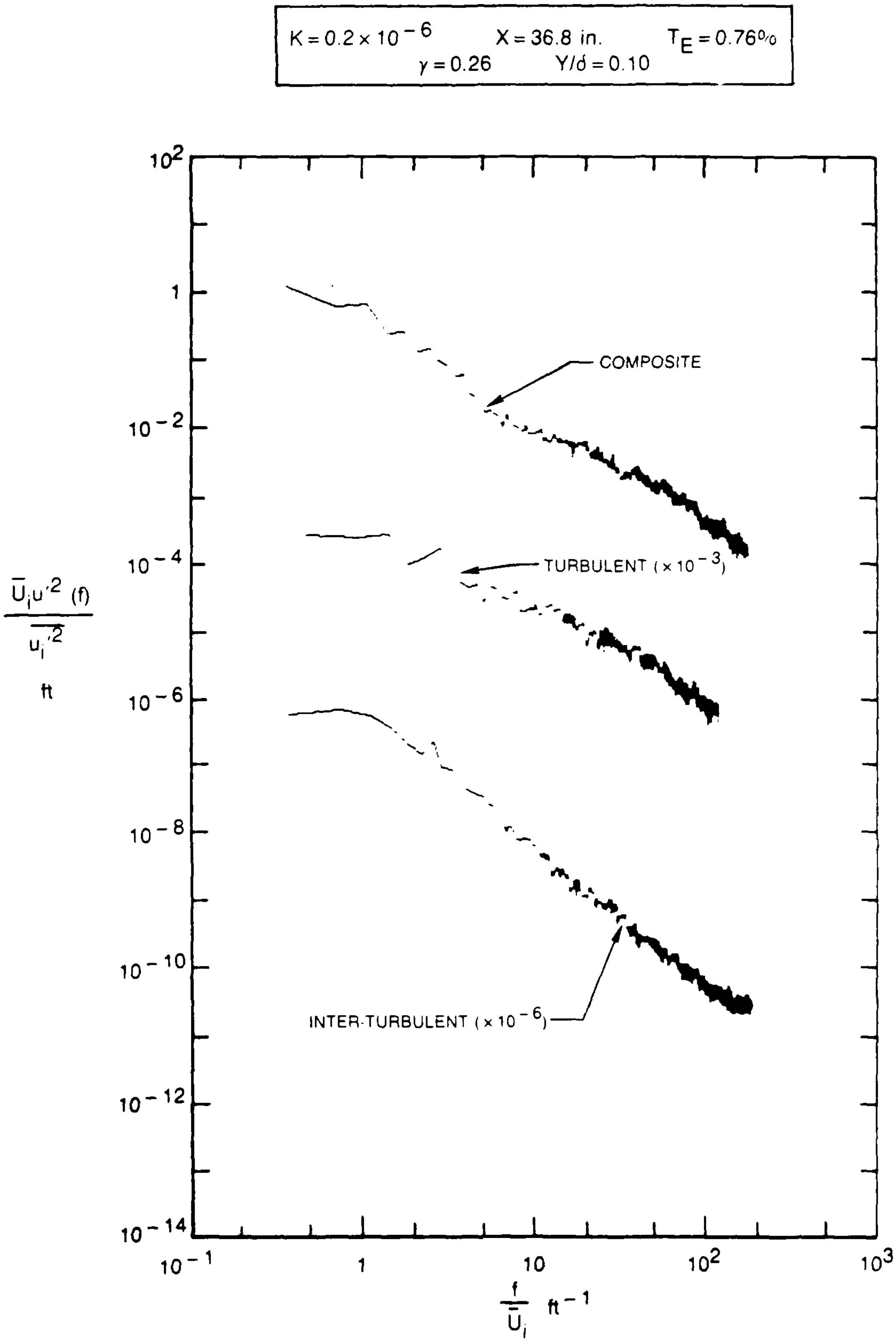

Figure 47. Conditionally Sampled Boundary Layer Spectral Distributions

87-10-44-14

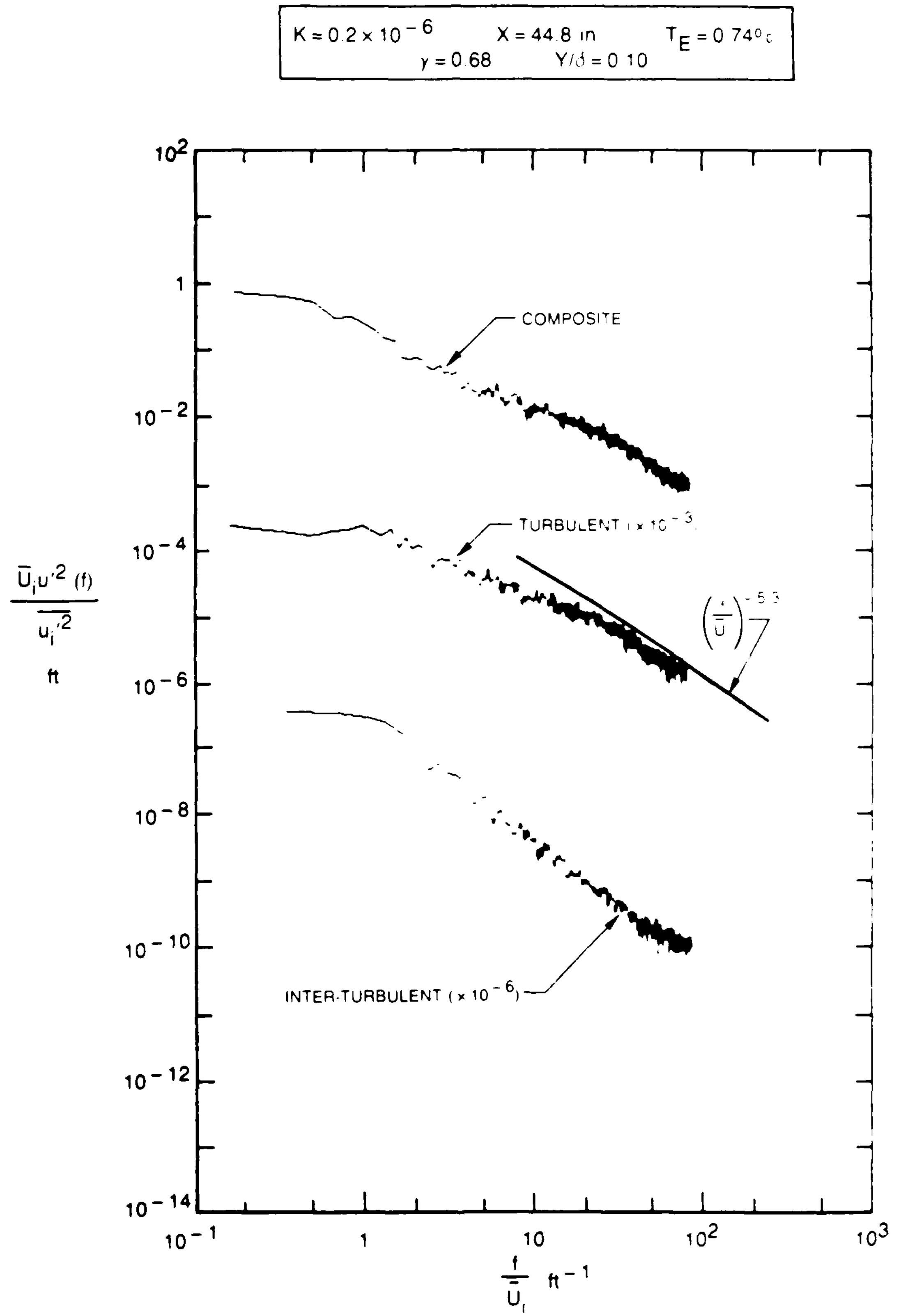

Figure 48. Conditionally Sampled Boundary Layer Spectral Distributions

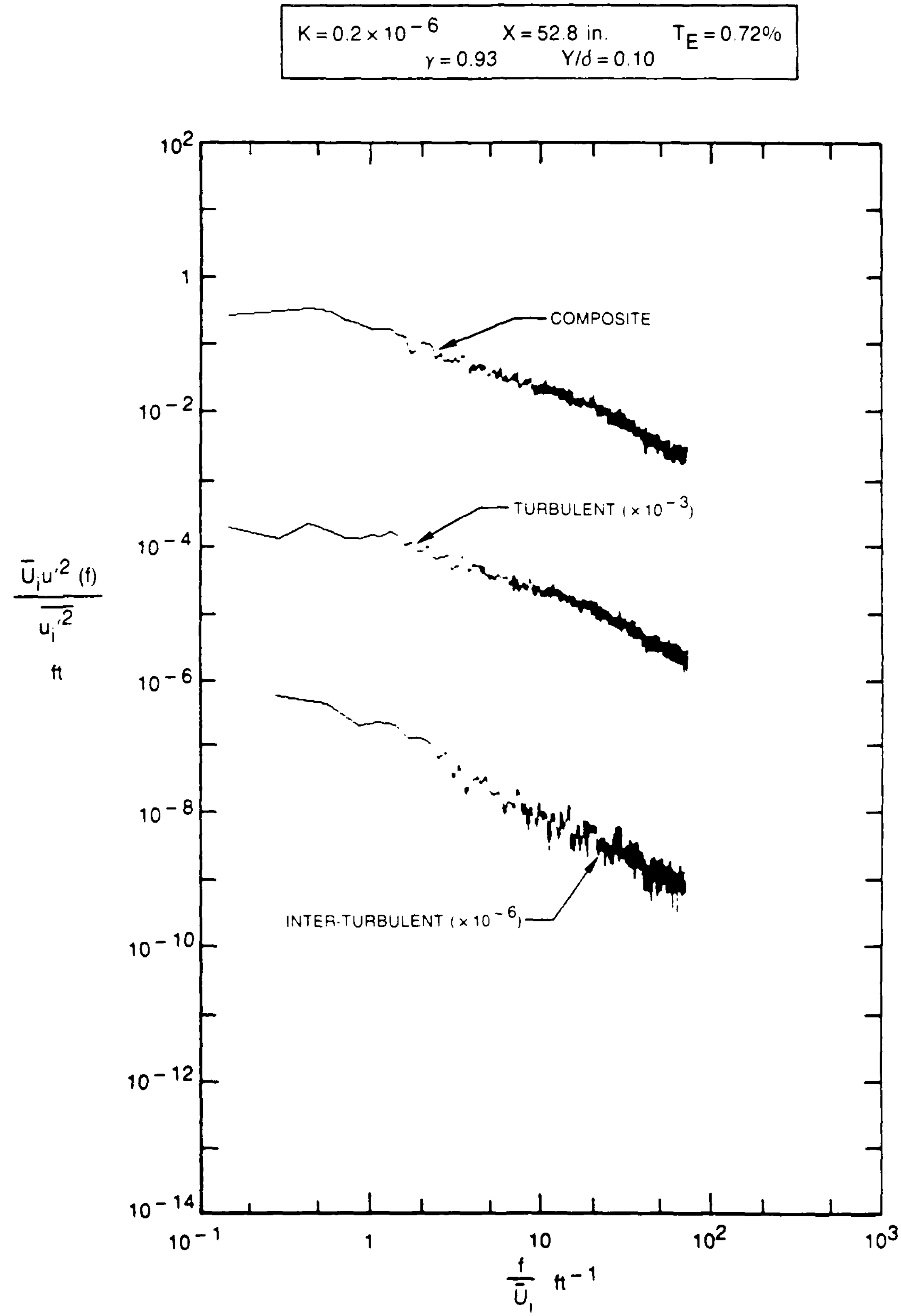

Figure 49. Conditionally Sampled Boundary Layer Spectral Distributions

87 - 10 - 44 - 12

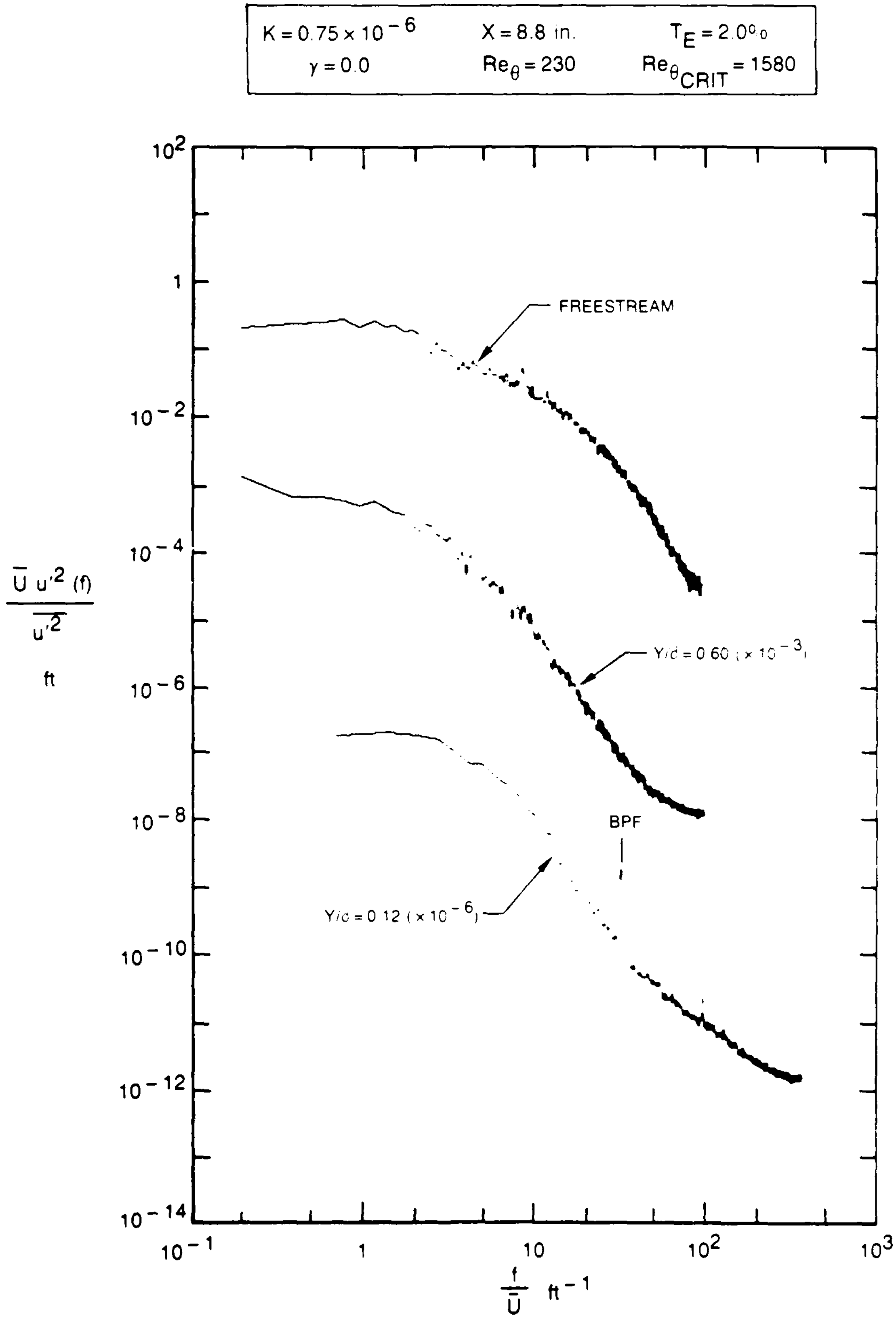

Figure 50. Boundary Layer Spectral Distributions

87-10-44-22

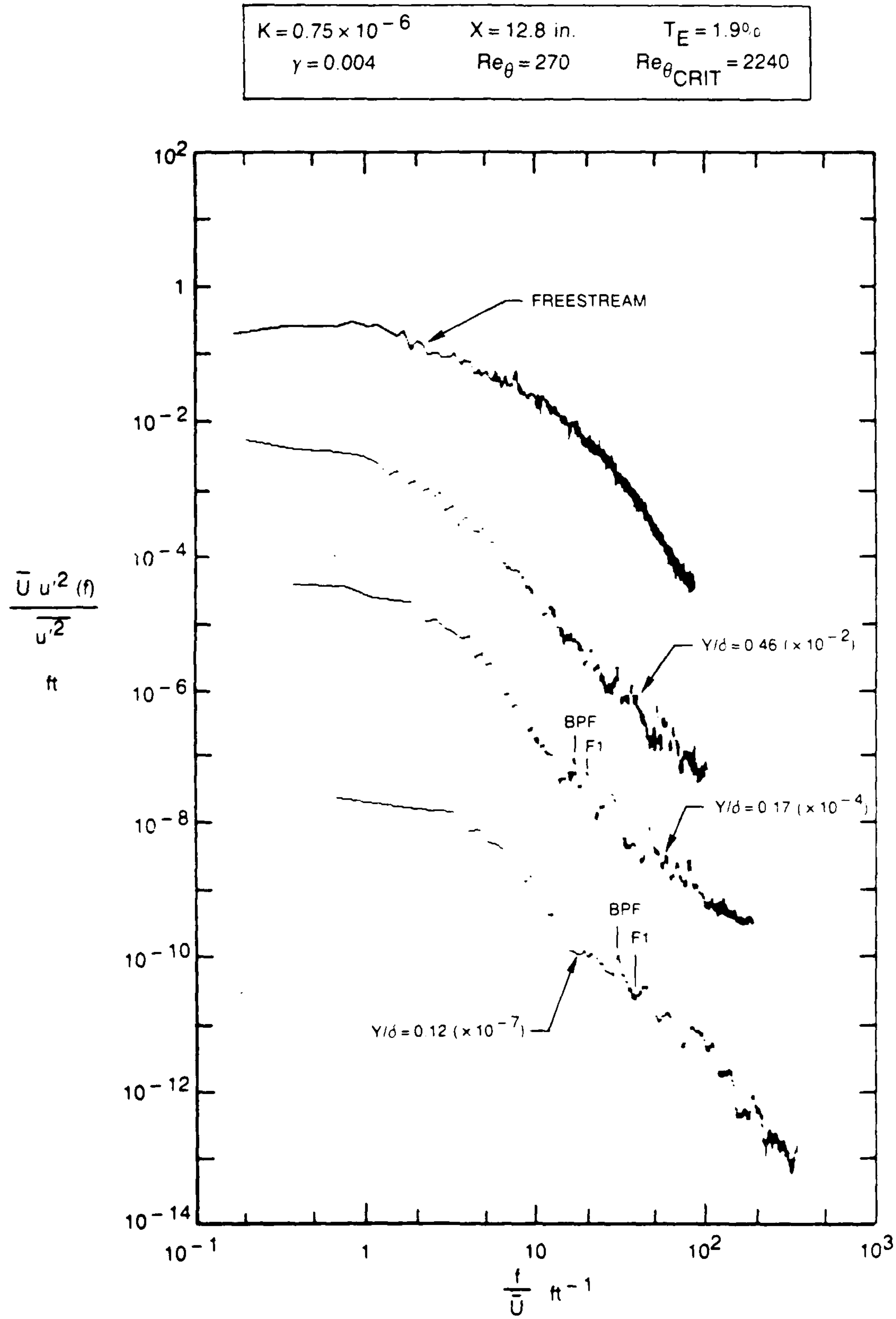

Figure 51. Boundary Layer Spectral Distributions

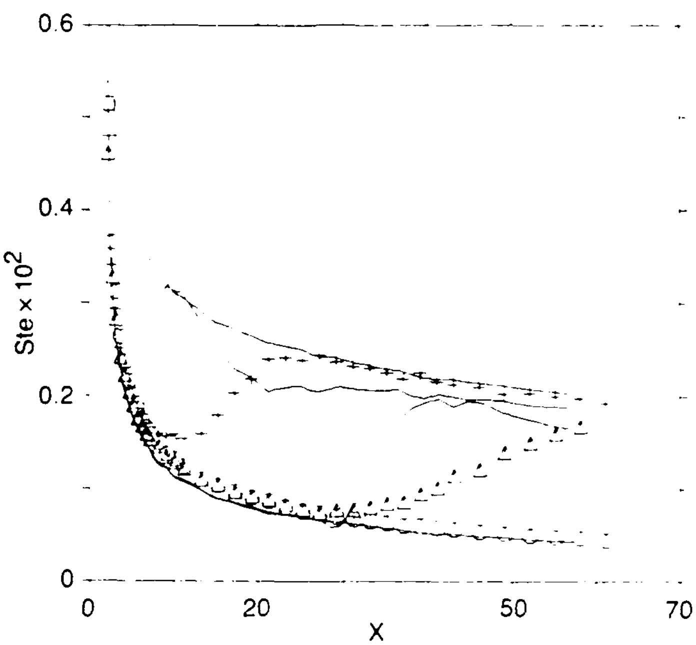

a) WEAK ACCELERATION K = 0.20E-06. O NO GRID. Δ GRID 1. + GRID 2

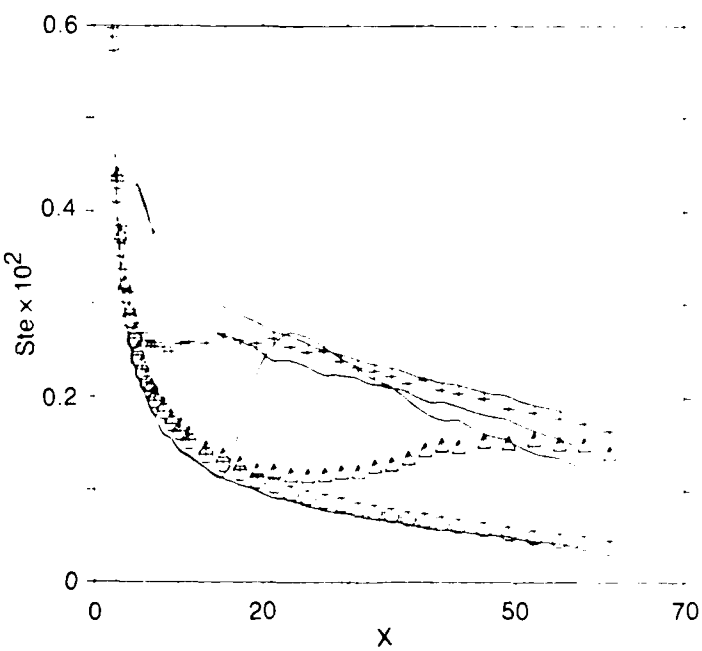

b) STRONG ACCELERATION K = .75E-06. O NO GRID. Δ GRID 1. + GRID 2

Figure 52. Predicted Heat Transfer-AbuGannom-Shaw Transition Model

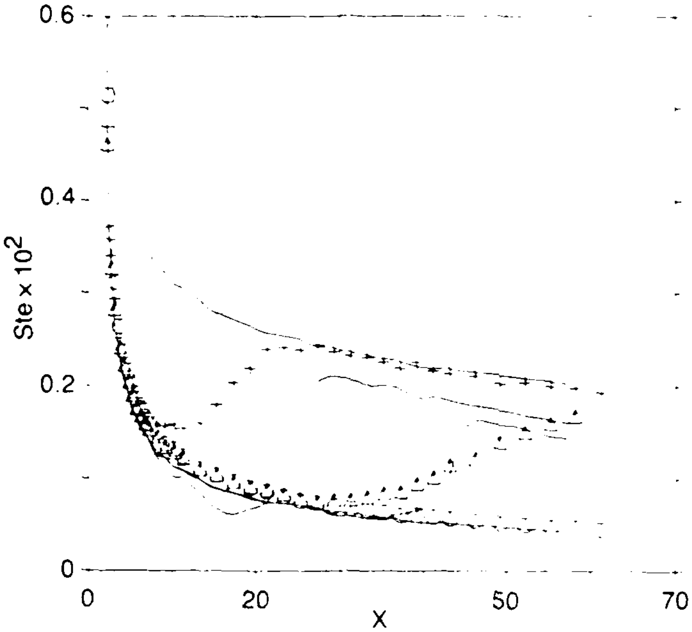

a) WEAK ACCELERATION KK = 0.20E-06. ○ NO GRID. △ GRID 1. + GRID 2

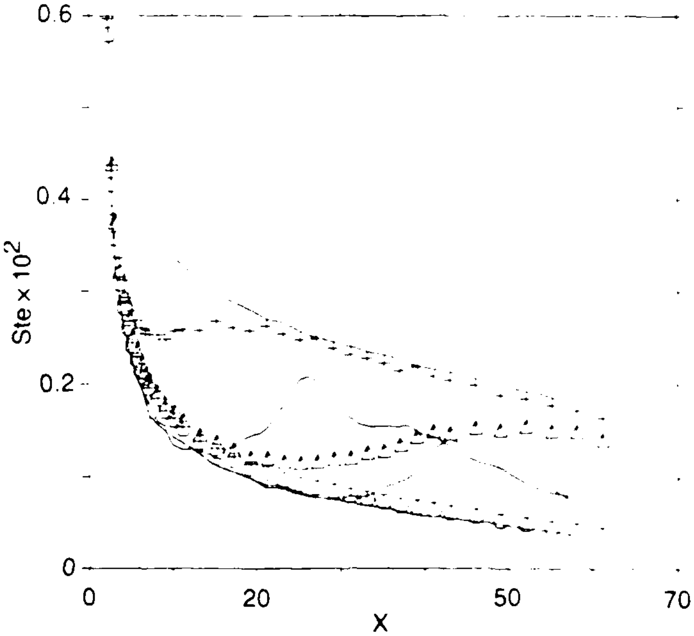

b) STRONG ACCELERATION K = 0.750E-06. ○ NO GRID. △ GRID 1. + GRID 2

Figure 53. Predicted Heat Transfer-McDonald-Kreskovsky Transition Model

8? - 10 - 44 - 35

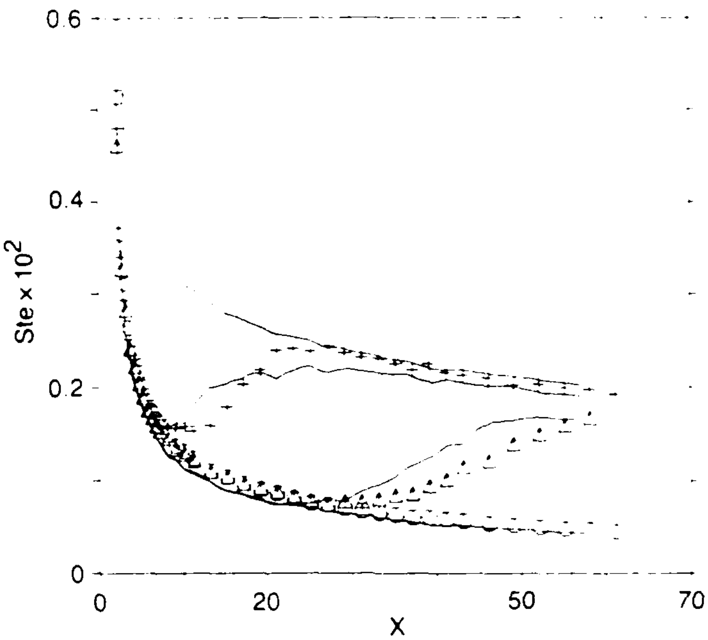

a) WEAK ACCELERATION K = 0.20E-06. O NO GRID. Δ GRID 1. + GRID 2

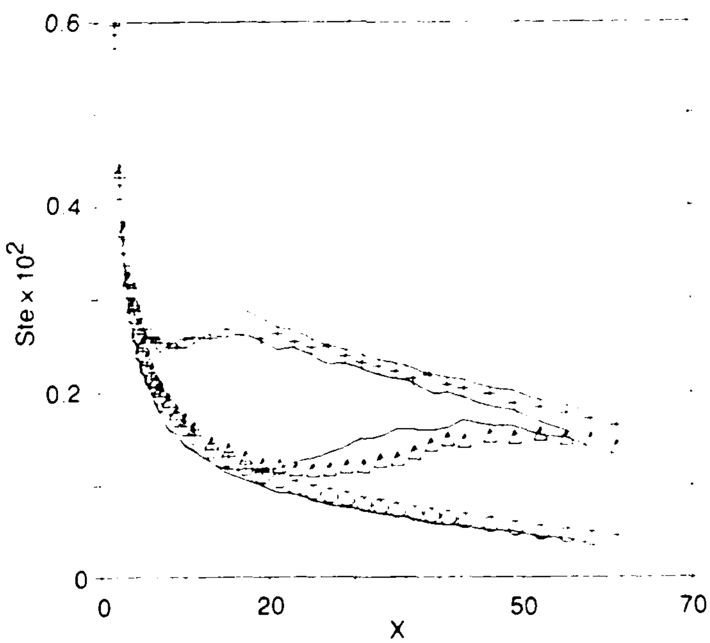

b) STRONG ACCELERATION K = 0.750E-06. O NO GRID. Δ GRID 1. + GRID 2

Figure 54. Predicted Heat Transfer-Cebeci-Smith Model with Experimental Intermittency

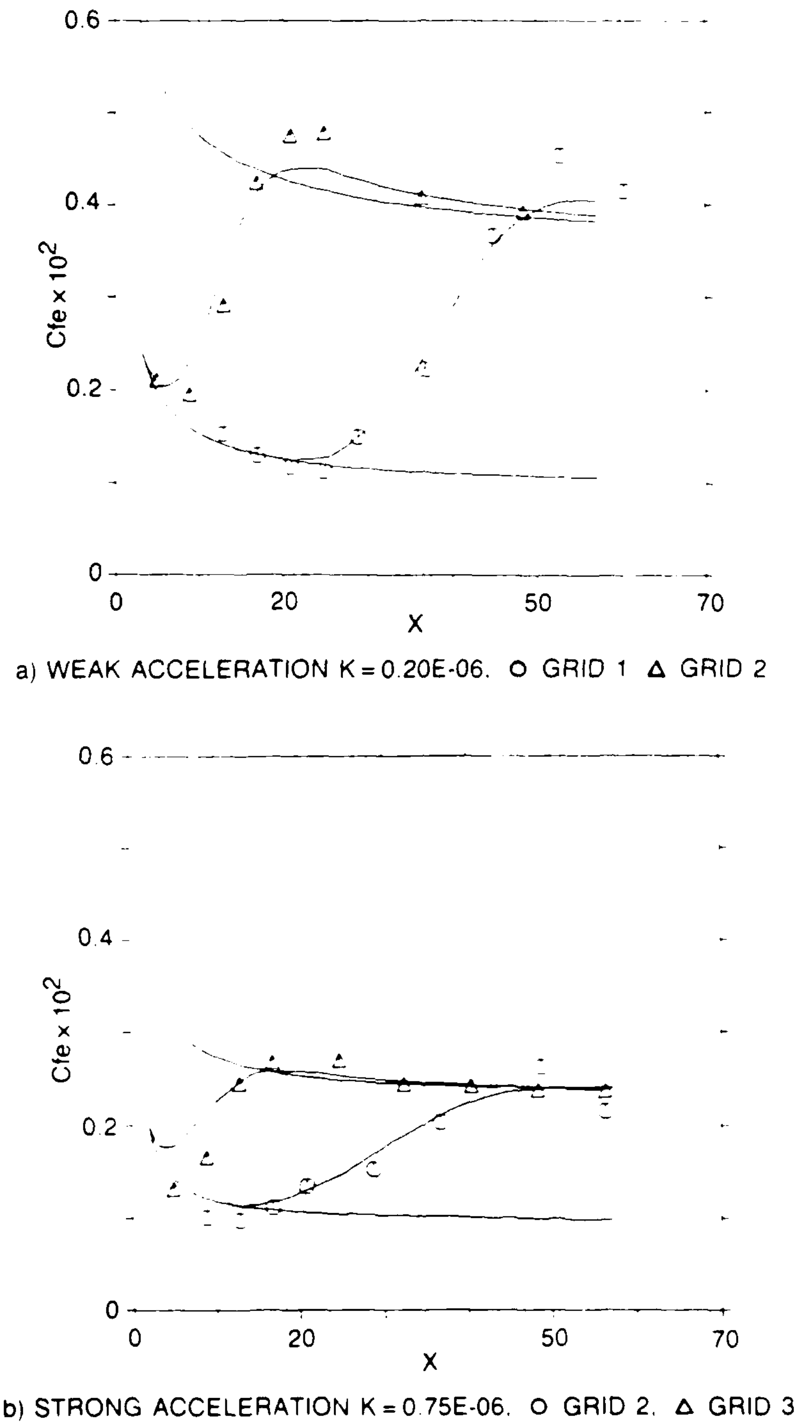

Figure 55. Predicted Skin Friction-Cebeci-Smith Model with Experimental Intermittency

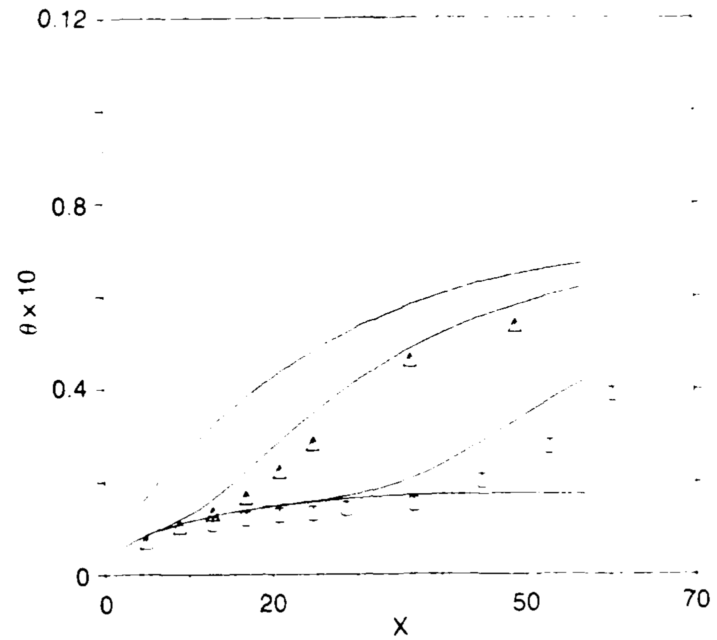

a) WEAK ACCELERATION K = 0.20E-06. O GRID 1. Δ GRID 2

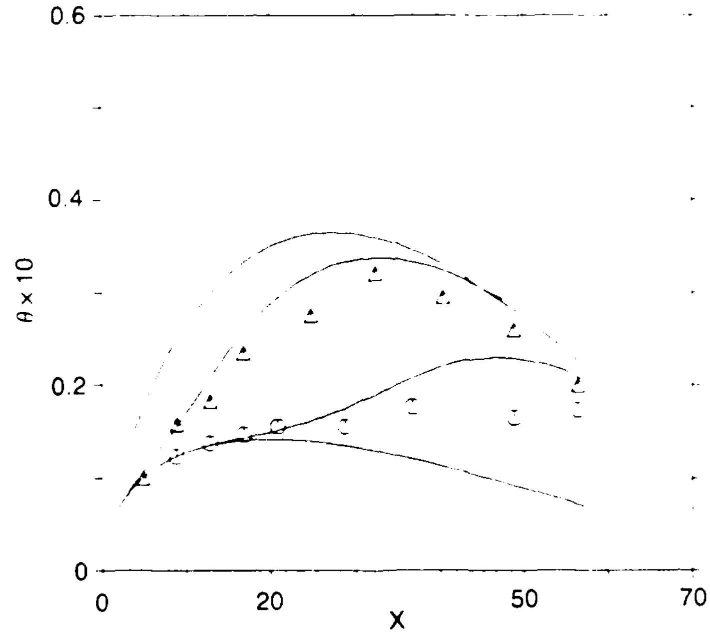

b) STRONG ACCELERATION K = 0.75E-06. O GRID 2. Δ GRID 3

Figure 56. Predicted Momentum Thickness-Cebeci-Smith Model with Experimental Intermittency

87-10-44-35

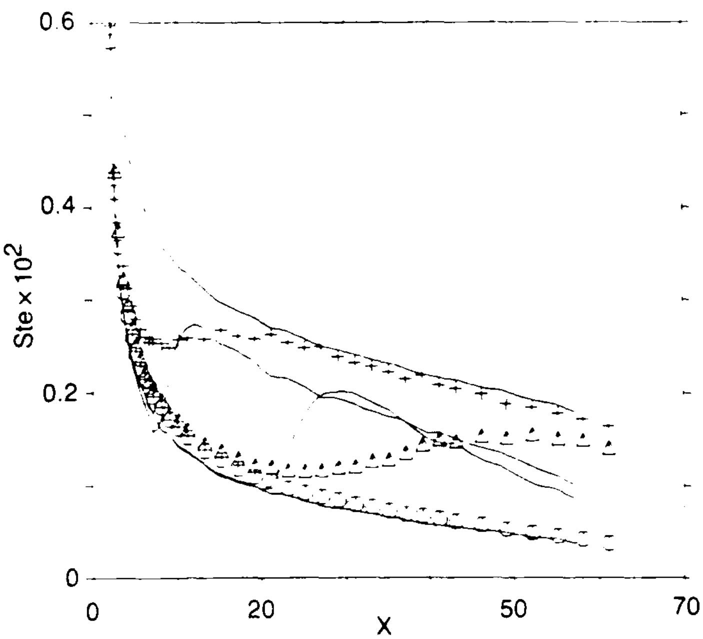

a) WEAK ACCELERATION K = 0.20E-06. O NO GRID. Δ GRID 1. + GRID 2

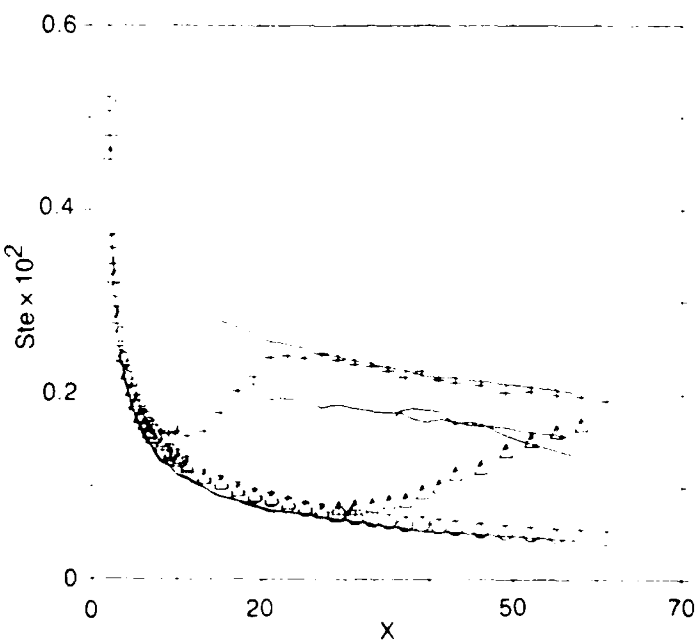

b) STRONG ACCELERATION K = 0.75E-06. O NO GRID. Δ GRID 1. + GRID 2

Figure 57. Predicted Heat Transfer-McDonald-Kreskovsky Model with Experimental Structural Coefficients

87-10-44-39

APPENDIX

PLOTTED AND TABULATED TURBULENCE PROFILES

$K \times 10^6$	GRID	FIGURE AND TABLE NUMBERS
0.2	1	A1 → A8
0.2	2	A9 → A14
0.75	2	A15 → A21
0.75	3	A22 → A26

87-10-44-68

PROFILES OF MEAN AND FLUCTUATING QUANTITIES

X = 12.8   K = 0.20 E−6   TE = 0.90 %

MEAN VELOCITY

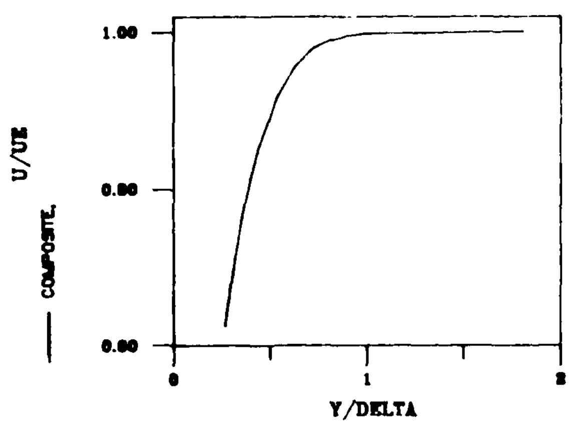

TURBULENCE COMPONENTS

COMPOSITE AVERAGE

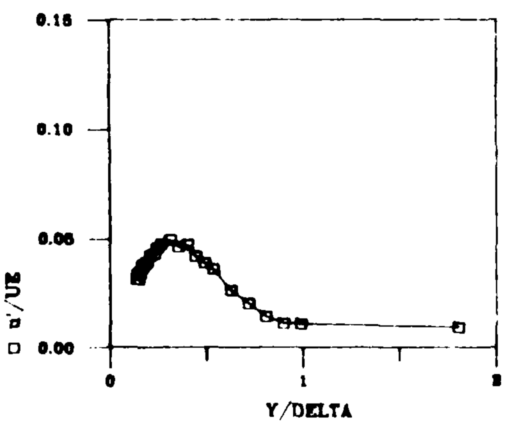

Figure A1

SINGLE WIRE PROFILE DATA

X = 12.8 GRID NO. 1 K = 0.2E-06

Y/DELTA	U/UE COMPOSITE	U/UE INTER-TURBULENT ZONE	U/UE TURBULENT ZONE	U'/UE COMPOSITE	U'/UE INTER-TURBULENT ZONE	U'/UE TURBULENT ZONE	GAMMA U	[illegible] U
0.1364	0.3475	0.0000	0.0000	0.0309	0.0000	0.0000	0.0000	0.0000
0.1426	0.3600	0.0000	0.0000	0.0331	0.0000	0.0000	0.0000	0.0000
0.1518	0.3841	0.0000	0.0000	0.0369	0.0000	0.0000	0.0000	0.0000
0.1591	0.3951	0.0000	0.0000	0.0339	0.0000	0.0000	0.0000	0.0000
0.1682	0.4221	0.0000	0.0000	0.0366	0.0000	0.0000	0.0000	0.0000
0.1764	0.4410	0.0000	0.0000	0.0374	0.0000	0.0000	0.0000	0.0000
0.1945	0.4849	0.0000	0.0000	0.0387	0.0000	0.0000	0.0000	0.0000
0.2136	0.5250	0.0000	0.0000	0.0418	0.0000	0.0000	0.0000	0.0000
0.2226	0.5630	0.0000	0.0000	0.0426	0.0000	0.0000	0.0000	0.0000
0.2452	0.5909	0.0000	0.0000	0.0455	0.0000	0.0000	0.0000	[illegible]
0.2691	0.6247	0.0000	0.0000	0.0473	0.0000	0.0000	0.0000	0.0000
0.3127	0.6956	0.0000	0.0000	0.0493	0.0000	0.0000	0.0000	[illegible]
0.3564	0.7617	0.0000	0.0000	0.0463	0.0000	0.0000	0.0000	[illegible]
0.4027	0.8149	0.0000	0.0000	0.0471	0.0000	0.0000	0.0000	0.0000
0.4455	0.8547	0.0000	0.0000	0.0416	0.0000	0.0000	0.0000	0.0000
0.4927	0.8855	0.0000	0.0000	0.0386	0.0000	0.0000	0.0000	[illegible]
0.5364	0.9171	0.0000	0.0000	0.0357	0.0000	0.0000	0.0435	[illegible]
0.6282	0.9534	0.0000	0.0000	0.0260	0.0000	0.0000	0.0564	[illegible]
0.7182	0.9786	0.0000	0.0000	0.0200	0.0000	0.0000	0.0282	[illegible]
0.8164	0.9898	0.0000	0.0000	0.0141	0.0000	0.0000	0.0307	[illegible]
0.9000	0.9954	0.0000	0.0000	0.0108	0.0000	0.0000	0.0000	[illegible]
0.99	0.9988	[illegible]	[illegible]	0.0107	0.0000	0.0000	[illegible]	[illegible]
1.8164	1.0015	[illegible]	0.0000	0.0090	0.0000	0.0000	0.0000	[illegible]
9.1782	1.0000	[illegible]	[illegible]	0.0064	0.0000	0.0000	[illegible]	[illegible]

TABLE A1

87-10-44-[illegible]

PROFILES OF MEAN AND FLUCTUATING QUANTITIES

X = 16.8 K = 0.20 E−6 TE = 0.85 %

MEAN VELOCITY

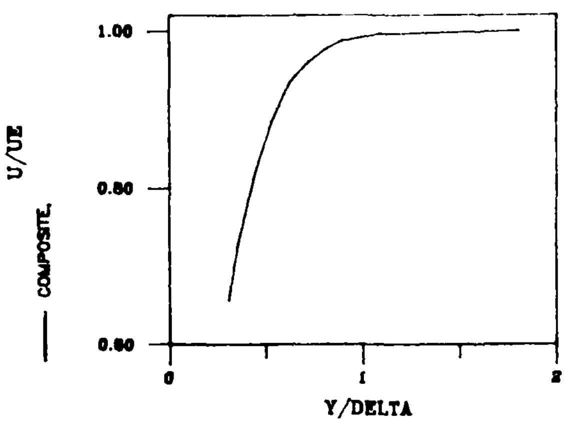

TURBULENCE COMPONENTS

COMPOSITE AVERAGE

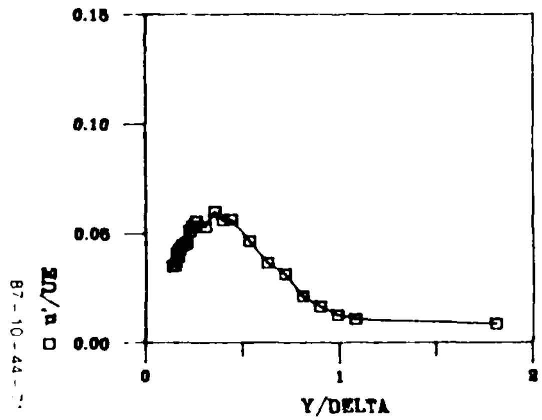

Figure A2

87-10-44-7

SINGLE WIRE PROFILE DATA

X = 16.8   GRID NO. 1   K = 0.2E-06

Y/DELTA	U/UE COMPOSITE	U/UE INTER-TURBULENT ZONE	U/UE TURBULENT ZONE	U'/UE COMPOSITE	U'/UE INTER-TURBULENT ZONE	U'/UE TURBULENT ZONE	GAMMA L	Y L
0.1364	0.2991	0.0000	0.0000	0.0348	0.0000	0.0000	0.0948	0.2001
0.1427	0.3145	0.0000	0.0000	0.0348	0.0000	0.0000	0.0000	0.0000
0.1545	0.3453	0.0000	0.0000	0.0352	0.0000	0.0000	0.1358	0.2001
0.1618	0.3660	0.0000	0.0000	0.0406	0.0000	0.0000	0.0000	0.0000
0.1700	0.3875	0.0000	0.0000	0.0391	0.0000	0.0000	0.0717	0.2001
0.1755	0.3988	0.0000	0.0000	0.0425	0.0000	0.0000	0.0000	0.0000
0.1936	0.4406	0.0000	0.0000	0.0445	0.0000	0.0000	0.0897	0.2001
0.2127	0.4884	0.0000	0.0000	0.0455	0.0000	0.0000	0.1127	0.2001
0.2300	0.5115	0.0000	0.0000	0.0510	0.0000	0.0000	0.0897	0.2001
0.2491	0.5517	0.0000	0.0000	0.0571	0.0000	0.0000	0.0000	0.0000
0.2664	0.5856	0.0000	0.0000	0.0555	0.0000	0.0000	0.0000	0.0000
0.3109	0.6551	0.0000	0.0000	0.0529	0.0000	0.0000	0.0000	0.0000
0.3582	0.7250	[illegible]	0.0000	0.0599	0.0000	0.0000	0.0000	0.0000
0.4009	0.7690	0.0000	0.0000	0.0559	0.0000	0.0000	0.0410	0.2001
0.4445	0.8151	0.0000	0.0000	0.0562	0.0000	0.0000	0.0000	0.0000
0.5264	0.8860	0.0000	0.0000	0.0460	0.0000	0.0000	0.0000	0.0000
0.6273	0.9351	0.0000	0.0000	0.0363	0.0000	0.0000	0.0000	0.0000
0.7177	0.9590	0.0000	0.0000	0.0220	0.0000	0.0000	0.0747	0.4002
0.8082	0.9765	0.0000	0.0000	0.0212	0.0000	0.0000	0.0589	0.4002
0.9000	0.9887	0.0000	0.0000	0.0164	0.0000	0.0000	0.0282	0.2001
0.9911	0.9917	0.0000	0.0000	0.0127	0.0000	0.0000	0.0564	0.4002
1.0827	0.9982	0.0000	0.0000	0.0116	0.0000	0.0000	0.0259	0.2001
1.8100	1.0007	0.0000	0.0000	0.0066	0.0000	0.0000	0.0000	0.0000
9.0827	0.9966	0.0000	0.0000	0.0080	0.0000	0.0000	0.0000	0.0000

TABLE A2

87-10-44-70

PROFILES OF MEAN AND FLUCTUATING QUANTITIES

X = 20.8   K = 0.20 E−6   TE = 0.82 %

MEAN VELOCITY

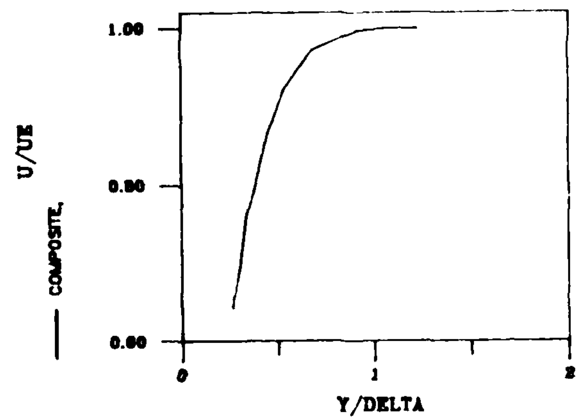

TURBULENCE COMPONENTS

COMPOSITE AVERAGE

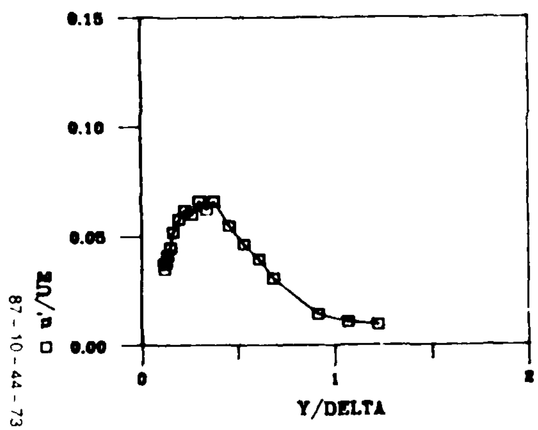

87 - 10 - 44 - 73

Figure A3

SINGLE WIRE PROFILE DATA

X = 20.8 GRID NO. 1 K = 0.2E-06

Y/DELTA	U/UE COMPOSITE	U/UE INTER-TURBULENT ZONE	U/UE TURBULENT ZONE	U'/UE COMPOSITE	U'/UE INTER-TURBULENT ZONE	U'/UE TURBULENT ZONE	GAMMA U	[illegible] U
0.1154	0.2771	0.0000	0.0000	0.0372	0.0000	0.0000	0.5840	[illegible]
0.1223	0.2958	0.0000	0.0000	0.0347	0.0000	0.0000	0.1230	0.2001
0.1308	0.3210	0.0000	0.0000	0.0377	0.0000	0.0000	0.3381	0.4002
0.1369	0.3431	0.0000	0.0000	0.0411	0.0000	0.0000	0.1537	0.2001
0.1531	0.3882	0.0000	0.0000	0.0447	0.0000	0.0000	0.2997	0.4002
0.1677	0.4314	0.0000	0.0000	0.0517	0.0000	0.0000	0.5507	[illegible]
0.1992	0.5029	0.0000	0.0000	0.0576	0.0000	0.0000	0.1306	0.6003
0.2285	0.5703	0.0000	0.0000	0.0616	0.0000	0.0000	0.2229	0.4002
0.2662	0.6422	0.0000	0.0000	0.0598	0.0000	0.0000	0.0000	[illegible]
0.3054	0.6953	[illegible]	[illegible]	0.0660	0.0000	0.0000	0.0000	[illegible]
0.3408	0.7605	0.0000	0.0000	0.0619	0.0000	0.0000	0.1870	0.4002
0.3808	0.7931	0.0000	0.0000	0.0658	0.0000	0.0000	0.1332	[illegible]
0.4577	0.8691	0.0000	0.0000	0.0546	0.0000	0.0000	0.4755	[illegible]
0.5338	0.9214	0.0000	0.0000	0.0462	0.0000	0.0000	0.5072	[illegible]
0.6115	0.9482	0.0000	0.0000	0.0392	0.0000	0.0000	0.1614	[illegible]
[illegible]	0.9718	0.0000	[illegible]	[illegible]	[illegible]	0.0000	[illegible]	[illegible]
0.9185	0.9971	0.0000	0.0000	0.0141	0.0000	0.0000	[illegible]	[illegible]
1.0700	1.0036	[illegible]	[illegible]	[illegible]	[illegible]	[illegible]	0.0256	[illegible]
1.2246	1.0061	[illegible]	0.0000	0.0093	0.0000	0.0000	0.0000	0.0000
2.3015	[illegible]	0.0000	0.0000	[illegible]	[illegible]	0.0000	[illegible]	[illegible]
[illegible]	1.0009	0.0000	0.0000	0.0080	0.0000	0.0000	0.0000	0.0000

TABLE A3

87-10-44-74

PROFILES OF MEAN AND FLUCTUATING QUANTITIES

X = 24.8   K = 0.20 E-6   TE = 0.80 %

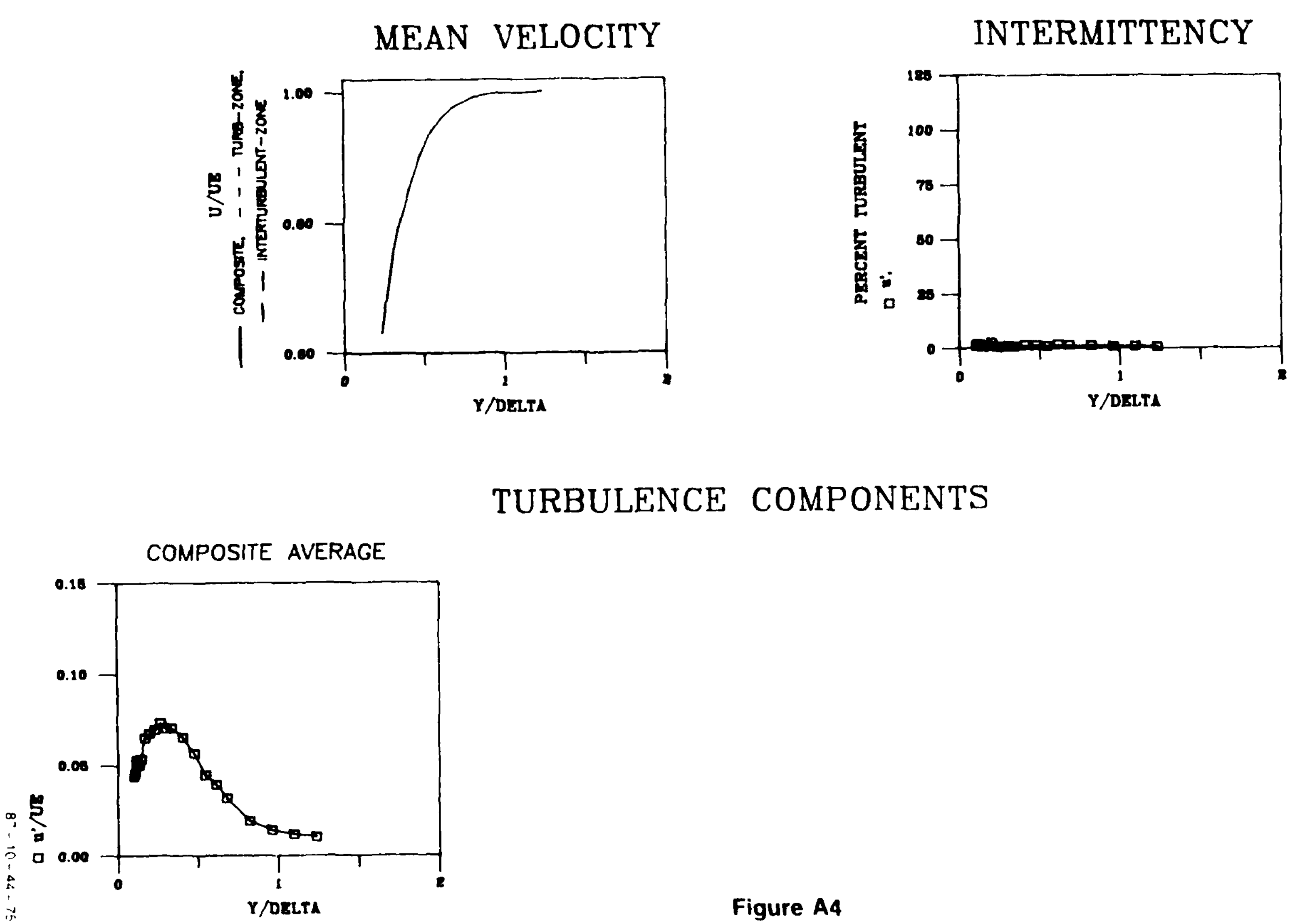

Figure A4

87-10-44-75

SINGLE WIRE PROFILE DATA

X = 24.8 GRID NO. 1 K = 0.2E-06

Y/DELTA	U/UE COMPOSITE	U/UE INTER-TURBULENT ZONE	U/UE TURBULENT ZONE	U'/UE COMPOSITE	U'/UE INTER-TURBULENT ZONE	U'/UE TURBULENT ZONE	GAMMA U	f U
0.1034	0.2731	0.0000	0.0000	0.0435	0.0000	0.0000	0.8940	1.0005
0.1083	0.2873	0.0000	0.0000	0.0453	0.0000	0.0000	1.0886	1.4007
0.1159	0.3160	0.0000	0.0000	0.0506	0.0000	0.0000	1.7341	2.4012
0.1207	0.3334	0.0000	0.0000	0.0526	0.0000	0.0000	1.8391	2.4012
0.1345	0.3754	0.0000	0.0000	0.0499	0.0000	0.0000	1.4933	2.0010
0.1483	0.4171	0.0000	0.0000	0.0573	0.0000	0.0000	0.6839	1.2006
0.1759	0.4896	0.0000	0.0000	0.0648	0.0000	0.0000	1.1936	1.6008
0.2041	0.5577	0.0000	0.0000	0.0672	0.0000	0.0000	2.7843	3.2016
0.2379	0.6374	0.0000	0.0000	0.0693	0.0000	0.0000	0.7403	1.4007
0.2731	0.6932	0.0000	0.0000	0.0731	0.0000	0.0000	0.9506	1.2006
0.3069	0.7535	0.0000	0.0000	0.0700	0.0000	0.0000	1.3064	2.2011
0.3414	0.7892	0.0000	0.0000	0.0703	0.0000	0.0000	0.9529	1.8009
0.4097	0.8534	0.0000	0.0000	0.0652	0.0000	0.0000	1.6086	2.8014
0.4779	0.9038	0.0000	0.0000	0.0567	0.0000	0.0000	1.3320	1.6008
0.5476	0.9411	0.0000	0.0000	0.0444	0.0000	0.0000	0.8427	1.6008
0.6172	0.9627	0.0000	0.0000	0.0390	0.0000	0.0000	1.5800	3.0015
0.6848	0.9777	0.0000	0.0000	0.0315	0.0000	0.0000	1.5138	2.8014
0.8224	0.9943	0.0000	0.0000	0.0191	0.0000	0.0000	1.3012	2.4012
0.9601	0.9996	0.0000	0.0000	0.0140	0.0000	0.0000	0.8735	2.2011
1.0993	1.0011	0.0000	0.0000	0.0117	0.0000	0.0000	0.8376	1.2006
1.2766	1.0019	0.0000	0.0000	0.0101	0.0000	0.0000	0.5277	1.6008
2.0641	1.0011	0.0000	0.0000	0.0081	0.0000	0.0000	0.0000	0.0000
6.8924	1.0000	0.0000	0.0000	0.0080	0.0000	0.0000	0.0000	0.0000

TABLE A4

87 - 10 - 44 - 76

PROFILES OF MEAN AND FLUCTUATING QUANTITIES

X = 28.8 K = 0.20 E−6 TE = 0.78 %

MEAN VELOCITY

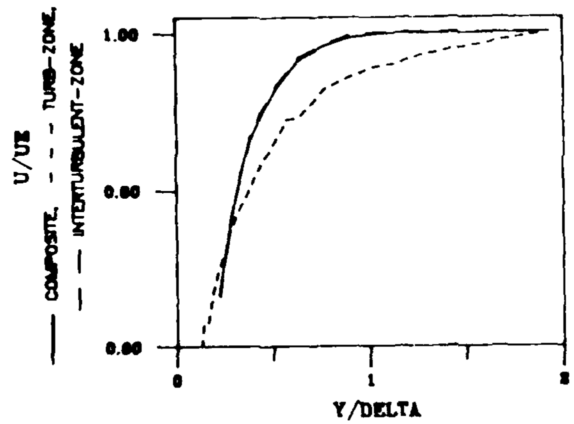

INTERMITTENCY

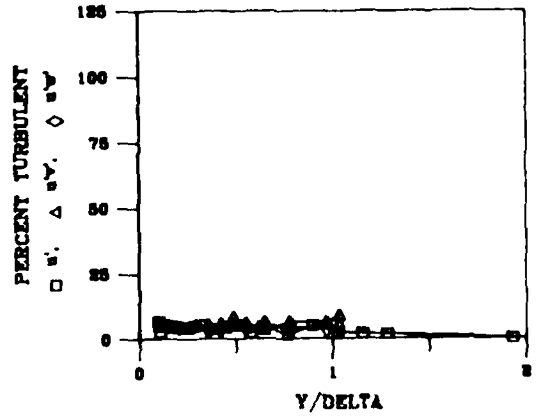

TURBULENCE COMPONENTS

COMPOSITE AVERAGE

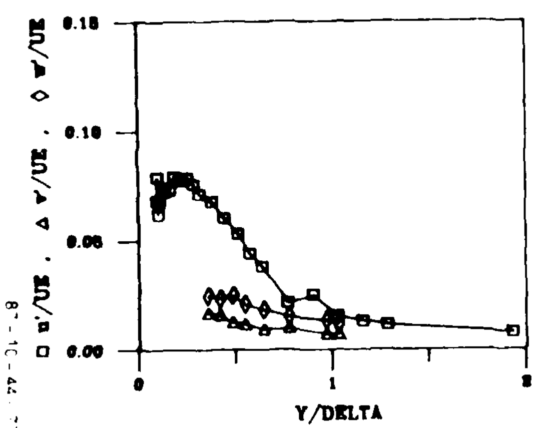

INTERTURB−ZONE AVERAGE

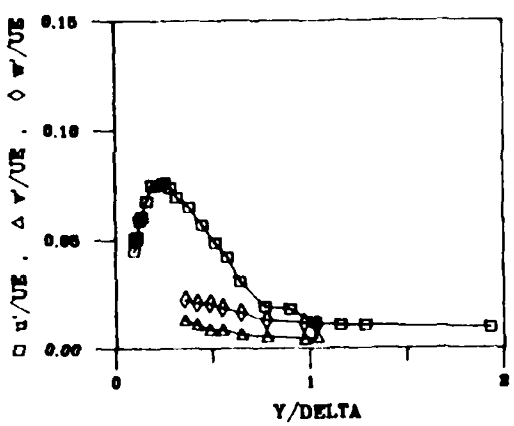

TURBULENT−ZONE AVERAGE

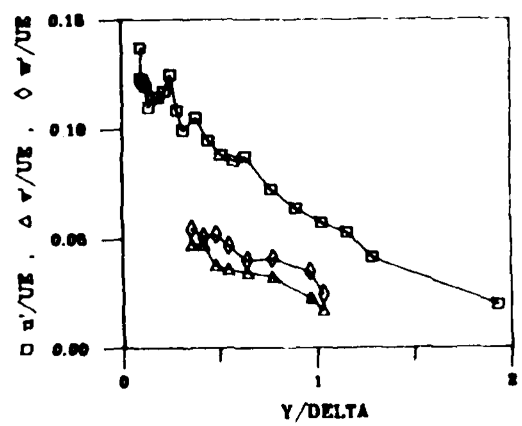

Figure A5-A

PROFILES OF TURBULENT STRESSES

$X = 28.8$ $K = 0.20\ E{-}6$ $TE = 0.78$ %

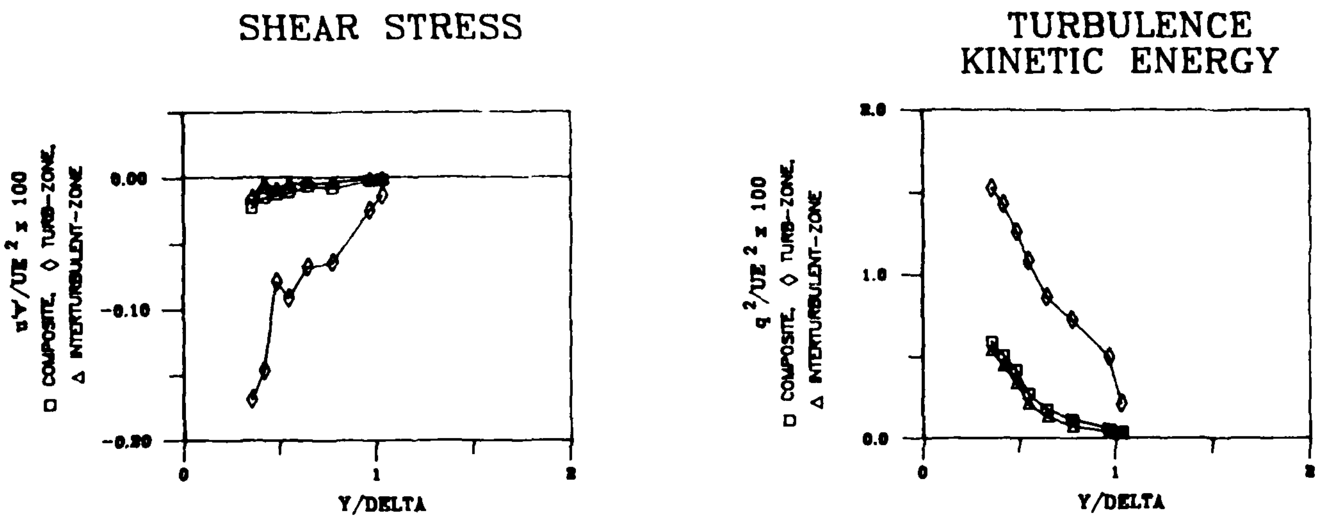

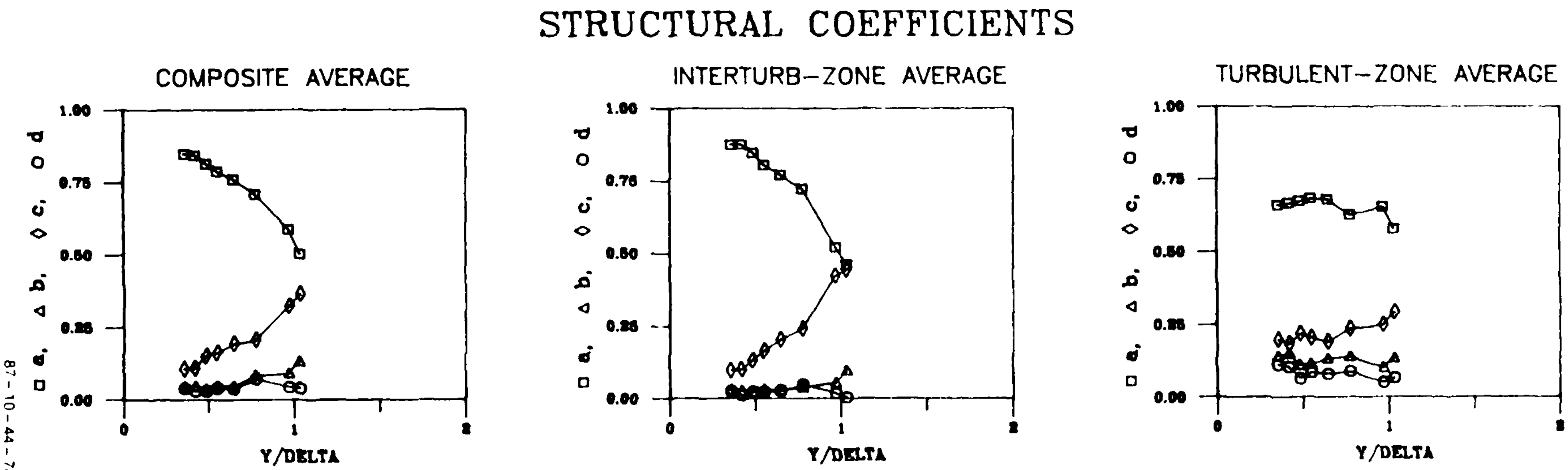

Figure A5-B

87-10-44-78

SINGLE WIRE PROFILE DATA

X = 28.8 GRID NO. 1 K = 0.2E-06

Y/DELTA	U/UE COMPOSITE	U/UE INTER-TURBULENT ZONE	U/UE TURBULENT ZONE	U'/UE COMPOSITE	U'/UE INTER-TURBULENT ZONE	U'/UE TURBULENT ZONE	GAMMA U	* U
0.0968	0.3369	0.3270	0.5176	0.0683	0.0446	0.1370	5.0820	6.0031
0.1013	0.3622	0.3478	0.5601	0.0789	0.0503	0.1229	6.6137	6.4033
0.1084	0.3696	0.3643	0.5559	0.0617	0.0498	0.1226	2.6742	3.4017
0.1142	0.3936	0.3852	0.5538	0.0674	0.0509	0.1211	4.8668	5.6029
0.1271	0.4413	0.4320	0.6000	0.0739	0.0584	0.1192	5.3663	5.6029
0.1413	0.4822	0.4743	0.6313	0.0721	0.0602	0.1094	5.1563	5.0026
0.1658	0.5304	0.5258	0.6311	0.0731	0.0673	0.1142	4.2059	4.8025
0.1903	0.5907	0.5867	0.6692	0.0790	0.0747	0.1140	4.8924	5.8030
0.2232	0.6653	0.6638	0.6988	0.0772	0.0747	0.1170	4.0907	4.8025
0.2555	0.7147	0.7144	0.7217	0.0783	0.0758	0.1245	4.2341	4.8025
0.2871	0.7589	0.7593	0.7494	0.0755	0.0735	0.1080	4.8361	5.4028
0.3174	0.7969	0.7964	0.7690	0.0712	0.0691	0.0989	5.3407	5.0026
0.3839	0.8652	0.8677	0.8177	0.0677	0.0646	0.1048	3.7756	4.6024
0.4471	0.8975	0.9003	0.8345	0.0602	0.0566	0.0943	4.2725	5.4028
0.5129	0.9278	0.9313	0.8634	0.0531	0.0483	0.0878	5.1231	[illegible]
0.5774	0.9479	0.9494	0.8911	0.0440	0.0417	0.0551	2.3847	5.0026
0.6394	0.9653	0.9686	0.8930	0.0379	0.0304	0.0570	4.4391	6.4033
0.7691	0.9846	0.9855	0.9291	0.0315	0.0191	0.0711	1.5215	3.4017
0.8961	0.9946	0.9973	0.9443	0.0251	0.0178	0.0636	5.0077	8.8045
1.0271	0.9994	1.0005	0.9571	0.0154	0.0117	0.0569	2.4641	4.0022
1.1568	1.0008	1.0016	0.9620	0.0133	0.0105	0.0527	1.8751	3.4017
1.2859	[illegible]	1.0007	0.9734	[illegible]	0.0109	0.0410	1.7162	[illegible]
1.9310	1.0020	1.0020	1.0021	0.0078	0.0093	0.0195	0.6615	3.4017
6.4477	1.0022	1.0022	0.9983	0.0077	0.0077	0.0000	0.0000	[illegible]

TABLE A5-A

87-10-44-79

CROSS WIRE PROFILE DATA

X = 28.8 GRID NO. 1 K = 0.2E-06

Y/DELTA	U'/UE COMPOSITE	U'/UE INTER-TURBULENT ZONE	U'/UE TURBULENT ZONE	V'/UE COMPOSITE	V'/UE INTER-TURBULENT ZONE	V'/UE TURBULENT ZONE	W'/UE COMPOSITE	W'/UE INTER-TURBULENT ZONE	W'/UE TURBULENT ZONE
0.3548	0.0705	0.0682	0.1002	0.0167	0.0130	0.0472	0.0247	0.0224	0.0547
0.4194	0.0650	0.0618	0.0974	0.0157	0.0110	0.0469	0.0232	0.0207	0.0535
0.4839	0.0576	0.0525	0.0918	0.0124	0.0087	0.0376	0.0247	0.0207	0.0517
0.5484	0.0459	0.0408	0.0858	0.0116	0.0083	0.0356	0.0207	0.0183	0.0463
0.6452	0.0361	0.0314	0.0762	0.0091	0.0062	0.0341	0.0181	0.0160	0.0398
0.7742	0.0281	0.0224	0.0671	0.0099	0.0053	0.0322	0.0150	0.0128	0.0407
0.9677	0.0180	0.0130	0.0551	0.0072	0.0043	0.0225	0.0133	0.0116	0.0346
1.0323	0.0137	0.0108	0.0346	0.0071	0.0051	0.0169	0.0115	0.0106	0.0240
6.4516	0.0086	0.0102	0.0092	0.0102	0.0100	0.0109	0.0090	0.0090	0.0104

Y/DELTA	U'**2/q**2 COMPOSITE	U'**2/q**2 INTER-TURBULENT ZONE	U'**2/q**2 TURBULENT ZONE	V'**2/q**2 COMPOSITE	V'**2/q**2 INTER-TURBULENT ZONE	V'**2/q**2 TURBULENT ZONE	W'**2/q**2 COMPOSITE	W'**2/q**2 INTER-TURBULENT ZONE	W'**2/q**2 TURBULENT ZONE
0.3548	0.8470	0.8733	0.6596	0.0462	0.0308	0.1424	0.1067	0.0961	0.1979
0.4194	0.8425	0.8731	0.6660	0.0478	0.0271	0.1506	0.1096	0.0998	0.1874
0.4839	0.8130	0.8463	0.6723	0.0363	0.0223	0.1101	0.1506	0.1314	0.2176
0.5484	0.7874	0.8035	0.6622	0.0492	0.0320	0.1146	0.1634	0.1645	0.2033
0.6452	0.7595	0.7682	0.6785	0.0463	0.0287	0.1321	0.1943	0.207[illegible]	0.1894
0.7742	0.7060	0.7205	0.6253	0.0649	0.0389	0.1399	0.2071	0.2405	0.2245
0.9677	0.5859	0.5207	0.6523	0.0909	0.0563	0.1000	0.3232	0.4229	0.2477
1.0323	0.5022	0.4607	0.5762	0.1329	0.0970	0.1335	0.3645	0.4427	0.2903
6.4516	0.2861	0.3655	0.2735	0.3922	0.3414	0.3713	0.3219	0.2901	0.3552

Y/DELTA	UV/Q**2 COMPOSITE	UV/Q**2 INTER-TURBULENT ZONE	UV/Q**2 TURBULENT ZONE	GAMMA UV	f UV	GAMMA W.	f W.
0.3548	-0.0396	-0.0253	-0.1107	5.2049	5.8030	3.4810	4.4023
0.4194	-0.0304	-0.0110	-0.1031	5.7633	7.2037	3.8320	4.4023
0.4839	-0.0308	-0.0243	-0.0627	5.6481	7.6039	7.0952	7.4038
0.5484	-0.0410	-0.0230	-0.0850	5.2894	7.6039	4.4903	6.0031
0.6452	-0.0779	-0.0270	-0.0788	3.7218	6.2032	5.0435	7.6039
0.7742	-0.0719	-0.0480	-0.0890	6.6393	9.6049	3.9626	5.8030
0.9677	-0.0432	-0.0188	-0.0502	6.4805	13.6070	3.6091	6.0031
1.0323	-0.0394	-0.0035	-0.0652	8.9267	18.4090	4.1137	8.4043
6.4516	0.0064	0.0014	0.0046	24.4110	50.2260	1.4447	7.6039

Y/DELTA	q**2/UE**2 COMPOSITE	q**2/UE**2 INTER-TURBULENT ZONE	q**2/UE**2 TURBULENT ZONE	UV/UE**2 COMPOSITE	UV/UE**2 INTER-TURBULENT ZONE	UV/UE**2 TURBULENT ZONE
0.3548	0.005871	0.005336	0.015237	-2.325E-04	-1.350E-04	-1.687E-03
0.4194	0.005034	0.004392	0.014237	-1.532E-04	-4.832E-05	-1.467E-03
0.4839	0.004159	0.003335	0.012571	-1.281E-04	-8.110E-05	-7.882E-04
0.5484	0.002657	0.002081	0.010798	-1.102E-04	-4.775E-05	-9.178E-04
0.6452	0.001728	0.001292	0.008576	-6.549E-05	-3.495E-05	-6.760E-04
0.7742	0.001119	0.000698	0.007212	-8.045E-05	-3.356E-05	-6.416E-04
0.9677	0.000561	0.000324	0.004945	-2.424E-05	-6.105E-06	-2.480E-04
1.0323	0.000374	0.000260	0.002067	-1.475E-05	-9.189E-07	-1.361E-04
6.4516	0.000260	0.000284	0.000312	1.660E-06	4.060E-07	1.440E-06

TABLE A5-B

87-10-44-80

PROFILES OF MEAN AND FLUCTUATING QUANTITIES

X = 36.8   K = 0.20 E−6   TE = 0.76 %

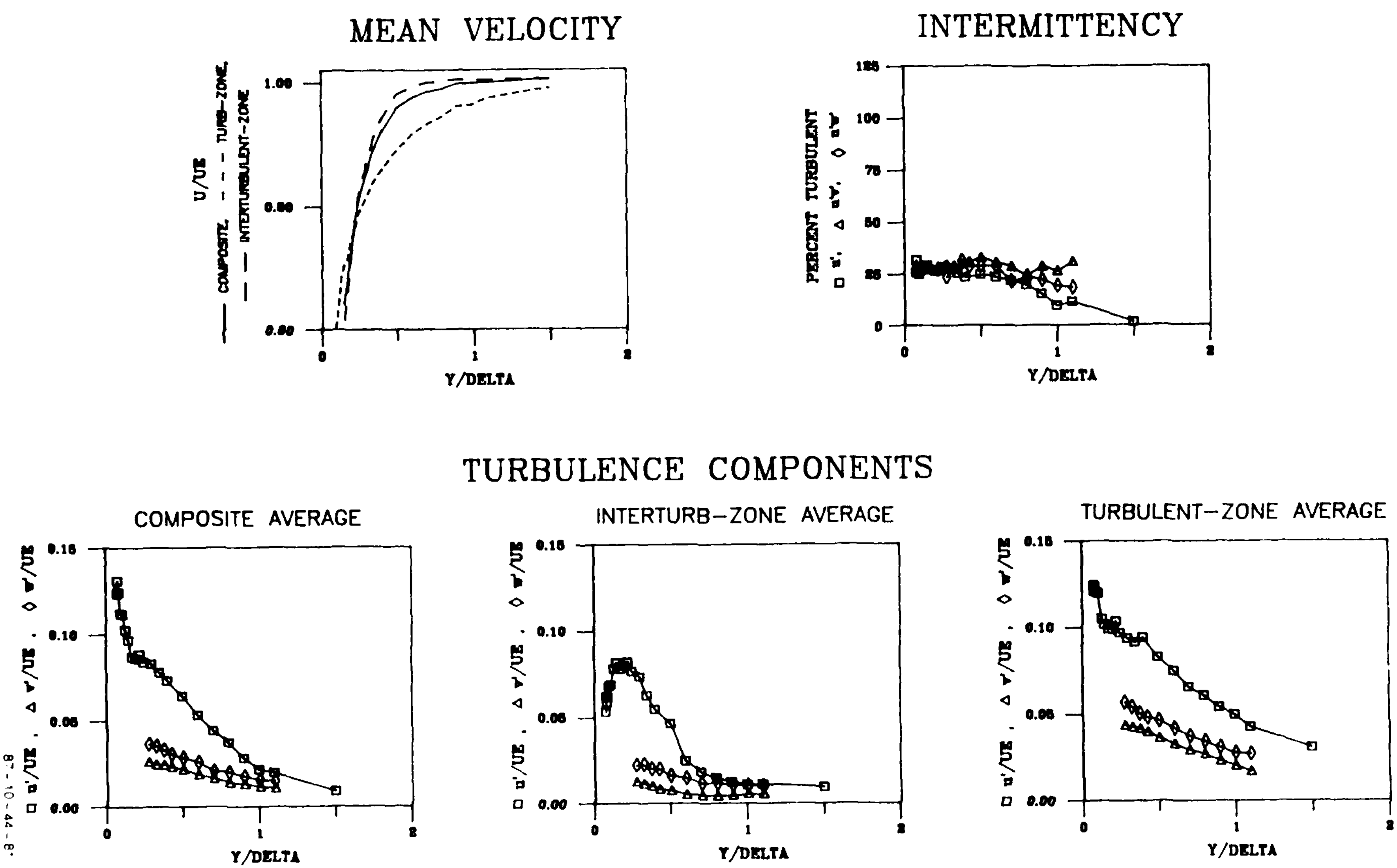

Figure A6-A

87-10-44-81

PROFILES OF TURBULENT STRESSES

X = 36.8   K = 0.20 E-6   TE = 0.76 %

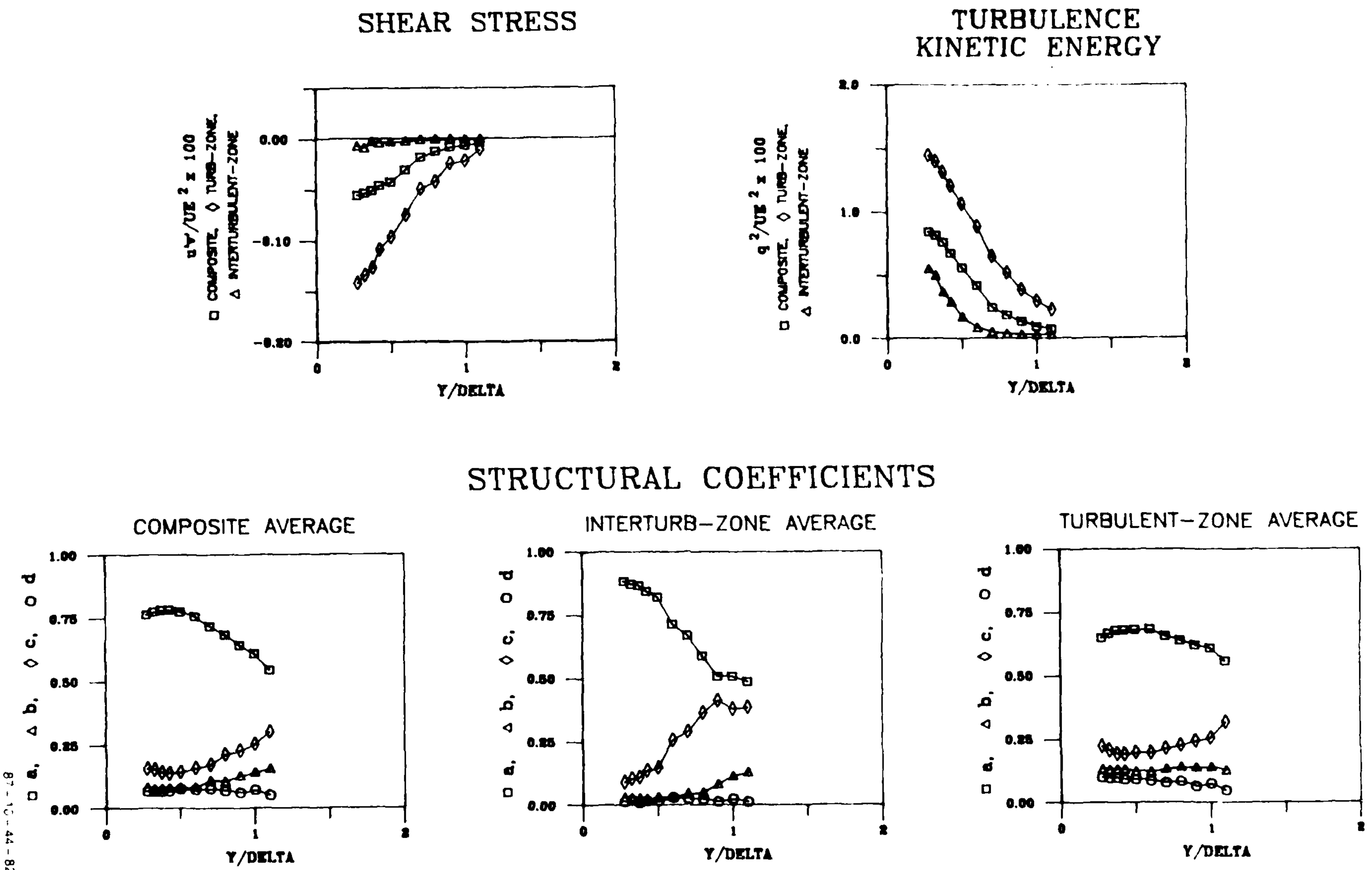

87-10-44-82

Figure A6-B

SINGLE WIRE PROFILE DATA

X = 36.8 GRID NO. 1 K = 0.2E-06

Y/DELTA	U/UE COMPOSITE	U/UE INTER-TURBULENT ZONE	U/UE TURBULENT ZONE	U'/UE COMPOSITE	U'/UE INTER-TURBULENT ZONE	U'/UE TURBULENT ZONE	GAMMA U	[illegible]
0.0750	0.3918	0.3345	0.5495	0.1233	0.0530	0.1242	25.4690	19.6100
0.0800	0.4356	0.3673	0.5794	0.1309	0.0620	0.1210	31.6290	21.6110
0.0850	0.4419	0.3817	0.5824	0.1242	0.0584	0.1234	28.2940	19.2100
0.0875	0.4571	0.3990	0.6037	0.1239	0.0617	0.1204	27.8020	19.4100
0.0985	0.4885	0.4453	0.6107	0.1117	0.0680	0.1201	24.6130	18.0090
0.1080	0.5197	0.4757	0.6338	0.1113	0.0687	0.1193	26.5290	18.6100
0.1285	0.5874	0.5529	0.6763	0.1024	0.0778	0.1046	27.4870	17.8090
0.1480	0.6410	0.6153	0.7030	0.0965	0.0816	0.1014	28.9700	21.4110
0.1730	0.6797	0.6666	0.7149	0.0866	0.0778	0.0987	26.9850	20.4100
0.1985	0.7294	[illegible]	0.7474	0.0857	0.0798	0.0986	26.1240	20.8110
0.2210	0.7678	0.7703	0.7614	0.0883	0.0818	0.1033	26.7260	22.2110
0.2460	0.8062	0.8142	0.7867	0.0877	0.0764	0.0967	28.3890	21.6110
0.2965	0.8518	0.8662	0.8142	0.0827	0.0734	0.0935	27.6130	22.4100
0.3465	0.8942	0.9130	0.8398	0.0777	0.0624	0.0913	25.2410	20.6110
0.3970	0.9209	0.9395	0.8591	0.0729	0.0544	0.0940	23.1890	20.6110
0.4975	0.9566	0.9800	0.8907	0.0642	0.0462	0.0825	24.4900	20.8110
0.5960	0.9751	0.9977	0.9168	0.0532	0.0245	0.0748	23.2860	21.2110
0.6955	0.9855	1.0044	0.9330	0.0441	0.0183	0.0655	21.5470	[illegible]
0.7960	0.9902	1.0015	0.9456	[illegible]	0.0146	0.0606	19.6850	20.2100
0.8955	0.9982	1.0049	0.9611	0.0282	0.0122	0.0538	15.1361	19.8100
0.9955	0.9997	1.0076	0.9643	0.0215	0.0106	0.0497	9.5748	15.605
1.0955	1.0006	1.0041	0.9748	0.0196	0.0111	0.0424	11.4290	19.2100
1.4950	1.0059	1.0061	0.9910	0.0088	0.0093	0.0306	1.5804	5.0026
4.9955	1.0047	1.0040	1.0107	0.0073	0.0073	0.0000	0.0000	0.0000

TABLE A6-A

87 - 10 - 44 - 83

CROSS WIRE PROFILE DATA

X = 36.8 GRID NO. 1 K = 0.2E-06

Y/DELTA	U'/UE COMPOSITE	U'/UE INTER-TURBULENT ZONE	U'/UE TURBULENT ZONE	V'/UE COMPOSITE	V'/UE INTER-TURBULENT ZONE	V'/UE TURBULENT ZONE	W'/UE COMPOSITE	W'/UE INTER-TURBULENT ZONE	W'/UE TURBULENT ZONE
0.2750	0.0800	0.0695	0.0967	0.0262	0.0127	0.0435	0.0363	0.0222	0.0566
0.3250	0.0793	0.0654	0.0963	0.0246	0.0115	0.0423	0.0352	0.0227	0.0538
0.3750	0.0769	0.0557	0.0942	0.0243	0.0099	0.0413	0.0328	0.0199	0.0501
0.4250	0.0725	0.0488	0.0904	0.0232	0.0082	0.0396	0.0305	0.0197	0.0479
0.5000	0.0657	0.0374	0.0850	0.0217	0.0074	0.0359	0.0283	0.0160	0.0459
0.6000	0.0559	0.0239	0.0774	0.0187	0.0050	0.0327	0.0258	0.0145	0.0416
0.7000	0.0414	0.0176	0.0648	0.0162	0.0046	0.0292	0.0204	0.0116	0.0371
0.8000	0.0352	0.0143	0.0573	0.0138	0.0042	0.0268	0.0198	0.0114	0.0342
0.9000	0.0290	0.0117	0.0484	0.0130	0.0047	0.0229	0.0174	0.0106	0.0305
1.0000	0.0237	0.0117	0.0421	0.0114	0.0056	0.0202	0.0153	0.0102	0.0274
1.1000	0.0195	0.0111	0.0343	0.0106	0.0057	0.0168	0.0147	0.0099	0.0268
5.0000	0.0080	0.0079	0.0085	0.0095	0.0092	0.0101	0.0083	0.0083	0.0068

Y/DELTA	U'**2/q**2 COMPOSITE	U'**2/q**2 INTER-TURBULENT ZONE	U'**2/q**2 TURBULENT ZONE	V'**2/q**2 COMPOSITE	V'**2/q**2 INTER-TURBULENT ZONE	V'**2/q**2 TURBULENT ZONE	W'**2/q**2 COMPOSITE	W'**2/q**2 INTER-TURBULENT ZONE	W'**2/q**2 TURBULENT ZONE
0.2750	0.7620	0.8812	0.6471	0.0823	0.0294	0.1318	0.1557	0.0894	0.2211
0.3250	0.7732	0.8693	0.6650	0.0748	0.0267	0.1287	0.1519	0.1040	0.2063
0.3750	0.7804	0.8637	0.6780	0.0784	0.0273	0.1307	0.1412	0.1090	0.1913
0.4250	0.7815	0.8411	0.6789	0.0807	0.0234	0.1312	0.1378	0.1355	0.1899
0.5000	0.7730	0.8195	0.6804	0.0842	0.0321	0.1218	0.1427	0.1485	0.1978
0.6000	0.7552	0.7125	0.6823	0.0850	0.0309	0.1218	0.1598	0.2566	0.1959
0.7000	0.7162	0.6664	0.6547	0.1103	0.0452	0.1328	0.1735	0.2863	0.2125
0.8000	0.6824	0.5864	0.6360	0.1051	0.0498	0.1394	0.2125	0.3637	0.2246
0.9000	0.6416	0.5063	0.6184	0.1295	0.0819	0.1383	0.2289	0.4118	0.2433
1.0000	0.6064	0.5065	0.6069	0.1416	0.1148	0.1393	0.2521	0.3786	0.2538
1.1000	0.5423	0.4852	0.5557	0.1566	0.1293	0.1266	0.3011	0.3855	0.3177
5.0000	0.2867	0.2918	0.2861	0.4051	0.3908	0.4055	0.3081	0.3174	0.3064

Y/DELTA	UV/Q**2 COMPOSITE	UV/Q**2 INTER-TURBULENT ZONE	UV/Q**2 TURBULENT ZONE	GAMMA UV	f UV	GAMMA WV	f WV
0.2750	-0.0662	-0.0129	-0.0984	29.4540	18.6100	23.2150	18.2090
0.3250	-0.0657	-0.0181	-0.0963	28.1860	21.4110	27.5970	22.4110
0.3750	-0.0672	-0.0068	-0.0970	29.7210	21.4110	31.1530	24.8130
0.4250	-0.0682	-0.0145	-0.0907	30.5710	25.0130	28.2910	21.4110
0.5000	-0.0763	-0.0161	-0.0909	32.6970	26.0130	28.7760	20.8110
0.6000	-0.0742	-0.0292	-0.0853	30.2410	23.2120	28.7010	23.4120
0.7000	-0.0766	-0.0239	-0.0773	28.4070	26.6140	21.0810	18.2090
0.8000	-0.0697	-0.0231	-0.0820	23.9750	24.2120	23.5990	20.4100
0.9000	-0.0621	-0.0122	-0.0637	28.3790	29.4150	21.7980	19.6100
1.0000	-0.0718	-0.0247	-0.0740	26.2730	32.6170	19.0470	19.8100
1.1000	-0.0516	-0.0123	-0.0478	30.7840	39.0200	18.1400	17.2090
5.0000	-0.0007	-0.0024	0.0024	32.2310	57.6300	1.7674	7.2037

Y/DELTA	q**2/UE**2 COMPOSITE	q**2/UE**2 INTER-TURBULENT ZONE	q**2/UE**2 TURBULENT ZONE	UV/UE**2 COMPOSITE	UV/UE**2 INTER-TURBULENT ZONE	UV/UE**2 TURBULENT ZONE
0.2750	0.008403	0.005492	0.014444	-5.560E-04	-7.096E-05	-1.422E-03
0.3250	0.008131	0.004950	0.013944	-5.339E-04	-8.971E-05	-1.343E-03
0.3750	0.007578	0.003628	0.013083	-5.092E-04	-2.480E-05	-1.269E-03
0.4250	0.006724	0.002857	0.012031	-4.584E-04	-4.157E-05	-1.091E-03
0.5000	0.005591	0.001715	0.010627	-4.266E-04	-2.759E-05	-9.662E-04
0.6000	0.004141	0.000811	0.008799	-3.072E-04	-2.366E-05	-7.508E-04
0.7000	0.002395	0.000467	0.006438	-1.835E-04	-1.117E-05	-4.976E-04
0.8000	0.001828	0.000354	0.005182	-1.273E-04	-8.177E-06	-4.250E-04
0.9000	0.001310	0.000272	0.003812	-8.141E-05	-3.320E-06	-2.429E-04
1.0000	0.000925	0.000272	0.002937	-6.647E-05	-6.720E-06	-2.173E-04
1.1000	0.000714	0.000252	0.002248	-3.687E-05	-3.106E-06	-1.075E-04
5.0000	0.000223	0.000216	0.000251	-1.584E-07	-5.090E-07	5.939E-07

TABLE A6-B

87-10-44-84

PROFILES OF MEAN AND FLUCTUATING QUANTITIES

X = 44.8 K = 0.20 E−6 TE = 0.74 %

MEAN VELOCITY

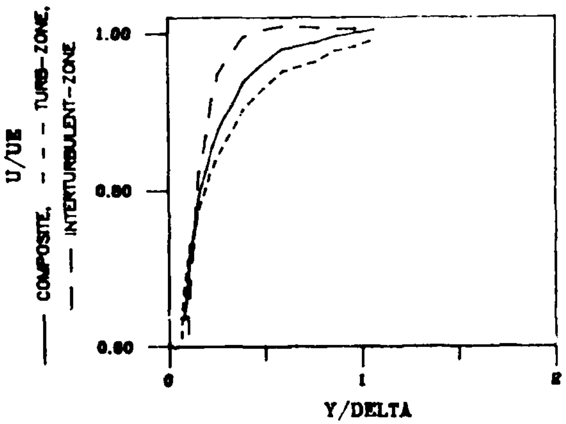

INTERMITTENCY

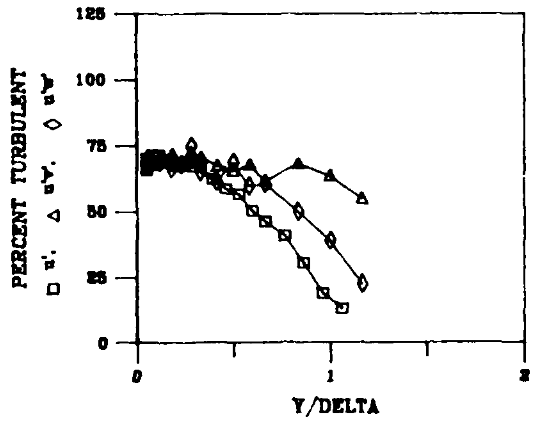

TURBULENCE COMPONENTS

COMPOSITE AVERAGE

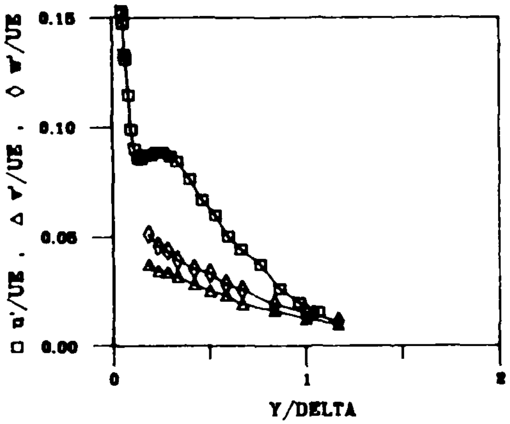

INTERTURB-ZONE AVERAGE

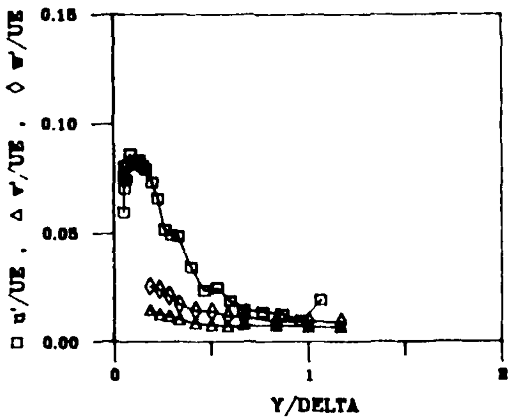

TURBULENT-ZONE AVERAGE

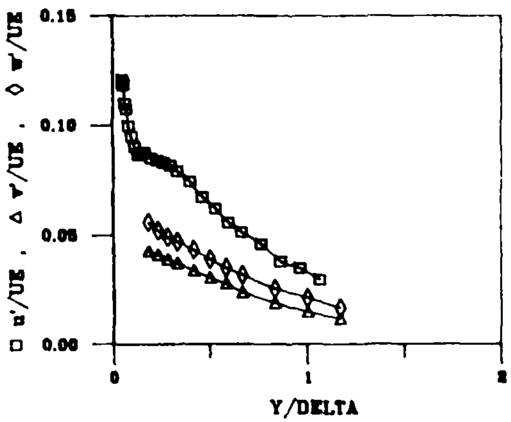

Figure A7-A

87-10-44-85

PROFILES OF TURBULENT STRESSES

X = 44.8 K = 0.20 E-6 TE = 0.74 %

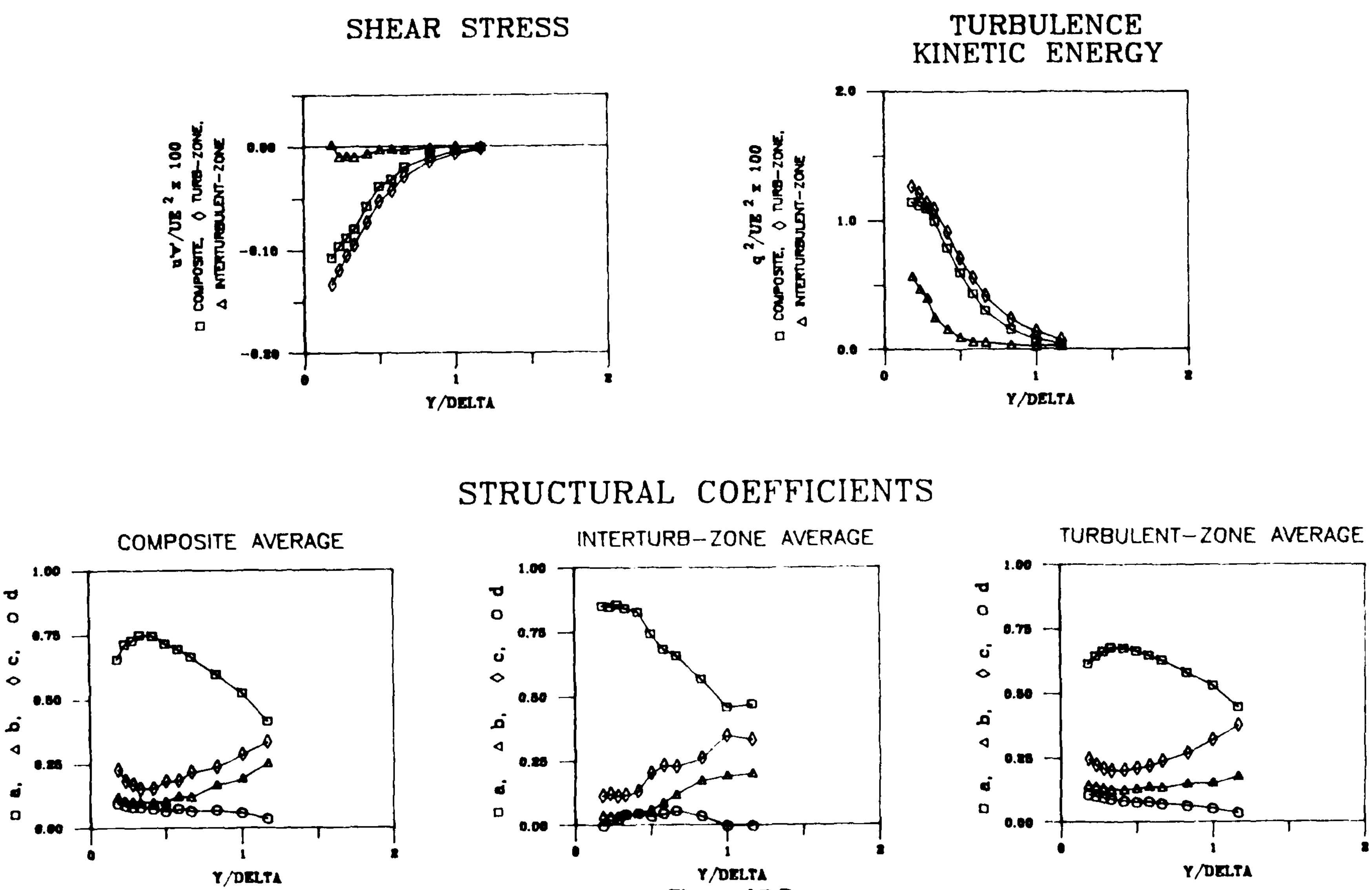

Figure A7-B

87-10-44-86

SINGLE WIRE PROFILE DATA

X = 44.8 GRID NO. 1 K = 0.2E-06

Y/DELTA	U/UE COMPOSITE	U/UE INTER-TURBULENT ZONE	U/UE TURBULENT ZONE	U' /UE COMPOSITE	U' /UE INTER-TURBULENT ZONE	U' /UE TURBULENT ZONE	GAMMA	[illegible]
0.0500	0.4491	0.2980	0.5278	0.1529	0.0754	0.1205	66.5110	26.4140
0.0533	0.4845	0.3149	0.5566	0.1518	0.0593	0.1180	69.8920	23.0120
0.0563	0.5025	0.3533	0.5692	0.1471	0.0803	0.1166	69.7230	24.6130
0.0583	0.5064	0.3625	0.5817	0.1475	0.0701	0.1187	65.5070	24.6130
0.0650	0.5525	0.4209	0.6105	0.1328	0.0741	0.1096	69.6900	23.8120
0.0717	0.5762	0.4532	0.6346	0.1306	0.0808	0.1071	68.1760	23.0120
0.0863	0.6349	0.5366	0.6746	0.1143	0.0860	0.0994	71.2270	23.6120
0.0997	0.6719	0.6156	0.6987	0.0986	0.0817	0.0947	67.4130	25.0130
0.1163	0.7154	0.6657	0.7276	0.0899	0.0823	0.0900	71.2220	25.8130
0.1310	0.7374	0.7252	0.7429	0.0856	0.0831	0.0862	65.5761	23.0120
0.1480	0.7674	0.7786	0.7626	0.0852	0.0806	0.0868	69.7870	25.2130
0.1637	0.7920	0.8221	0.7782	0.0870	0.0790	0.0872	68.5431	25.[illegible]
0.1977	0.8222	0.8669	0.8018	0.0869	0.0730	0.0847	67.5[illegible]	25.6[illegible]
0.2303	0.8552	0.9156	0.8281	0.0882	0.0656	0.0836	68.6420	26.6140
0.2637	0.8784	0.9486	0.8461	0.0881	0.0513	0.0826	65.5730	27.4140
0.2977	0.8948	0.9625	0.8616	0.0864	0.0490	0.0814	67.0800	28.4151
0.3310	0.9172	0.9778	0.8750	0.0841	0.0484	0.0788	67.4740	26.2130
0.3970	0.9391	0.9958	0.9048	0.0762	0.0342	0.0742	62.1391	30.2150
0.4637	0.9548	1.0020	0.9221	0.0664	0.0274	0.0677	58.5761	30.8161
0.5302	0.9679	1.0068	0.9375	0.0597	0.0247	0.0617	56.3990	30.8160
0.5970	0.9804	1.0089	0.9519	0.0530	0.0167	0.0554	50.1410	34.2161
0.6641	0.9621	1.0067	0.9558	0.0441	0.0144	0.0510	46.1271	35.8181
0.7637	0.9854	1.0059	0.9622	0.0372	0.0125	0.0457	40.6191	35.818
0.8637	0.9961	1.0044	0.9774	0.0261	0.0126	0.0376	30.2381	41.4210
0.9641	1.0002	1.0047	0.9822	0.0197	0.0096	0.0347	18.6910	36.6191
1.0637	1.0047	1.0066	0.9904	0.0154	0.0193	0.0294	12.8530	[illegible].4163
3.3310	1.0064	1.0064	1.0114	0.0068	0.0068	0.0000	0.0000	0.0000

TABLE A7-A

87-10-44-87

CROSS WIRE PROFILE DATA

X = 44.8 GRID NO. 1 K = 0.2E-06

Y/DELTA	U'/UE COMPOSITE	U'/UE INTER-TURBULENT ZONE	U'/UE TURBULENT ZONE	V'/UE COMPOSITE	V'/UE INTER-TURBULENT ZONE	V'/UE TURBULENT ZONE	W'/UE COMPOSITE	W'/UE INTER-TURBULENT ZONE	W'/UE TURBULENT ZONE
0.1833	0.0864	0.0693	0.0879	0.0370	0.0145	0.0424	0.0510	0.0254	0.0556
0.2333	0.0890	0.0622	0.0882	0.0341	0.0124	0.0407	0.0453	0.0238	0.0517
0.2833	0.0892	0.0582	0.0867	0.0334	0.0117	0.0386	0.0432	0.0211	0.0486
0.3333	0.0863	0.0455	0.0857	0.0314	0.0101	0.0368	0.0390	0.0171	0.0466
0.4167	0.0765	0.0356	0.0782	0.0280	0.0083	0.0336	0.0349	0.0142	0.0429
0.5000	0.0652	0.0261	0.0685	0.0248	0.0074	0.0302	0.0330	0.0137	0.0386
0.5833	0.0544	0.0195	0.0596	0.0230	0.0069	0.0275	0.0282	0.0114	0.0347
0.6667	0.0444	0.0186	0.0507	0.0189	0.0079	0.0234	0.0256	0.0110	0.0314
0.8333	0.0300	0.0133	0.0366	0.0159	0.0074	0.0187	0.0190	0.0091	0.0251
1.0000	0.0201	0.0103	0.0264	0.0122	0.0067	0.0144	0.0149	0.0091	0.0209
1.1667	0.0122	0.0104	0.0176	0.0095	0.0068	0.0113	0.0110	0.0088	0.0164
3.3333	0.0077	0.0098	0.0076	0.0092	0.0087	0.0096	0.0078	0.0078	0.0087

Y/DELTA	U'**2/q**2 COMPOSITE	U'**2/q**2 INTER-TURBULENT ZONE	U'**2/q**2 TURBULENT ZONE	V'**2/q**2 COMPOSITE	V'**2/q**2 INTER-TURBULENT ZONE	V'**2/q**2 TURBULENT ZONE	W'**2/q**2 COMPOSITE	W'**2/q**2 INTER-TURBULENT ZONE	W'**2/q**2 TURBULENT ZONE
0.1833	0.6536	0.8497	0.6127	0.1200	0.0374	0.1430	0.2263	0.1129	0.2443
0.2333	0.7117	0.8457	0.6429	0.1051	0.0330	0.1373	0.1832	0.1212	0.2198
0.2833	0.7274	0.8551	0.6613	0.1023	0.0341	0.1319	0.1703	0.1108	0.2069
0.3333	0.7483	0.8403	0.6761	0.0995	0.0415	0.1248	0.1522	0.1182	0.1990
0.4167	0.7451	0.8247	0.6733	0.1003	0.0453	0.1250	0.1546	0.1300	0.2017
0.5000	0.7141	0.7402	0.6618	0.1035	0.0585	0.1292	0.1823	0.2013	0.2091
0.5833	0.6919	0.6817	0.6446	0.1236	0.0865	0.1372	0.1845	0.2318	0.2180
0.6667	0.6621	0.6557	0.6272	0.1205	0.1183	0.1342	0.2174	0.2261	0.2386
0.8333	0.5949	0.5654	0.5794	0.1679	0.1737	0.1509	0.2372	0.2608	0.2697
1.0000	0.5222	0.4579	0.5281	0.1928	0.1934	0.1529	0.2850	0.3486	0.3190
1.1667	0.4132	0.4688	0.4453	0.2522	0.2000	0.1786	0.3346	0.3312	0.3761
3.3333	0.2905	0.4140	0.2578	0.4142	0.3290	0.4118	0.2954	0.2570	0.3303

Y/DELTA	UV/Q**2 COMPOSITE	UV/Q**2 INTER-TURBULENT ZONE	UV/Q**2 TURBULENT ZONE	GAMMA UV	f UV	GAMMA WV	f WV
0.1833	-0.0941	0.0037	-0.1058	71.8950	24.2120	66.1270	19.4100
0.2333	-0.0863	-0.0209	-0.0986	67.3080	25.0130	67.8710	23.0120
0.2833	-0.0805	-0.0224	-0.0926	71.9030	23.8120	74.6880	21.6110
0.3333	-0.0800	-0.0416	-0.0877	70.3380	24.4130	64.7980	25.8130
0.4167	-0.0734	-0.0433	-0.0807	67.1880	27.8140	61.0170	26.2130
0.5000	-0.0646	-0.0320	-0.0748	65.2820	28.4150	68.5250	26.0130
0.5833	-0.0739	-0.0446	-0.0772	67.7590	27.0140	59.5110	27.0140
0.6667	-0.0652	-0.0539	-0.0699	61.6140	34.6180	60.4070	27.2140
0.8333	-0.0686	-0.0339	-0.0627	68.0610	38.0190	49.6110	32.8170
1.0000	-0.0571	0.0034	-0.0505	63.4120	46.0240	38.6010	35.0180
1.1667	-0.0348	0.0041	-0.0339	54.6620	54.2280	22.1540	29.4150
3.3333	0.0191	0.0167	0.0141	45.7070	64.0330	2.4283	9.0046

Y/DELTA	q**2/UE**2 COMPOSITE	q**2/UE**2 INTER-TURBULENT ZONE	q**2/UE**2 TURBULENT ZONE	UV/UE**2 COMPOSITE	UV/UE**2 INTER-TURBULENT ZONE	UV/UE**2 TURBULENT ZONE
0.1833	0.011427	0.005672	0.012621	-1.075E-03	2.085E-05	-1.335E-03
0.2333	0.011138	0.004660	0.012091	-9.618E-04	-9.760E-05	-1.193E-03
0.2833	0.010936	0.004000	0.011358	-8.801E-04	-8.951E-05	-1.052E-03
0.3333	0.009947	0.002459	0.010870	-7.957E-04	-1.022E-04	-9.536E-04
0.4167	0.007851	0.001541	0.009090	-5.763E-04	-6.679E-05	-7.340E-04
0.5000	0.005958	0.000928	0.007097	-3.846E-04	-2.966E-05	-5.307E-04
0.5833	0.004286	0.000557	0.005515	-3.169E-04	-2.483E-05	-4.259E-04
0.6667	0.002991	0.000531	0.004112	-1.949E-04	-2.859E-05	-2.875E-04
0.8333	0.001519	0.000317	0.002331	-1.043E-04	-1.076E-05	-1.462E-04
1.0000	0.000780	0.000234	0.001363	-4.455E-05	8.059E-07	-6.877E-05
1.1667	0.000362	0.000232	0.000714	-1.261E-05	9.498E-07	-2.423E-05
3.3333	0.000205	0.000233	0.000227	3.915E-06	3.900E-06	3.196E-06

TABLE A7-B

PROFILES OF MEAN AND FLUCTUATING QUANTITIES

X = 52.8 K = 0.20 E−6 TE = 0.72 %

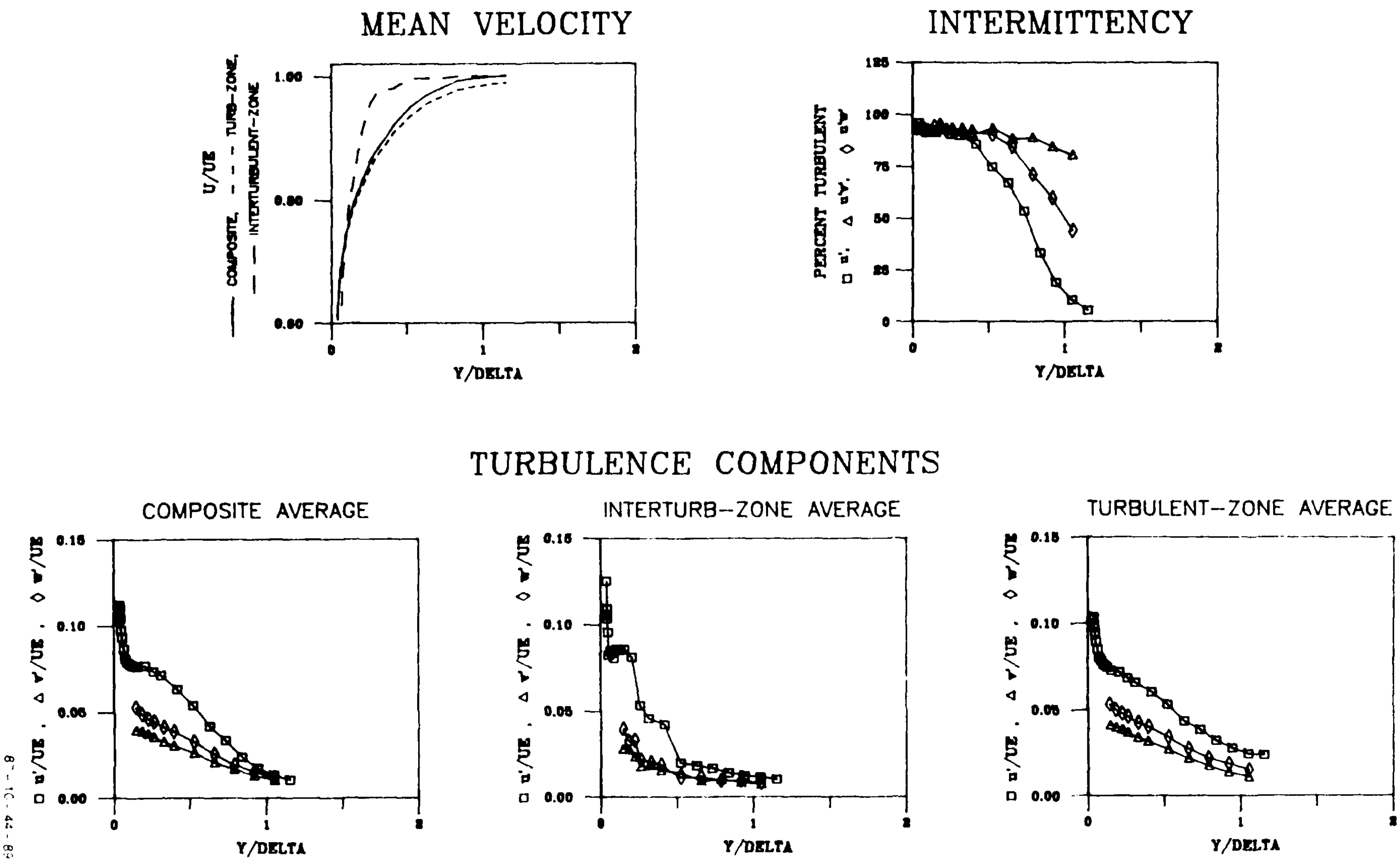

Figure A8-A

87-10-44-89

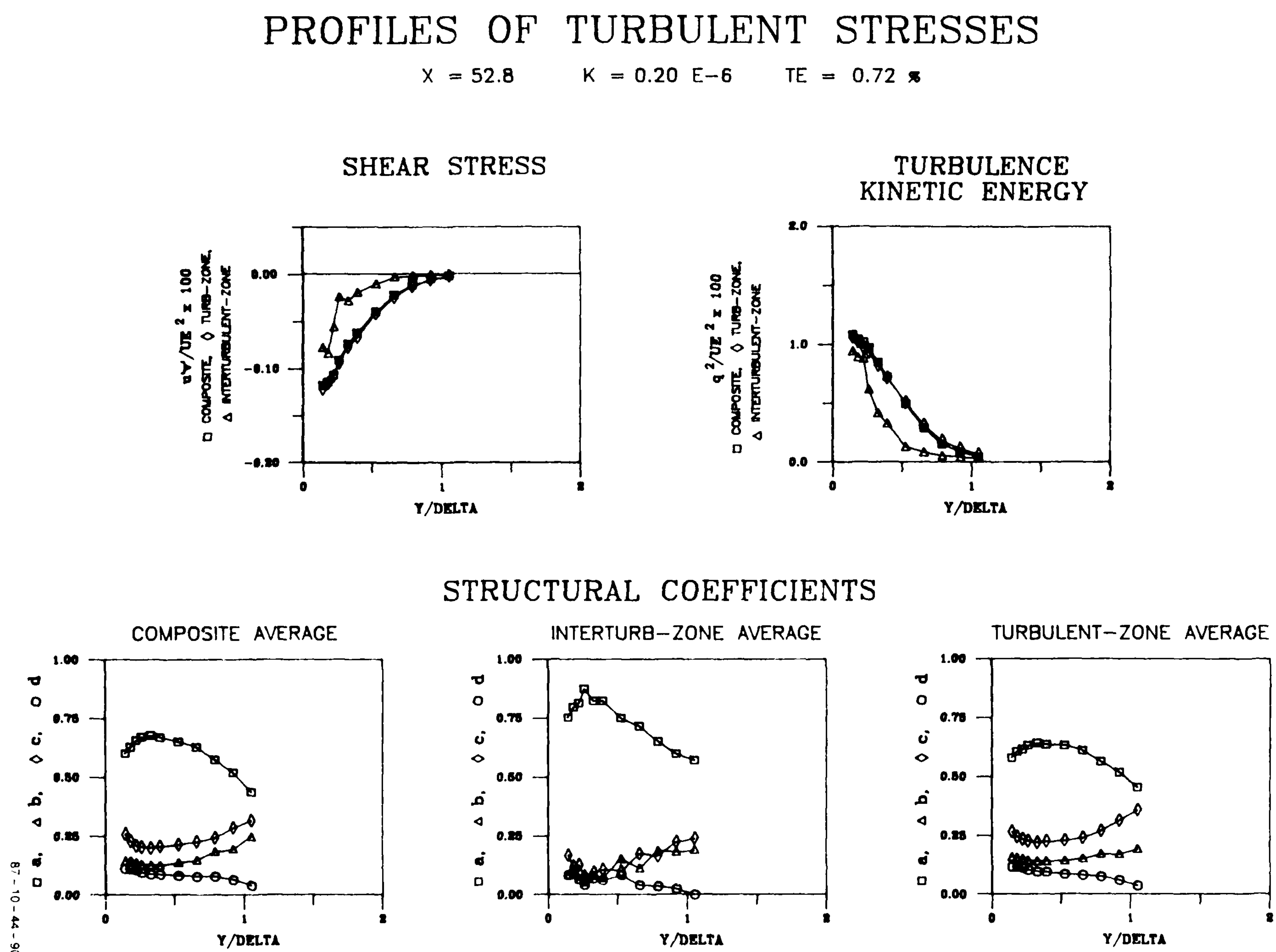

Figure A8-B

87-10-44-90

SINGLE WIRE PROFILE DATA

X = 52.8 GRID NO. 1 K = 0.2E-06

Y/DELTA	U/UE COMPOSITE	U/UE INTER-TURBULENT ZONE	U/UE TURBULENT ZONE	U'/UE COMPOSITE	U'/UE INTER-TURBULENT ZONE	U'/UE TURBULENT ZONE	GAMMA	[illegible]
0.0395	0.5846	0.4368	0.5966	0.1119	0.1054	0.1035	93.1860	9.0046
0.0418	0.5940	0.5171	0.6062	0.1099	0.1250	0.1021	93.2990	9.8050
0.0437	0.6112	0.4952	0.6186	0.1037	0.1090	0.0989	95.6510	7.6079
0.0463	0.6177	0.5135	0.6301	0.1045	0.1032	0.0975	92.0770	7.6039
0.0513	0.6414	0.5662	0.6484	0.0973	0.0953	0.0946	94.0270	11.2060
0.0566	0.6587	0.5518	0.6663	0.0930	0.0820	0.0891	93.9750	9.0046
0.0679	0.6854	0.6284	0.6912	0.0866	0.0846	0.0848	92.2540	9.6049
0.0784	0.7085	0.6754	0.7109	0.0806	0.0834	0.0799	93.3940	7.8040
0.0911	0.7247	0.7182	0.7254	0.0785	0.0804	0.0783	[illegible]	[illegible]
0.1042	0.7453	0.7583	0.7435	0.0775	0.0855	0.0762	92.7460	[illegible]
0.1166	0.7610	0.7844	0.7579	0.0769	0.0856	0.0753	91.7370	10.4150
0.1297	0.7757	0.8061	0.7714	0.0765	0.0851	0.0743	92.2260	10.8[illegible]
0.1566	0.7980	0.8397	0.7911	0.0762	0.0855	0.0724	[illegible]	[illegible]
0.2069	0.8326	0.9091	0.8242	0.0767	0.0811	0.0715	92.6590	11.4[illegible]
0.2618	0.8633	0.9566	0.8527	0.0734	0.0532	0.0680	90.3690	11.6[illegible]
0.3134	0.8841	0.9759	0.8731	0.0712	0.0457	0.0657	89.7750	14.4[illegible]
0.4187	0.9209	0.9804	0.9094	0.0630	0.0420	0.0601	85.5300	21.8110
0.5239	0.9505	0.9969	0.9349	0.0537	0.0198	0.0528	74.6720	[illegible]
0.6292	0.9686	0.9963	0.9550	0.0415	0.0183	0.0433	66.8706	41.4210
0.7345	0.9813	0.9974	0.9674	0.0334	0.0166	0.0363	53.3710	51.8[illegible]
0.8397	0.9928	1.0003	0.9783	0.0238	0.0138	0.0322	33.1280	54.6[illegible]
0.9451	0.9966	0.9999	0.9833	0.0172	0.0124	0.0277	18.9520	44.5[illegible]
1.0503	0.9999	1.0013	0.9878	0.0131	0.0114	0.0243	10.2790	31.416
1.1555	1.0010	1.0016	0.9895	0.0105	0.0101	0.0236	5.22[illegible]	[illegible]
2.6292	1.0018	1.0018	1.0051	0.0066	0.0066	0.0000	0.0000	0.00

TABLE A8-A

87-10-44-91

CROSS WIRE PROFILE DATA

X = 52.8 GRID NO. 1 K = 0.2E-06

Y/DELTA	U'/UE COMPOSITE	U'/UE INTER-TURBULENT ZONE	U'/UE TURBULENT ZONE	V'/UE COMPOSITE	V'/UE INTER-TURBULENT ZONE	V'/UE TURBULENT ZONE	W'/UE COMPOSITE	W'/UE INTER-TURBULENT ZONE	W'/UE TURBULENT ZONE
0.1447	0.0804	0.0837	0.0784	0.0394	0.0279	0.0409	0.0527	0.0396	0.0530
0.1842	0.0807	0.0836	0.0785	0.0389	0.0277	0.0397	0.0486	0.0324	0.0496
0.2237	0.0817	0.0843	0.0772	0.0373	0.0234	0.0384	0.0459	0.0331	0.0475
0.2632	0.0807	0.0732	0.0766	0.0354	0.0178	0.0365	0.0443	0.0215	0.0457
0.3289	0.0757	0.0583	0.0725	0.0326	0.0183	0.0339	0.0409	0.0199	0.0423
0.3947	0.0695	0.0517	0.0673	0.0303	0.0152	0.0316	0.0386	0.0186	0.0400
0.5263	0.0565	0.0304	0.0564	0.0260	0.0140	0.0268	0.0325	0.0112	0.0339
0.6579	0.0422	0.0239	0.0435	0.0206	0.0094	0.0217	0.0254	0.0118	0.0272
0.7895	0.0293	0.0181	0.0315	0.0166	0.0099	0.0174	0.0190	0.0092	0.0218
0.9211	0.0208	0.0151	0.0235	0.0129	0.0083	0.0136	0.0155	0.0093	0.0185
1.0526	0.0137	0.0125	0.0165	0.0103	0.0073	0.0109	0.0116	0.0081	0.0149
2.6316	0.0070	0.0095	0.0071	0.0085	0.0080	0.0089	0.0070	0.0070	0.0081

Y/DELTA	U'**2/q**2 COMPOSITE	U'**2/q**2 INTER-TURBULENT ZONE	U'**2/q**2 TURBULENT ZONE	V'**2/q**2 COMPOSITE	V'**2/q**2 INTER-TURBULENT ZONE	V'**2/q**2 TURBULENT ZONE	W'**2/q**2 COMPOSITE	W'**2/q**2 INTER-TURBULENT ZONE	W'**2/q**2 TURBULENT ZONE
0.1447	0.5989	0.7514	0.5779	0.1434	0.0822	0.1573	0.2577	0.1664	0.2648
0.1842	0.6265	0.7951	0.6044	0.1454	0.0864	0.1542	0.2282	0.1184	0.2414
0.2237	0.6557	0.8123	0.6152	0.1364	0.0622	0.1513	0.2079	0.1255	0.2335
0.2632	0.6695	0.8728	0.6319	0.1285	0.0516	0.1428	0.2020	0.0756	0.2253
0.3289	0.6764	0.8229	0.6419	0.1255	0.0813	0.1395	0.1981	0.0958	0.2185
0.3947	0.6676	0.8224	0.6350	0.1261	0.0708	0.1399	0.2063	0.1069	0.2251
0.5263	0.6490	0.7487	0.6305	0.1369	0.1525	0.1414	0.2140	0.0988	0.2280
0.6579	0.6259	0.7146	0.6097	0.1477	0.1113	0.1511	0.2264	0.1741	0.2392
0.7895	0.5728	0.6497	0.5617	0.1846	0.1870	0.1701	0.2426	0.1633	0.2682
0.9211	0.5188	0.5961	0.5162	0.1954	0.1803	0.1700	0.2857	0.2236	0.3139
1.0526	0.4368	0.5701	0.4524	0.2471	0.1901	0.1911	0.3162	0.2397	0.3564
2.6316	0.2838	0.4458	0.2584	0.4259	0.3155	0.4050	0.2904	0.2387	0.336[illegible]

Y/DELTA	UV/Q**2 COMPOSITE	UV/Q**2 INTER-TURBULENT ZONE	UV/Q**2 TURBULENT ZONE	GAMMA UV	f UV	GAMMA WV	f WV
0.1447	-0.1092	-0.0828	-0.1149	91.4110	10.0050	93.8930	7.8040
0.1842	-0.1102	-0.0950	-0.1135	95.0790	8.4043	94.4930	7.6039
0.2237	-0.1052	-0.0643	-0.1117	93.4840	7.8040	92.0570	9.6049
0.2632	-0.0939	-0.0392	-0.1016	93.2740	9.8050	92.3670	9.8050
0.3289	-0.0873	-0.0689	-0.0943	91.6500	12.2060	92.0700	9.6049
0.3947	-0.0859	-0.0600	-0.0935	90.4120	11.8060	91.2780	10.6050
0.5263	-0.0809	-0.0827	-0.0833	93.4070	11.0060	90.0490	13.0070
0.6579	-0.0774	-0.0396	-0.0799	88.1990	18.2090	84.2320	19.4100
0.7895	-0.0776	-0.0342	-0.0736	88.9110	24.4130	70.9990	29.4150
0.9211	-0.0634	-0.0228	-0.0585	84.3800	26.4140	59.5440	38.8200
1.0526	-0.0381	0.0012	-0.0337	80.4020	41.2210	43.6990	45.4230
2.6316	0.0150	0.0075	0.0134	54.4850	65.6340	3.8934	12.4060

Y/DELTA	q**2/UE**2 COMPOSITE	q**2/UE**2 INTER-TURBULENT ZONE	q**2/UE**2 TURBULENT ZONE	UV/UE**2 COMPOSITE	UV/UE**2 INTER-TURBULENT ZONE	UV/UE**2 TURBULENT ZONE
0.1447	0.010809	0.009425	0.010623	-1.180E-03	-7.803E-04	-1.221E-03
0.1842	0.010391	0.008880	0.010200	-1.145E-03	-8.435E-04	-1.157E-03
0.2237	0.010177	0.008746	0.009697	-1.071E-03	-5.627E-04	-1.083E-03
0.2632	0.009725	0.006146	0.009296	-9.130E-04	-2.412E-04	-9.440E-04
0.3289	0.008471	0.004128	0.008193	-7.397E-04	-2.842E-04	-7.725E-04
0.3947	0.007237	0.003254	0.007135	-6.217E-04	-1.951E-04	-6.673E-04
0.5263	0.004934	0.001283	0.005049	-3.990E-04	-1.061E-04	-4.205E-04
0.6579	0.002855	0.000799	0.003103	-2.209E-04	-3.167E-05	-2.480E-04
0.7895	0.001498	0.000524	0.001771	-1.162E-04	-1.794E-05	-1.304E-04
0.9211	0.000845	0.000384	0.001091	-5.357E-05	-8.773E-06	-6.380E-05
1.0526	0.000430	0.000277	0.000622	-1.641E-05	3.360E-07	-2.099E-05
2.6316	0.000171	0.000205	0.000196	2.566E-06	1.542E-06	2.622E-06

TABLE A8-B

PROFILES OF MEAN AND FLUCTUATING QUANTITIES

X = 4.8   K = 0.20 E−6   TE = 2.0 %

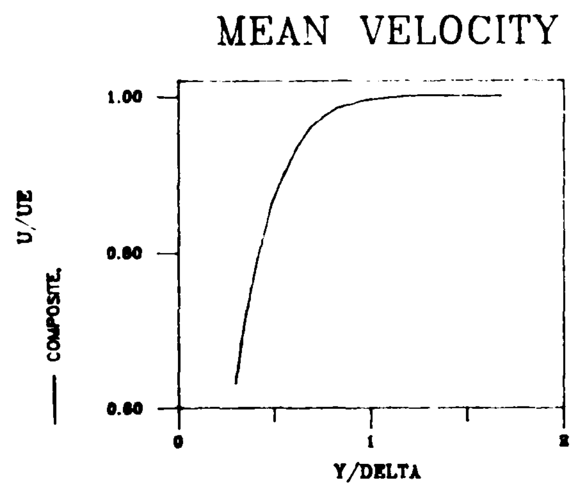

TURBULENCE COMPONENTS

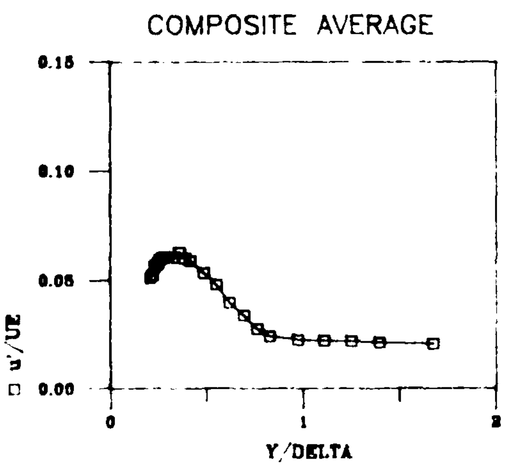

87-10-44-93

Figure A9

SINGLE WIRE PROFILE DATA

X = 4.8 GRID NO. 2 K = 0.2E-06

Y DELTA	U/UE COMPOSITE	U/UE INTER-TURBULENT ZONE	U/UE TURBULENT ZONE	U'/UE COMPOSITE	U'/UE INTER-TURBULENT ZONE	U'/UE TURBULENT ZONE	GAMMA U	U
0.2113	0.4560			0.0508				
0.2239	0.4801			0.0521				
0.2366	0.5061			0.0561				
0.2507	0.5384			0.0572				
0.2592	0.5474			0.0591				
0.2732	0.5804			0.0601				
0.3014	0.6312			0.0602				
0.3296	0.6515			0.0607				
0.3592	0.7249			0.0627				
0.3887	0.7622			0.0599				
0.4169	0.7976			0.0597				
0.4873	0.8626			0.0572				
0.5521	0.9015			0.0478				
0.6197	0.9351			0.0395				
0.6930	0.9612			0.0337				
0.7674	0.9757			0.0274				
0.8292	0.9857			0.0244				
[illegible]	0.9959			0.0227				
1.1099	0.9953			0.0221				
[illegible]	1.0017			0.0217				
1.7958	0.9996			0.0211				
[illegible]	[illegible]			[illegible]				
14.0662	0.9997			0.0176				

TABLE A9

87 - 10 - 44 - 94

PROFILES OF MEAN AND FLUCTUATING QUANTITIES

X = 8.8   K = 0.20 E-6   TE = 1.9 %

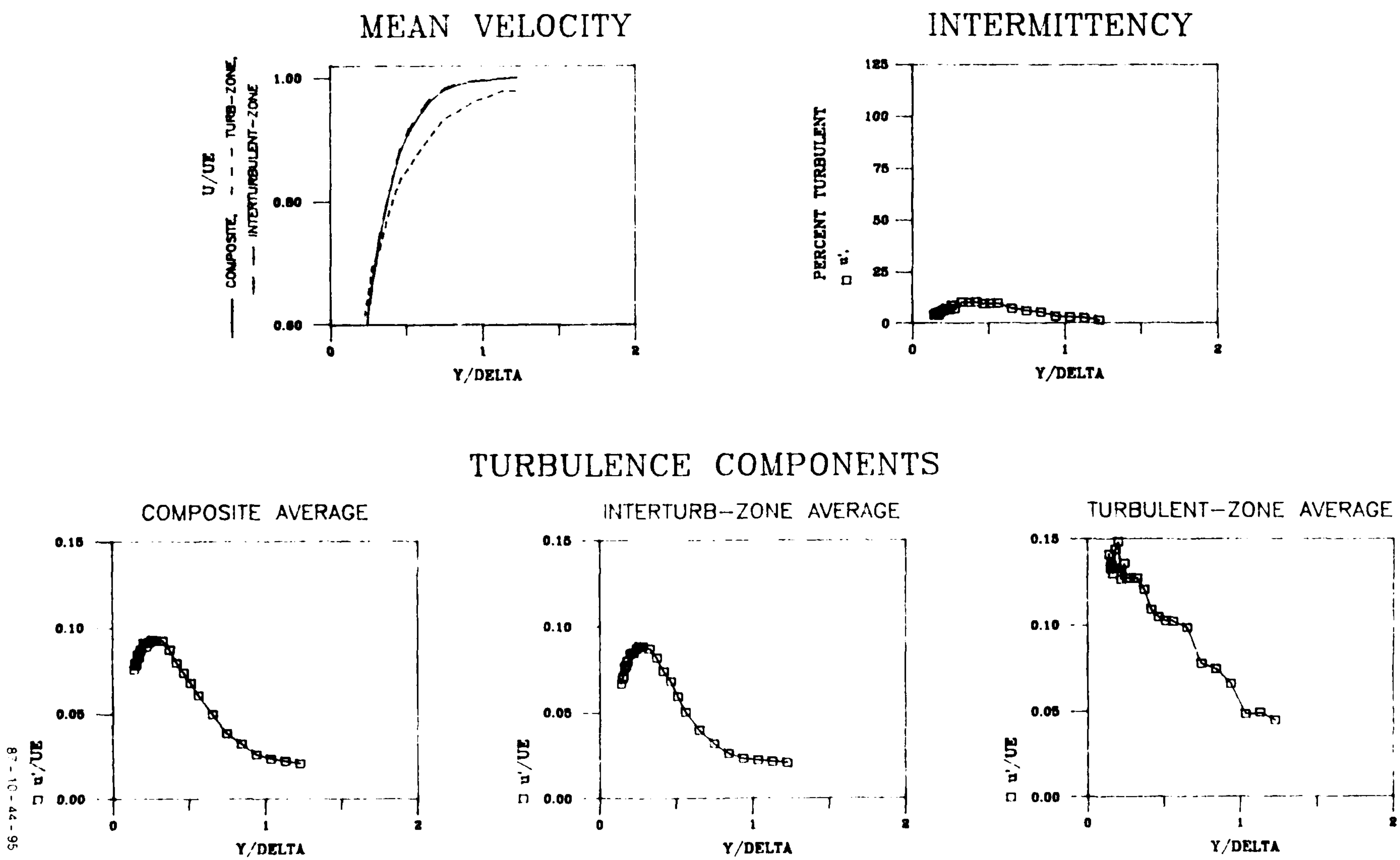

Figure A10

SINGLE WIRE PROFILE DATA

X = 8.8 GRID NO. 2 K = 0.2E-06

Y/DELTA	U/UE COMPOSITE	U/UE INTER-TURBULENT ZONE	U/UE TURBULENT ZONE	U'/UE COMPOSITE	U'/UE INTER-TURBULENT ZONE	U'/UE TURBULENT ZONE	GAMMA U	* U
0.1429	0.3653	0.3599	0.4912	0.0756	0.0663	0.1407	3.9063	8.2042
0.1533	0.3912	0.3847	0.5246	0.0793	0.0696	0.1325	4.3929	9.8050
0.1581	0.4109	0.4059	0.5051	0.0781	0.0705	0.1344	4.7515	11.8060
0.1686	0.4312	0.4256	0.4932	0.0841	0.0760	0.1294	4.9898	12.0060
0.1781	0.4581	0.4538	0.5596	0.0827	0.0771	0.1326	3.7910	9.4048
0.1867	0.4857	0.4801	0.5707	0.0870	0.0796	0.1436	5.3945	11.4060
0.2057	0.5307	0.5262	0.5949	0.0911	0.0839	0.1482	6.2013	14.4070
0.2257	0.5712	0.5679	0.6136	0.0898	0.0843	0.1262	6.9877	16.2081
0.2443	0.6022	0.5997	0.6364	0.0914	0.0868	0.1355	6.4985	17.2091
0.2619	0.6764	0.6742	0.6575	0.0927	0.0882	0.1269	8.7782	23.0120
0.281	0.6660	0.6675	0.6945	0.0923	0.0883	0.1269	7.0056	19.6111
0.3286	0.7422	0.7443	0.7242	0.0922	0.0869	0.1269	10.3250	26.2170
0.3762	0.7930	0.7958	0.7693	0.0869	0.0817	0.1213	10.0690	28.8150
0.4011	0.8475	0.8487	0.8146	0.0784	0.0737	0.1087	10.3617	29.2150
0.4676	0.8809	0.8873	0.8382	0.0737	0.0678	0.1044	9.3161	25.6130
0.5177	0.9077	0.9142	0.8501	0.0677	0.0591	0.1021	9.5261	27.6141
0.5629	0.9289	0.9355	0.8722	0.0606	0.0500	0.1019	9.6311	31.4161
0.6547	0.9615	0.9666	0.9022	0.0494	0.0395	0.0982	7.0927	25.4111
0.7495	0.9817	0.9836	0.9336	0.0382	0.0319	0.0772	6.0651	19.8111
0.8441	0.9898	0.9924	0.9465	0.0322	0.0258	0.0747	5.3689	18.8111
0.9411	0.9944	0.9956	0.9615	0.0251	0.0229	0.0659	3.3478	11.6161
1.0361	0.9971	0.9979	0.9693	0.0234	0.0221	0.0481	2.9450	10.8161
1.1305	1.0000	1.0005	0.9789	0.0221	0.0212	0.0491	2.5128	9.1146
1.2276	1.0014	1.0013	0.9759	0.0206	0.0205	0.0445	1.4191	7.6105
9.5114	0.9994	0.9994	0.9882	0.0165	0.0165	0.0000	0.0000	0.0000

TABLE A10

87-10-44-96

PROFILES OF MEAN AND FLUCTUATING QUANTITIES

X = 12.8   K = 0.20 E-6   TE = 1.8 %

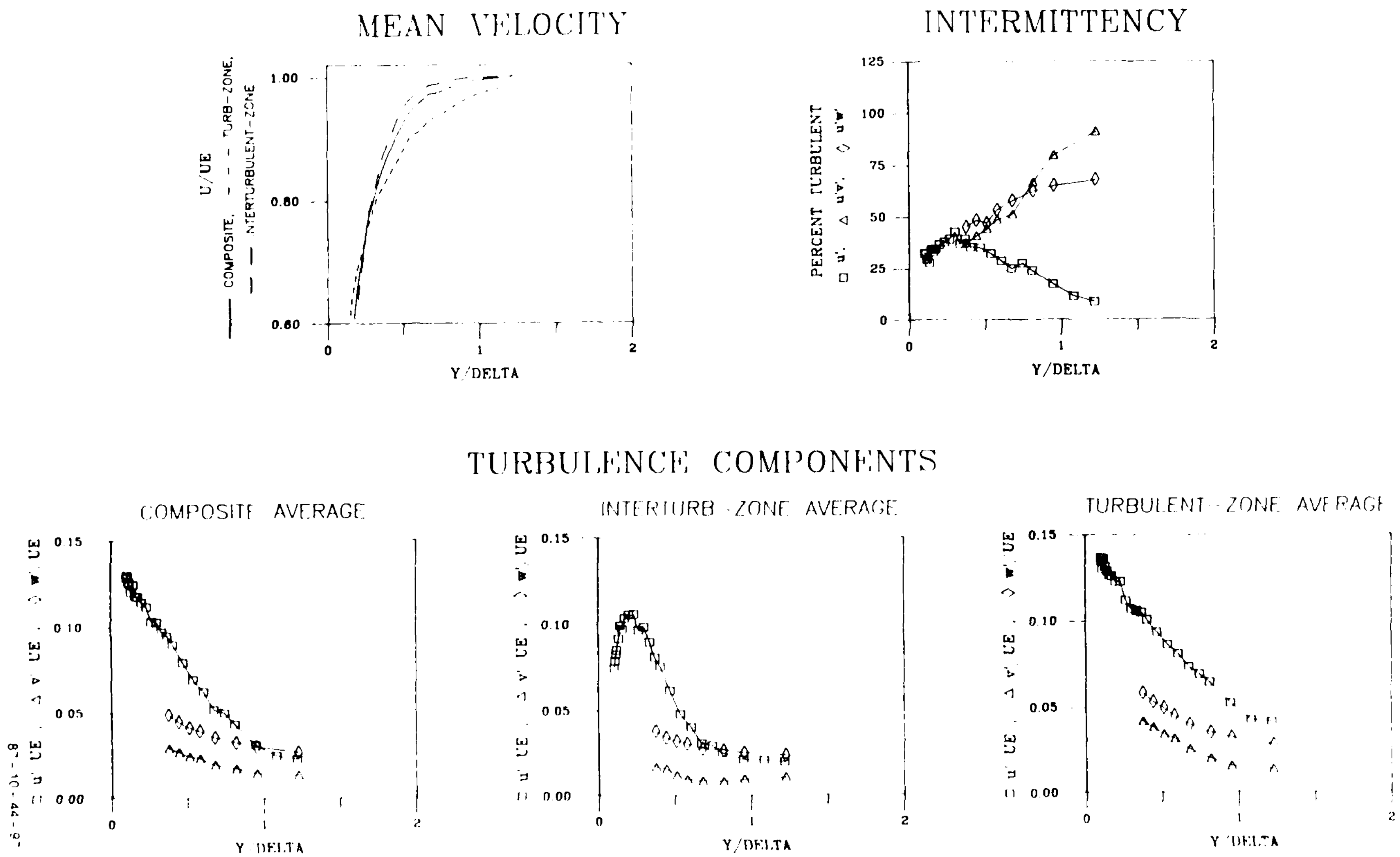

Figure A11-A

PROFILES OF TURBULENT STRESSES

X = 12.8 K = 0.20 E-6 TE = 1.8 %

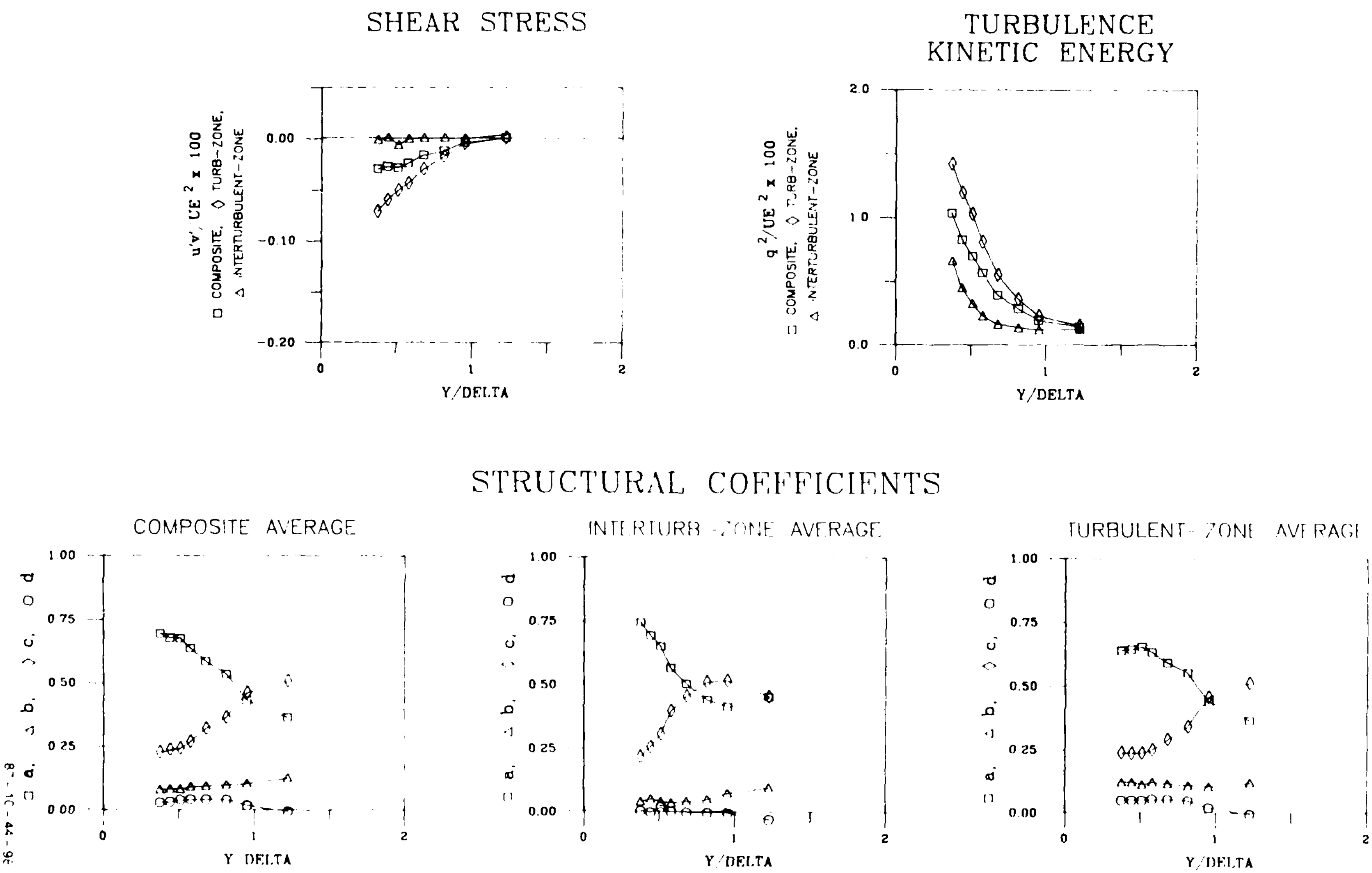

Figure A11-B

SINGLE WIRE PROFILE DATA

X = 12.8 GRID NO. 2 K = 0.2E-06

Y DELTA	U/UE COMPOSITE	U/UE INTER-TURBULENT ZONE	U/UE TURBULENT ZONE	U'/UE COMPOSITE	U'/UE INTER-TURBULENT ZONE	U'/UE TURBULENT ZONE	GAMMA U	[illegible]
0.1020	0.3946	0.3374	0.5109	0.1284	0.0743	0.1364	32.0850	36.6190
0.1085	0.4204	0.3628	0.5379	0.1297	0.0783	0.1344	32.1670	36.2190
0.1156	0.4395	0.3885	0.5579	0.1259	0.0822	0.1300	29.2520	34.6180
0.1197	0.4361	0.3889	0.5464	0.1252	0.0848	0.1361	29.2670	35.6180
0.1333	0.4875	0.4498	0.5820	0.1201	0.0914	0.1313	27.5740	36.0180
0.1469	0.5339	0.4919	0.6134	0.1243	0.0988	0.1287	34.0340	41.2210
0.1605	0.5741	0.5399	0.6413	0.1177	0.0969	0.1259	32.8380	37.8190
0.1741	0.6077	0.5808	0.6577	0.1175	0.1032	0.1260	34.1680	39.2200
0.2007	0.6552	0.6389	0.6905	0.1142	0.1052	0.1226	36.3650	[illegible]
0.2340	0.7132	0.7080	0.7210	0.1117	0.1055	0.1227	37.6460	45.8240
0.2680	0.7676	0.7727	0.7607	0.1030	0.0962	0.1117	39.0190	45.2250
0.3021	0.7974	0.8075	0.7842	0.1023	0.0979	0.1069	42.6840	[illegible]
0.3361	0.8283	0.8392	0.8164	0.0967	0.0892	0.1057	36.8710	50.8250
0.3687	0.8571	0.8736	0.8273	0.0943	0.0803	0.1047	39.2010	[illegible]
0.4034	0.8756	0.8962	0.8395	0.0892	0.0752	0.1003	35.1750	[illegible]
0.4694	0.9122	0.9369	0.8672	0.0735	0.0610	0.0931	34.7620	[illegible]
0.5374	0.9421	0.9625	0.9010	0.0690	0.0472	0.0855	32.0180	53.6270
0.6054	0.9577	0.9764	0.9126	0.0620	0.0397	0.0805	28.4860	[illegible]
0.6741	0.9731	0.9876	0.9311	0.0513	0.0300	0.0731	24.8620	41.4010
0.7475	0.9762	0.9917	0.9389	0.0495	0.0289	0.0689	27.4150	47.6220
0.8102	0.9879	0.9953	0.9493	0.0429	0.0246	0.0642	23.8470	[illegible]
0.9476	0.9945	1.0010	0.9682	0.0310	0.0206	0.0520	17.1930	33.8170
1.0877	0.9956	1.0011	0.9806	0.0243	0.0202	0.0420	11.4290	27.0140
1.2177	1.0011	1.0026	0.9858	0.0223	0.0195	0.0405	8.6256	22.6120
6.7966	1.0011	1.0011	0.9942	0.0157	0.0157	0.0000	0.0000	[illegible]

TABLE A11-A

87-10-44-99

CROSS WIRE PROFILE DATA

X = 12.8 GRID NO. 2 K = 0.2E-06

Y/DELTA	U'/UE COMPOSITE	U'/UE INTER-TURBULENT ZONE	U'/UE TURBULENT ZONE	V'/UE COMPOSITE	V'/UE INTER-TURBULENT ZONE	V'/UE TURBULENT ZONE	W'/UE COMPOSITE	W'/UE INTER-TURBULENT ZONE	W'/UE TURBULENT ZONE
0.3741	0.0846	0.0697	0.0952	0.0288	0.0163	0.0416	0.0484	0.0377	[illegible]
0.4422	0.0746	0.0550	0.0875	0.0264	0.0153	0.0381	0.0442	0.0377	[illegible]
0.5102	0.0684	0.0457	0.0819	0.0242	0.0115	0.0339	0.0410	0.0316	[illegible]
0.5782	0.0599	0.0356	0.0713	0.0230	0.0090	0.0313	0.0390	0.0300	0.0447
0.6803	0.0475	0.0282	0.0568	0.0192	0.0081	0.0253	0.0352	0.0268	0.0398
0.8163	0.0390	0.0247	0.0445	0.0169	0.0081	0.0198	0.0322	0.0262	[illegible]
0.9524	0.0288	0.0219	0.0314	0.0143	0.0093	0.0153	0.0298	0.0246	[illegible]
1.2245	0.0223	0.0232	0.0232	0.0132	0.0108	0.0134	0.0263	0.0234	[illegible]
6.8027	0.0170	0.0243	0.0170	0.0220	0.0209	0.0221	0.0200	0.0189	[illegible]

Y/DELTA	U'**2/q**2 COMPOSITE	U'**2/q**2 INTER-TURBULENT ZONE	U'**2/q**2 TURBULENT ZONE	V'**2/q**2 COMPOSITE	V'**2/q**2 INTER-TURBULENT ZONE	V'**2/q**2 TURBULENT ZONE	W'**2/q**2 COMPOSITE	W'**2/q**2 INTER-TURBULENT ZONE	W'**2/q**2 TURBULENT ZONE
0.3741	0.6971	0.7471	0.6795	0.0793	0.0461	0.1215	0.2271	0.2169	[illegible]
0.4422	0.6777	0.6919	0.6479	0.0842	0.0524	0.1212	0.2384	0.2567	[illegible]
0.5102	0.6747	0.6511	0.6526	0.0876	0.0407	0.1110	0.2421	[illegible]	[illegible]
0.5782	0.6767	[illegible]	0.6711	0.0977	0.0757	0.1212	[illegible]	0.7987	[illegible]
0.6803	0.5877	0.5103	0.5912	0.0946	0.0417	0.1167	0.3217	0.4555	[illegible]
0.8163	0.5744	0.4795	[illegible]	0.1002	0.0491	[illegible]	0.3654	[illegible]	[illegible]
0.9524	0.4014	[illegible]	[illegible]	0.1059	[illegible]	0.1073	0.4628	[illegible]	[illegible]
1.2245	0.3679	0.4517	0.3657	[illegible]	0.0954	0.1217	0.5089	0.4541	[illegible]
6.8027	0.2461	0.4747	0.2475	0.4115	[illegible]	[illegible]	[illegible]	[illegible]	[illegible]

Y/DELTA	UV/Q**2 COMPOSITE	UV/Q**2 INTER-TURBULENT ZONE	UV/Q**2 TURBULENT ZONE	GAMMA UV	? UV	GAMMA WV	? WV
0.3741	[illegible]	[illegible]	-0.0505	37.1520	51.0261	44.9130	[illegible]
0.4422	[illegible]	[illegible]	-0.0507	40.6150	54.2281	48.1630	[illegible]
0.5102	-0.0412	-0.0194	-0.0490	44.0570	58.4300	46.6190	50.6260
0.5782	-0.0426	-0.0017	-0.0541	48.4810	58.6300	53.2250	60.2311
0.6803	-0.0415	0.0074	-0.0549	51.1600	60.0310	57.8300	[illegible]
0.8163	-0.0407	0.0048	-0.0479	66.6340	56.0290	62.4130	57.8300
0.9524	-0.0182	0.0069	-0.0204	79.5930	50.2260	64.9900	[illegible]
1.2245	0.0064	0.0309	0.0045	90.9780	29.0150	67.9120	58.0300
6.8027	0.0271	0.0078	0.0283	97.5670	10.4050	76.4040	55.2281

Y/DELTA	q**2/UE**2 COMPOSITE	q**2/UE**2 INTER-TURBULENT ZONE	q**2/UE**2 TURBULENT ZONE	UV/UE**2 COMPOSITE	UV/UE**2 INTER-TURBULENT ZONE	UV/UE**2 TURBULENT ZONE
0.3741	0.010745	0.006594	0.014189	-3.006E-04	-1.420E-05	-7.169E-04
0.4422	0.008247	0.004458	0.011907	-2.720E-04	1.318E-05	-5.959E-04
0.5102	0.006972	[illegible]	0.010282	-2.845E-04	-6.297E-05	-5.047E-04
0.5782	0.005657	0.002271	0.008059	-2.411E-04	-1.678E-06	-4.365E-04
0.6803	0.003874	0.001583	0.005462	-1.619E-04	5.318E-06	-2.996E-04
0.8163	0.002547	0.001745	[illegible]	-1.155E-04	6.409E-06	-1.726E-04
0.9524	0.001937	0.001181	0.002254	-3.499E-05	8.084E-06	-4.610E-05
1.2245	0.001365	0.001209	0.001477	8.679E-06	3.733E-05	6.606E-06
6.8027	[illegible]	0.001799	0.002192	3.177E-05	5.384E-06	7.775E-05

TABLE A11-B

87-10-44-100

PROFILES OF MEAN AND FLUCTUATING QUANTITIES

X = 16.8   K = 0.20 E-6   TI = 1.7 %

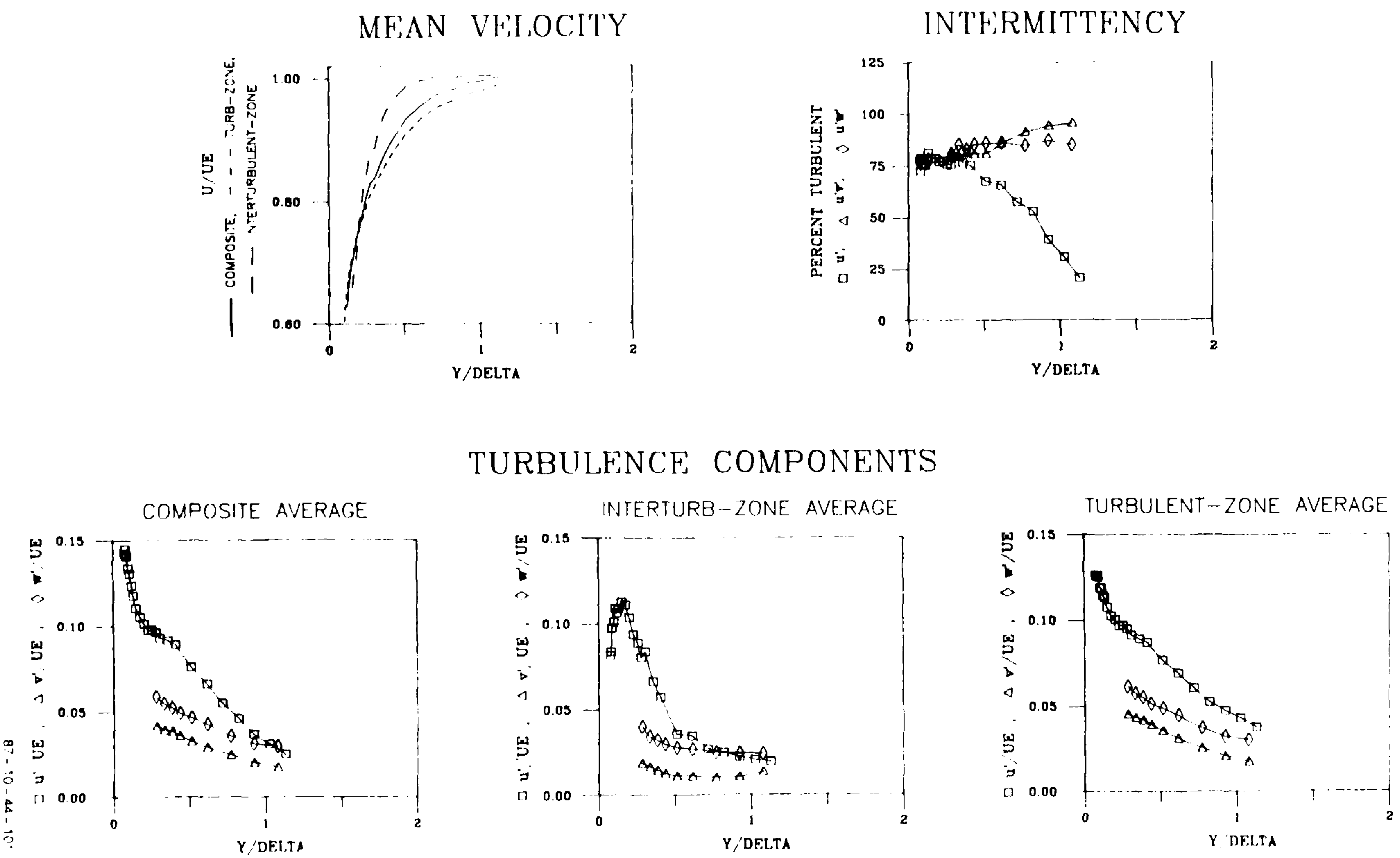

Figure A12-A

PROFILES OF TURBULENT STRESSES

X = 16.8   K = 0.20 E−6   TE = 1.7 %

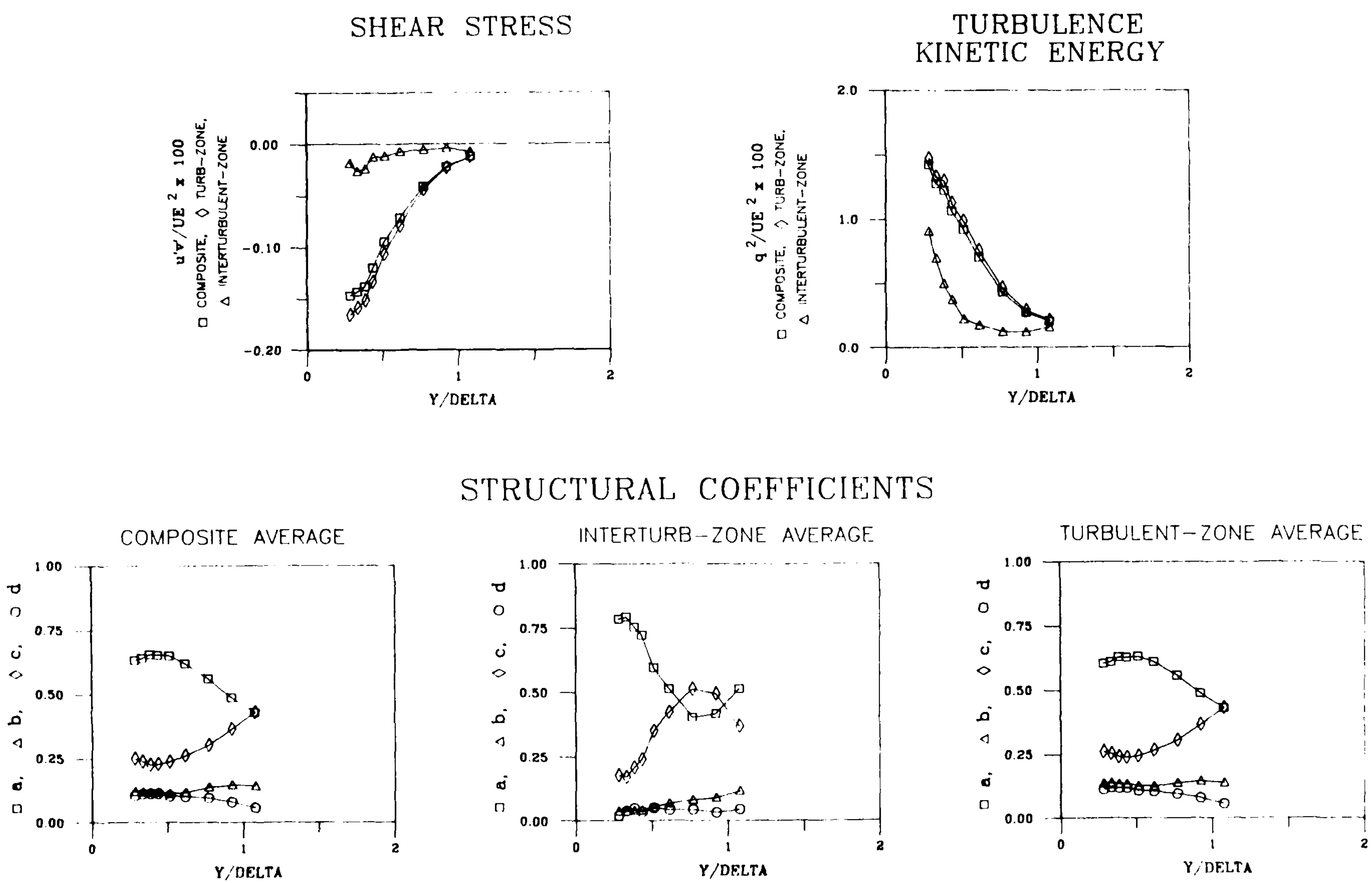

Figure A12-B

SINGLE WIRE PROFILE DATA

X = 16.8 GRID NO. 2 K = 0.2E-06

Y/DELTA	U/UE COMPOSITE	U/UE INTER-TURBULENT ZONE	U/UE TURBULENT ZONE	U'/UE COMPOSITE	U'/UE INTER-TURBULENT ZONE	U'/UE TURBULENT ZONE	GAMMA	[illegible]
0.0769	0.4736	0.3213	0.5168	0.1425	0.0814	0.1255	77.3640	33.6170
0.0821	0.4855	0.3428	0.5383	0.1448	0.0836	0.1259	72.2870	35.8180
0.0872	0.5252	0.3816	0.5638	0.1411	0.0971	0.1252	78.3860	33.4170
0.0923	0.5221	0.3905	0.5672	0.1406	0.0973	0.1261	75.4660	36.2190
0.1026	0.5654	0.4424	0.6038	0.1337	0.1009	0.1187	76.1140	33.0170
0.1128	0.5970	0.4926	0.6295	0.1304	0.1068	0.1189	75.2740	32.6170
0.1231	0.6287	0.5727	0.6549	0.1233	0.1061	0.1144	77.6000	32.4170
0.1333	0.6597	0.5872	0.6755	0.1174	0.1087	0.1132	81.3810	32.2160
0.1538	0.6952	0.6584	0.7050	0.1102	0.1125	0.1075	78.5120	37.0170
0.1795	0.7293	0.7030	0.7362	0.1050	0.1108	0.1023	78.5760	31.0160
0.2051	0.7584	0.7661	0.7569	0.1011	0.1034	0.1003	76.9190	33.1170
0.2308	0.7864	0.8154	0.7784	0.0972	0.0935	0.0967	77.4150	37.8190
0.2564	0.8085	0.8453	0.7963	0.0976	0.0855	0.0970	75.7990	37.2190
0.2821	0.8317	0.8649	0.8149	0.0963	0.0811	0.0948	75.3000	40.6210
0.3077	0.8386	0.8876	0.8264	0.0930	0.0836	0.0912	79.3650	35.0180
0.3590	0.8711	0.9366	0.8520	0.0916	0.0663	0.0892	76.5650	40.4210
0.4103	0.8952	0.9604	0.8741	0.0868	0.0570	0.0871	75.2840	40.6220
0.5128	0.9345	0.9851	0.9101	0.0758	0.0355	0.0767	67.5100	45.2250
0.6154	0.9571	0.9974	0.9362	0.0661	0.0345	0.0651	65.4590	50.6260
0.7179	0.9732	1.0018	0.9524	0.0548	0.0267	0.0606	57.4720	56.2290
0.8205	0.9811	1.0018	0.9677	0.0453	0.0246	0.0522	52.5410	[illegible]
0.9231	0.9925	1.0039	0.9752	0.0367	0.0219	0.0472	38.8240	59.4300
1.0256	0.9962	1.0077	0.9817	0.0307	0.0213	0.0428	30.5520	50.2260
1.1282	1.0024	1.0058	0.9856	0.0248	0.0194	0.0374	23.4640	46.4240
5.1282	1.0054	1.0054	1.0118	0.0151	0.0151	0.0000	0.0000	0.0000

TABLE A12-A

87 - 10 - 44 - 103

CROSS WIRE PROFILE DATA

X = 16.8 GRID NO. 2 K = 0.2E-06

Y/DELTA	U'/UE COMPOSITE	U'/UE INTER-TURBULENT ZONE	U'/UE TURBULENT ZONE	V'/UE COMPOSITE	V'/UE INTER-TURBULENT ZONE	V'/UE TURBULENT ZONE	W'/UE COMPOSITE	W'/UE INTER-TURBULENT ZONE	W'/UE TURBULENT ZONE
0.2821	0.0947	0.0932	0.0942	0.0417	0.0187	0.0453	0.0588	0.0396	0.0612
0.3333	0.0905	0.0731	0.0899	0.0395	0.0163	0.0432	0.0548	0.0341	0.0577
0.3846	0.0895	0.0605	0.0902	0.0385	0.0143	0.0419	0.0521	0.0319	0.0552
0.4359	0.0832	0.0510	0.0879	0.0359	0.0125	0.0392	0.0489	0.0295	0.0517
0.5128	0.0771	0.0355	0.0787	0.0325	0.0111	0.0355	0.0463	0.0276	0.0486
0.6154	0.0658	0.0296	0.0677	0.0291	0.0109	0.0310	0.0425	0.0267	0.0444
0.7692	0.0488	0.0219	0.0505	0.0245	0.0101	0.0254	0.0356	0.0246	0.0371
0.9231	0.0362	0.0223	0.0372	0.0201	0.0105	0.0206	0.0312	0.0241	0.0320
1.0769	0.0293	0.0284	0.0301	0.0171	0.0138	0.0173	0.0292	0.0239	0.0311
5.1282	0.0164	0.0161	0.0164	0.0201	0.0203	0.0200	0.0194	0.0179	0.0195

Y/DELTA	U'**2/q**2 COMPOSITE	U'**2/q**2 INTER-TURBULENT ZONE	U'**2/q**2 TURBULENT ZONE	V'**2/q**2 COMPOSITE	V'**2/q**2 INTER-TURBULENT ZONE	V'**2/q**2 TURBULENT ZONE	W'**2/q**2 COMPOSITE	W'**2/q**2 INTER-TURBULENT ZONE	W'**2/q**2 TURBULENT ZONE
0.2821	0.6318	0.7647	0.6034	0.1201	0.0386	0.1368	0.2481	0.1773	0.2599
0.3333	0.6411	0.7924	0.6099	0.1199	0.0374	0.1361	0.2389	0.1701	0.2521
0.3846	0.6556	0.7524	0.6276	0.1191	0.0402	0.1328	0.2254	0.2074	0.2396
0.4359	0.6505	0.7193	0.6275	0.1191	0.0412	0.1344	0.2234	0.2391	0.2381
0.5128	0.6474	0.5949	0.6304	0.1170	0.0546	0.1260	0.2375	0.3505	0.2436
0.6154	0.6196	0.5109	0.6097	0.1185	0.0672	0.1250	0.2619	0.4219	0.2657
0.7692	0.5593	0.4077	0.5569	0.1382	0.0834	0.1381	0.3020	0.5133	0.3049
0.9231	0.4869	0.4159	0.4877	0.1476	0.0905	0.1459	0.3656	0.4936	0.3662
1.0769	0.4284	0.5174	0.4293	0.1426	0.1187	0.1390	0.4251	0.3685	0.4717
5.1282	0.2561	0.2617	0.2574	0.3772	0.410	0.3719	0.3667	0.3257	0.3747

Y/DELTA	UV/q**2 COMPOSITE	UV/q**2 INTER-TURBULENT ZONE	UV/q**2 TURBULENT ZONE	GAMMA UV	f UV	GAMMA WV	f WV
0.2821	-0.1078	-0.0212	-0.1127	80.2540	34.2160	80.5510	29.2151
0.3333	-0.1127	-0.0273	-0.1199	79.4600	35.0180	85.0490	26.2130
0.3846	-0.1171	-0.0454	-0.1171	81.4110	29.6150	82.6720	29.6150
0.4359	-0.1128	-0.0336	-0.1191	80.7920	32.2160	85.3970	27.2140
0.5128	-0.1027	-0.0506	-0.1080	80.8860	32.2160	85.9550	27.2140
0.6154	-0.1014	-0.0409	-0.1046	85.7270	32.6170	85.8320	30.2150
0.7692	-0.0958	-0.0446	-0.0951	91.1730	23.6120	84.5160	32.8170
0.9231	-0.0807	-0.0315	-0.0801	94.2210	18.8100	86.8440	32.4170
1.0769	-0.0576	-0.0458	-0.0569	95.7200	13.8070	84.8920	33.4170
5.1282	-0.0176	-0.0435	-0.0166	96.9310	15.2080	80.3970	46.8240

Y/DELTA	q**2/UE**2 COMPOSITE	q**2/UE**2 INTER-TURBULENT ZONE	q**2/UE**2 TURBULENT ZONE	UV/UE**2 COMPOSITE	UV/UE**2 INTER-TURBULENT ZONE	UV/UE**2 TURBULENT ZONE
0.2821	0.014200	0.009070	0.014713	-1.474E-03	-1.832E-04	-1.658E-03
0.3333	0.012775	0.006969	0.013277	-1.435E-03	-2.633E-04	-1.590E-03
0.3846	0.012241	0.004982	0.012964	-1.383E-03	-2.409E-04	-1.518E-03
0.4359	0.010631	0.003717	0.011230	-1.200E-03	-1.250E-04	-1.338E-03
0.5128	0.009179	0.002208	0.009845	-9.427E-04	-1.117E-04	-1.064E-03
0.6154	0.007011	0.001723	0.007541	-7.106E-04	-7.050E-05	-7.888E-04
0.7692	0.004271	0.001196	0.004605	-4.090E-04	-5.334E-05	-4.380E-04
0.9231	0.002711	0.001199	0.002852	-2.180E-04	-3.770E-05	-2.285E-04
1.0769	0.002018	0.001580	0.002125	-1.162E-04	-7.237E-05	-1.210E-04
5.1282	0.001048	0.000988	0.001062	-1.842E-05	-4.293E-05	-1.764E-05

TABLE A12-B

87 - 10 - 44 - 104

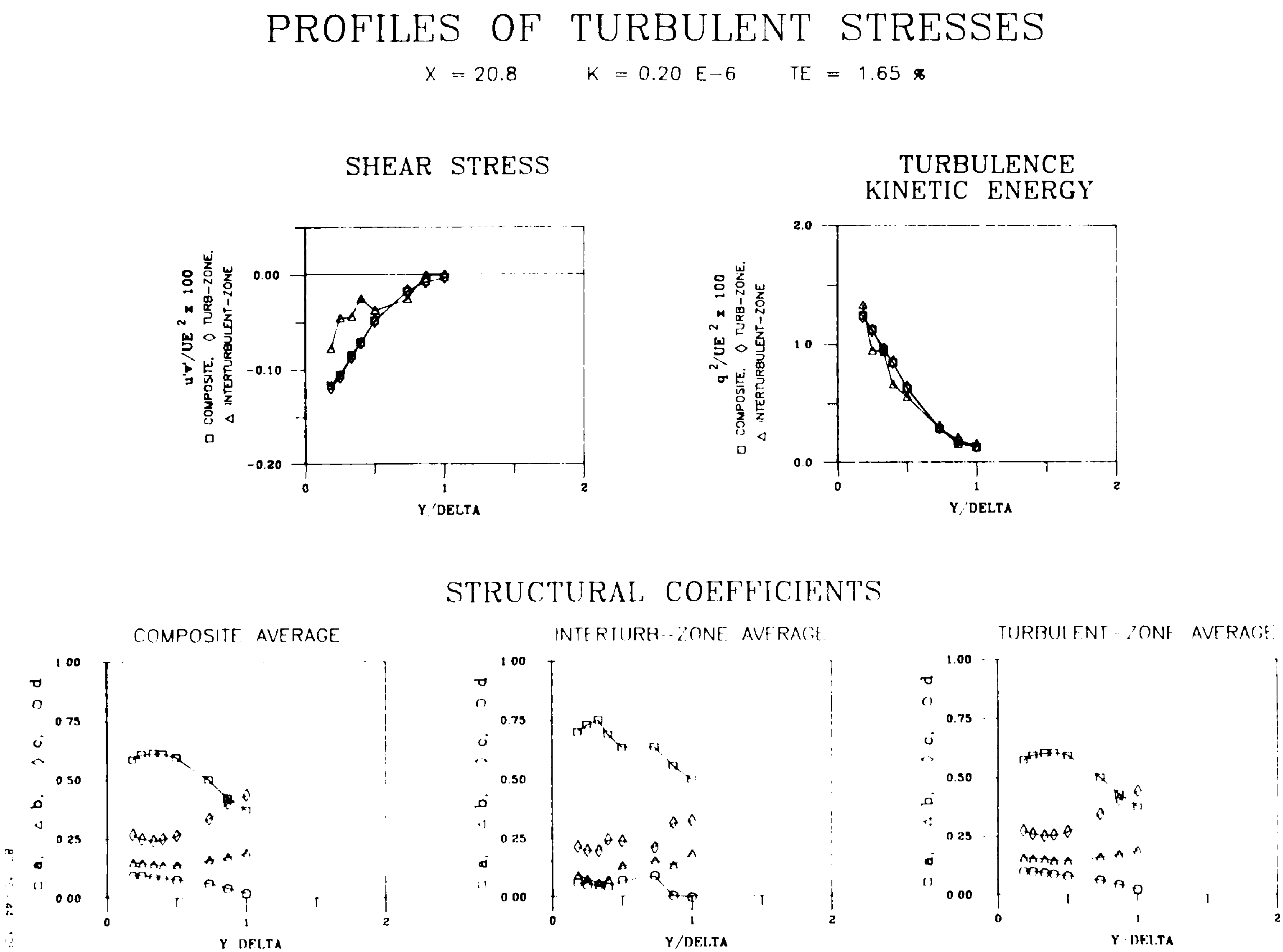

PROFILES OF TURBULENT STRESSES
X = 20.8 K = 0.20 E-6 TE = 1.65 %
SHEAR STRESS
u'v'/UE 2 x 100
□ COMPOSITE, ◇ TURB-ZONE,
△ INTERTURBULENT-ZONE
Y/DELTA
TURBULENCE KINETIC ENERGY
q 2/UE 2 x 100
□ COMPOSITE, ◇ TURB-ZONE,
△ INTERTURBULENT-ZONE
Y/DELTA
STRUCTURAL COEFFICIENTS
COMPOSITE AVERAGE
INTERTURB-ZONE AVERAGE
TURBULENT-ZONE AVERAGE
□ a, △ b, ◇ c, ○ d
Y/DELTA

Figure A13-A

PROFILES OF MEAN AND FLUCTUATING QUANTITIES

X = 20.8 K = 0.20 E−6 TE = 1.65 %

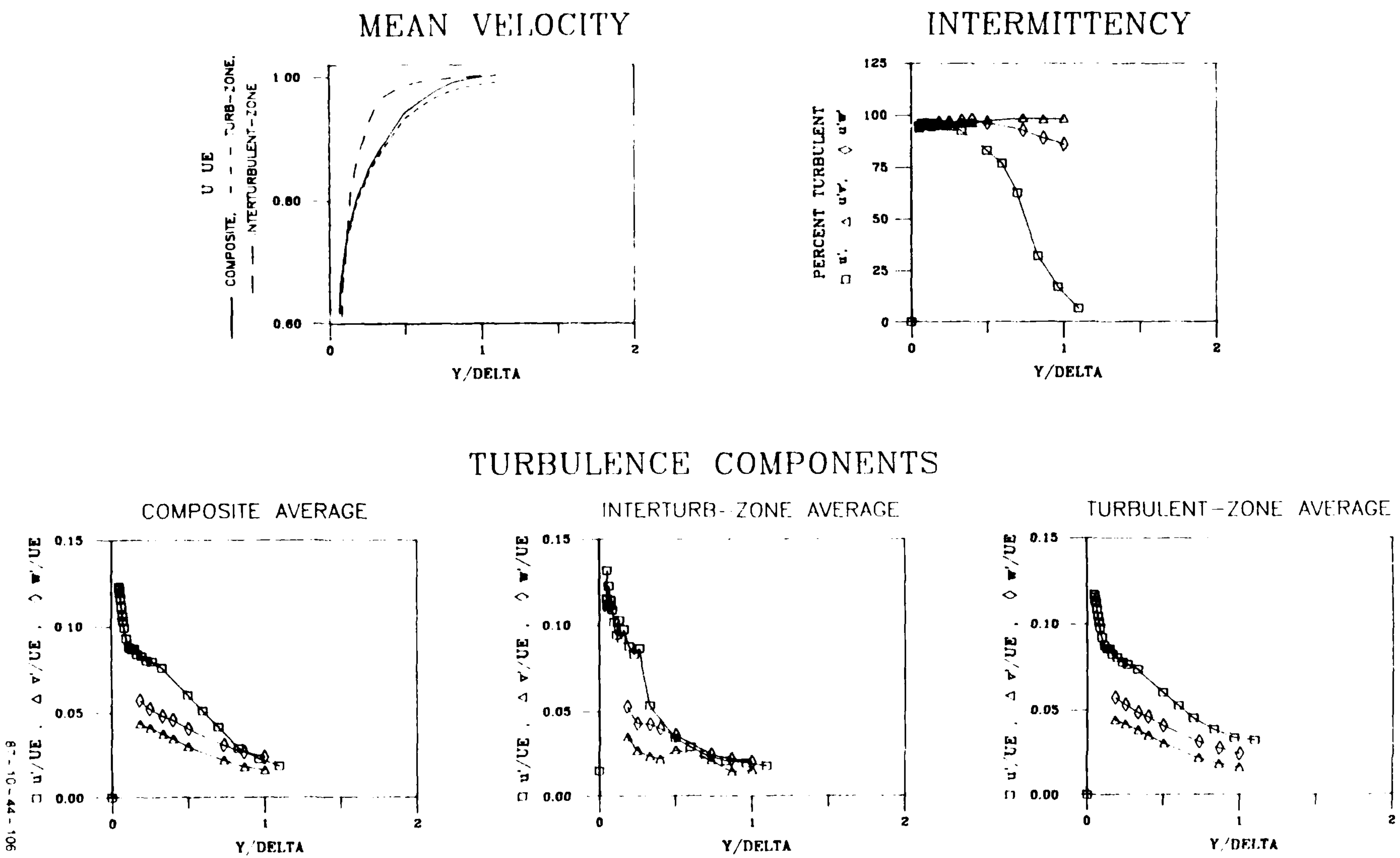

Figure A13-B

SINGLE WIRE PROFILE DATA

X = 20.8 GRID NO. 2 K = 0.2E-06

Y/DELTA	U/UE COMPOSITE	U/UE INTER-TURBULENT ZONE	U/UE TURBULENT ZONE	U'/UE COMPOSITE	U'/UE INTER-TURBULENT ZONE	U'/UE TURBULENT ZONE	GAMMA U	[illegible]
0.0500	0.5362	0.4144	0.5455	0.1228	0.1316	0.1170	94.6950	11.2[illegible]
0.0523	0.5506	0.3980	0.5601	0.1215	0.1149	0.1154	94.6160	11.6060
0.0557	0.5652	0.4241	0.5753	0.1194	0.1114	0.1134	93.6090	11.8060
0.0597	0.5915	0.4680	0.5990	0.1162	0.1100	0.1123	94.6390	12.2060
0.0660	0.6162	0.5622	0.6219	0.1112	0.1225	0.1085	94.8540	11.4060
0.0727	0.6449	0.5811	0.6482	0.1058	0.1113	0.1045	95.6500	11.6150
0.0783	0.6610	0.6058	0.6648	0.1029	0.1142	0.1011	95.3050	11.2060
0.0867	0.6776	0.6560	0.6798	0.0989	0.1086	0.0976	94.9641	10.4150
0.0990	0.7050	0.6860	0.7062	0.0928	0.1014	0.0921	95.5380	10.0650
0.1157	0.7311	0.7230	0.7309	0.0874	0.0938	0.0872	96.1910	8.4140
0.1323	0.7549	0.7793	0.7533	0.0866	0.1026	0.0854	94.4720	11.2060
0.1477	0.7675	0.8194	0.7640	0.0869	0.0918	0.0854	94.9051	9.6743
0.1651	0.7846	0.8799	0.7821	0.0837	0.0973	0.0822	96.0370	8.6144
0.1970	0.8110	0.8751	0.8067	0.0824	0.0875	0.0803	95.2021	12.41[illegible]
0.2307	0.8305	0.9[illegible]	0.8259	0.0799	0.0825	0.0776	94.7440	[illegible]
0.2647	0.8531	0.9287	0.8479	0.0794	0.0863	0.0767	94.6210	[illegible]
0.3310	0.8817	0.9645	0.8744	0.0758	0.0531	0.0734	92.2870	[illegible]
0.4970	0.9421	0.9877	0.9326	0.0601	0.0342	0.0602	82.8920	35.2[illegible]
0.5[illegible]	0.9[illegible]	0.9974	0.9515	0.0509	0.0255	0.0523	76.6960	4[illegible]
0.6977	0.9776	0.9959	0.9672	0.0413	0.0242	0.0452	62.4710	65.[illegible]
0.8[illegible]	1.[illegible]	0.9997	0.9813	0.0299	0.0218	0.0387	31.9110	65.[illegible]
0.9[illegible]	1.0[illegible]	1.0026	0.9882	0.0227	0.0193	0.0336	16.9520	46.4[illegible]
1.0977	1.0[illegible]	1.0035	0.9915	0.0187	0.0178	0.0320	6.5[illegible]	21.8[illegible]
3.7[illegible]	1.0041	1.0041	0.9943	0.0147	0.0147	0.0000	0.0000	0.0[illegible]
0.0000	1.0[illegible]	0.0000	0.0000	0.0000	0.0001	0.0000	0.0000	0.0[illegible]

TABLE A13-A

87-10-44-107

CROSS WIRE PROFILE DATA

X = 20.8 GRID NO. 2 K = 0.2E-06

Y/DELTA	U'/UE COMPOSITE	U'/UE INTER-TURBULENT ZONE	U'/UE TURBULENT ZONE	V'/UE COMPOSITE	V'/UE INTER-TURBULENT ZONE	V'/UE TURBULENT ZONE	W'/UE COMPOSITE	W'/UE INTER-TURBULENT ZONE	W'/UE TURBULENT ZONE
0.1833	0.0851	0.0964	0.0838	0.0433	0.0349	0.0441	0.0570	0.0526	[illegible]
0.2500	0.0825	0.0830	0.0812	0.0406	0.0267	0.0414	0.0522	0.0426	[illegible]
0.3333	0.0768	0.0874	0.0758	0.0374	0.0232	0.0380	0.0478	0.0421	0.0483
0.4000	0.0717	0.0666	0.0714	0.0345	0.0215	0.0350	0.0455	0.0395	0.0455
0.5000	0.0608	0.0591	0.0610	0.0299	0.0272	0.0302	0.0403	0.0357	0.0416
0.7333	0.0376	0.0425	0.0379	0.0217	0.0214	0.0217	0.0306	0.0244	[illegible]
0.8667	0.0276	0.0288	0.0282	0.0179	0.0144	0.0180	0.0266	0.0217	[illegible]
1.0000	0.0219	0.0249	0.0227	0.0159	0.0153	0.0160	0.0235	0.0200	[illegible]
3.3333	0.0160	0.0246	0.0161	0.0199	0.0177	0.0199	0.0184	0.0169	[illegible]

Y/DELTA	U'**2/q**2 COMPOSITE	U'**2/q**2 INTER-TURBULENT ZONE	U'**2/q**2 TURBULENT ZONE	V'**2/q**2 COMPOSITE	V'**2/q**2 INTER-TURBULENT ZONE	V'**2/q**2 TURBULENT ZONE	W'**2/q**2 COMPOSITE	W'**2/q**2 INTER-TURBULENT ZONE	W'**2/q**2 TURBULENT ZONE
0.1833	0.5840	0.6984	0.5735	0.1484	0.0996	0.1553	0.2673	0.2120	[illegible]
0.2500	[illegible]	0.7295	0.5971	0.1453	0.0741	0.1511	0.2477	0.1967	[illegible]
0.3333	0.6146	0.7499	[illegible]	0.1429	0.0567	0.1487	0.2425	0.1975	0.2462
0.4000	0.6114	0.6886	0.6040	0.1388	0.0690	0.1424	0.2509	0.2424	[illegible]
0.5000	[illegible]	[illegible]	0.5917	0.1462	0.1718	0.1416	0.2655	[illegible]	[illegible]
0.7333	0.5003	0.6365	0.4975	0.1670	0.1551	0.1599	0.3361	0.2064	0.3426
0.8667	0.4275	[illegible]	[illegible]	0.1744	0.1317	0.1705	0.4021	[illegible]	0.4075
1.0000	0.3714	[illegible]	[illegible]	0.1526	0.1810	0.1877	0.4360	[illegible]	0.4414
3.3333	0.2597	0.5125	0.2563	0.3923	0.2465	0.3863	0.3488	0.2751	0.3565

Y/DELTA	UV/Q**2 COMPOSITE	UV/Q**2 INTER-TURBULENT ZONE	UV/Q**2 TURBULENT ZONE	GAMMA UV	[illegible] UV	GAMMA WV	[illegible] WV
0.1833	-0.0943	-0.0569	-0.0976	95.5940	8.4043	96.1550	9.6049
0.2500	-0.0944	-0.0493	-0.0978	95.9810	6.8035	96.2450	9.4049
0.3333	-0.0888	-0.0477	-0.0917	96.0940	9.6049	97.0820	7.4033
0.4000	-0.0844	-0.0781	-0.0857	96.2120	10.0050	97.6020	6.4037
0.5000	-0.0772	-0.0652	-0.0780	97.5670	7.2037	96.0990	11.6061
0.7333	-0.0616	-0.0591	-0.0594	98.6140	5.0026	92.5560	21.4110
0.8667	-0.0407	-0.0020	-0.0406	97.9000	8.2042	88.8320	31.6160
1.0000	-0.0201	0.0051	-0.0212	98.2990	8.2042	85.7610	41.2210
3.3333	0.0273	0.0089	0.0284	97.7640	11.2060	76.5090	47.4240

Y/DELTA	q**2/UE**2 COMPOSITE	q**2/UE**2 INTER-TURBULENT ZONE	q**2/UE**2 TURBULENT ZONE	UV/UE**2 COMPOSITE	UV/UE**2 INTER-TURBULENT ZONE	UV/UE**2 TURBULENT ZONE
0.1833	0.012407	0.013303	0.012274	-1.170E-03	-7.833E-04	-1.197E-03
0.2500	0.011215	0.009445	0.011125	-1.058E-03	-4.565E-04	-1.079E-03
0.3333	[illegible]	0.009336	0.009532	-8.518E-04	-4.420E-04	-8.704E-04
0.4000	0.008415	0.006570	0.008444	-7.108E-04	-2.533E-04	-7.237E-04
0.5000	0.006621	[illegible]	0.006722	-4.819E-04	-3.762E-04	-4.916E-04
0.7333	0.002874	0.002905	0.002891	-1.747E-04	-2.589E-04	-1.717E-04
0.8667	[illegible]	0.001536	0.001666	-7.319E-05	-3.061E-06	-7.569E-05
1.0000	0.001293	0.001261	0.001335	-2.595E-05	6.368E-06	-2.832E-05
3.3333	0.000987	0.001242	0.001009	2.700E-05	1.111E-05	2.864E-05

TABLE A13-B

87-10-44-108

PROFILES OF MEAN AND FLUCTUATING QUANTITIES

X = 24.8   K = 0.20 E−6   TE = 1.60 %

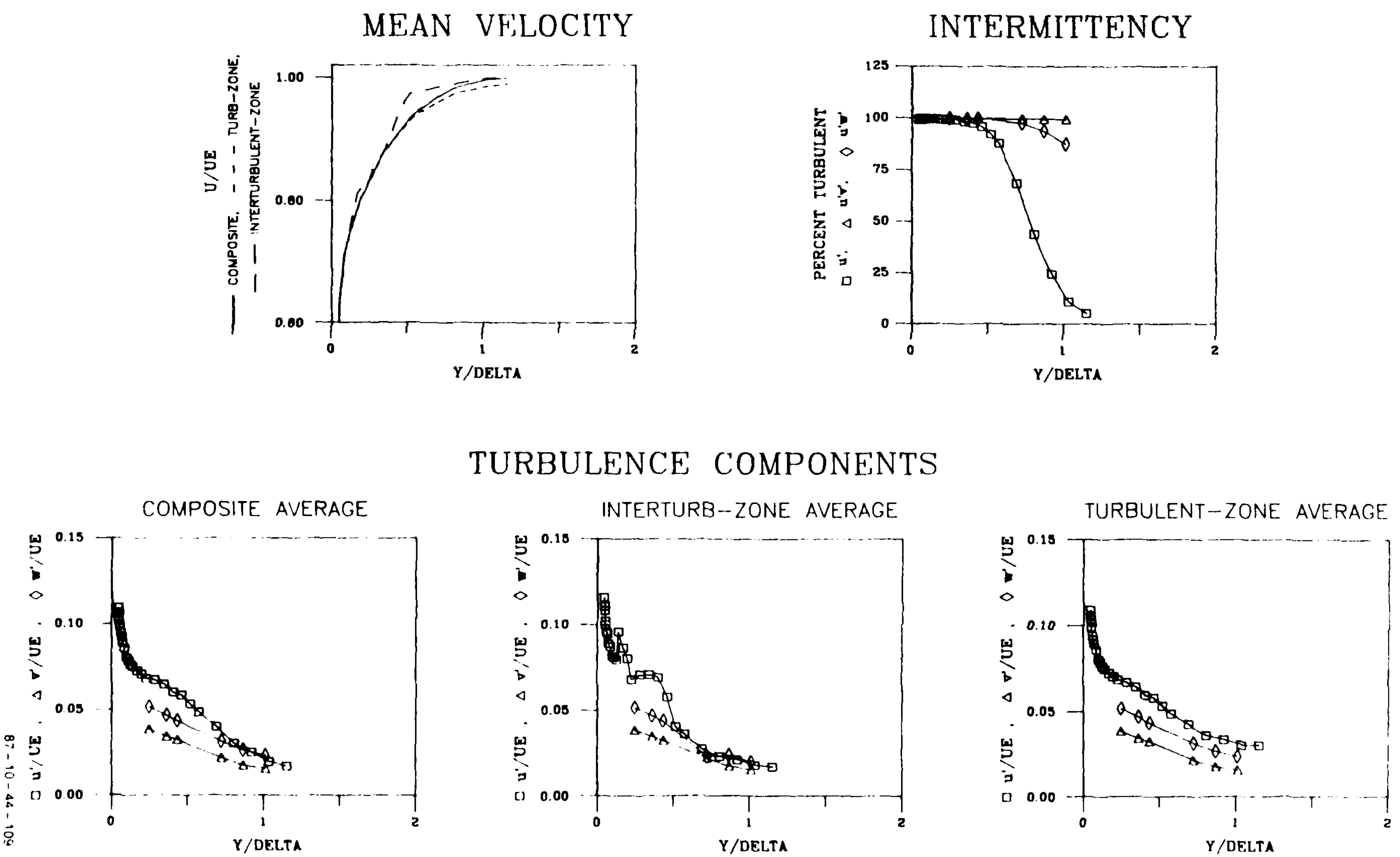

Figure A14-A

PROFILES OF TURBULENT STRESSES

X = 24.8 K = 0.20 E-6 TE = 1.60 %

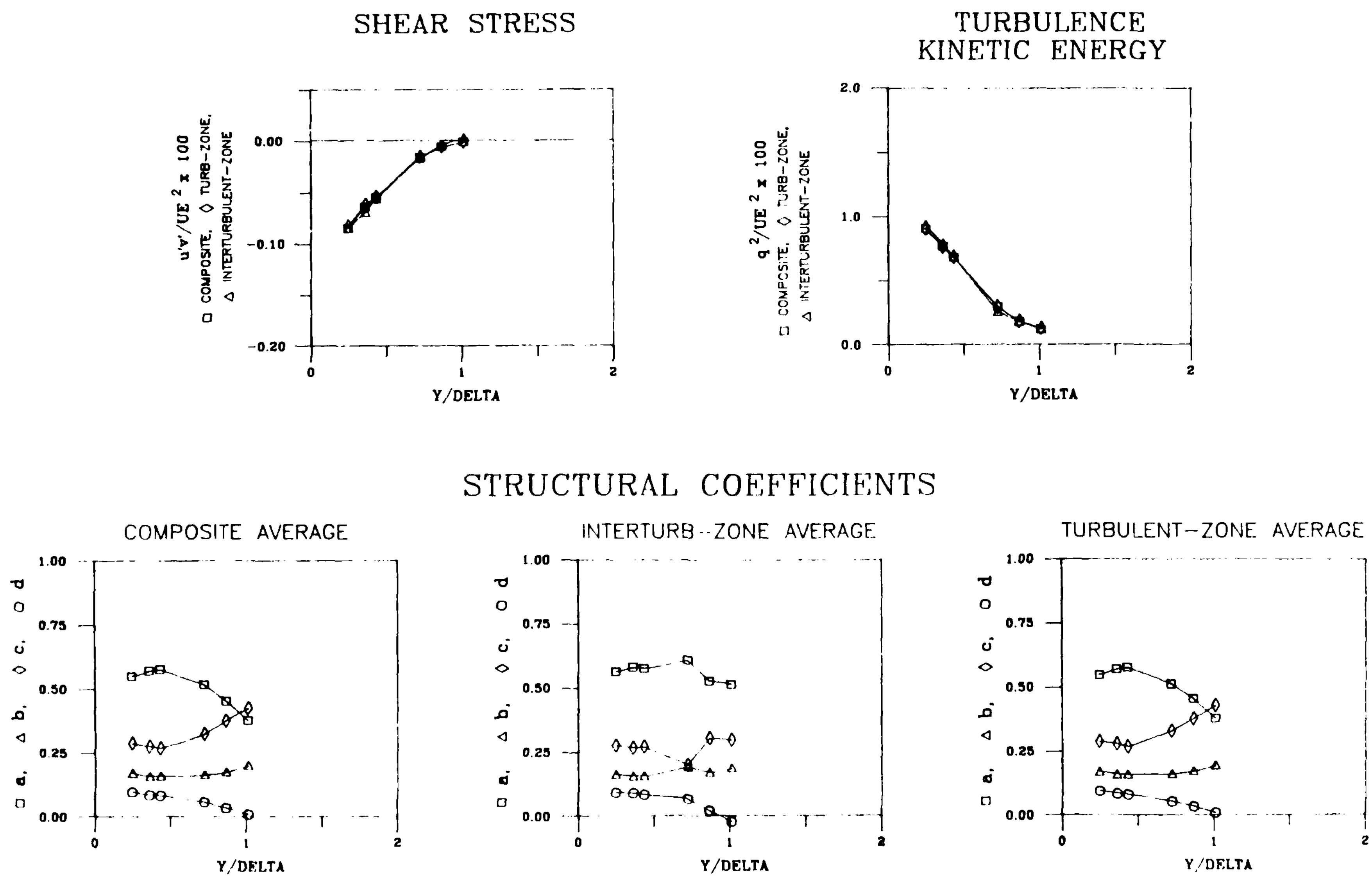

Figure A14-B

87 - 10 - 44 - 110

SINGLE WIRE PROFILE DATA

X = 24.8 GRID NO. 2 K = 0.2E-06

Y/DELTA	U/UE COMPOSITE	U/UE INTER-TURBULENT ZONE	U/UE TURBULENT ZONE	U'/UE COMPOSITE	U'/UE INTER-TURBULENT ZONE	U'/UE TURBULENT ZONE	GAMMA [illegible]	[illegible]
0.0434	0.5774	0.5678	0.5780	0.1090	0.1155	0.1086	98.9700	1.8009
0.0462	0.5932	0.5868	0.5945	0.1061	0.1103	0.1053	99.0800	1.6008
0.0487	0.6018	0.5937	0.6023	0.1037	0.1078	0.1034	99.2930	1.2006
0.0512	0.6172	0.6130	0.6155	0.1016	0.1016	0.1016	99.1650	1.8009
0.0566	0.6379	0.6332	0.6380	0.0989	0.0995	0.0987	98.8270	2.6013
0.0627	0.6507	0.6515	0.6484	0.0949	0.0954	0.0937	99.4290	0.8004
0.0685	0.6664	0.6652	0.6668	0.0923	0.0944	0.0916	99.4290	1.2006
0.0737	0.6818	0.6752	0.6818	0.0888	0.0885	0.0888	99.0390	[illegible]
0.0857	0.7015	0.7084	0.7011	0.0856	0.0869	0.0856	99.2420	[illegible]
0.1016	0.7216	0.7207	0.7217	0.0799	0.0810	0.0798	99.2730	[illegible]
0.1139	0.7373	0.7386	0.7371	0.0782	0.0805	0.0781	99.3850	[illegible]
0.1277	0.7518	0.7615	0.7514	0.0761	0.0791	0.0759	99.3850	[illegible]
0.1419	0.7619	0.7768	0.7615	0.0748	0.0955	0.0747	99.2900	[illegible]
0.1711	0.7846	0.8124	0.7839	0.0727	0.0861	0.0729	99.2651	[illegible]
[illegible]	0.8165	0.8217	0.8055	[illegible]	0.0798	0.0699	99.0880	[illegible]
0.2292	0.8191	0.8171	0.8202	0.0678	0.0674	0.0682	99.249	[illegible]
[illegible]	0.8499	0.8559	0.8457	[illegible]	0.0714	0.0665	[illegible]	[illegible]
0.3445	0.8773	0.8771	0.8773	0.0645	0.0714	0.0675	98.0790	[illegible]
0.4026	0.8969	0.9194	0.8957	[illegible]	0.0688	0.0597	97.2570	[illegible]
0.4593	0.9155	0.9531	0.9135	0.0582	0.0574	0.0577	95.5510	[illegible]
[illegible]	0.9339	[illegible]	[illegible]	[illegible]	[illegible]	[illegible]	91.714	[illegible]
0.5754	0.9464	0.9781	0.9419	0.0453	0.0358	0.0484	87.4620	[illegible]
[illegible]	0.9671	[illegible]	[illegible]	[illegible]	[illegible]	0.0422	[illegible]	[illegible]
0.8069	0.9828	0.9961	0.9740	[illegible]	0.0228	0.0759	[illegible]	[illegible]
0.9223	[illegible]	0.9945	[illegible]	0.0249	0.0208	0.0333	[illegible]	[illegible]
1.0383	0.9978	0.9993	0.9867	0.0196	0.0189	0.0302	[illegible]	[illegible]
1.1575	0.9987	0.9993	0.9894	0.0173	0.0168	0.0300	5.0410	[illegible]
2.8876	0.9999	0.9999	1.0067	0.0136	0.0136	0.0000	[illegible]	[illegible]

TABLE A14-A

CROSS WIRE PROFILE DATA

X = 24.8 GRID NO. 2 K = 0.2E-06

Y/DELTA	U'/UE COMPOSITE	U'/UE INTER-TURBULENT ZONE	U'/UE TURBULENT ZONE	V'/UE COMPOSITE	V'/UE INTER-TURBULENT ZONE	V'/UE TURBULENT ZONE	W'/UE COMPOSITE	W'/UE INTER-TURBULENT ZONE	W'/UE TURBULENT ZONE
0.2457	0.0704	0.0725	0.0712	0.0384	0.0384	0.0383	0.0515	0.0515	0.0515
0.3617	0.0661	0.0676	0.0657	0.0341	0.0344	0.0340	0.0464	0.0464	0.0465
0.4335	0.0626	0.0629	0.0627	0.0303	0.0303	0.0324	0.0473	0.0476	0.0473
0.7225	0.0389	0.0395	0.0387	0.0216	0.0218	0.0214	0.0317	0.0323	0.0318
0.8671	0.0285	0.0307	0.0287	0.0174	0.0172	0.0174	0.0263	0.0277	0.0265
1.0116	0.0213	0.0250	0.0216	0.0153	0.0151	0.0153	0.0229	0.0195	0.0234
2.8902	0.0149	0.0287	0.0150	0.0181	0.0198	0.0181	0.0174	0.0162	[illegible]

Y/DELTA	U'**2/q**2 COMPOSITE	U'**2/q**2 INTER-TURBULENT ZONE	U'**2/q**2 TURBULENT ZONE	V'**2/q**2 COMPOSITE	V'**2/q**2 INTER-TURBULENT ZONE	V'**2/q**2 TURBULENT ZONE	W'**2/q**2 COMPOSITE	W'**2/q**2 INTER-TURBULENT ZONE	W'**2/q**2 TURBULENT ZONE
0.2457	0.5476	0.5626	0.5467	0.1674	0.1619	0.1676	0.2850	0.2755	0.2861
0.3617	0.5707	0.5811	0.5687	0.1559	0.1544	0.1561	0.2734	0.2655	[illegible]
0.4335	0.5757	0.5748	0.5767	0.1577	0.1556	0.1577	0.2669	[illegible]	[illegible]
0.7225	0.5150	0.6091	0.5112	0.1625	0.1516	0.1614	[illegible]	0.1994	[illegible]
0.8671	0.4517	0.5066	0.4574	0.1777	0.1697	0.1711	0.3751	0.3041	[illegible]
1.0116	0.3760	0.5135	0.3775	0.1999	0.1878	0.1944	0.4240	0.2984	0.4081
2.8902	0.2615	[illegible]	0.2599	[illegible]	0.2492	0.3891	0.3477	0.1587	[illegible]

Y/DELTA	UV/Q**2 COMPOSITE	UV/Q**2 INTER-TURBULENT ZONE	UV/Q**2 TURBULENT ZONE	GAMMA UV	[illegible] UV	GAMMA WV	[illegible] W
0.2457	[illegible]	[illegible]	-0.0825	99.675	[illegible]	99.45	[illegible]
0.3617	-0.0841	-0.0867	-0.0817	[illegible]	[illegible]	99.324	[illegible]
0.4335	[illegible]	-0.0822	-0.0810	99.559	0.607	[illegible]	[illegible]
0.7225	[illegible]	[illegible]	-0.0526	99.475	[illegible]	97.216	[illegible]
0.8671	[illegible]	[illegible]	[illegible]	[illegible]	[illegible]	[illegible]	[illegible]
1.0116	[illegible]	[illegible]	[illegible]	[illegible]	4.8025	[illegible]	[illegible]
2.8902	[illegible]	[illegible]	[illegible]	[illegible]	[illegible]	75.991	[illegible]

Y/DELTA	q**2/UE**2 COMPOSITE	q**2/UE**2 INTER-TURBULENT ZONE	q**2/UE**2 TURBULENT ZONE	UV/UE**2 COMPOSITE	UV/UE**2 INTER-TURBULENT ZONE	UV/UE**2 TURBULENT ZONE
0.2457	0.009043	0.009349	0.009009	-8.537E-04	-8.545E-04	-8.332E-04
0.3617	0.007666	0.007873	0.007610	-6.448E-04	-6.983E-04	-6.232E-04
0.4335	0.006917	0.006866	0.006824	-5.515E-04	-5.642E-04	-5.474E-04
0.7225	0.002952	0.002561	0.002943	-1.627E-04	-1.706E-04	-1.548E-04
0.8671	0.001796	0.001795	0.001824	-5.916E-05	-3.660E-05	-5.966E-05
1.0116	0.001205	0.001244	0.001241	-9.870E-06	2.712E-05	-1.122E-05
2.8902	0.000854	0.001617	0.000866	4.074E-05	1.289E-04	4.009E-05

TABLE A14-B

87-10-44-112

PROFILES OF MEAN AND FLUCTUATING QUANTITIES

X = 8.8 K = 0.75 E−6 TE = 2.0 %

MEAN VELOCITY

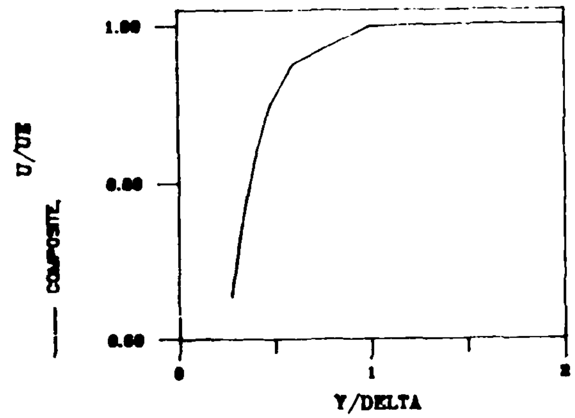

TURBULENCE COMPONENTS

COMPOSITE AVERAGE

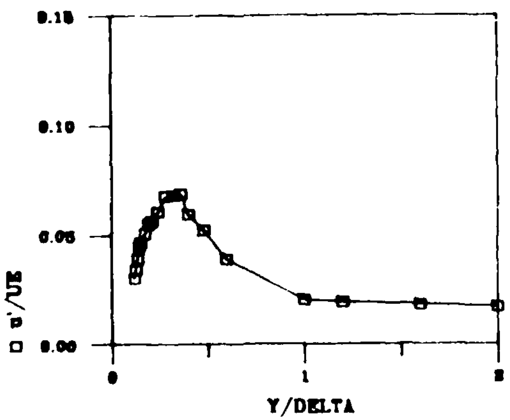

87-10-44-113

Figure A15

SINGLE WIRE PROFILE DATA

X = 8.8 GRID NO. 2 K = 0.75E-06

Y/DELTA	U/UE COMPOSITE	U/UE INTER-TURBULENT ZONE	U/UE TURBULENT ZONE	U'/UE COMPOSITE	U'/UE INTER-TURBULENT ZONE	U'/UE TURBULENT ZONE	GAMMA U	[illegible]
0.1200	0.2604	0.0000	0.0000	0.0301	0.0000	0.0000	0.0000	[illegible]
0.1288	0.2857	0.0000	0.0000	0.0340	0.0000	0.0000	0.0000	0.0000
0.1392	0.3171	0.0000	0.0000	0.0390	0.0000	0.0000	0.0000	[illegible]
0.1472	0.3455	0.0000	0.0000	0.0447	0.0000	0.0000	0.0000	[illegible]
0.1552	0.3698	0.0000	0.0000	0.0466	0.0000	0.0000	0.0000	[illegible]
0.1760	0.4176	0.0000	0.0000	0.0507	0.0000	0.0000	0.0435	[illegible]
0.1936	0.4639	0.0000	0.0000	0.0549	0.0000	0.0000	0.0359	0.2061
0.2120	0.5153	0.0000	0.0000	0.0562	0.0000	0.0000	0.0000	[illegible]
0.2424	0.5761	0.0000	0.0000	0.0605	0.0000	0.0000	0.0000	[illegible]
0.2792	[illegible]	0.0000	0.0000	0.0675	0.0000	0.0000	0.0307	[illegible]
0.3224	0.7313	0.0000	0.0000	0.0679	0.0000	0.0000	0.0000	[illegible]
0.3600	0.7822	0.0000	0.0000	0.0686	0.0000	0.0000	0.0000	[illegible]
0.4000	[illegible]	0.0000	0.0000	0.0593	0.0000	0.0000	[illegible]	[illegible]
0.4800	[illegible]	0.0000	0.0000	0.0520	0.0000	0.0000	0.1366	[illegible]
0.6000	0.9513	0.0000	0.0000	0.0389	0.0000	0.0000	[illegible]	[illegible]
1.0000	[illegible]	0.0000	0.0000	0.0202	0.0000	0.0000	[illegible]	[illegible]
1.2000	1.0013	[illegible]	0.0000	0.0192	0.0000	0.0000	0.0000	[illegible]
1.6000	[illegible]	[illegible]	[illegible]	[illegible]	[illegible]	[illegible]	[illegible]	[illegible]
2.0000	1.0014	0.0000	0.0000	[illegible]	0.0000	0.0000	[illegible]	[illegible]
4.0000	0.9978	[illegible]	0.0000	0.0169	0.0000	[illegible]	[illegible]	[illegible]

TABLE A15

PROFILES OF MEAN AND FLUCTUATING QUANTITIES

X = 12.8 K = 0.75 E−6 TE = 1.9 %

MEAN VELOCITY

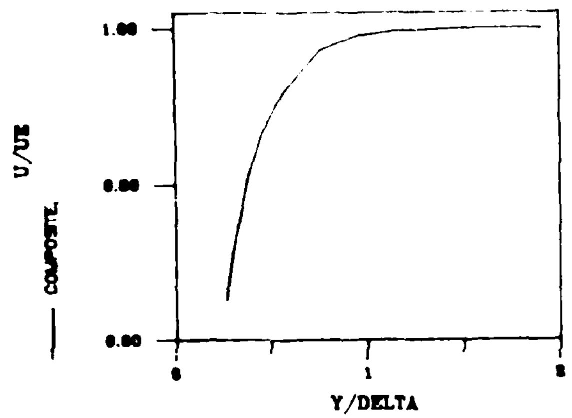

TURBULENCE COMPONENTS

COMPOSITE AVERAGE

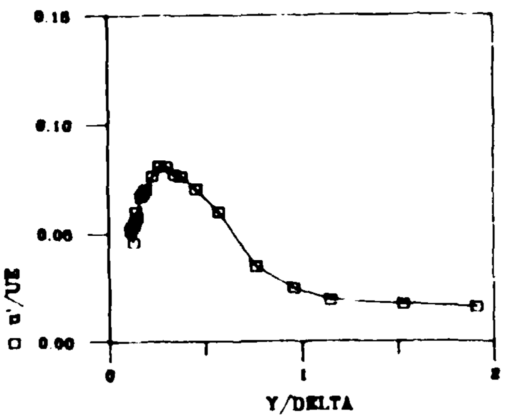

Figure A16

SINGLE WIRE PROFILE DATA

X = 12.8 GRID NO. 2 K = 0.75E-06

Y/DELTA	U/UE COMPOSITE	U/UE INTER-TURBULENT ZONE	U/UE TURBULENT ZONE	U /UE COMPOSITE	U /UE INTER-TURBULENT ZONE	U /UE TURBULENT ZONE	GAMMA U	U
0.1145	0.2888	0.0000	0.0000	0.0512	0.0000	0.0000	0.5712	1.2006
0.1252	0.3138	0.0000	0.0000	0.0526	0.0000	0.0000	0.3714	0.6003
0.1328	0.3418	0.0000	0.0000	0.0458	0.0000	0.0000	0.0589	0.2001
0.1389	0.3604	0.0000	0.0000	0.0542	0.0000	0.0000	0.5661	1.0005
0.1458	0.3852	0.0000	0.0000	0.0598	0.0000	0.0000	1.0528	2.2011
0.1519	0.3983	0.0000	0.0000	0.0569	0.0000	0.0000	0.3893	0.6003
0.1718	0.4489	0.0000	0.0000	0.0665	0.0000	0.0000	0.2382	0.6003
0.1847	0.4809	0.0000	0.0000	0.0680	0.0000	0.0000	0.1819	0.4002
0.1992	0.5091	0.0000	0.0000	0.0698	0.0000	0.0000	0.5379	1.2006
0.2305	0.5916	0.0000	0.0000	0.0761	0.0000	0.0000	0.5763	0.6003
0.2687	0.6507	0.0000	0.0000	0.0807	0.0000	0.0000	0.1204	0.4002
0.3061	0.7128	0.0000	0.0000	0.0805	0.0000	0.0000	0.0640	0.4002
0.3435	0.7555	0.0000	0.0000	0.0767	0.0000	0.0000	0.3566	[illegible]
0.3817	0.8049	0.0000	0.0000	0.0759	0.0000	0.0000	0.4995	1.2006
0.4580	0.8658	0.0000	0.0000	0.0701	0.0000	0.0000	0.8325	1.6008
0.5725	0.9189	0.0000	0.0000	0.0595	0.0000	0.0000	0.9093	[illegible]
0.7634	0.9723	0.0000	0.0000	0.0346	0.0000	0.0000	0.3023	1.4007
0.9542	[illegible]	0.0000	0.0000	0.0244	0.0000	0.0000	0.3407	1.6008
1.1450	0.9964	0.0000	0.0000	0.0189	0.0000	0.0000	0.0000	[illegible]
1.5267	1.0005	0.0000	0.0000	0.0171	0.0000	0.0000	0.0000	[illegible]
1.9084	1.0000	0.0000	0.0000	0.0155	0.0000	0.0000	0.0000	[illegible]
3.8168	0.9951	[illegible]	[illegible]	0.0151	0.0000	0.0000	0.0000	[illegible]

TABLE A16

87 - 10 - 44 - 116

PROFILES OF MEAN AND FLUCTUATING QUANTITIES

X = 16.8 K = 0.75 E-6 TE = 1.7 %

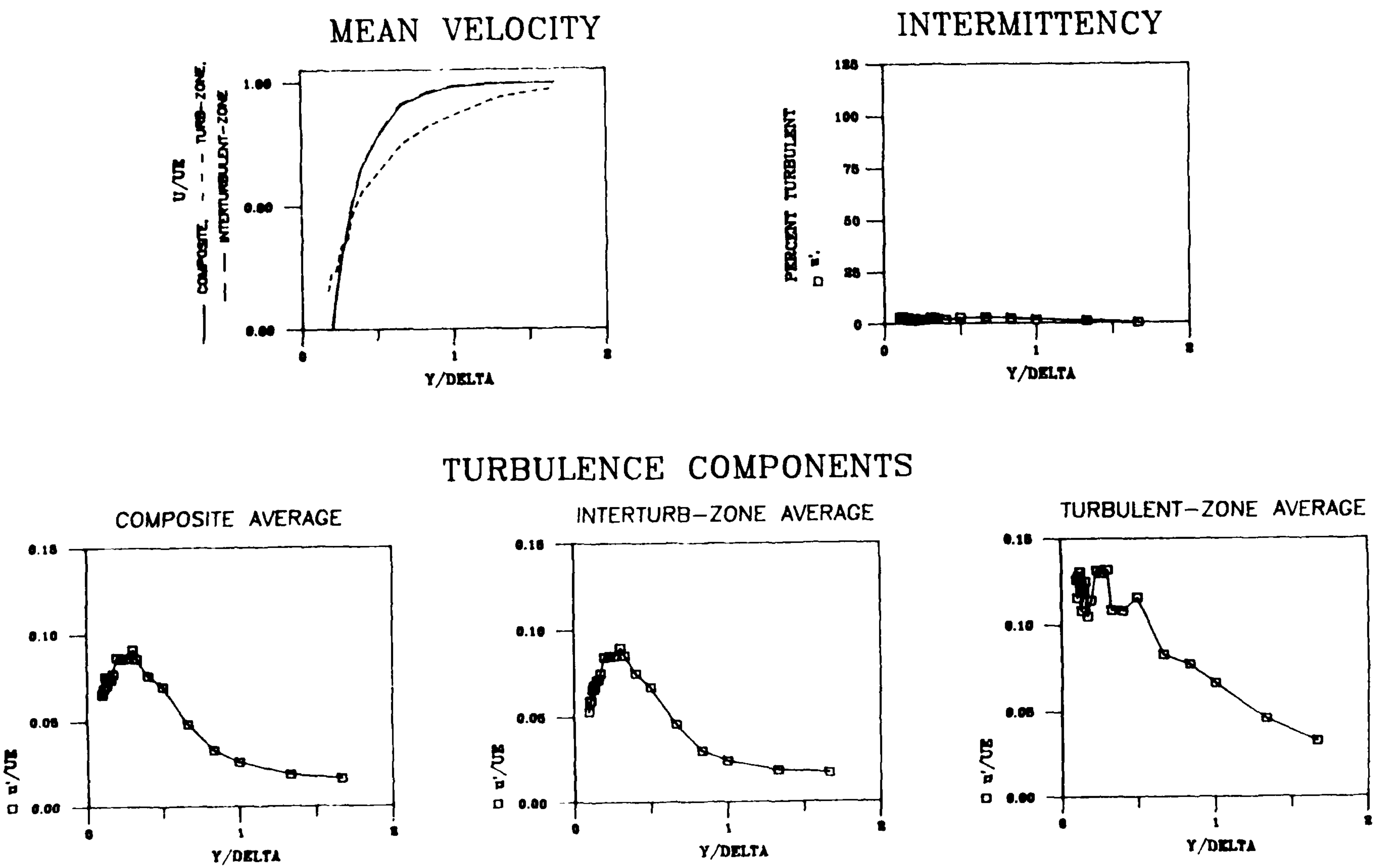

Figure A17

SINGLE WIRE PROFILE DATA

X = 16.8 GRID NO. 2 K = 0.75E-06

Y/DELTA	U/UE COMPOSITE	U/UE INTER-TURBULENT ZONE	U/UE TURBULENT ZONE	U'/UE COMPOSITE	U'/UE INTER-TURBULENT ZONE	U'/UE TURBULENT ZONE	GAMMA U	[illegible] U
0.1000	0.3523	0.3461	0.5370	0.0659	0.0528	0.1260	3.1404	3.8019
0.1080	0.3747	0.3714	0.5344	0.0649	0.0590	0.1153	2.1311	3.0015
0.1147	0.3910	0.3860	0.5547	0.0687	0.0594	0.1281	2.8279	4.4023
0.1233	0.4269	0.4210	0.5872	0.0755	0.0658	0.1304	3.4144	4.2022
0.1313	0.4366	0.4322	0.5817	0.0747	0.0679	0.1251	2.8458	4.2022
0.1347	0.4500	0.4470	0.6114	0.0703	0.0658	0.1078	1.7674	2.4012
0.1500	0.4877	0.4846	0.5977	0.0751	0.0712	0.1188	2.5768	3.4017
0.1613	0.5179	0.5163	0.5993	0.0735	0.0713	0.1249	1.7649	3.2016
0.1753	0.5393	0.5374	0.6628	0.0770	0.0750	0.1047	1.4600	2.4012
0.2000	0.6069	0.6044	0.6928	0.0863	0.0842	0.1135	2.6630	3.6018
0.2347	0.6642	0.6636	0.6962	0.0857	0.0846	0.1313	1.6265	3.0150
0.2660	0.7140	0.7136	0.7345	0.0860	0.0849	0.1295	1.8929	3.4017
0.3047	0.7637	0.7641	0.7486	0.0912	0.0896	0.1317	3.0200	5.4028
0.3313	0.7983	0.7986	0.7830	0.0857	0.0850	0.1082	2.8356	4.6024
0.4073	0.8629	0.8637	0.8244	0.0757	0.0748	0.1079	1.9851	3.2016
0.5000	0.9116	0.9135	0.8510	0.0696	0.0668	0.1157	3.0789	4.8025
0.6667	0.9635	0.9653	0.9013	0.0479	0.0454	0.0825	2.7561	5.4028
0.8333	0.9829	0.9844	0.9257	0.0325	0.0298	0.0769	2.5307	6.6035
1.0000	0.9929	0.9938	0.9460	0.0258	0.0229	0.0663	1.8951	4.8025
1.3333	0.9961	0.9983	0.9770	0.0125	0.0184	0.0456	1.1051	3.2016
1.6667	0.9987	0.9987	0.9899	0.0162	0.0169	0.0335	0.2333	1.0005
3.3333	1.0024	1.0024	0.9966	0.0147	0.0147	[illegible]	[illegible]	[illegible]

TABLE A17

87-10-44-118

PROFILES OF MEAN AND FLUCTUATING QUANTITIES

X = 20.8 K = 0.75 E-6 TE = 1.6 %

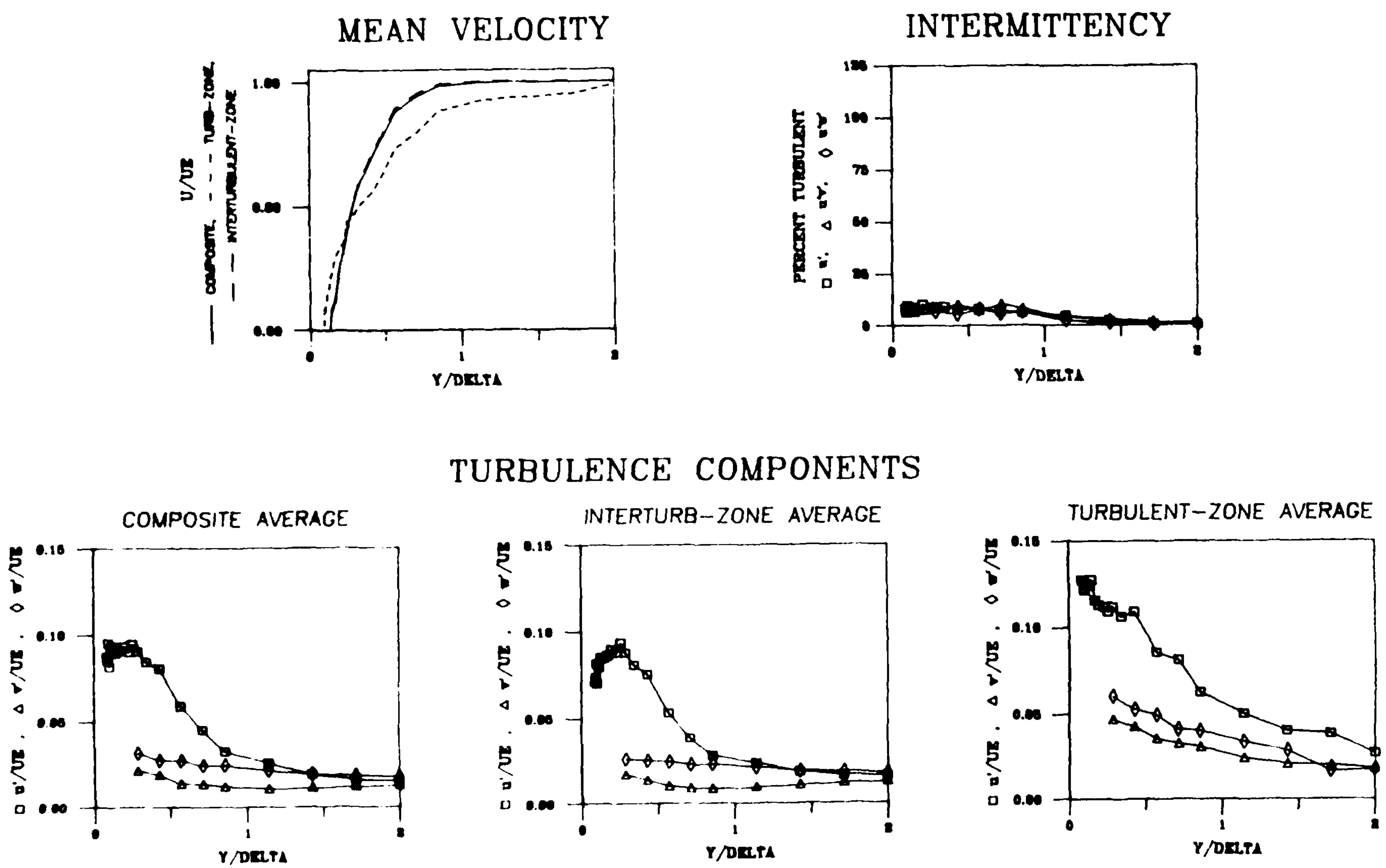

Figure A18-A

PROFILES OF TURBULENT STRESSES

x = 20.8 K = 0.75 E−6 TE = 1.6 %

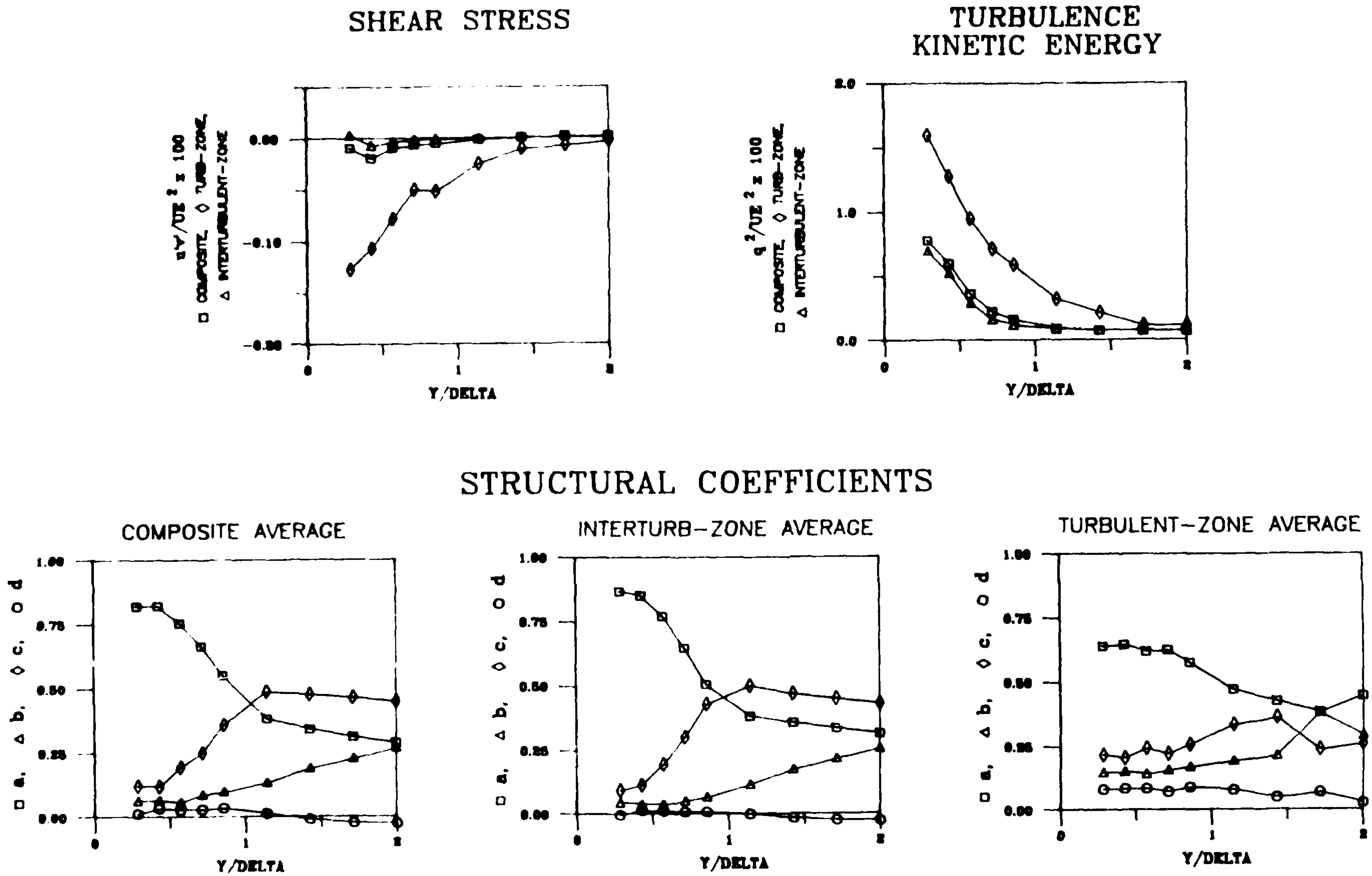

Figure A18-B

87-10-44-120

SINGLE WIRE PROFILE DATA

X = 20.8 GRID NO. 2 K = 0.75E-06

Y/DELTA	U/UE COMPOSITE	U/UE INTER-TURBULENT ZONE	U/UE TURBULENT ZONE	U'/UE COMPOSITE	U'/UE INTER-TURBULENT ZONE	U'/UE TURBULENT ZONE	GAMMA U	F U
0.0857	0.4436	0.4315	0.5780	0.0872	0.0711	0.1271	8.3017	9.2047
0.0943	0.4767	0.4677	0.6078	0.0851	0.0734	0.1272	6.2423	7.0036
0.1000	0.5115	0.4961	0.6346	0.0952	0.0813	0.1218	9.5825	9.8050
0.1040	0.5054	0.4964	0.6270	0.0815	0.0698	0.1212	6.7264	7.0036
0.1154	0.5436	0.5337	0.6559	0.0905	0.0793	0.1250	7.7843	7.4038
0.1274	0.5742	0.5654	0.6635	0.0933	0.0848	0.1239	8.7526	10.4050
0.1389	0.6049	0.5979	0.6867	0.0912	0.0844	0.1240	7.7024	8.4043
0.1514	0.6357	0.6316	0.6903	0.0894	0.0847	0.1274	6.6163	8.8045
0.1731	0.6540	0.6484	0.7192	0.0908	0.0861	0.1154	7.6255	8.0041
0.1994	0.6973	0.6934	0.7310	0.0931	0.0897	0.1127	10.2130	10.2050
0.2314	0.7341	0.7333	0.7430	0.0898	0.0877	0.1117	7.6691	9.2047
0.2589	0.7685	0.7677	0.7761	0.0944	0.0933	0.1088	8.5809	10.4050
0.2857	0.8004	0.8019	0.7847	0.0901	0.0876	0.1119	9.0110	9.8050
0.3446	0.8435	0.8475	0.8052	0.0841	0.0806	0.1061	9.1829	10.2050
0.4303	0.8869	0.8923	0.8261	0.0804	0.0752	0.1088	7.9150	11.8060
0.5714	0.9523	0.9575	0.8940	0.0587	0.0529	0.0854	7.8842	11.6060
0.7143	0.9772	0.9814	0.9199	0.0450	0.0382	0.0811	6.6470	11.6060
0.8571	0.9938	0.9964	0.9534	0.0325	0.0281	0.0625	5.9554	[illegible]
1.1429	0.9997	1.0011	0.9706	0.0257	0.0236	0.0502	4.3981	11.6161
1.4286	1.0006	1.0012	0.9762	0.0190	0.0185	0.0400	2.1004	6.6034
1.7143	[illegible]	1.0001	0.9802	0.0158	0.0163	0.0383	0.6071	[illegible]
[illegible]	[illegible]	[illegible]	0.9946	[illegible]	0.0159	0.0269	0.3662	[illegible]
3.4286	0.9962	0.9962	0.9912	0.0135	0.0135	0.0006	0.0007	[illegible]

TABLE A18-A

87-10-44-121

CROSS WIRE PROFILE DATA

X = 20.8 GRID NO. 2 K = 0.75E-06

Y/DELTA	U'/UE COMPOSITE	U'/UE INTER-TURBULENT ZONE	U'/UE TURBULENT ZONE	V'/UE COMPOSITE	V'/UE INTER-TURBULENT ZONE	V'/UE TURBULENT ZONE	W'/UE COMPOSITE	W'/UE INTER-TURBULENT ZONE	W'/UE TURBULENT ZONE
0.2857	0.0797	0.0775	0.1008	0.0212	0.0168	0.0469	0.0314	0.0260	0.0603
0.4286	0.0699	0.0662	0.0904	0.0189	0.0136	0.0425	0.0273	0.0250	0.0524
0.5714	0.0515	0.0465	0.0764	0.0136	0.0100	0.0353	0.0270	0.0243	0.0492
0.7143	0.0383	0.0321	0.0665	0.0134	0.0088	0.0324	0.0242	0.0226	0.0407
0.8571	0.0293	0.0241	0.0579	0.0119	0.0085	0.0305	0.0244	0.0229	0.0399
1.1429	0.0183	0.0177	0.0384	0.0105	0.0095	0.0240	0.0212	0.0209	0.0335
1.4286	0.0156	0.0160	0.0298	0.0113	0.0109	0.0205	0.0190	0.0189	0.0284
1.7143	0.0146	0.0154	0.0200	0.0122	0.0121	0.0197	0.0184	0.0184	0.0164
2.0000	0.0137	0.0146	0.0224	0.0128	0.0128	0.0178	0.0176	0.0176	0.0177
3.4286	0.0131	0.0136	0.0088	0.0160	0.0159	0.0230	0.0158	0.0158	0.0000

Y/DELTA	U'**2/q**2 COMPOSITE	U'**2/q**2 INTER-TURBULENT ZONE	U'**2/q**2 TURBULENT ZONE	V'**2/q**2 COMPOSITE	V'**2/q**2 INTER-TURBULENT ZONE	V'**2/q**2 TURBULENT ZONE	W'**2/q**2 COMPOSITE	W'**2/q**2 INTER-TURBULENT ZONE	W'**2/q**2 TURBULENT ZONE
0.2857	0.8190	0.8649	0.6387	0.0616	0.0432	0.1461	0.1194	0.0919	0.2152
0.4286	0.8196	0.8491	0.6455	0.0631	0.0379	0.1508	0.1174	0.1131	0.2037
0.5714	0.7521	0.7682	0.6185	0.0549	0.0370	0.1400	0.1929	0.1948	0.2415
0.7143	0.6636	0.6468	0.6242	0.0868	0.0513	0.1565	0.2496	0.3019	0.2193
0.8571	0.5476	0.5046	0.5749	0.0959	0.0660	0.1688	0.3565	0.4292	0.2562
1.1429	0.3810	0.3824	0.4709	0.1332	0.1169	0.1933	0.4858	0.5007	0.3358
1.4286	0.3389	0.3566	0.4247	0.1881	0.1746	0.2127	0.4731	0.4686	0.3626
1.7143	0.3101	0.3343	0.3822	0.2278	0.2168	0.3808	0.4621	0.4459	0.2369
2.0000	0.2865	0.3133	0.4468	0.2675	0.2562	0.2940	0.4460	0.4306	0.2592
3.4286	0.2548	0.2699	0.2176	0.3994	0.3898	0.7824	0.3458	0.3400	0.0000

Y/DELTA	UV/Q**2 COMPOSITE	UV/Q**2 INTER-TURBULENT ZONE	UV/Q**2 TURBULENT ZONE	GAMMA UV	f UV	GAMMA WV	f WV
0.2857	-0.0124	0.0046	-0.0801	8.4200	9.4046	6.5300	7.2037
0.4286	-0.0326	-0.0136	-0.0840	10.1000	12.4064	5.4800	7.2037
0.5714	-0.0269	-0.0116	-0.0832	7.1300	12.2063	7.5500	8.0041
0.7143	-0.0292	-0.0079	-0.0703	10.2700	13.4069	5.6400	8.2041
0.8571	-0.0336	-0.0072	-0.0891	7.9200	11.2057	6.2900	10.4053
1.1429	-0.0123	0.0007	-0.0781	3.7833	9.4048	2.1800	6.2032
1.4286	0.0113	0.0172	-0.0478	2.8893	8.4043	0.9200	3.4017
1.7143	0.0243	0.0255	-0.0677	1.1194	4.4023	0.2200	1.2006
2.0000	0.0272	0.0270	-0.0275	0.7351	3.8019	0.0300	0.2001
3.4286	0.0430	0.0429	-0.0572	0.5661	3.0015	0.0000	0.0000

Y/DELTA	q**2/UE**2 COMPOSITE	q**2/UE**2 INTER-TURBULENT ZONE	q**2/UE**2 TURBULENT ZONE	UV/UE**2 COMPOSITE	UV/UE**2 INTER-TURBULENT ZONE	UV/UE**2 TURBULENT ZONE
0.2857	0.007765	0.006954	0.015941	-9.633E-05	3.168E-05	-1.277E-03
0.4286	0.005976	0.005191	0.012709	-1.949E-04	-7.170E-05	-1.068E-03
0.5714	0.003573	0.002852	0.009431	-9.620E-05	-3.311E-05	-7.850E-04
0.7143	0.002206	0.001599	0.007112	-6.440E-05	-1.264E-05	-4.998E-04
0.8571	0.001575	0.001155	0.005851	-5.290E-05	-8.261E-06	-5.213E-04
1.1429	0.000876	0.000820	0.003157	-1.082E-05	5.723E-07	-2.467E-04
1.4286	0.000721	0.000719	0.002095	8.142E-06	1.235E-05	-1.002E-04
1.7143	0.000692	0.000712	0.001074	1.684E-05	1.820E-05	-7.270E-05
2.0000	0.000654	0.000677	0.001138	1.775E-05	1.829E-05	-3.130E-05
3.4286	0.000683	0.000691	0.000718	2.926E-05	2.965E-05	-4.112E-05

TABLE A18-B

87-10-44-122

PROFILES OF MEAN AND FLUCTUATING QUANTITIES

X = 28.8   K = 0.75 E−6   TE = 1.4 %

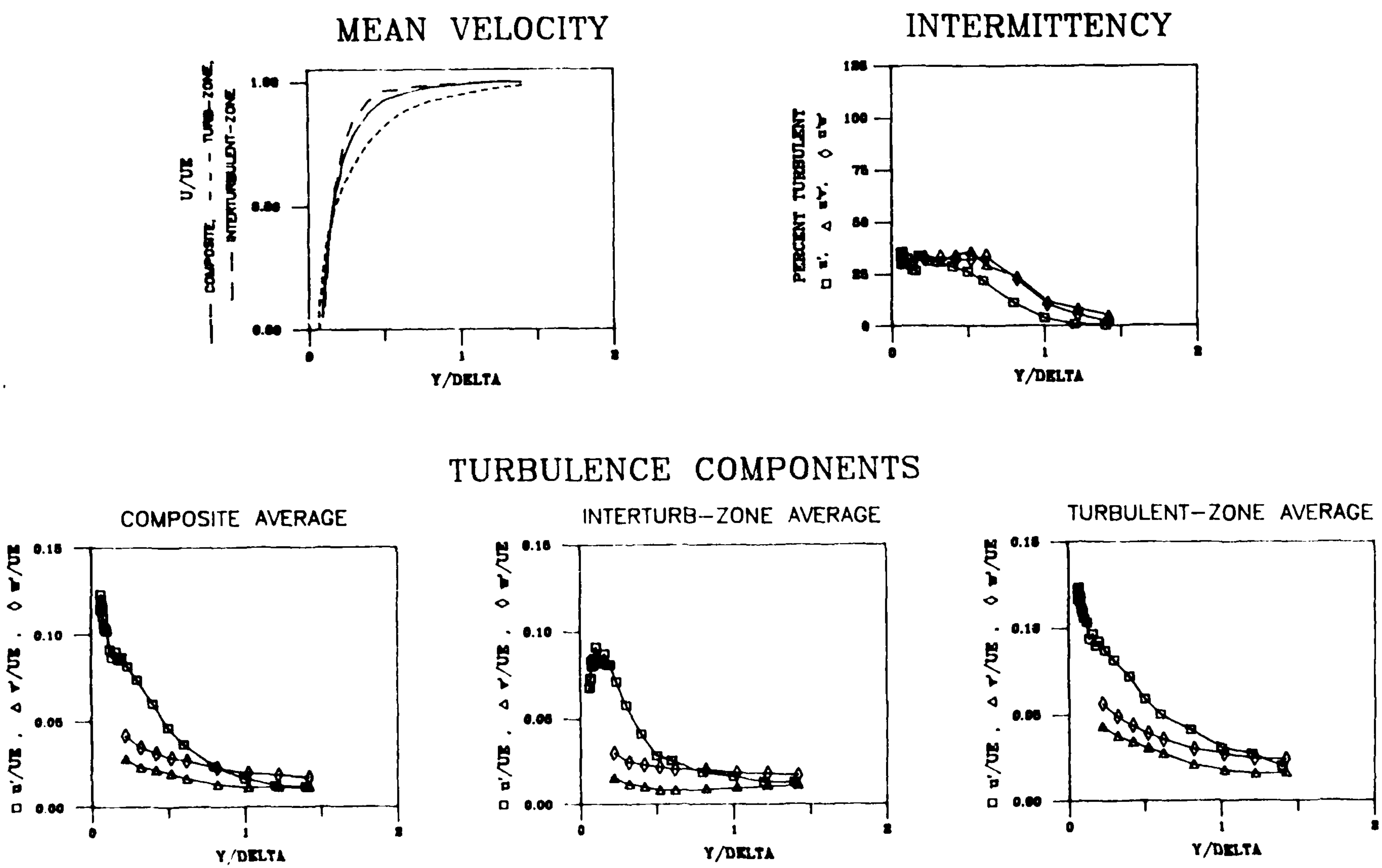

Figure A19-A

87-10-44-123

PROFILES OF TURBULENT STRESSES

X = 28.8 K = 0.75 E−6 TE = 1.4 %

SHEAR STRESS

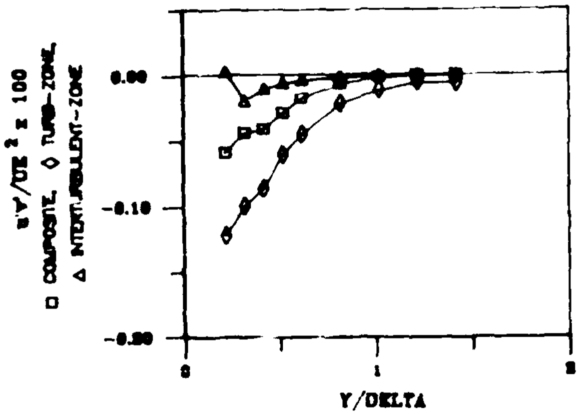

TURBULENCE KINETIC ENERGY

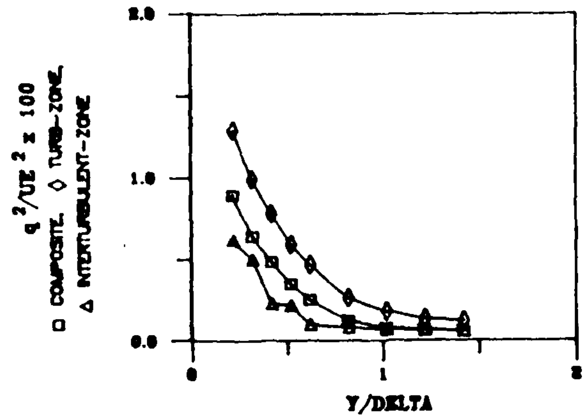

STRUCTURAL COEFFICIENTS

COMPOSITE AVERAGE

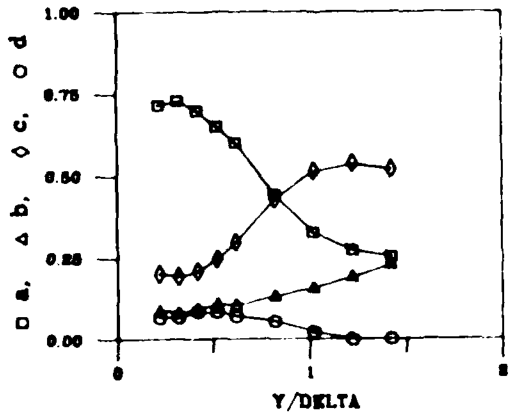

INTERTURB–ZONE AVERAGE

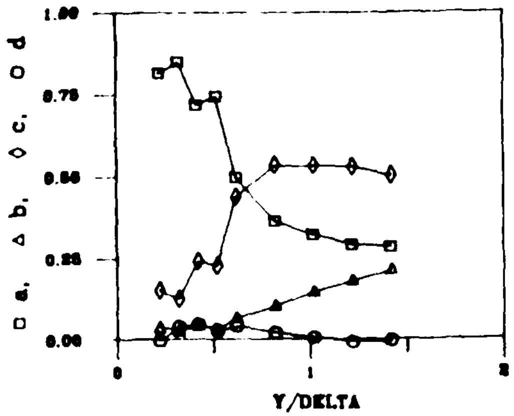

TURBULENT–ZONE AVERAGE

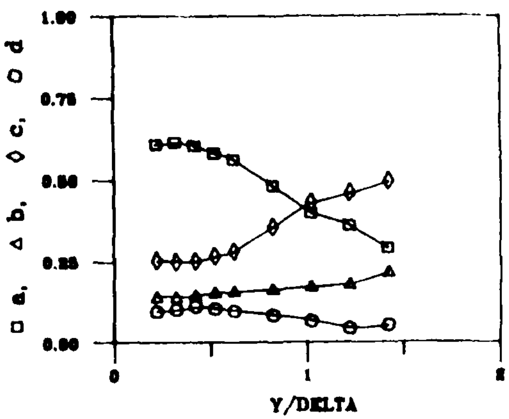

Figure A19-B

87 - 10 - 44 - 124

SINGLE WIRE PROFILE DATA

X = 28.8 GRID NO. 2 K = 0.75E-06

Y/DELTA	U/UE COMPOSITE	U/UE INTER-TURBULENT ZONE	U/UE TURBULENT ZONE	U'/UE COMPOSITE	U'/UE INTER-TURBULENT ZONE	U'/UE TURBULENT ZONE	GAMMA	[illegible]
0.0600	0.4635	0.4019	0.5766	0.1231	0.0674	0.1221	35.1510	22.6120
0.0660	0.4882	0.4390	0.6019	0.1137	0.0680	0.1166	30.0000	[illegible]
0.0684	0.5053	0.4514	0.6089	0.1194	0.0728	0.1233	[illegible]	[illegible]
0.0720	0.5381	0.4920	0.6330	0.1163	0.0732	0.1183	35.5350	[illegible]
0.0772	0.5582	0.5133	0.6456	0.1149	0.0833	0.1176	[illegible]	[illegible]
0.0800	0.5564	0.5177	0.6488	0.1097	0.0801	0.1156	[illegible]	[illegible]
0.0886	0.5914	0.5587	0.6679	0.1037	0.0806	0.1111	[illegible]	[illegible]
0.0960	0.6204	0.5919	0.6867	0.1024	0.0846	[illegible]	[illegible]	[illegible]
0.1048	0.6613	0.6379	0.7078	[illegible]	[illegible]	[illegible]	[illegible]	[illegible]
0.1224	0.7044	0.6915	0.7329	[illegible]	[illegible]	[illegible]	[illegible]	[illegible]
0.1392	0.7474	[illegible]	0.7576	[illegible]	0.0824	[illegible]	[illegible]	[illegible]
0.1604	0.7852	0.7865	[illegible]	[illegible]	[illegible]	[illegible]	[illegible]	[illegible]
[illegible]	0.8195	[illegible]	[illegible]	[illegible]	[illegible]	[illegible]	[illegible]	[illegible]
0.2000	0.8348	[illegible]	[illegible]	[illegible]	[illegible]	[illegible]	[illegible]	[illegible]
0.2400	[illegible]	[illegible]	[illegible]	[illegible]	[illegible]	[illegible]	[illegible]	[illegible]
[illegible]	[illegible]	[illegible]	[illegible]	[illegible]	[illegible]	[illegible]	[illegible]	[illegible]
[illegible]	[illegible]	[illegible]	[illegible]	0.0599	[illegible]	[illegible]	[illegible]	[illegible]
[illegible]	[illegible]	[illegible]	[illegible]	[illegible]	[illegible]	[illegible]	[illegible]	[illegible]
[illegible]	[illegible]	0.9884	[illegible]	[illegible]	[illegible]	[illegible]	[illegible]	[illegible]
[illegible]	[illegible]	[illegible]	[illegible]	[illegible]	[illegible]	[illegible]	[illegible]	[illegible]
[illegible]	[illegible]	[illegible]	[illegible]	[illegible]	[illegible]	[illegible]	[illegible]	[illegible]
[illegible]	[illegible]	[illegible]	[illegible]	[illegible]	[illegible]	[illegible]	[illegible]	[illegible]
[illegible]	[illegible]	[illegible]	[illegible]	[illegible]	[illegible]	[illegible]	[illegible]	[illegible]
[illegible]	[illegible]	[illegible]	[illegible]	[illegible]	[illegible]	[illegible]	[illegible]	[illegible]

TABLE A19-A

CROSS WIRE PROFILE DATA

X = 28.8 GRID NO. 2 K = 0.75E-06

Y/DELTA	U/UE COMPOSITE	U/UE INTER-TURBULENT ZONE	U/UE TURBULENT ZONE	V/UE COMPOSITE	V/UE INTER-TURBULENT ZONE	V/UE TURBULENT ZONE	W/UE COMPOSITE	W/UE INTER-TURBULENT ZONE	W/UE TURBULENT ZONE
0.2200	0.078?	[illegible]	[illegible]	[illegible]	[illegible]	[illegible]	0.041?	[illegible]	0.058?
0.32??	0.066?	[illegible]	[illegible]	[illegible]	[illegible]	[illegible]	0.0246	0.0245	0.045?
0.42??	0.0578	[illegible]	[illegible]	[illegible]	[illegible]	[illegible]	[illegible]	0.0225	0.047?
0.52??	0.047?	[illegible]	[illegible]	[illegible]	[illegible]	[illegible]	[illegible]	[illegible]	[illegible]
0.6200	0.0385	[illegible]	[illegible]	[illegible]	[illegible]	[illegible]	0.0266	[illegible]	0.0275?
0.82??	0.0222?	[illegible]	[illegible]	[illegible]	[illegible]	[illegible]	[illegible]	[illegible]	0.0299?
1.02??	0.0156	[illegible]	0.0264?	[illegible]	[illegible]	[illegible]	[illegible]	[illegible]	[illegible]
1.22??	[illegible]	[illegible]	[illegible]	[illegible]	[illegible]	[illegible]	0.0164?	[illegible]	[illegible]
1.420?	[illegible]	[illegible]	[illegible]	[illegible]	[illegible]	[illegible]	[illegible]	[illegible]	[illegible]
1.42??	[illegible]	[illegible]	[illegible]	[illegible]	[illegible]	[illegible]	[illegible]	[illegible]	[illegible]

Y/DELTA [illegible]

INTER-TURBULENT ZONE

TURBULENT ZONE

[illegible]

[illegible]

Y/DELTA	[illegible] COMPOSITE	INTER-TURBULENT ZONE	TURBULENT ZONE	COMPOSITE	INTER-TURBULENT ZONE	TURBULENT ZONE
[illegible]	[illegible]	[illegible]	[illegible]	-5.869E-04?	2.847E-05	-1.225E-0?
[illegible]	[illegible]	[illegible]	[illegible]	-4.?E-04	-1.959E-04	-9.9?E-04
[illegible]	[illegible]	[illegible]	[illegible]	-4.084E-04	-1.047E-04	-8.640E-04
[illegible]	[illegible]	[illegible]	[illegible]	-3.867E-04?	-6.051E-05?	-6.06?E-04
[illegible]	[illegible]	[illegible]	[illegible]	[illegible]	-3.667E-05	-4.497E-04?
[illegible]	[illegible]	[illegible]	0.00255?	-6.702E-05	-1.491E-05	-2.174E-04
[illegible]	[illegible]	[illegible]	0.00176?	-1.615E-05	-2.865E-06	-1.162E-04
[illegible]	[illegible]	[illegible]	[illegible]	6.770E-07?	5.128E-06	-5.552E-05?
[illegible]	[illegible]	[illegible]	0.00119?	-4.942E-07	2.341E-06	-6.288E-05
1.42?	[illegible]	[illegible]	0.00058?	5.346E-06	3.920E-06	2.116E-05

TABLE A19-B

87-10-44-126

AD-A191 698 STUDY OF THE STRUCTURE OF TURBULENCE IN ACCELERATING 3/3
TRANSITIONAL BOUNDAR..(U) UNITED TECHNOLOGIES RESEARCH
CENTER EAST HARTFORD CT M F BLAIR ET AL. 23 DEC 87
UNCLASSIFIED UTRC/R87-956900-1 AFOSR-TR-88-0017 F/G 20/4 NL

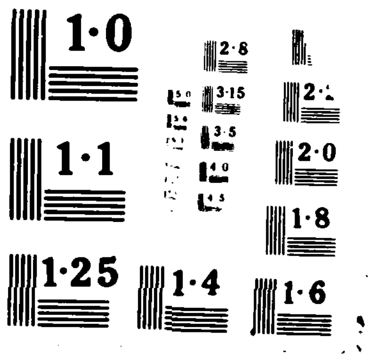
1·0
2·8
3·15
3·5
4·0
4·5
1·1
2·0
1·8
1·25
1·4
1·6

PROFILES OF MEAN AND FLUCTUATING QUANTITIES

X = 36.8 K = 0.75 E-6 TE = 1.2 %

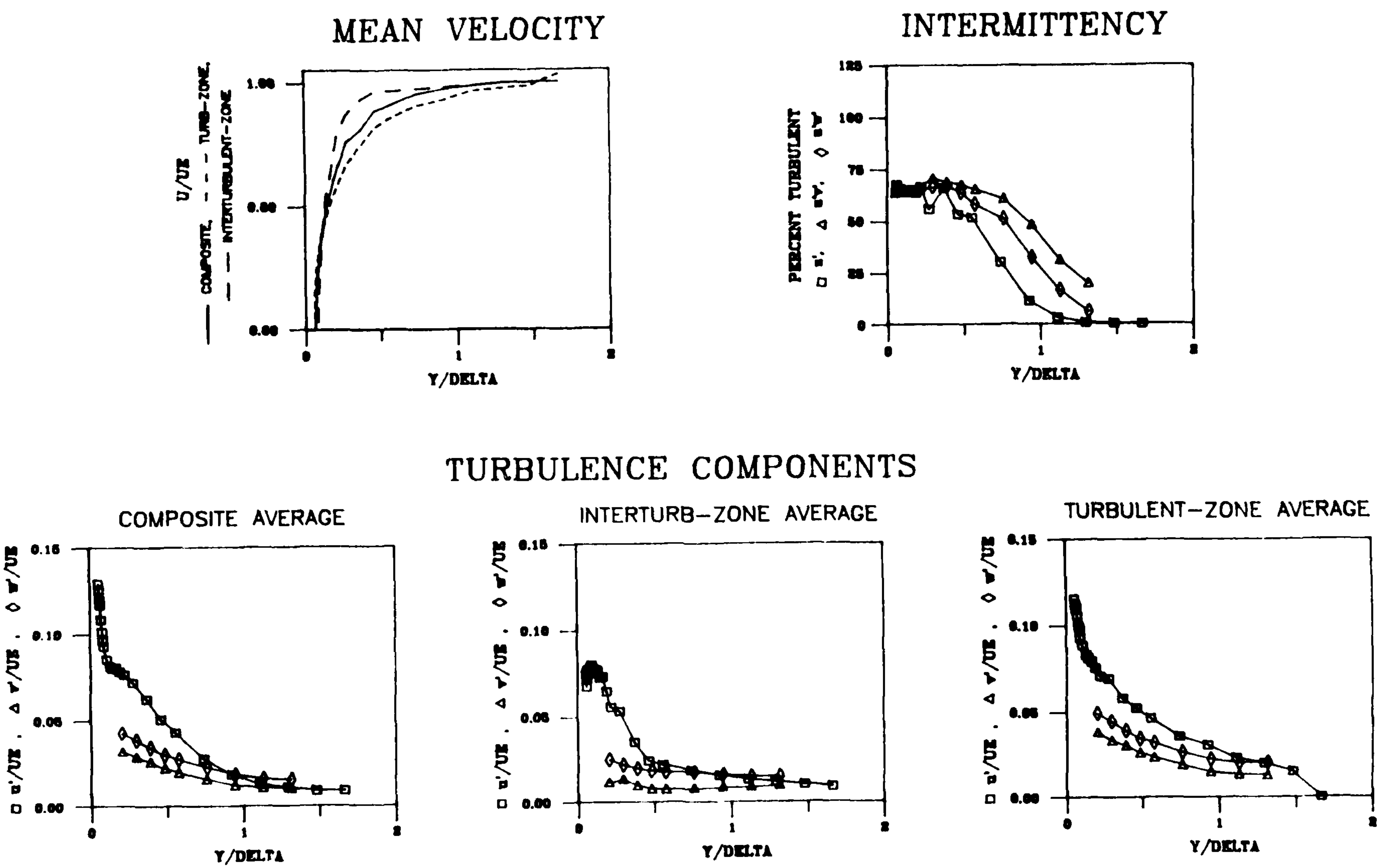

Figure A20-A

87-10-44-127

PROFILES OF TURBULENT STRESSES

X = 36.8 K = 0.75 E-6 TE = 1.2 %

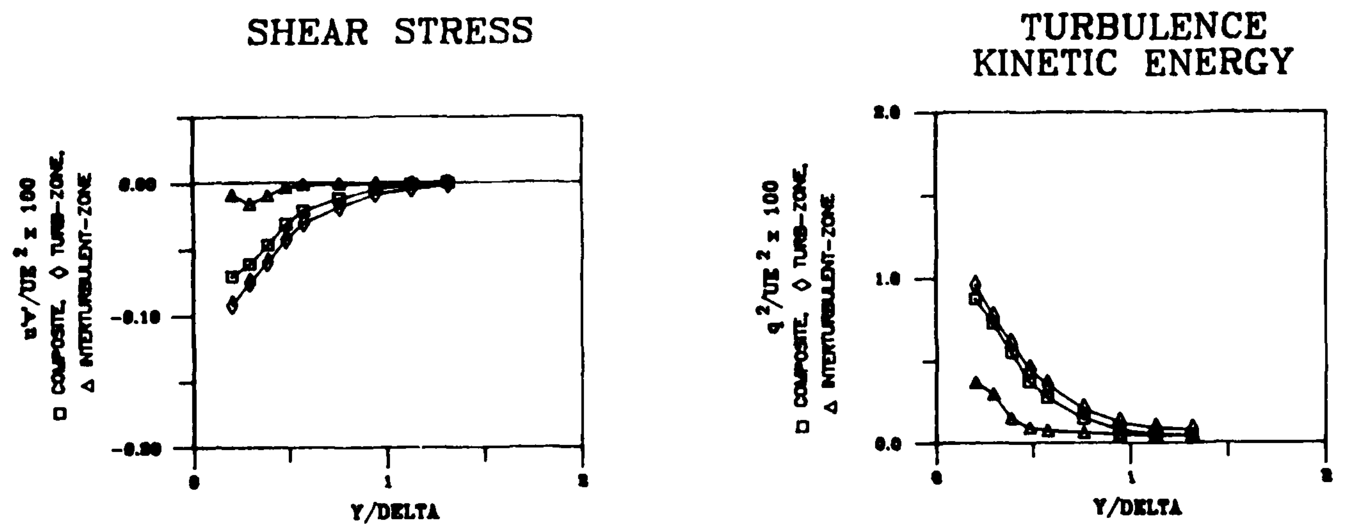

STRUCTURAL COEFFICIENTS

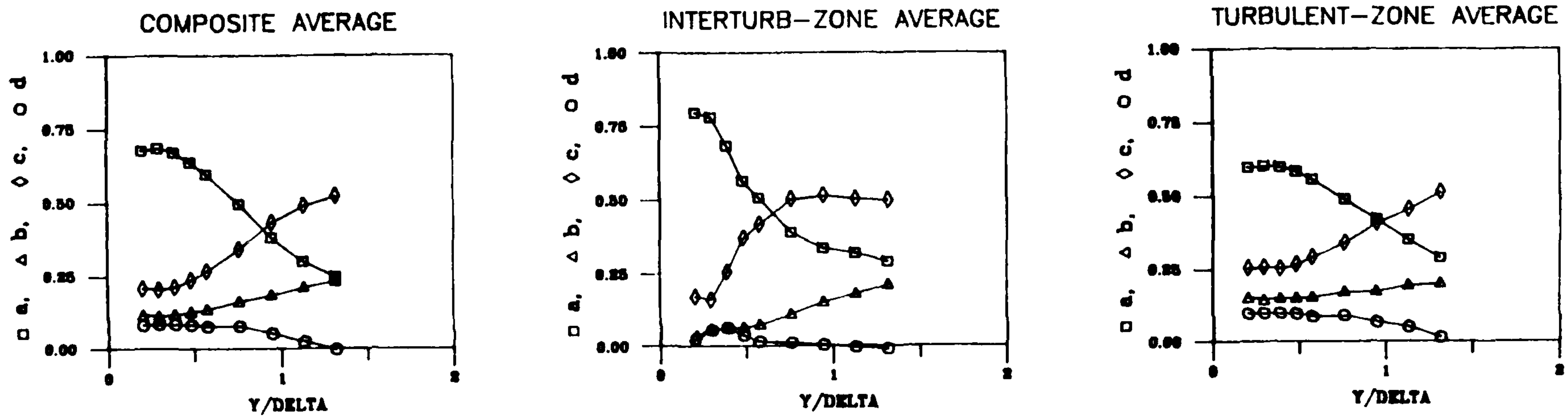

Figure A20-B

87-10-44-128

SINGLE WIRE PROFILE DATA

X = 36.8 GRID NO. 2 K = 0.75E-06

Y/DELTA	U/UE COMPOSITE	U/UE INTER-TURBULENT ZONE	U/UE TURBULENT ZONE	U'/UE COMPOSITE	U'/UE INTER-TURBULENT ZONE	U'/UE TURBULENT ZONE	GAMMA U	f U
0.0556	0.5372	0.4352	0.5983	0.1289	0.0746	0.1152	63.4860	21.2110
0.0611	0.5639	0.4577	0.6181	0.1251	0.0672	0.1125	65.9450	22.0110
0.0630	0.5893	0.4980	0.6333	0.1177	0.0723	0.1099	67.4400	20.6105
0.0667	0.6002	0.5075	0.6497	0.1193	0.0767	0.1094	64.6290	20.2100
0.0685	0.6088	0.5285	0.6548	0.1165	0.0769	0.1103	64.1270	23.2120
0.0741	0.6361	0.5680	0.6726	0.1080	0.0748	0.1054	65.1020	23.4120
0.0815	0.6664	0.6122	0.6974	0.1010	0.0776	0.0998	64.1980	23.0120
0.0889	0.6852	0.6448	0.7072	0.0962	0.0783	0.0980	65.3130	23.2120
0.0941	0.6995	0.6622	0.7202	0.0925	0.0798	0.0927	64.0470	21.6110
0.1096	0.7405	0.7273	0.7478	0.0851	0.0776	0.0883	64.3010	21.8110
0.1300	0.7740	0.7820	0.7693	0.0810	0.0768	0.0830	64.0780	23.6120
0.1467	0.7963	0.8182	0.7840	0.0797	0.0725	0.0810	63.8140	23.8120
0.1667	0.8179	0.8457	0.8006	0.0803	0.0730	0.0791	64.8850	23.6120
0.1926	0.8432	0.8840	0.8196	0.0779	0.0644	0.0753	63.6240	22.2110
0.2222	0.8665	0.9203	0.8383	0.0763	0.0553	0.0706	66.3760	20.8110
0.2778	0.9043	0.9482	0.8690	0.0715	0.0529	0.0691	55.6330	25.0130
0.3704	0.9233	0.9724	0.8982	0.0619	0.0348	0.0578	65.7790	22.0110
0.4630	0.9540	0.9849	0.9272	0.0503	0.0240	0.0521	53.0530	30.2150
0.5556	0.9624	0.9857	0.9409	0.0425	0.0216	0.0461	51.3730	36.6190
0.7407	0.9815	0.9895	0.9627	0.0274	0.0183	0.0354	29.9590	41.6210
0.9259	0.9907	0.9926	0.9729	0.0182	0.0153	0.0304	11.1530	31.0160
1.1111	0.9946	0.9951	0.9852	0.0125	0.0130	0.0228	3.1634	14.0070
1.2963	0.9992	0.9992	0.9900	0.0106	0.0116	0.0196	0.5891	3.2016
1.4815	1.0003	1.0003	0.9943	0.0088	0.0102	0.0149	0.1050	0.6003
1.6667	1.0010	1.0010	1.0126	0.0089	0.0089	0.0000	0.0000	0.0000
2.9630	0.9944	0.9944	0.9927	0.0083	0.0083	0.0000	0.0000	0.0000

TABLE A20-A

87 – 10 – 44 – 129

CROSS WIRE PROFILE DATA

X = 36.8 GRID NO. 2 K = 0.75E-06

Y/DELTA	U'/UE COMPOSITE	U'/UE INTER-TURBULENT ZONE	U'/UE TURBULENT ZONE	V'/UE COMPOSITE	V'/UE INTER-TURBULENT ZONE	V'/UE TURBULENT ZONE	W'/UE COMPOSITE	W'/UE INTER-TURBULENT ZONE	W'/UE TURBULENT ZONE
0.2037	0.0768	0.0538	0.0756	0.0319	0.0116	0.0381	0.0424	0.0248	0.0491
0.2963	0.0703	0.0479	0.0678	0.0286	0.0134	0.0332	0.0382	0.0216	0.0442
0.3889	0.0605	0.0317	0.0602	0.0256	0.0096	0.0303	0.0339	0.0193	0.0389
0.4815	0.0486	0.0225	0.0509	0.0218	0.0077	0.0260	0.0295	0.0182	0.0343
0.5741	0.0402	0.0189	0.0439	0.0193	0.0073	0.0233	0.0269	0.0172	0.0318
0.7593	0.0269	0.0152	0.0314	0.0155	0.0081	0.0188	0.0223	0.0172	0.0262
0.9444	0.0170	0.0127	0.0226	0.0119	0.0086	0.0146	0.0181	0.0156	0.0222
1.1296	0.0123	0.0117	0.0173	0.0104	0.0089	0.0131	0.0156	0.0146	0.0198
1.3148	0.0104	0.0112	0.0148	0.0101	0.0097	0.0127	0.0151	0.0147	0.0201

Y/DELTA	U'**2/q**2 COMPOSITE	U'**2/q**2 INTER-TURBULENT ZONE	U'**2/q**2 TURBULENT ZONE	V'**2/q**2 COMPOSITE	V'**2/q**2 INTER-TURBULENT ZONE	V'**2/q**2 TURBULENT ZONE	W'**2/q**2 COMPOSITE	W'**2/q**2 INTER-TURBULENT ZONE	W'**2/q**2 TURBULENT ZONE
0.2037	0.6768	0.7940	0.5967	0.1161	0.0363	0.1504	0.2071	0.1696	0.2530
0.2963	0.6845	0.7792	0.6009	0.1122	0.0611	0.1429	0.2033	0.1597	0.2562
0.3889	0.6696	0.6830	0.5979	0.1190	0.0621	0.1505	0.2115	0.2549	0.2516
0.4815	0.6363	0.5634	0.5822	0.1276	0.0653	0.1517	0.2361	0.3713	0.2661
0.5741	0.5962	0.5065	0.5553	0.1366	0.0752	0.1539	0.2672	0.4180	0.2908
0.7593	0.4952	0.3884	0.4879	0.1632	0.1098	0.1724	0.3416	0.5018	0.3397
0.9444	0.3807	0.3342	0.4193	0.1863	0.1521	0.1738	0.4330	0.5137	0.4069
1.1296	0.2988	0.3170	0.3501	0.2124	0.1812	0.1957	0.4888	0.5017	0.4542
1.3148	0.2460	0.2900	0.2677	0.2327	0.2124	0.2003	0.5213	0.4977	0.5120

Y/DELTA	UV/Q**2 COMPOSITE	UV/Q**2 INTER-TURBULENT ZONE	UV/Q**2 TURBULENT ZONE	GAMMA UV	f UV	GAMMA WV	f WV
0.2037	-0.0809	-0.0252	-0.0958	66.2990	24.4130	65.0900	22.4110
0.2963	-0.0843	-0.0542	-0.0977	70.4330	24.8130	66.3650	22.6120
0.3889	-0.0846	-0.0636	-0.0984	68.5300	22.4110	66.6090	23.8120
0.4815	-0.0824	-0.0367	-0.0954	67.2670	25.0130	63.5860	25.8130
0.5741	-0.0762	-0.0149	-0.0857	65.0200	30.4160	57.8410	26.8140
0.7593	-0.0779	-0.0095	-0.0887	60.5070	30.6160	50.8200	30.8160
0.9444	-0.0514	-0.0025	-0.0662	47.9640	42.8220	32.1570	37.4190
1.1296	-0.0232	0.0057	-0.0496	30.7990	45.0230	16.2140	33.8170
1.3148	0.0041	0.0109	-0.0135	19.5770	49.8260	5.8940	17.2090

Y/DELTA	q**2/UE**2 COMPOSITE	q**2/UE**2 INTER-TURBULENT ZONE	q**2/UE**2 TURBULENT ZONE	UV/UE**2 COMPOSITE	UV/UE**2 INTER-TURBULENT ZONE	UV/UE**2 TURBULENT ZONE
0.2037	0.008718	0.003662	0.009592	-7.051E-04	-9.245E-05	-9.193E-04
0.2963	0.007240	0.002940	0.007669	-6.102E-04	-1.592E-04	-7.492E-04
0.3889	0.005472	0.001474	0.006059	-4.630E-04	-9.379E-05	-5.964E-04
0.4815	0.003715	0.000899	0.004445	-3.061E-04	-3.296E-05	-4.240E-04
0.5741	0.002722	0.000714	0.003490	-2.074E-04	-1.064E-05	-2.991E-04
0.7593	0.001459	0.000595	0.002029	-1.137E-04	-5.652E-06	-1.799E-04
0.9444	0.000759	0.000479	0.001222	-3.900E-05	-1.189E-06	-8.089E-05
1.1296	0.000507	0.000436	0.000865	-1.168E-05	2.468E-06	-4.292E-05
1.3148	0.000439	0.000436	0.000797	1.802E-06	4.756E-06	-1.079E-05

TABLE A20-B

87-10-44-130

PROFILES OF MEAN AND FLUCTUATING QUANTITIES

X = 48.8 K = 0.75 E-6 TE = 0.9 %

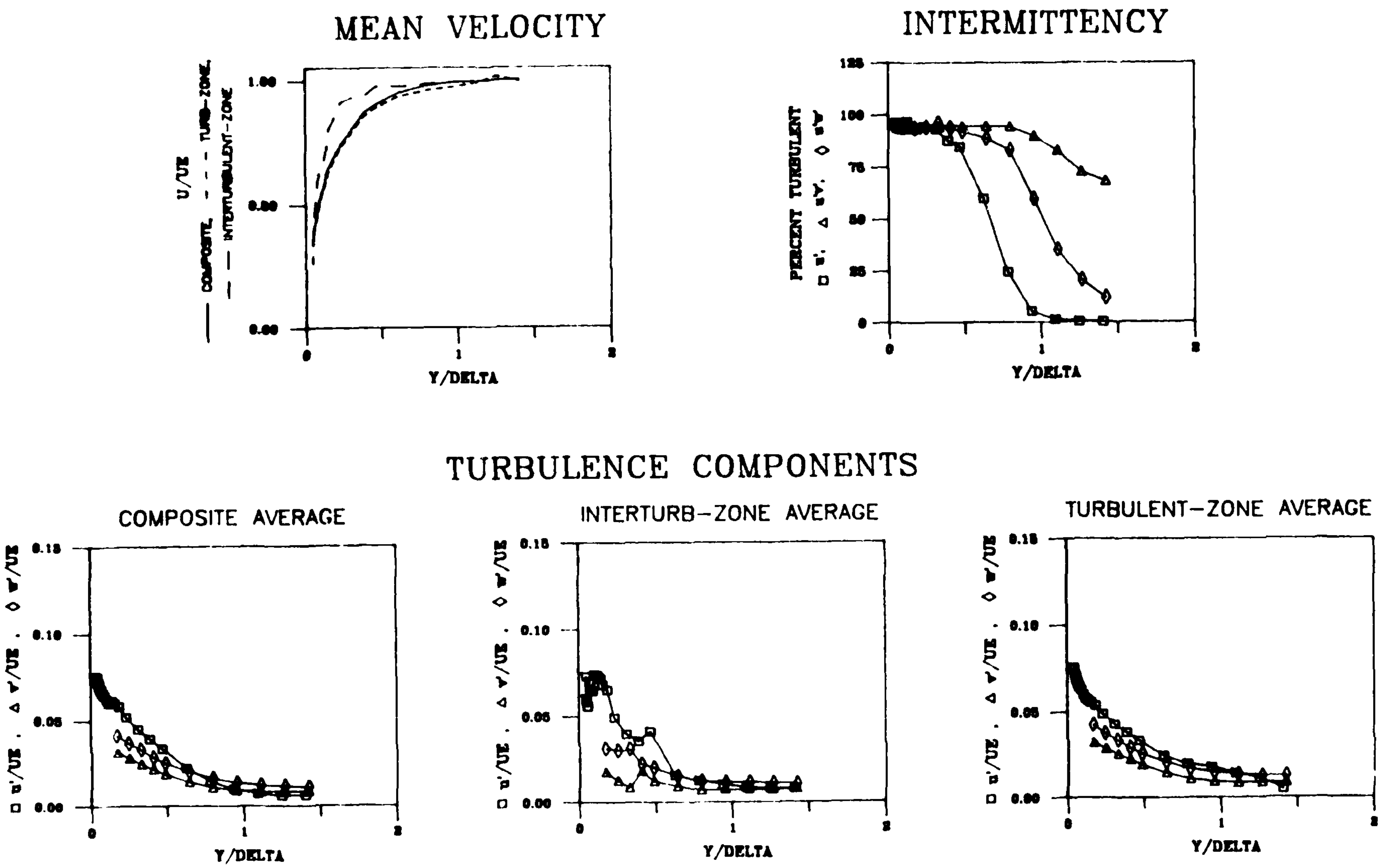

Figure A21-A

87-10-44-131

PROFILES OF TURBULENT STRESSES

X = 48.8 K = 0.75 E−6 TE = 0.9 %

SHEAR STRESS

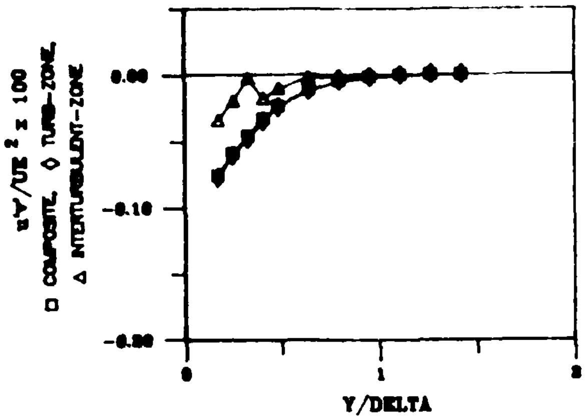

TURBULENCE KINETIC ENERGY

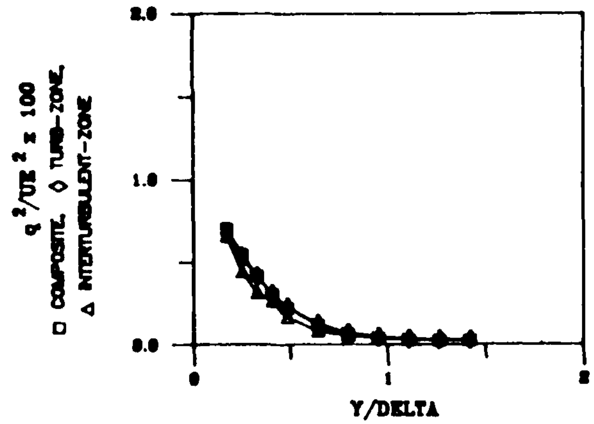

STRUCTURAL COEFFICIENTS

COMPOSITE AVERAGE

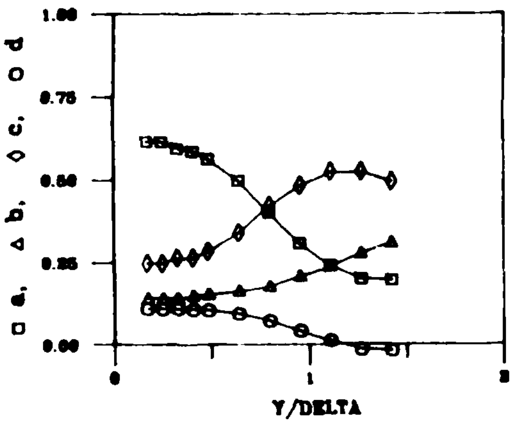

INTERTURB-ZONE AVERAGE

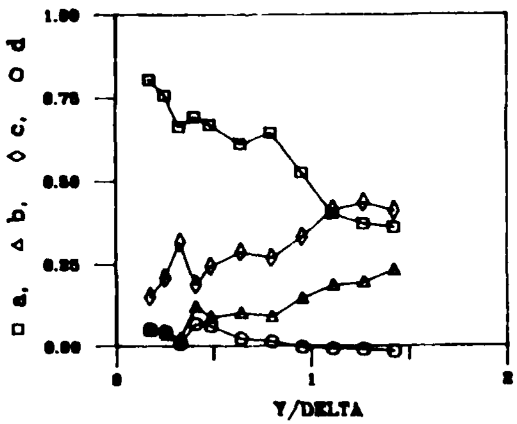

TURBULENT-ZONE AVERAGE

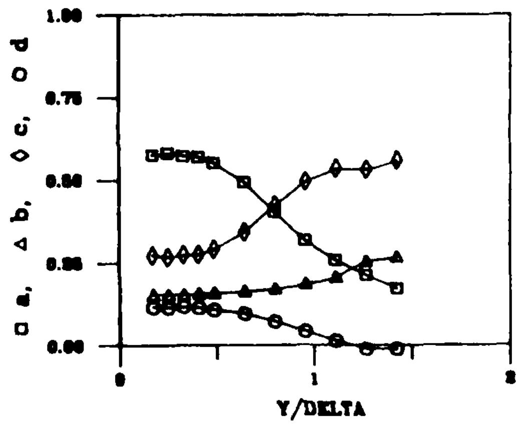

Figure A21-B

87 - 10 - 44 - 132

SINGLE WIRE PROFILE DATA

X = 48.8 GRID NO. 2 K = 0.75E-06

Y/DELTA	U/UE	U/UE	U/UE	U'/UE	U'/UE	U'/UE	GAMMA	f
	COMPOSITE	INTER-TURBULENT ZONE	TURBULENT ZONE	COMPOSITE	INTER-TURBULENT ZONE	TURBULENT ZONE	U	U
0.0469	0.7351	0.7162	0.7359	0.0753	0.0729	0.0753	95.8120	7.4038
0.0500	0.7361	0.7021	0.7383	0.0745	0.0601	0.0748	94.2060	6.0031
0.0531	0.7471	0.7423	0.7473	0.0717	0.0583	0.0722	96.0480	5.0026
0.0563	0.7511	0.7533	0.7510	0.0707	0.0586	0.0715	93.4020	7.6039
0.0594	0.7598	0.7721	0.7589	0.0699	0.0554	0.0707	93.4140	8.4043
0.0625	0.7650	0.7872	0.7639	0.0681	0.0557	0.0685	95.0080	7.4038
0.0700	0.7720	0.8090	0.7695	0.0676	0.0698	0.0669	94.3010	6.4033
0.0750	0.7779	0.8128	0.7761	0.0659	0.0655	0.0654	95.1920	7.4038
0.0813	0.7913	0.8357	0.7871	0.0656	0.0647	0.0643	92.7590	9.8050
0.0938	0.8039	0.8476	0.8002	0.0640	0.0644	0.0627	94.0270	8.0041
0.1094	0.8194	0.8602	0.8162	0.0618	0.0738	0.0598	96.0660	7.2037
0.1250	0.8290	0.8680	0.8258	0.0597	0.0733	0.0575	96.7210	5.0026
0.1406	0.8469	0.8901	0.8397	0.0613	0.0718	0.0565	93.0990	7.0036
0.1563	0.8588	0.9211	0.8525	0.0599	0.0680	0.0554	93.3220	8.4043
0.1875	0.8751	0.9364	0.8658	0.0579	0.0650	0.0535	92.9660	8.6044
0.2344	0.8976	0.9647	0.8926	0.0517	0.0491	0.0485	94.0630	8.6044
0.3125	0.9229	0.9730	0.9184	0.0447	0.0396	0.0427	92.7540	9.0046
0.3906	0.9455	0.9752	0.9401	0.0391	0.0353	0.0378	87.2770	13.8070
0.4688	0.9619	0.9904	0.9564	0.0335	0.0410	0.0330	84.4290	21.8110
0.6250	0.9810	0.9903	0.9749	0.0220	0.0155	0.0243	59.6030	62.0320
0.7813	0.9911	0.9975	0.9831	0.0145	0.0124	0.0196	24.2260	55.8290
0.9375	0.9961	0.9966	0.9881	0.0097	0.0102	0.0176	5.3099	19.0100
1.0938	0.9982	0.9953	0.9935	0.0071	0.0086	0.0142	1.3192	7.0036
1.2500	1.0030	1.0000	1.0057	0.0061	0.0080	0.0108	0.1511	0.6003
1.4063	1.0011	1.0011	0.9972	0.0062	0.0080	0.0049	0.0845	0.6003
2.5000	1.0007	1.0003	0.9948	0.0056	0.0056	0.0000	0.0000	0.0000

TABLE A21-A

87 - 10 - 44 - 133

CROSS WIRE PROFILE DATA

X = 48.8 GRID NO. 2 K = 0.75E-06

Y/DELTA	U'/UE COMPOSITE	U'/UE INTER-TURBULENT ZONE	U'/UE TURBULENT ZONE	V'/UE COMPOSITE	V'/UE INTER-TURBULENT ZONE	V'/UE TURBULENT ZONE	W'/UE COMPOSITE	W'/UE INTER-TURBULENT ZONE	W'/UE TURBULENT ZONE
0.1719	0.0655	0.0723	0.0619	0.0315	0.0177	0.0322	0.0413	0.0312	0.0424
0.2500	0.0578	0.0570	0.0554	0.0279	0.0126	0.0286	0.0365	0.0300	0.0373
0.3281	0.0496	0.0433	0.0484	0.0245	0.0085	0.0252	0.0330	0.0311	0.0333
0.4063	0.0423	0.0425	0.0418	0.0216	0.0180	0.0221	0.0284	0.0220	0.0289
0.4844	0.0352	0.0332	0.0353	0.0186	0.0122	0.0191	0.0249	0.0199	0.0255
0.6406	0.0241	0.0221	0.0246	0.0140	0.0091	0.0143	0.0199	0.0150	0.0205
0.7969	0.0157	0.0184	0.0163	0.0106	0.0070	0.0107	0.0160	0.0120	0.0167
0.9531	0.0108	0.0141	0.0118	0.0090	0.0076	0.0091	0.0135	0.0114	0.0147
1.1094	0.0083	0.0107	0.0093	0.0083	0.0077	0.0084	0.0121	0.0114	0.0134
1.2656	0.0071	0.0102	0.0079	0.0084	0.0075	0.0087	0.0114	0.0111	0.0124
1.4219	0.0068	0.0098	0.0071	0.0087	0.0080	0.0089	0.0108	0.0105	0.0128
2.5156	0.0066	0.0101	0.0088	0.0108	0.0098	0.0091	0.0097	0.0095	0.0111

Y/DELTA	U'**2/q**2 COMPOSITE	U'**2/q**2 INTER-TURBULENT ZONE	U'**2/q**2 TURBULENT ZONE	V'**2/q**2 COMPOSITE	V'**2/q**2 INTER-TURBULENT ZONE	V'**2/q**2 TURBULENT ZONE	W'**2/q**2 COMPOSITE	W'**2/q**2 INTER-TURBULENT ZONE	W'**2/q**2 TURBULENT ZONE
0.1719	0.6140	0.8027	0.5754	0.1400	0.0472	0.1535	0.2459	0.1501	0.2711
0.2500	0.6127	0.7558	0.5812	0.1410	0.0357	0.1528	0.2463	0.2085	0.2660
0.3281	0.5928	0.6609	0.5725	0.1430	0.0228	0.1534	0.2642	0.3163	0.2741
0.4063	0.5844	0.6911	0.5688	0.1504	0.1217	0.1566	0.2652	0.1872	0.2745
0.4844	0.5619	0.6678	0.5512	0.1547	0.0894	0.1583	0.2834	0.2428	0.2905
0.6406	0.4961	0.6106	0.4934	0.1640	0.1028	0.1635	0.3399	0.2866	0.3431
0.7969	0.3999	0.6436	0.4039	0.1786	0.0893	0.1713	0.4215	0.2670	0.4248
0.9531	0.3076	0.5236	0.3178	0.2102	0.1454	0.1869	0.4822	0.3311	0.4953
1.1094	0.2401	0.4006	0.2585	0.2378	0.1860	0.2067	0.5221	0.4134	0.5348
1.2656	0.1990	0.3700	0.2127	0.2784	0.1953	0.2555	0.5226	0.4347	0.5318
1.4219	0.1957	0.3591	0.1725	0.3113	0.2318	0.2682	0.4930	0.4090	0.5593
2.5156	0.1715	0.3572	0.2834	0.4526	0.3282	0.2866	0.3758	0.3146	0.4301

Y/DELTA	UV/Q**2 COMPOSITE	UV/Q**2 INTER-TURBULENT ZONE	UV/Q**2 TURBULENT ZONE	GAMMA UV	f UV	GAMMA WV	f WV
0.1719	-0.1084	-0.0524	-0.1158	94.8870	6.2032	93.1510	7.4038
0.2500	-0.1075	-0.0445	-0.1147	94.7690	9.2047	93.6630	7.0036
0.3281	-0.1100	-0.0077	-0.1174	93.9930	8.6044	95.8710	3.8019
0.4063	-0.1065	-0.0682	-0.1132	94.8920	8.2042	93.1860	10.0050
0.4844	-0.1039	-0.0612	-0.1069	94.2670	10.6050	91.7670	11.0060
0.6406	-0.0933	-0.0241	-0.0951	94.1570	12.2060	88.3630	12.4060
0.7969	-0.0717	-0.0130	-0.0709	94.0700	13.4070	82.8280	27.2140
0.9531	-0.0411	0.0041	-0.0413	89.5540	26.6140	59.4540	51.4260
1.1094	-0.0100	0.0084	-0.0135	82.7020	43.8220	34.8280	55.8290
1.2656	0.0156	0.0104	0.0122	72.3030	59.2300	20.1050	40.6210
1.4219	0.0189	0.0163	0.0124	67.8560	59.4300	11.6090	31.2160
2.5156	0.0324	0.0120	-0.0633	73.2040	59.2300	10.4710	26.8140

Y/DELTA	q**2/UE**2 COMPOSITE	q**2/UE**2 INTER-TURBULENT ZONE	q**2/UE**2 TURBULENT ZONE	UV/UE**2 COMPOSITE	UV/UE**2 INTER-TURBULENT ZONE	UV/UE**2 TURBULENT ZONE
0.1719	0.007005	0.006549	0.006695	-7.591E-04	-3.429E-04	-7.752E-04
0.2500	0.005461	0.004379	0.005283	-5.870E-04	-1.949E-04	-6.061E-04
0.3281	0.004161	0.003101	0.004103	-4.576E-04	-2.391E-05	-4.817E-04
0.4063	0.003067	0.002616	0.003083	-3.268E-04	-1.784E-04	-3.491E-04
0.4844	0.002215	0.001648	0.002267	-2.301E-04	-1.009E-04	-2.422E-04
0.6406	0.001175	0.000799	0.001234	-1.096E-04	-1.921E-05	-1.174E-04
0.7969	0.000618	0.000547	0.000667	-4.432E-05	-7.105E-06	-4.730E-05
0.9531	0.000382	0.000394	0.000442	-1.568E-05	1.618E-06	-1.826E-05
1.1094	0.000286	0.000318	0.000337	-2.871E-06	2.680E-06	-4.544E-06
1.2656	0.000252	0.000287	0.000294	3.917E-06	2.989E-06	3.577E-06
1.4219	0.000240	0.000273	0.000295	4.519E-06	4.429E-06	3.652E-06
2.5156	0.000253	0.000290	0.000288	8.179E-06	3.487E-06	-1.826E-05

TABLE A21-B

87-10-44-134

PROFILES OF MEAN AND FLUCTUATING QUANTITIES

X = 4.8 K = 0.75 E-6 TE = 4.7 %

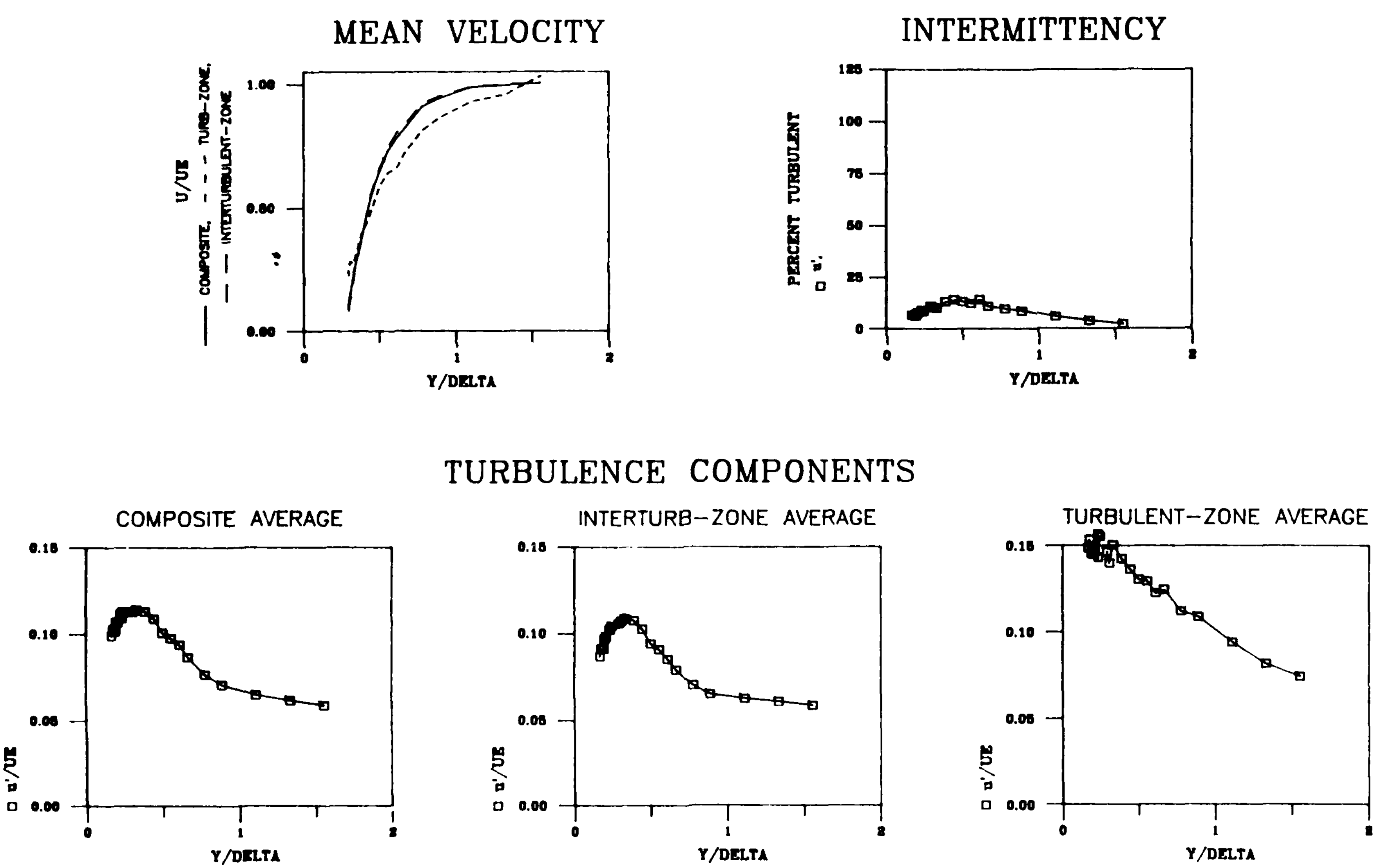

Figure A22

87-10-44-135

SINGLE WIRE PROFILE DATA

X = 4.8 GRID NO. 3 K = 0.75E-06

Y/DELTA	U/UE COMPOSITE	U/UE INTER-TURBULENT ZONE	U/UE TURBULENT ZONE	U'/UE COMPOSITE	U'/UE INTER-TURBULENT ZONE	U'/UE TURBULENT ZONE	GAMMA U	f U
0.1678	0.3892	0.3797	0.5153	0.0987	0.0867	0.1485	6.5900	16.8090
0.1789	0.4177	0.4084	0.5384	0.1026	0.0912	0.1534	6.6598	17.6090
0.1933	0.4446	0.4357	0.5730	0.1013	0.0911	0.1449	6.0605	16.4080
0.2000	0.4602	0.4506	0.5770	0.1068	0.0968	0.1467	7.2157	19.0100
0.2089	0.4827	0.4742	0.5762	0.1066	0.0981	0.1445	7.8356	20.2100
0.2333	0.5162	0.5079	0.5985	0.1115	0.1024	0.1564	8.7500	24.6130
0.2344	0.5285	0.5215	0.5954	0.1089	0.1023	0.1428	8.9421	23.8120
0.2456	0.5505	0.5421	0.6341	0.1128	0.1041	0.1552	8.5015	23.0120
2.6556	0.5912	0.5826	0.6685	0.1152	0.1074	0.1492	9.4826	25.2130
0.2933	0.6396	0.6329	0.6899	0.1127	0.1057	0.1461	11.0710	29.4150
0.3089	0.6603	0.6538	0.7138	0.1127	0.1071	0.1396	10.3480	26.6150
0.3311	0.6920	0.6899	0.7098	0.1138	0.1085	0.1502	10.0790	26.6140
0.3889	0.7544	0.7534	0.7604	0.1128	0.1073	0.1422	13.2680	37.4190
0.4444	0.8183	0.8225	0.7945	0.1086	0.1024	0.1361	14.2110	39.4200
0.5000	0.8604	0.8646	0.8355	0.1005	0.0939	0.1302	13.1070	36.4190
0.5556	0.8923	0.8975	0.8575	0.0973	0.0906	0.1291	12.2260	36.0180
0.6111	0.9130	0.9214	0.8657	0.0936	0.0850	0.1224	14.1110	38.2200
0.6667	0.9297	0.9349	0.8895	0.0865	0.0788	0.1243	10.9070	35.4180
0.7778	0.9637	0.9683	0.9249	0.0764	0.0699	0.1119	9.6030	32.0160
0.8889	0.9772	0.9804	0.9456	0.0705	0.0647	0.1085	8.5528	26.0130
1.1111	0.9959	0.9974	0.9729	0.0646	0.0621	0.0938	5.7454	19.6100
1.3333	0.9991	0.9997	0.9839	0.0613	0.0604	0.0814	3.7141	17.6070
1.5556	1.0022	1.0019	1.0126	0.0585	0.0582	0.0741	2.2490	8.8045
2.7778	0.9986	0.9983	1.0546	0.0536	0.0537	0.0549	0.2690	1.2006

TABLE A22

87-10-44-136

PROFILES OF MEAN AND FLUCTUATING QUANTITIES

X = 8.8 K = 0.75 E-6 TE = 4.4 %

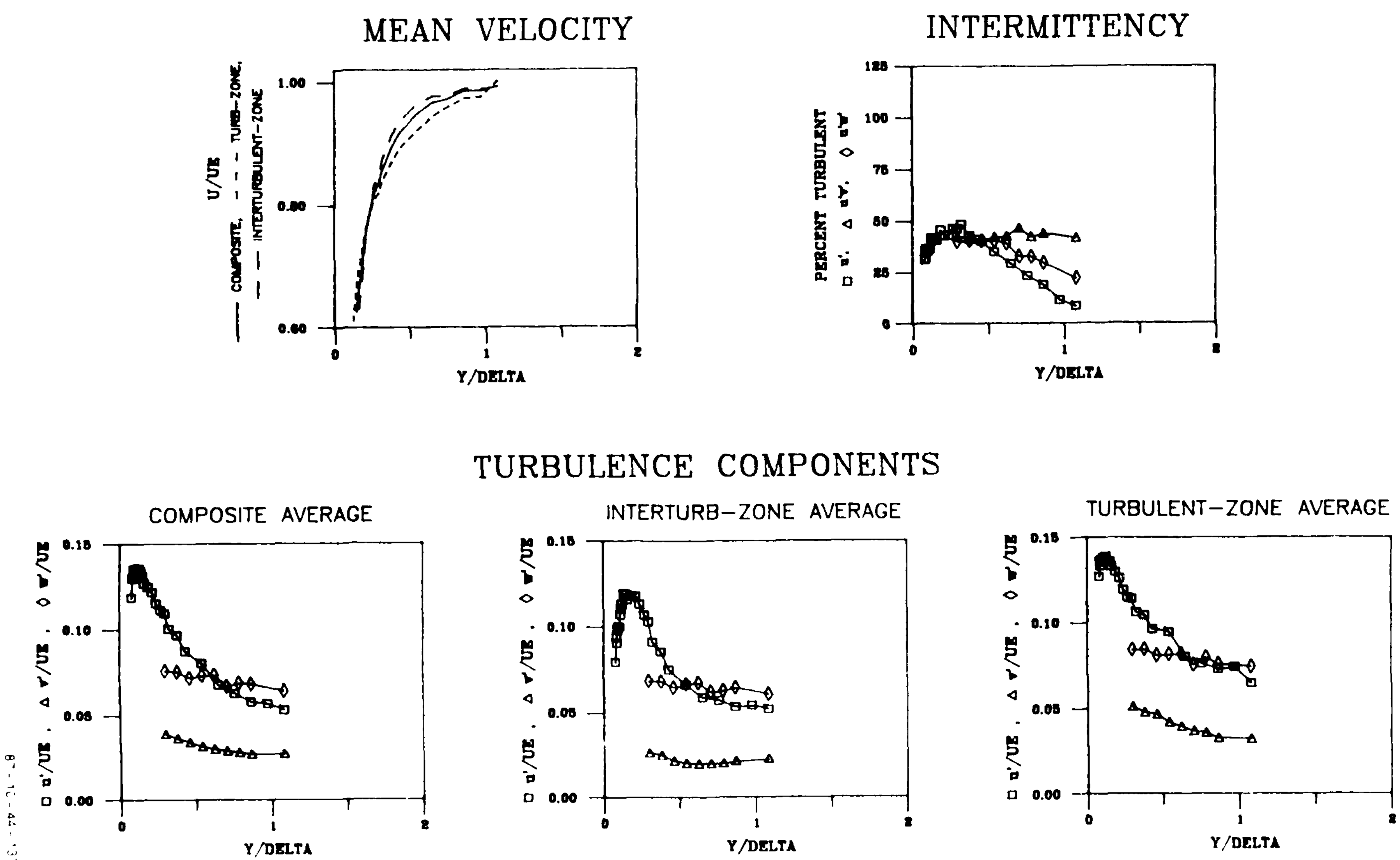

Figure A23-A

87-10-44-137

PROFILES OF TURBULENT STRESSES

X = 8.8   K = 0.75 E−6   TE = 4.4 %

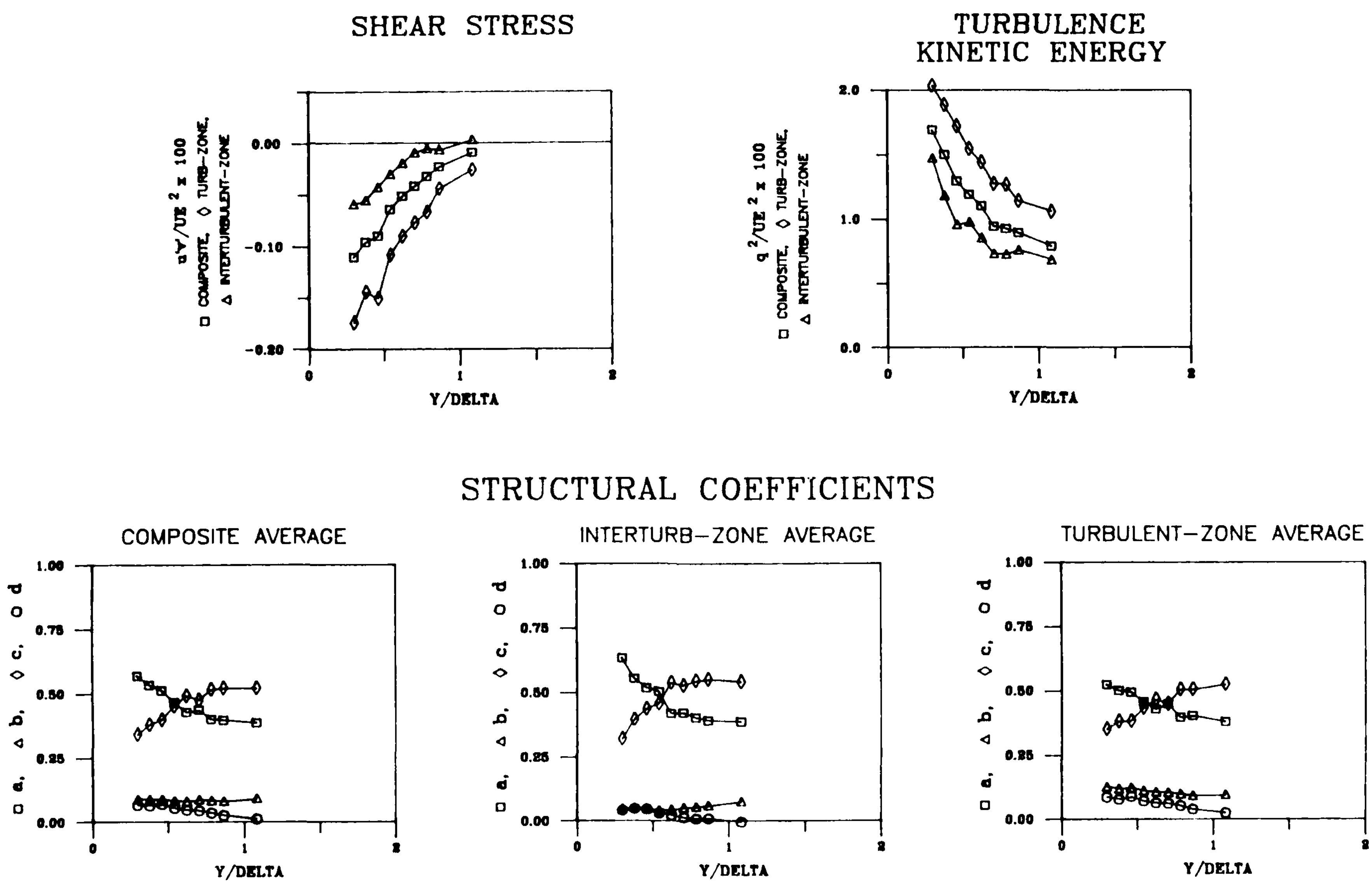

Figure A23-B

87 - 10 - 44 - 138

SINGLE WIRE PROFILE DATA

X = 8.8 GRID NO. 3 K = 0.75E-06

Y/DELTA	U/UE COMPOSITE	U/UE INTER-TURBULENT ZONE	U/UE TURBULENT ZONE	U'/UE COMPOSITE	U'/UE INTER-TURBULENT ZONE	U'/UE TURBULENT ZONE	GAMMA U	f U
0.0811	0.3388	0.2923	0.4378	0.1184	0.0795	0.1268	30.9760	47.2240
0.0881	0.3770	0.3285	0.4760	0.1296	0.0940	0.1358	31.5700	43.2220
0.0914	0.3973	0.3425	0.4918	0.1299	0.0905	0.1332	35.7270	46.4240
0.0951	0.4105	0.3546	0.5043	0.1351	0.0982	0.1365	36.3650	48.4250
0.1005	0.4335	0.3810	0.5256	0.1335	0.0994	0.1359	35.1080	46.8240
0.1070	0.4631	0.4123	0.5507	0.1326	0.1002	0.1358	35.6790	45.2230
0.1135	0.4956	0.4495	0.5740	0.1336	0.1070	0.1378	36.4470	45.4230
0.1195	0.5159	0.4721	0.5885	0.1322	0.1106	0.1353	36.3190	48.2250
0.1270	0.5484	0.5022	0.6100	0.1356	0.1130	0.1387	41.7260	51.2260
0.1395	0.5852	0.5471	0.6373	0.1336	0.1191	0.1355	40.8580	47.8240
0.1514	0.6250	0.5952	0.6662	0.1309	0.1188	0.1357	41.1320	47.4241
0.1622	0.6553	0.6295	0.6918	0.1268	0.1157	0.1329	40.4710	46.6240
0.1892	0.7030	0.6882	0.7203	0.1245	0.1181	0.1296	45.6120	49.4250
0.2162	0.7566	0.7518	0.7627	0.1215	0.1179	0.1259	42.8660	53.2270
0.2432	0.7953	0.7977	0.7916	0.1149	0.1132	0.1190	43.0460	52.8270
0.2703	0.8222	0.8323	0.8110	0.1110	0.1068	0.1145	46.4290	55.0261
0.2973	0.8356	0.8490	0.8207	0.1090	0.1028	0.1139	46.2910	59.8310
0.3243	0.8590	0.8764	0.8414	0.1001	0.0909	0.1059	48.4140	59.0311
0.3784	0.8922	0.9116	0.8676	0.0965	0.0853	0.1042	42.8230	57.2290
0.4324	0.9174	0.9358	0.8922	0.0871	0.0748	0.0961	41.0450	56.4300
0.5405	0.9466	0.9619	0.9192	0.0799	0.0661	0.0943	34.7310	59.2300
0.6486	0.9664	0.9764	0.9434	0.0674	0.0586	0.0800	29.0860	55.6281
0.7568	0.9732	0.9777	0.9596	0.0625	0.0567	0.0760	23.2510	47.2240
0.8649	0.9860	0.9891	0.9737	0.0576	0.0539	0.0727	18.9730	44.8221
0.9730	0.9868	0.9882	0.9764	0.0566	0.0539	0.0740	11.4220	32.0260
1.0811	0.9930	0.9922	1.0008	0.0529	0.0517	0.0647	8.4042	26.8141

TABLE A23-A

87-10-44-139

CROSS WIRE PROFILE DATA

X = 8.8 GRID NO. 3 K = 0.75E-06

Y/DELTA	U'/UE COMPOSITE	U'/UE INTER-TURBULENT ZONE	U'/UE TURBULENT ZONE	V'/UE COMPOSITE	V'/UE INTER-TURBULENT ZONE	V'/UE TURBULENT ZONE	W'/UE COMPOSITE	W'/UE INTER-TURBULENT ZONE	W'/UE TURBULENT ZONE
0.2973	0.0979	0.0964	0.1031	0.0389	0.0263	0.0509	0.0757	0.0683	0.0841
0.3784	0.0893	0.0805	0.0969	0.0362	0.0248	0.0474	0.0751	0.0679	0.0842
0.4595	0.0813	0.0702	0.0920	0.0340	0.0214	0.0463	0.0715	0.0643	0.0817
0.5405	0.0744	0.0699	0.0838	0.0313	0.0200	0.0415	0.0729	0.0664	0.0813
0.6216	0.0686	0.0595	0.0784	0.0298	0.0196	0.0392	0.0732	0.0672	0.0815
0.7027	0.0641	0.0552	0.0752	0.0289	0.0196	0.0364	0.0665	0.0616	0.0751
0.7838	0.0607	0.0538	0.0707	0.0278	0.0199	0.0354	0.0687	0.0624	0.0796
0.8649	0.0594	0.0543	0.0675	0.0269	0.0213	0.0323	0.0679	0.0642	0.0755
1.0811	0.0552	0.0513	0.0631	0.0271	0.0227	0.0319	0.0638	0.0604	0.0742
2.4324	0.0479	0.0462	0.0522	0.0360	0.0334	0.0397	0.0573	0.0562	0.0662

Y/DELTA	U'**2/q**2 COMPOSITE	U'**2/q**2 INTER-TURBULENT ZONE	U'**2/q**2 TURBULENT ZONE	V'**2/q**2 COMPOSITE	V'**2/q**2 INTER-TURBULENT ZONE	V'**2/q**2 TURBULENT ZONE	W'**2/q**2 COMPOSITE	W'**2/q**2 INTER-TURBULENT ZONE	W'**2/q**2 TURBULENT ZONE
0.2973	0.5698	0.6327	0.5227	0.0888	0.0466	0.1262	0.3423	0.3206	0.3511
0.3784	0.5333	0.5534	0.5001	0.0864	0.0515	0.1184	0.3803	0.3951	0.3815
0.4595	0.5117	0.5162	0.4935	0.0884	0.0476	0.1234	0.3998	0.4362	0.3831
0.5405	0.4665	0.5024	0.4561	0.0816	0.0407	0.1108	0.4519	0.4569	0.4331
0.6216	0.4283	0.4178	0.4261	0.0796	0.0446	0.1058	0.4920	0.5376	0.4661
0.7027	0.4371	0.4206	0.4480	0.0879	0.0524	0.1032	0.4750	0.5266	0.4457
0.7838	0.4004	0.4015	0.3967	0.0828	0.0543	0.0979	0.5168	0.5442	0.5054
0.8649	0.3973	0.3902	0.4029	0.0833	0.0595	0.0910	0.5224	0.5502	0.5061
1.0811	0.3864	0.3850	0.3792	0.0919	0.0750	0.0950	0.5217	0.5399	0.5258
2.4324	0.3326	0.3319	0.3139	0.1859	0.1720	0.1788	0.4815	0.4961	0.5073

Y/DELTA	UV/Q**2 COMPOSITE	UV/Q**2 INTER-TURBULENT ZONE	UV/Q**2 TURBULENT ZONE	GAMMA UV	f UV	GAMMA WV	f WV
0.2973	-0.0654	-0.0402	-0.0858	42.2260	49.0250	39.7260	46.6240
0.3784	-0.0639	-0.0469	-0.0767	41.3830	48.4250	40.3640	47.0240
0.4595	-0.0695	-0.0443	-0.0878	40.1540	49.6250	40.3590	49.4250
0.5405	-0.0538	-0.0305	-0.0703	42.1210	56.6290	40.0540	52.0270
0.6216	-0.0464	-0.0226	-0.0626	42.6490	51.8270	38.8550	48.0250
0.7027	-0.0440	-0.0126	-0.0604	46.5470	61.0310	32.5850	49.2250
0.7838	-0.0348	-0.0071	-0.0527	42.2690	61.2310	32.4180	47.8240
0.8649	-0.0254	-0.0085	-0.0386	43.9340	58.8300	29.5470	47.6240
1.0811	-0.0112	0.0050	-0.0244	41.6240	61.0310	21.8880	40.6210
2.4324	0.0043	0.0058	0.0010	37.5820	64.8330	9.8950	26.8140

Y/DELTA	q**2/UE**2 COMPOSITE	q**2/UE**2 INTER-TURBULENT ZONE	q**2/UE**2 TURBULENT ZONE	UV/UE**2 COMPOSITE	UV/UE**2 INTER-TURBULENT ZONE	UV/UE**2 TURBULENT ZONE
0.2973	0.016900	0.014712	0.020333	-1.106E-03	-5.921E-04	-1.745E-03
0.3784	0.014993	0.011785	0.018818	-9.586E-04	-5.529E-04	-1.444E-03
0.4595	0.012931	0.009559	0.017176	-8.987E-04	-4.238E-04	-1.507E-03
0.5405	0.011884	0.009744	0.015423	-6.389E-04	-2.972E-04	-1.084E-03
0.6216	0.011014	0.008498	0.014392	-5.113E-04	-1.920E-04	-9.005E-04
0.7027	0.009411	0.007272	0.012706	-4.140E-04	-9.136E-05	-7.680E-04
0.7838	0.009217	0.007224	0.012649	-3.204E-04	-5.108E-05	-6.660E-04
0.8649	0.008902	0.007565	0.011378	-2.261E-04	-6.460E-05	-4.387E-04
1.0811	0.007886	0.006823	0.010577	-8.829E-05	3.413E-05	-2.576E-04
2.4324	0.006892	0.006420	0.008715	2.944E-05	3.700E-05	8.800E-06

TABLE A23-B

87 - 10 - 44 - 140

PROFILES OF MEAN AND FLUCTUATING QUANTITIES

X = 12.8 K = 0.75 E−6 TE = 4.2 %

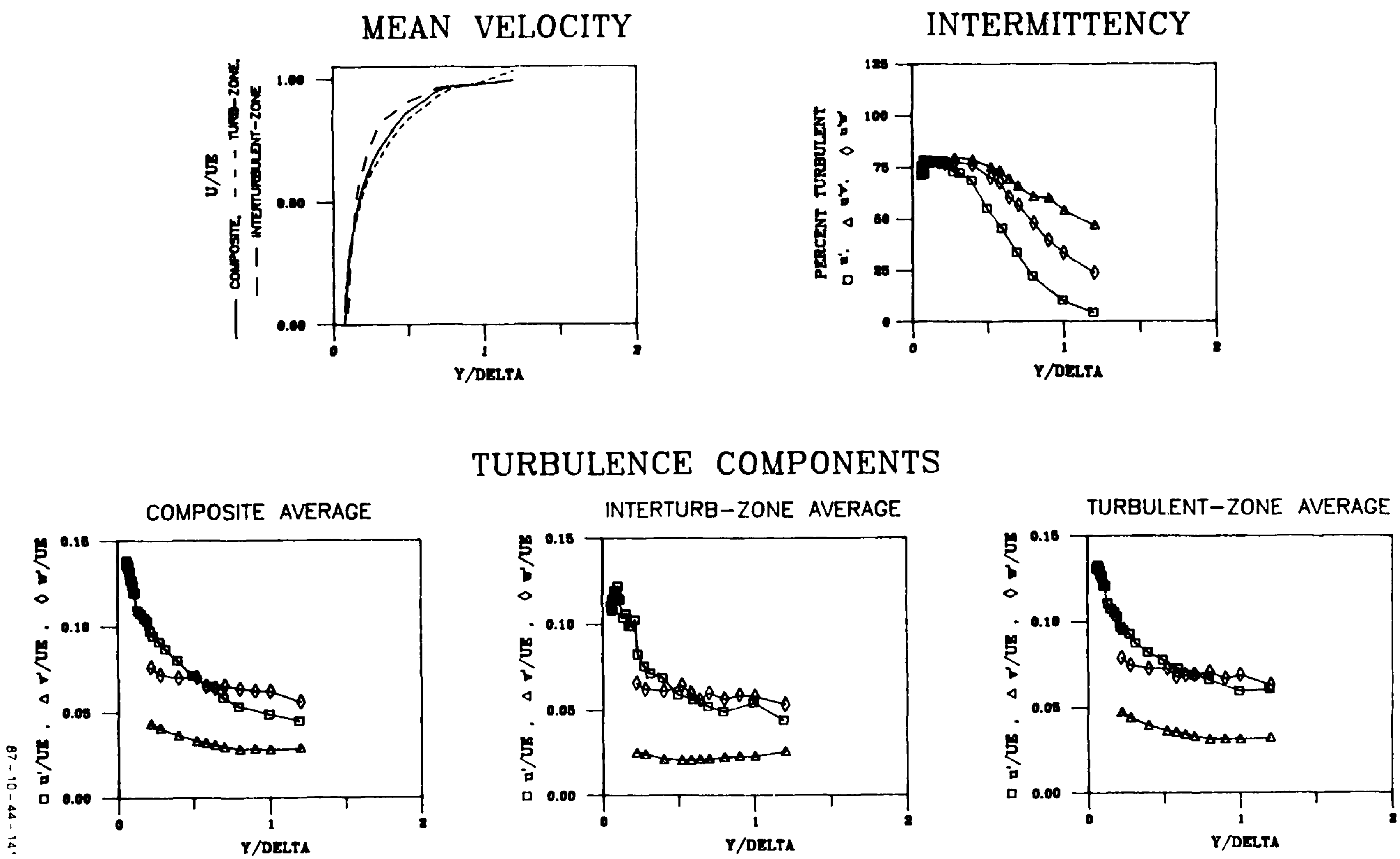

Figure A24-A

PROFILES OF TURBULENT STRESSES

X = 12.8 K = 0.75 E−6 TE = 4.2 %

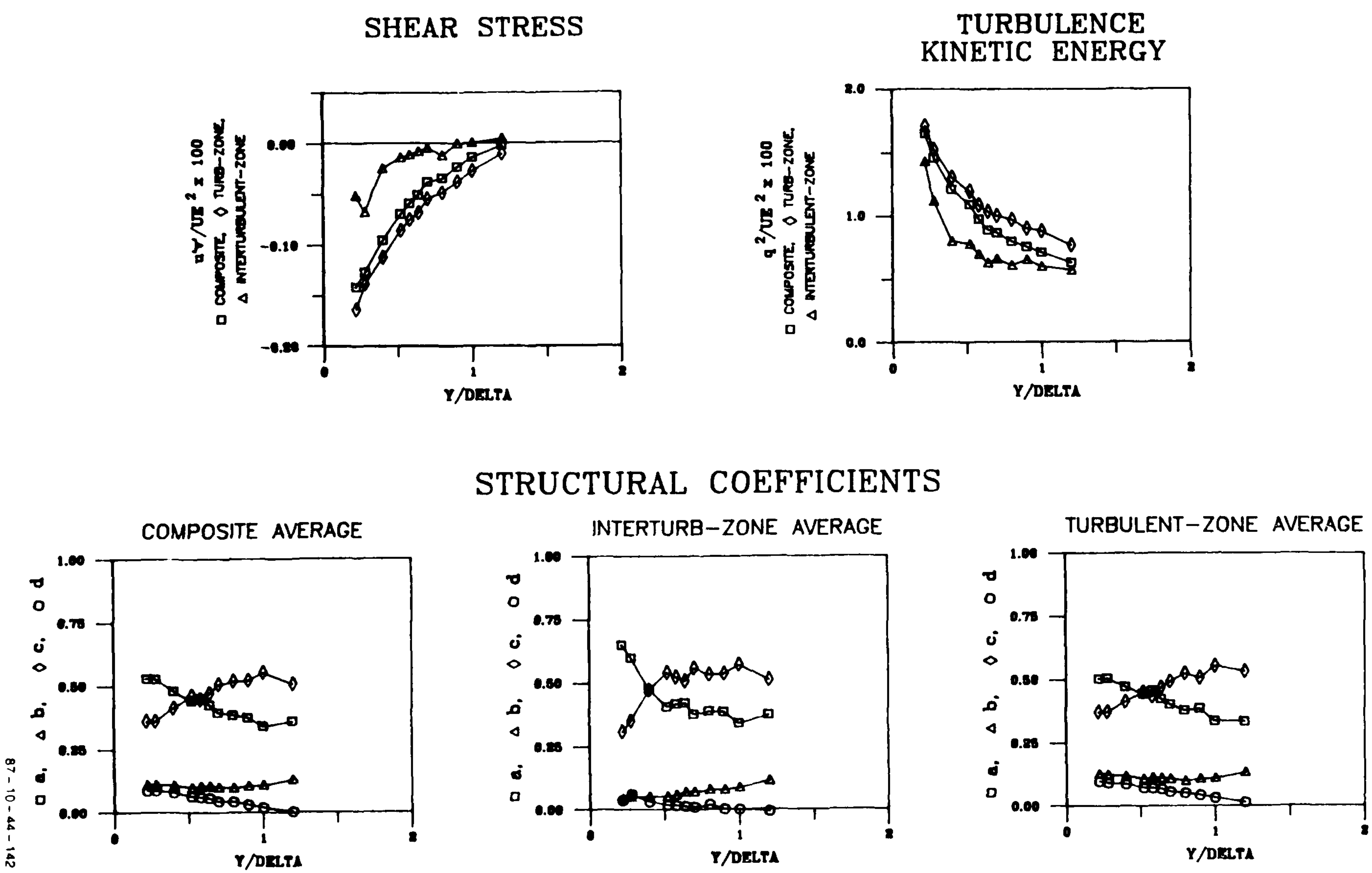

Figure A24-B

SINGLE WIRE PROFILE DATA

X = 12.8 GRID NO. 3 K = 0.75E-06

Y/DELTA	U/UE COMPOSITE	U/UE INTER-TURBULENT ZONE	U/UE TURBULENT ZONE	U'/UE COMPOSITE	U'/UE INTER-TURBULENT ZONE	U'/UE TURBULENT ZONE	GAMMA U	f U
0.0600	0.5003	0.4040	0.5377	0.1382	0.1077	0.1305	70.9120	46.2240
0.0632	0.5310	0.4436	0.5580	0.1353	0.1109	0.1306	75.4790	47.0240
0.0668	0.5376	0.4535	0.5698	0.1363	0.1086	0.1320	71.4930	47.0240
0.0708	0.5619	0.4911	0.5859	0.1344	0.1137	0.1324	73.8110	44.2230
0.0740	0.5769	0.5005	0.6044	0.1348	0.1145	0.1309	72.9100	42.0220
0.0772	0.6002	0.5258	0.6202	0.1322	0.1137	0.1297	78.2430	38.6200
0.0820	0.6108	0.5540	0.6329	0.1315	0.1191	0.1295	71.3270	42.6220
0.0860	0.6388	0.5954	0.6514	0.1271	0.1162	0.1274	76.7210	35.2180
0.0940	0.6630	0.6202	0.6749	0.1267	0.1182	0.1264	77.4720	39.0200
0.1020	0.6815	0.6391	0.6927	0.1237	0.1220	0.1217	78.3020	39.4200
0.1084	0.7041	0.6827	0.7103	0.1196	0.1144	0.1204	77.2620	34.8180
0.1176	0.7199	0.7065	0.7237	0.1192	0.1139	0.1204	76.9310	36.0180
0.1360	0.7488	0.7499	0.7485	0.1089	0.1034	0.1103	78.0050	38.2200
0.1556	0.7782	0.7973	0.7729	0.1072	0.1059	0.1070	77.7460	35.2180
0.1760	0.7999	0.8271	0.7926	0.1046	0.0987	0.1049	77.9230	39.2200
0.1952	0.8164	0.8461	0.8077	0.1029	0.0986	0.1026	76.3880	40.0200
0.2156	0.8327	0.8611	0.8242	0.0971	0.1023	0.0964	77.7480	40.0200
0.2340	0.8459	0.8826	0.8353	0.0942	0.0822	0.0947	76.8080	40.0200
0.2752	0.8691	0.9045	0.8560	0.0906	0.0753	0.0926	72.8380	49.4250
0.3152	0.8873	0.9288	0.8720	0.0867	0.0710	0.0872	72.2030	45.8230
0.3948	0.9155	0.9428	0.9038	0.0799	0.0683	0.0818	68.5960	56.2300
0.4944	0.9457	0.9627	0.9326	0.0711	0.0586	0.0773	54.9870	58.4300
0.5932	0.9628	0.9726	0.9517	0.0648	0.0558	0.0724	45.3360	67.0340
0.6936	0.9800	0.9849	0.9708	0.0584	0.0519	0.0687	33.3890	59.6310
0.7932	0.9885	0.9897	0.9845	0.0532	0.0489	0.0660	22.0360	49.8260
0.9936	0.9927	0.9917	0.9955	0.0485	0.0540	0.0594	10.0280	29.6150
1.1932	0.9988	0.9981	1.0134	0.0447	0.0439	0.0607	4.2367	15.4080
2.1924	1.0044	1.0034	0.9834	0.0416	0.0521	0.0228	0.1644	1.0005

TABLE A24-A

87 - 10 - 44 - 143

CROSS WIRE PROFILE DATA

X = 12.8 GRID NO. 3 K = 0.75E-06

Y/DELTA	U'/UE COMPOSITE	U'/UE INTER-TURBULENT ZONE	U'/UE TURBULENT ZONE	V'/UE COMPOSITE	V'/UE INTER-TURBULENT ZONE	V'/UE TURBULENT ZONE	W'/UE COMPOSITE	W'/UE INTER-TURBULENT ZONE	W'/UE TURBULENT ZONE
0.2200	0.0932	0.0947	0.0925	0.0433	0.0251	0.0472	0.0762	0.0656	0.0787
0.2800	0.0876	0.0814	0.0876	0.0407	0.0241	0.0438	0.0717	0.0618	0.0743
0.4000	0.0760	0.0611	0.0782	0.0364	0.0209	0.0394	0.0698	0.0606	0.0723
0.5200	0.0692	0.0560	0.0727	0.0332	0.0205	0.0362	0.0701	0.0640	0.0724
0.5800	0.0660	0.0537	0.0700	0.0322	0.0205	0.0354	0.0651	0.0594	0.0675
0.6400	0.0614	0.0513	0.0659	0.0308	0.0212	0.0341	0.0638	0.0556	0.0686
0.7000	0.0584	0.0497	0.0633	0.0298	0.0215	0.0331	0.0653	0.0598	0.0692
0.8000	0.0553	0.0485	0.0604	0.0283	0.0223	0.0313	0.0634	0.0561	0.0703
0.9000	0.0531	0.0499	0.0588	0.0285	0.0230	0.0316	0.0619	0.0585	0.0666
1.0000	0.0491	0.0452	0.0541	0.0281	0.0232	0.0315	0.0618	0.0577	0.0688
1.2000	0.0475	0.0459	0.0504	0.0291	0.0258	0.0324	0.0557	0.0530	0.0629
2.2000	0.0431	0.0473	0.0446	0.0368	0.0338	0.0396	0.0526	0.0520	0.0572

Y/DELTA	U'**2/q**2 COMPOSITE	U'**2/q**2 INTER-TURBULENT ZONE	U'**2/q**2 TURBULENT ZONE	V'**2/q**2 COMPOSITE	V'**2/q**2 INTER-TURBULENT ZONE	V'**2/q**2 TURBULENT ZONE	W'**2/q**2 COMPOSITE	W'**2/q**2 INTER-TURBULENT ZONE	W'**2/q**2 TURBULENT ZONE
0.2200	0.5286	0.6487	0.5015	0.1108	0.0430	0.1273	0.3606	0.3083	0.3712
0.2800	0.5274	0.5986	0.5048	0.1109	0.0508	0.1231	0.3617	0.3506	0.3722
0.4000	0.4795	0.4746	0.4712	0.1071	0.0536	0.1167	0.4134	0.4719	0.4121
0.5200	0.4403	0.4064	0.4430	0.0985	0.0527	0.1072	0.4612	0.5409	0.4499
0.5800	0.4494	0.4179	0.4550	0.1043	0.0595	0.1130	0.4463	0.5226	0.4319
0.6400	0.4249	0.4223	0.4227	0.1045	0.0705	0.1098	0.4705	0.5072	0.4675
0.7000	0.3945	0.3751	0.4019	0.1000	0.0686	0.1069	0.5054	0.5563	0.4911
0.8000	0.3844	0.3886	0.3777	0.0980	0.0797	0.0990	0.5176	0.5316	0.5232
0.9000	0.3740	0.3853	0.3860	0.1054	0.0789	0.1084	0.5206	0.5358	0.5056
1.0000	0.3408	0.3413	0.3367	0.1088	0.0880	0.1107	0.5504	0.5707	0.5526
1.2000	0.3612	0.3744	0.3349	0.1322	0.1150	0.1339	0.5066	0.5106	0.5312
2.2000	0.3084	0.3724	0.2897	0.2200	0.1806	0.2230	0.4716	0.4469	0.4873

Y/DELTA	UV/Q**2 COMPOSITE	UV/Q**2 INTER-TURBULENT ZONE	UV/Q**2 TURBULENT ZONE	GAMMA UV	f UV	GAMMA WV	f WV
0.2200	-0.0861	-0.0361	-0.0960	76.9470	33.8170	76.6700	30.0150
0.2800	-0.0870	-0.0608	-0.0913	79.6360	35.4180	77.5080	35.4180
0.4000	-0.0791	-0.0309	-0.0863	78.7010	37.2190	76.2060	39.0200
0.5200	-0.0638	-0.0179	-0.0718	75.0950	44.2230	69.9410	46.4240
0.5800	-0.0607	-0.0162	-0.0696	73.2350	44.4230	67.7000	48.6250
0.6400	-0.0573	-0.0130	-0.0663	69.0320	50.0260	60.1230	54.8280
0.7000	-0.0440	-0.0071	-0.0548	65.6220	55.8290	56.4190	55.2280
0.8000	-0.0430	-0.0197	-0.0504	60.5870	63.8330	47.7430	60.8310
0.9000	-0.0305	-0.0005	-0.0421	59.8310	64.0330	39.4700	58.2300
1.0000	-0.0194	0.0008	-0.0310	53.6680	65.4340	32.9870	55.0280
1.2000	-0.0034	0.0084	-0.0136	46.6930	66.8340	23.4860	46.0240
2.2000	0.0041	0.0131	-0.0111	41.9010	66.8340	11.1190	29.4150

Y/DELTA	q**2/UE**2 COMPOSITE	q**2/UE**2 INTER-TURBULENT ZONE	q**2/UE**2 TURBULENT ZONE	UV/UE**2 COMPOSITE	UV/UE**2 INTER-TURBULENT ZONE	UV/UE**2 TURBULENT ZONE
0.2200	0.016476	0.014290	0.017084	-1.418E-03	-5.163E-04	-1.640E-03
0.2800	0.014554	0.011146	0.015205	-1.266E-03	-6.780E-04	-1.388E-03
0.4000	0.012080	0.007971	0.013006	-9.560E-04	-2.464E-04	-1.123E-03
0.5200	0.010902	0.007768	0.011952	-6.958E-04	-1.388E-04	-8.584E-04
0.5800	0.009727	0.006924	0.010811	-5.903E-04	-1.124E-04	-7.523E-04
0.6400	0.008871	0.006239	0.010306	-5.086E-04	-8.102E-05	-6.829E-04
0.7000	0.008649	0.006582	0.009976	-3.806E-04	-4.661E-05	-5.472E-04
0.8000	0.007965	0.006069	0.009666	-3.426E-04	-1.194E-04	-4.875E-04
0.9000	0.007543	0.006538	0.008973	-2.304E-04	-3.141E-06	-3.775E-04
1.0000	0.007103	0.005983	0.008768	-1.379E-04	4.566E-06	-2.721E-04
1.2000	0.006263	0.005639	0.007631	-2.106E-05	4.765E-05	-1.036E-04
2.2000	0.006015	0.006188	0.006869	2.437E-05	8.125E-05	-7.623E-05

TABLE A24-B

PROFILES OF MEAN AND FLUCTUATING QUANTITIES

X = 16.8 K = 0.75 E−6 TE = 3.7 %

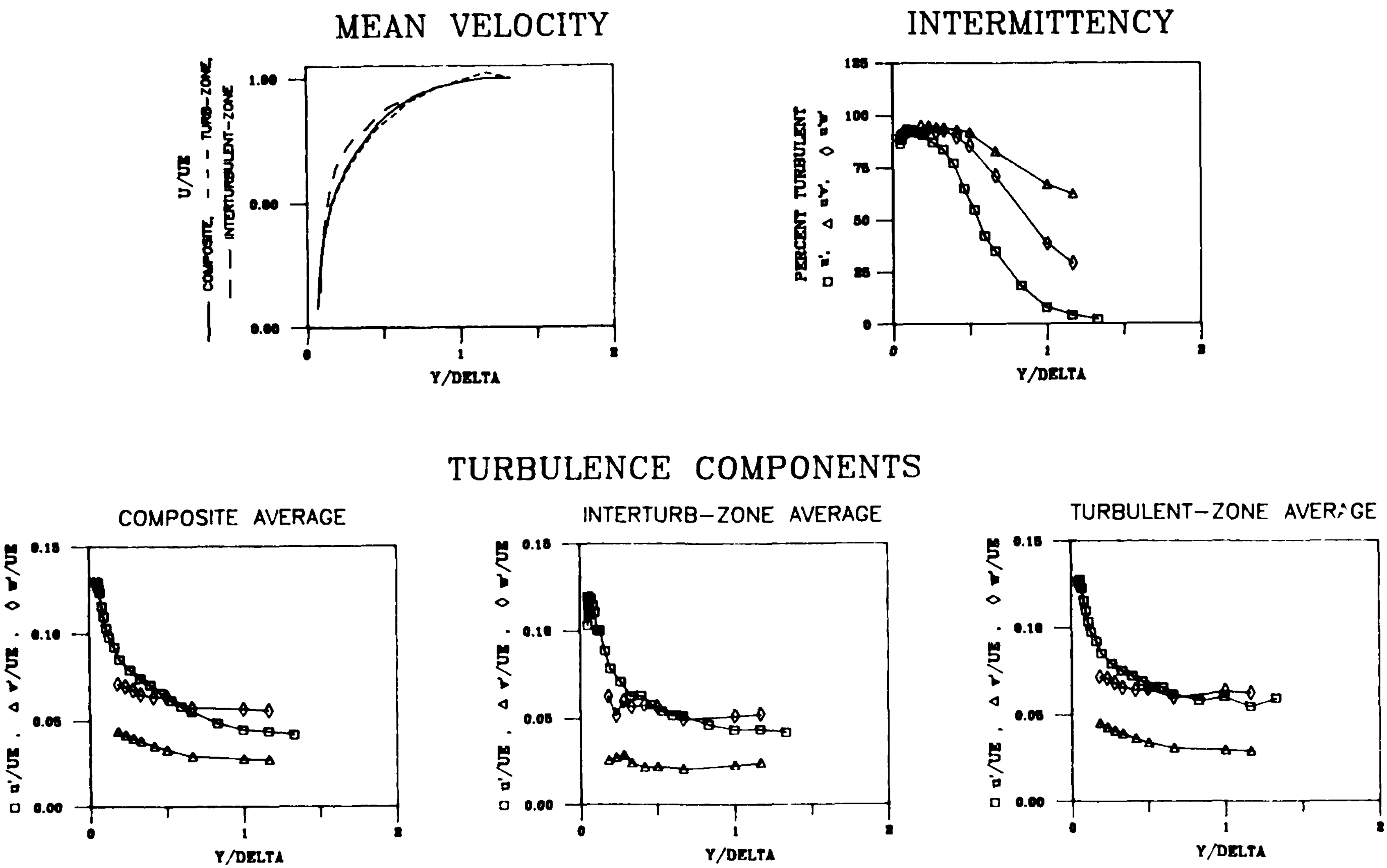

Figure A25-A

87 - 10 - 44 - 145

PROFILES OF TURBULENT STRESSES

X = 16.8 K = 0.75 E-6 TE = 3.7 %

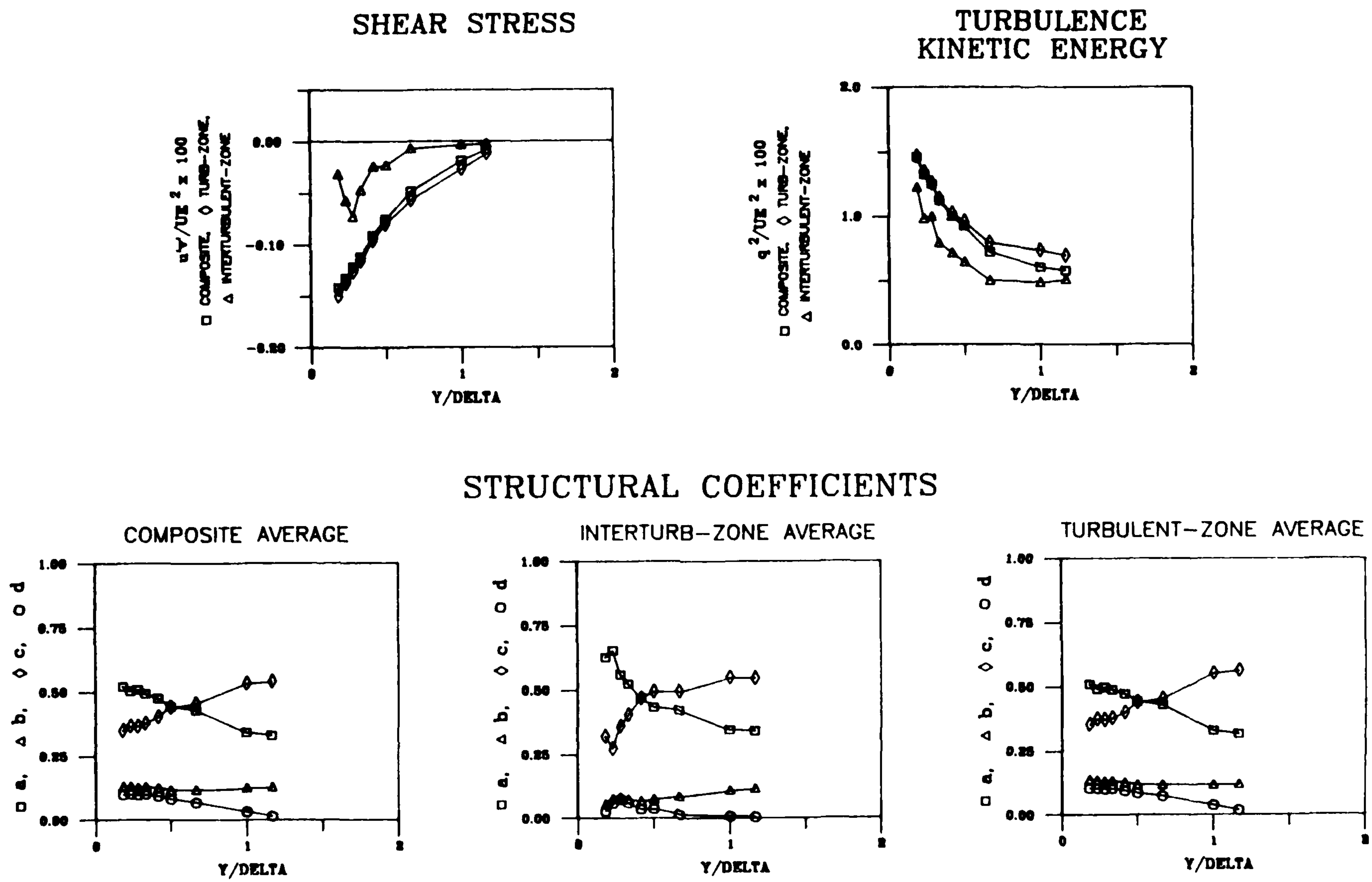

Figure A25-B

87-10-44-146

SINGLE WIRE PROFILE DATA

X = 16.8 GRID NO. 3 K = 0.75E-06

Y/DELTA	U/UE COMPOSITE	U/UE INTER-TURBULENT ZONE	U/UE TURBULENT ZONE	U'/UE COMPOSITE	U'/UE INTER-TURBULENT ZONE	U'/UE TURBULENT ZONE	GAMMA U	[illegible] U
0.0500	0.5127	0.4207	0.5266	0.1286	0.1029	0.1263	86.3930	35.8181
0.0533	0.5343	0.4412	0.5466	0.1297	0.1195	0.1259	89.3830	31.2160
0.0567	0.5540	0.4848	0.5644	0.1278	0.1158	0.1262	89.0190	25.8130
0.0590	0.5658	0.4807	0.5754	0.1289	0.1103	0.1273	90.3460	22.6120
0.0623	0.5807	0.5042	0.5921	0.1259	0.1088	0.1244	88.4400	25.2130
0.0713	0.6306	0.5724	0.6367	0.1234	0.1182	0.1224	91.1350	20.2100
0.0853	0.6806	0.6566	0.6833	0.1154	0.1143	0.1153	91.5800	18.8100
0.0987	0.7163	0.7188	0.7161	0.1095	0.1104	0.1095	93.1580	15.8080
0.1153	0.7430	0.7527	0.7420	0.1029	0.0997	0.1032	93.1250	18.6100
0.1303	0.7608	0.7847	0.7587	0.0977	0.1001	0.0973	92.0210	18.8100
0.1640	0.7990	0.8321	0.7948	0.0922	0.0884	0.0919	91.5910	19.6100
0.1980	0.8229	0.8579	0.8188	0.0850	0.0782	0.0849	90.4870	24.2120
0.2643	0.8564	0.8883	0.8517	0.0789	0.0707	0.0790	86.8600	32.4170
0.3303	0.8829	0.9107	0.8776	0.0741	0.0624	0.0751	83.6300	36.6200
0.3973	0.9039	0.9200	0.8991	0.0704	0.0628	0.0720	77.1000	53.4270
0.4637	0.9265	0.9391	0.9204	0.0657	0.0575	0.0659	64.8340	63.4320
0.5310	0.9422	0.9531	0.9335	0.0613	0.0538	0.0655	54.7210	64.2330
0.5981	0.9552	0.9614	0.9470	0.0561	0.0513	0.0655	42.1441	64.2770
0.6640	0.9655	0.9673	0.9623	0.0550	0.0513	0.0613	34.8280	61.0310
0.8713	0.9842	0.9847	0.9822	0.0487	0.0460	0.0579	16.2221	42.4220
0.9970	0.9939	0.9937	0.9958	0.0445	0.0431	0.0599	7.8432	26.6141
1.1647	1.0068	1.0024	1.0091	0.0425	0.0422	0.0545	3.9857	13.617[illegible]
1.3310	1.0009	1.0005	0.9987	0.0417	0.0415	0.0592	2.0056	7.6029
3.3307	1.0046	1.0046	1.0778	0.0355	0.0358	0.0411	0.0282	0.2[illegible]

TABLE A25-A

87-10-44-147

CROSS WIRE PROFILE DATA

X = 16.8 GRID NO. 3 K = 0.75E-06

Y/DELTA	U'/UE COMPOSITE	U'/UE INTER-TURBULENT ZONE	U'/UE TURBULENT ZONE	V'/UE COMPOSITE	V'/UE INTER-TURBULENT ZONE	V'/UE TURBULENT ZONE	W'/UE COMPOSITE	W'/UE INTER-TURBULENT ZONE	W'/UE TURBULENT ZONE
0.1833	0.0869	0.0870	0.0862	0.0437	0.0257	0.0450	0.0711	0.0624	0.0716
0.2333	0.0814	0.0796	0.0810	0.0416	0.0274	0.0425	0.0695	0.0513	0.0706
0.2833	0.0796	0.0745	0.0789	0.0396	0.0287	0.0405	0.0673	0.0596	0.068[illegible]
0.3333	0.0742	0.0643	0.0743	0.0381	0.0241	0.0389	0.0648	0.0563	0.065[illegible]
0.4167	0.0687	0.0576	0.0693	0.0351	0.0216	0.0360	0.0632	0.0574	0.063[illegible]
0.5000	0.0638	0.0526	0.0650	0.0328	0.0219	0.0336	0.0635	0.0561	0.064[illegible]
0.6667	0.0554	0.0456	0.0582	0.0291	0.0207	0.0305	0.0569	0.0493	0.055[illegible]
1.0000	0.0452	0.0406	0.0490	0.0275	0.0229	0.0294	0.0563	0.0511	[illegible]
1.1667	0.0435	0.0414	0.0466	0.0272	0.0242	0.0289	0.0555	0.0522	[illegible]
3.3333	0.0359	0.0354	0.0380	0.0403	0.0375	0.0426	0.0417	0.0405	0.047[illegible]

Y/DELTA	U'**2/q**2 COMPOSITE	U'**2/q**2 INTER-TURBULENT ZONE	U'**2/q**2 TURBULENT ZONE	V'**2/q**2 COMPOSITE	V'**2/q**2 INTER-TURBULENT ZONE	V'**2/q**2 TURBULENT ZONE	W'**2/q**2 COMPOSITE	W'**2/q**2 INTER-TURBULENT ZONE	W'**2/q**2 TURBULENT ZONE
0.1833	0.5197	0.6258	0.5087	0.1307	0.0537	0.1379	0.3496	0.3205	0.3534
0.2333	0.5026	0.6524	0.4907	0.1298	0.0761	0.1341	0.3676	0.2715	[illegible]
0.2833	0.5087	0.5585	0.4979	0.1248	0.0821	0.1301	0.3665	0.3595	[illegible]
0.3333	0.4929	0.5227	0.4883	0.1289	0.0728	0.1325	0.3782	0.4045	[illegible]
0.4167	0.4737	0.4677	0.4721	0.1231	0.0654	0.1263	0.4032	0.4669	0.401[illegible]
0.5000	0.4430	0.4322	0.4422	0.1160	0.0744	0.1174	0.4410	0.4925	0.4414
0.6667	0.4284	0.4205	0.4294	0.1170	0.0857	0.1169	0.4546	0.4938	0.4527
1.0000	0.3417	0.3439	0.3295	0.1253	0.1082	0.1177	0.5330	0.5460	0.55[illegible]
1.1667	0.3308	0.3397	0.3164	0.1287	0.1156	0.1198	0.5406	0.5446	0.56[illegible]
3.3333	0.2765	0.2915	0.2654	0.3475	0.3248	0.3269	0.3758	0.3877	0.4057

Y/DELTA	UV/Q**2 COMPOSITE	UV/Q**2 INTER-TURBULENT ZONE	UV/Q**2 TURBULENT ZONE	GAMMA UV	f UV	GAMMA WV	f WV
0.1833	-0.0979	-0.0261	-0.1028	91.9420	15.6080	94.1570	11.6060
0.2333	-0.1004	-0.0585	-0.1030	94.0750	12.2060	93.5530	11.6060
0.2833	-0.0975	-0.0732	-0.1007	94.2520	12.6060	91.8780	15.8080
0.3333	-0.1000	-0.0592	-0.1022	93.6860	16.2080	92.7560	14.8080
0.4167	-0.0915	-0.0337	-0.0941	92.9590	17.2090	89.5240	22.8120
0.5000	-0.0818	-0.0358	-0.0837	91.5730	27.8140	85.3230	32.4170
0.6667	-0.0674	-0.0137	-0.0720	82.6380	42.4220	70.9580	53.8280
1.0000	-0.0312	-0.0064	-0.0367	66.7620	60.2310	38.5810	57.8300
1.1667	-0.0139	-0.0037	-0.0173	62.0620	67.8350	28.8240	51.0260
3.3333	0.0085	0.0095	0.0066	53.2100	67.0340	15.8560	38.4200

Y/DELTA	q**2/UE**2 COMPOSITE	q**2/UE**2 INTER-TURBULENT ZONE	q**2/UE**2 TURBULENT ZONE	UV/UE**2 COMPOSITE	UV/UE**2 INTER-TURBULENT ZONE	UV/UE**2 TURBULENT ZONE
0.1833	0.014547	0.012223	0.014617	-1.423E-03	-3.185E-04	-1.503E-03
0.2333	0.013216	0.009776	0.013372	-1.326E-03	-5.720E-04	-1.377E-03
0.2833	0.012460	0.009952	0.012525	-1.215E-03	-7.280E-04	-1.261E-03
0.3333	0.011181	0.007901	0.011315	-1.118E-03	-4.675E-04	-1.156E-03
0.4167	0.009959	0.007106	0.010189	-9.109E-04	-2.395E-04	-9.589E-04
0.5000	0.009210	0.006411	0.009559	-7.529E-04	-2.294E-04	-8.005E-04
0.6667	0.007172	0.004954	0.007893	-4.835E-04	-6.788E-05	-5.680E-04
1.0000	0.005986	0.004796	0.007297	-1.866E-04	-3.057E-05	-2.676E-04
1.1667	0.005729	0.005040	0.006903	-7.940E-05	-1.846E-05	-1.192E-04
3.3333	0.004652	0.004306	0.005473	3.945E-05	4.103E-05	3.620E-05

TABLE A25-B

PROFILES OF MEAN AND FLUCTUATING QUANTITIES

X = 24.8 K = 0.75 E-6 TE = 3.1 %

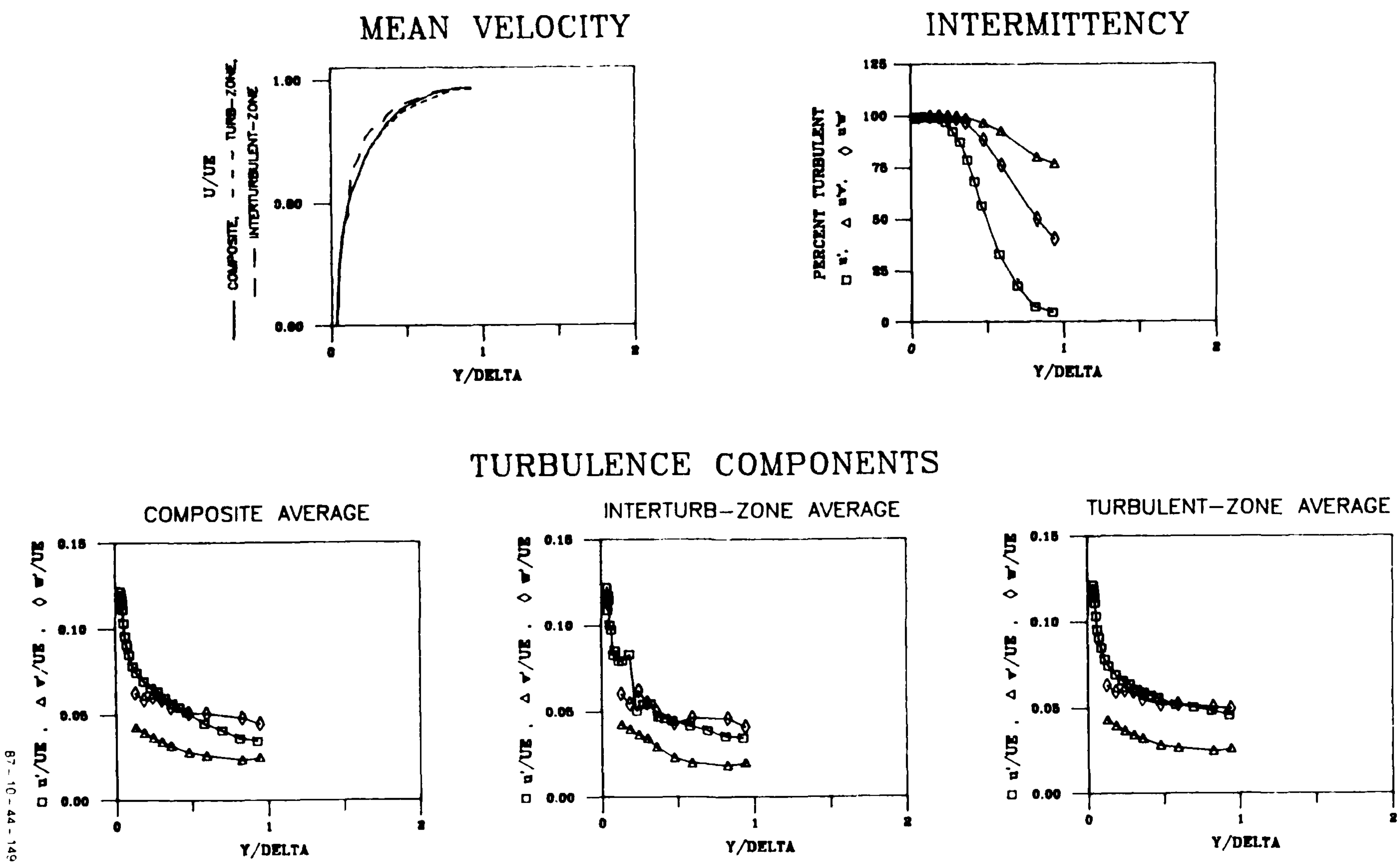

Figure A26-A

PROFILES OF TURBULENT STRESSES

X = 24.8 K = 0.75 E−6 TE = 3.1 %

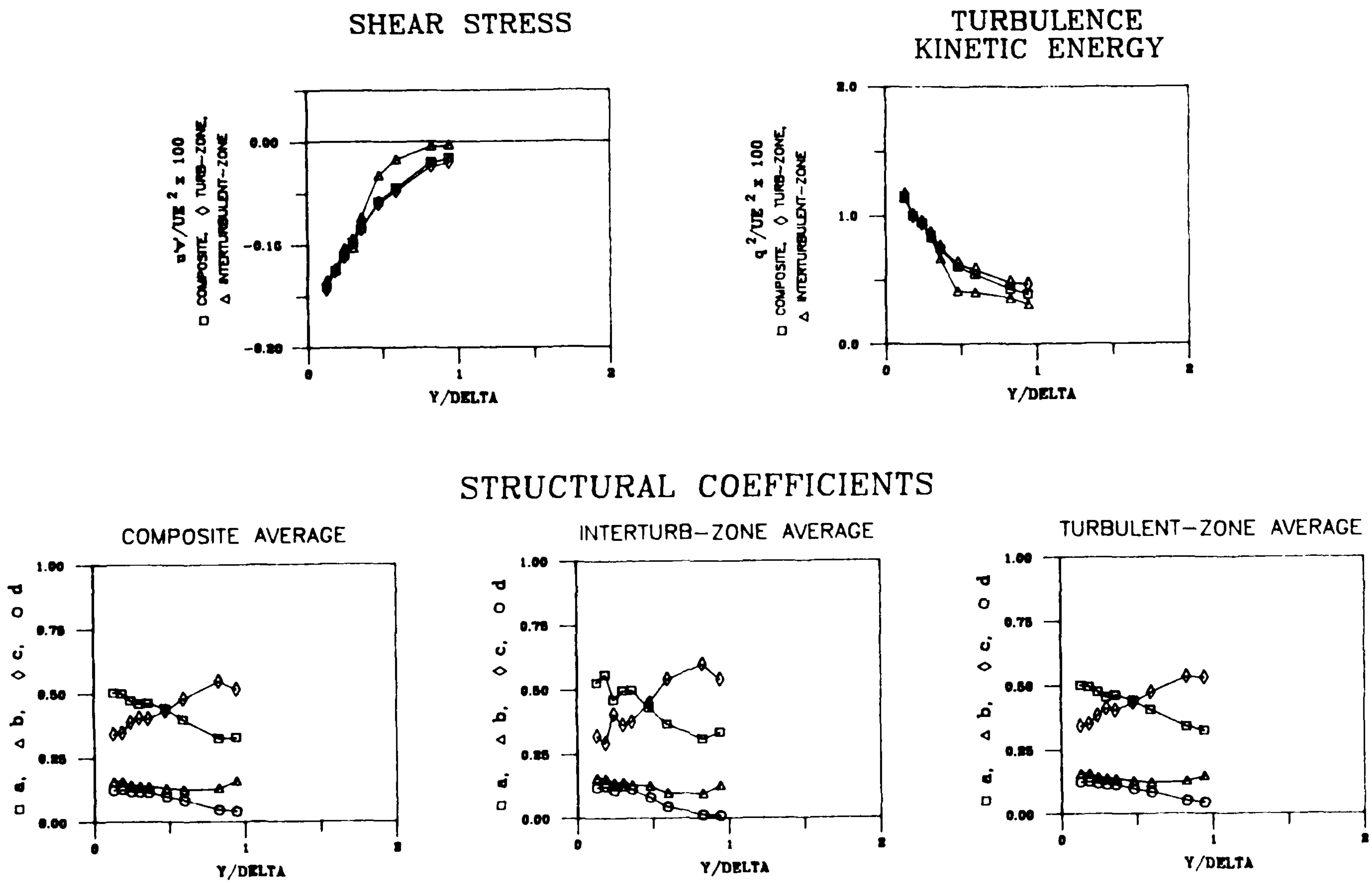

Figure A26-B

87 - 10 - 44 - 150

SINGLE WIRE PROFILE DATA

X = 24.8 GRID NO. 3 K = 0.75E-06

Y/DELTA	U/UE COMPOSITE	U/UE INTER-TURBULENT ZONE	U/UE TURBULENT ZONE	U'/UE COMPOSITE	U'/UE INTER-TURBULENT ZONE	U'/UE TURBULENT ZONE	GAMMA U	f U
0.0349	0.5794	0.5168	0.5806	0.1216	0.1219	0.1213	98.4070	3.6018
0.0374	0.6003	0.5689	0.6007	0.1191	0.1175	0.1190	98.8680	3.8019
0.0386	0.6028	0.5223	0.6042	0.1178	0.1170	0.1173	98.5300	4.8025
0.0412	0.6220	0.5958	0.6223	0.1169	0.1084	0.1169	99.2190	2.2011
0.0437	0.6372	0.6309	0.6377	0.1152	0.1155	0.1152	98.9880	3.2016
0.0451	0.6467	0.6504	0.6465	0.1141	0.1171	0.1140	98.9930	3.2016
0.0498	0.6645	0.6772	0.6643	0.1108	0.1144	0.1107	99.1010	2.4012
0.0591	0.6993	0.6981	0.6993	0.1029	0.0999	0.1029	99.0060	2.4012
0.0684	0.7228	0.7243	0.7228	0.0953	0.0971	0.0952	99.3930	1.8009
0.0795	0.7476	0.7670	0.7474	0.0903	0.0823	0.0904	99.1240	2.0010
0.0919	0.7666	0.7698	0.7664	0.0846	0.0851	0.0846	99.0290	1.8009
0.1144	0.7925	0.7789	0.7930	0.0779	0.0789	0.0779	99.0910	3.4017
0.1381	0.8174	0.8517	0.8169	0.0742	0.0792	0.0740	98.8370	3.4017
0.1847	0.8452	0.8723	0.8448	0.0692	0.0828	0.0689	98.7270	5.2027
0.2314	0.8765	0.9065	0.8754	0.0653	0.0499	0.0655	96.5800	12.0060
0.2770	0.8960	0.9210	0.8979	0.0634	0.0539	0.0636	92.1290	25.0131
0.3244	0.9114	0.9224	0.9098	0.0595	0.0543	0.0603	87.0980	38.4200
0.3705	0.9294	0.9419	0.9260	0.0566	0.0465	0.0588	78.3040	49.6267
0.4172	0.9400	0.9523	0.9345	0.0542	0.0455	0.0571	67.9760	63.2320
0.4635	0.9526	0.9601	0.9469	0.0512	0.0441	0.0557	56.0810	68.4350
0.5795	0.9672	0.9700	0.9617	0.0447	0.0410	0.0514	32.5440	61.6320
0.6960	0.9789	0.9815	0.9719	0.0407	0.0385	0.0501	17.3230	42.8020
0.8126	0.9868	0.9869	0.9845	0.0360	0.0352	0.0481	7.0441	22.6120
0.9286	0.9881	0.9880	0.9857	0.0343	0.0341	0.0454	4.4698	16.008
2.3240	0.9999	0.9998	1.0008	0.0264	0.0264	0.0000	0.0000	0.0000

TABLE A26-A

87 - 10 - 44 - 151

CROSS WIRE PROFILE DATA

X = 24.8 GRID NO. 3 K = 0.75E-06

Y/DELTA	U'/UE COMPOSITE	U'/UE INTER-TURBULENT ZONE	U'/UE TURBULENT ZONE	V'/UE COMPOSITE	V'/UE INTER-TURBULENT ZONE	V'/UE TURBULENT ZONE	W'/UE COMPOSITE	W'/UE INTER-TURBULENT ZONE	W'/UE TURBULENT ZONE
0.1279	0.0761	0.0772	0.0763	0.0426	0.0422	0.0428	0.0625	0.0600	0.0623
0.1860	0.0705	0.0749	0.0703	0.0394	0.0393	0.0394	0.0586	0.0540	0.0569
0.2442	0.0666	0.0663	0.0669	0.0365	0.0362	0.0366	0.0602	0.0619	0.0596
0.3023	0.0623	0.0640	0.0623	0.0341	0.0341	0.0341	0.0583	0.0546	0.0590
0.3605	0.0586	0.0573	0.0588	0.0319	0.0292	0.0320	0.0544	0.0496	0.0547
0.4767	0.0514	0.0419	0.0524	0.0279	0.0227	0.0282	0.0507	0.0426	0.0517
0.5930	0.0462	0.0380	0.0481	0.0259	0.0195	0.0264	0.0505	0.0460	0.0518
0.8256	0.0371	0.0329	0.0401	0.0236	0.0183	0.0247	0.0480	0.0457	0.0501
0.9419	0.0357	0.0321	0.0387	0.0249	0.0198	0.0262	0.0444	0.0406	0.0494
2.3256	0.0282	0.0287	0.0286	0.0334	0.0000	0.0348	0.0352	0.0340	0.0393

Y/DELTA	U'**2/q**2 COMPOSITE	U'**2/q**2 INTER-TURBULENT ZONE	U'**2/q**2 TURBULENT ZONE	V'**2/q**2 COMPOSITE	V'**2/q**2 INTER-TURBULENT ZONE	V'**2/q**2 TURBULENT ZONE	W'**2/q**2 COMPOSITE	W'**2/q**2 INTER-TURBULENT ZONE	W'**2/q**2 TURBULENT ZONE
0.1279	0.5025	0.5254	0.5010	0.1563	0.1553	0.1564	0.3412	0.3194	0.3426
0.1860	0.4989	0.5574	0.4950	0.1542	0.1514	0.1542	0.3469	0.2912	0.3508
0.2442	0.4717	0.4596	0.4755	0.1406	0.1358	0.1410	0.3877	0.4046	0.3835
0.3023	0.4586	0.4970	0.4542	0.1365	0.1393	0.1353	0.4047	0.3636	0.4105
0.3605	0.4624	0.4977	0.4617	0.1358	0.1277	0.1355	0.4018	0.3746	0.4028
0.4767	0.4396	0.4284	0.4412	0.1289	0.1245	0.1268	0.4315	0.4471	0.4320
0.5930	0.3977	0.3658	0.4057	0.1237	0.0953	0.1211	0.4786	0.5390	0.4732
0.8256	0.3245	[illegible]	[illegible]	0.1298	0.0944	0.1274	0.5457	0.5975	[illegible]
0.9419	0.3282	0.3349	0.3238	0.1587	0.1267	0.1465	0.5132	0.5385	0.5297
2.3256	0.2524	0.4134	0.2292	0.3504	0.0007	0.3350	0.3972	0.5866	0.4358

Y/DELTA	UV/Q**2 COMPOSITE	UV/Q**2 INTER-TURBULENT ZONE	UV/Q**2 TURBULENT ZONE	GAMMA UV	f UV	GAMMA WV	f WV
0.1279	-0.1226	-0.1186	-0.1237	99.2160	1.4007	99.1680	1.0005
0.1860	-0.1255	-0.1232	-0.1254	99.3720	1.6008	99.2750	1.0005
0.2442	-0.1173	-0.1079	-0.1184	99.3160	1.4007	98.9860	1.8009
0.3023	-0.1153	-0.1249	-0.1135	98.9140	3.4017	98.5300	6.6034
0.3605	-0.1134	-0.1111	-0.1129	98.9160	5.2027	96.6880	11.4060
0.4767	-0.0968	-0.0796	-0.0959	96.2470	15.2080	88.2220	29.4150
0.5930	-0.0833	-0.0432	-0.0831	92.3640	24.4130	75.8480	46.4240
0.8256	-0.0459	-0.0128	-0.0497	79.6440	48.4250	49.8160	60.0310
0.9419	-0.0401	-0.0097	-0.0423	76.5830	53.0270	40.0690	56.2290
2.3256	0.0101	0.0000	0.0111	68.2740	63.2320	20.8480	45.4230

Y/DELTA	q**2/UE**2 COMPOSITE	q**2/UE**2 INTER-TURBULENT ZONE	q**2/UE**2 TURBULENT ZONE	UV/UE**2 COMPOSITE	UV/UE**2 INTER-TURBULENT ZONE	UV/UE**2 TURBULENT ZONE
0.1279	0.011537	0.011372	0.011609	-1.414E-03	-1.349E-03	-1.436E-03
0.1860	0.009978	0.010099	0.009977	-1.252E-03	-1.244E-03	-1.252E-03
0.2442	0.009417	0.009559	0.009410	-1.104E-03	-1.032E-03	-1.114E-03
0.3023	0.008465	0.008267	0.008547	-9.758E-04	-1.032E-03	-9.697E-04
0.3605	0.007417	0.006620	0.007486	-8.411E-04	-7.353E-04	-8.450E-04
0.4767	0.006011	0.004093	0.006233	-5.822E-04	-3.260E-04	-5.974E-04
0.5930	0.005376	0.003961	0.005714	-4.478E-04	-1.709E-04	-4.746E-04
0.8256	0.004255	0.003523	0.004749	-1.955E-04	-4.509E-05	-2.359E-04
0.9419	0.003878	0.003079	0.004640	-1.555E-04	-2.981E-05	-1.961E-04
2.3256	0.003152	0.001986	0.003580	3.192E-05	0.000E+00	3.985E-05

TABLE A26-B

87 - 10 - 44 - 152

END
DATE
FILMED
5-88
DTIC